DEVELOPMENT OF GUIDELINES FOR TRANSVERSE WEB FRAME DESIGN IN POLAR CLASS SHIPS USING NON-LINEAR FINITE ELEMENT ANALYSIS

By

© Edward Moakler, B.Eng.

A thesis submitted to the School of Graduate Studies

in partial fulfillment of the requirements for the degree of

Masters of Engineering

Faculty of Engineering and Applied Science

Memorial University of Newfoundland

May 2018

St. John's Newfoundland and Labrador Canada

Abstract

This thesis aims to fill in the gaps that exist for transverse web frame design in polar class ships. The International Association of Classification Societies (IACS) has developed a set of harmonized rules that govern the design and construction of many different types of vessels. Traditional ship design used an elastic design point whereas the new Polar Class rules use a plastic design point. For polar class ships an agreement could not be reached within IACS governing bodies with regards to transverse web frame design. As no agreement was reached each classification society has adopted their own methods for the design and construction of transverse web frames. Many of the classification societies have adapted their rules from traditional steel vessel designs until an agreement can be made within IACS. The problem with this (aside from there not being harmonized rules across the classification societies) is that the design point for web frames using traditional steel vessel rules is elastic, while the design point of all the surrounding is plastic. This causes a mismatch in design philosophies where the web frames must be overly large in order to remain elastic under the design load. This thesis looks at the plastic behaviour of transverse web frames in two different polar class ships, at the design load and in overload scenarios, using non-linear finite element analysis and a "design of experiments" statistical approach. This thesis presents guidance on how to develop accurate finite element models for polar class ships and provides guidance on appropriate acceptance criteria for the plastic design/behaviour of transverse web frames.

Acknowledgements

I would like to thank the following people for their continual guidance and help with my research and graduate studies:

1) Dr. Bruce Quinton, my graduate supervisor, for his guidance and expertise, his positive attitude and his ability to motivate even during the difficult times. Without Bruce I would have never had this amazing opportunity. He was nothing less than a perfect supervisor.
2) My mother and father, Rose and Bob Moakler, for their constant support and love. They made it possible for me to carry out my research and still maintain a life outside of my academics.
3) My brother, Michael Moakler, for always being supportive and helping me relax and take my mind off of my research.
4) John Dolny of ABS, for his help with my research. John was always able to guide me in my research and push me to strive for more.
5) Dan Oldford of ABS, for always being around to bounce ideas off of, his knowledge of ship design/construction and his willingness to help.
6) The ONAE faculty at MUN, for always being helpful in all things naval related as well as career guidance.

Table of Contents

List of Tables

List of Figures

List of Symbols, Nomenclature or Abbreviations

ABS	American Bureau of Shipping
ANOVA	Analysis of Variance
DNV	Det Norske Veritas
FEA	Finite Element Analysis
NFEA	Nonlinear Finite Element Analysis
IACS	International Association of Classification Societies
P_{avg}	Average Uniform Pressure
H-L	Hughes-Liu
B-T	Belytscho-Tsay
DOF	Degrees of Freedom
WSD	Working Stress Design
DOE	Design of Experiments

List of Appendices

Chapter 1 Introduction

As Arctic waters have become more accessible there has been an increase in marine traffic through the Arctic Ocean. This increase in traffic has led to new design rules for ships in ice environments. The International Association of Classification societies (IACS), a group of leading classification societies such as the American Bureau of Shipping (ABS), Det Norske Veritas (DNV) and Lloyd's Register, creates unified rules for various topics to ensure certain key design points are uniform across all classification societies. In the early 2000s IACS released a set of unified Polar Class rules for vessels that operate in ice infested polar waters. These rules prescribe minimum requirements for many different aspects of ice-strengthened ship design such as plating thickness, internal structure size, and machinery/power requirements. For the structural design of polar class ships a new approach (IACS, 2011) was taken by IACS. Instead of classical ship design which tends to ensure that ship structures respond only in the linear elastic range, it was decided to use a plastic limit state, comparable to plastic three hinge collapse. This design point allows for some plastic deformation without collapse. Not all parties in IACS could come to agreement over the design criteria for large structural members (such as transverse web frames) in polar class ships. The currently prescribed criteria are to ensure that the web frames respond in the elastic range, to the design load. This causes the web frames to be overly large, increasing their weight, as they must bear even more load due to the surrounding structure which uses a plastic design point.

In order to better understand the plastic response of transverse web frames, nonlinear finite element models were created for a “high” and “low” polar class ship design. Using the initial model results, side studies were used to identify specific design characteristics that influence the web frames response. From these studies, guidelines have been proposed on how to develop an accurate non-linear finite element model, and acceptance criteria to determine if a web frame has been sized appropriately.

This thesis is divided into four main chapters. This chapter, the introductory chapter, outlines the scope and objective of this thesis; description of the literature review done for this thesis; an overview of polar class ship rules and briefly describes the finite element code used for developing and solving the numerical model. Chapter 2 discusses the methodology used for completing the research within this thesis. Chapter 3 discusses the development of the numerical models created in order to study transverse web frame plastic response. Chapter 4 discusses the results from the numerical models developed in Chapter 3. Chapter 5 presents the conclusions and recommendations for future research.

1.1 Scope/mission

This thesis investigates the nonlinear structural response of transverse web frames in polar class ships subject to accidental overload scenarios, and presents nonlinear finite element analysis (NFEM) guidelines that may be used for similar structural analysis work. In the IACS Polar Class rules the design scenario that governs the design of a ship’s structure is a glancing blow across the bow, which has been simplified as a static

pressure patch load. This load patch is scaled as appropriate for the non-bow sections of the hull. All web frames studied in this thesis were in a non-bow location.

The IACS Polar class rules state (IACS 2011) that transverse web frames must be able to withstand the load patch determined in the Polar class rules with little other guidance. This leads many designers and classification societies to oversize the web frames using elastic design principles. In order to verify that the web frame sizing is sufficient, finite element analysis (FEA) is commonly used to check the structure. Very little guidance is given on how to develop an accurate finite element model so that a web frame design can be proven. This verification process significantly increases the amount of time a designer must spend in order to ensure their design is sound. In order to create an accurate numerical model many design details such as access openings, brackets and penetrations should be modeled, but will significantly increase the amount of time required to complete the analysis. This thesis investigates which structural design details should be included in a numerical model, in order to ensure accuracy without significantly increasing the time to model and complete the analysis.

In order to complete this scope, finite element models of different polar class ship side shell structural arrangements were created and analyzed using an explicit time-integration non-linear FEA code. The models were subjected to an overload, up to 2 times the design load, and the results were analyzed. The failure modes of the web frames as well as the

corresponding displacements and forces were extracted from the numerical models and used to develop guidelines for undertaking future, similar non-linear finite element analyses.

In short the scope of this thesis is to; develop numerical models of different polar class ship structures; investigate the different factors which influence the strength of transverse web frames; determine which design details should be modeled for future analysis, and develop appropriate guidelines for web frame design in polar class ships.

1.2 Literature Review

1.2.1 Polar Class Related Research

The topic of plastic design of transverse structures for polar class ships is a relatively new area for research. Due to this, very little literature exists to draw from. Much of the work completed in the past investigated other structure responses, such as simple frames and their failure modes, but very little related to web frames. Extensive research has been done to show that plastic three hinge collapse is an appropriate design point for polar class ships. General guidelines on how to properly develop a non-linear finite element model for ship structural analysis to verify these polar class designs has also been researched.

Much of the early work done by researchers was first centered on the development of ship rules (Daley et al. 2002; Daley 2002) around a plastic design point. As discussed above,

ship design in the past has always used an elastic design approach, specifically a Working/Allowable Stress Design (WSD) approach (FMA and SMA 2010). This caps the allowable stress in a specific structural member at a certain percentage of the yield stress. This causes structures to have a large factor of safety when loads do not exceed yield (Daley et al. 2007) but can often leave very little capacity in the plastic response region. Using a plastic design point, a new set of rules was developed that considers post yield behaviour. Although it is impossible to know a deformed shape of an entire structure, like a side shell grillage, the problem can be solved by breaking up the structure into singular frames and analyzing each one individually. This type of assumption has several advantages. One is that a singular frame will deform in a predictable way depending on the load location and type (point load, patch load, etc.) thus allowing for the structures dimension to be determined or inversely for a given structural frame the force to cause collapse can be determined (Daley et al. 2002). Another advantage is that this method does not take into account all of the different mechanisms that resist load within a structure, such as the membrane response, strain hardening, strain-rate hardening, or the interaction of neighbouring frames on the response (Daley 2002). This will give a conservative structure that is better optimized for a plastic response than traditional elastic design. Overall this will create a structure that is safe but also more cost efficient to construct.

As mentioned above a structural grillage, made up of many different frames and other structural details will have a very different response than that of a single frame. There is

currently one very idealized method for determining the collapse pressure/force for a given grillage or for determining the required frame dimensions for a given loading scenario (Daley et al. 2005). In the absence of specific rules governing the design of large transverse structural members, many researchers and designers have used non-linear finite element analysis to aid in their design or analysis. Based on the results of the analysis the designers/analysts can determine if a structure is compliant.

Det Norske Veritas (DNV) has developed guidelines for applying NFEA with regards to polar class ship design for static loads applying a statistical approach (Det Norske Veritas 2013). Others, such as Quinton et al. (2016) have also published guidelines/suggestions for completing NFEA of ship structures; but focused on moving loads. Although outside of the scope of this thesis it is important to note that many class rules use a limit state approach and a statistical approach to prescribe different loading scenarios where it must be proven that the ships structure can withstand the design load. The main limit states described in the rules are the ultimate limit state (ULS), Accidental Limit State (ALS), Fatigue Limit State (FLS) and the Serviceability Limit State (SLS) (Det Norske Veritas 2013). Each of the limit states has an associated probability and load which can be static or cyclic, depending on the limit state. By knowing these limit states the structural behaviour can be studied to determine the instabilities that will cause failure such as buckling or fatigue due to cyclic loads. The structure can then be designed to resist these instabilities.

Choice of FE code is often overlooked when completing a NFEA. The choice of whether or not to include "time" (and thus dynamics) to the simulation can have a large effect on the accuracy of the results. NFEA of ship structures may result in highly deformed structures. For implicit static codes, accuracy of the solution can require many incremental solutions before the final solution to the fully applied load is achieved. For FE codes including time, this may require that the timestep be very small in order to appropriately capture the behaviour, if the behaviour involves elastic or plastic instabilities. Small timesteps are more efficiently solved with an explicit time integration FE code; as a small timestep is already required to ensure the results will be stable (Quinton et al. 2016). An implicit code, however, has to invert large matrices at each and every time and/or load step, increasing the computational time significantly for a small time step. This becomes even more computationally expensive for moving loads. In general, it is suggested by Quinton et al. (2016) to use an explicit code for highly nonlinear cases, cases involving elastic or plastic instabilities, or moving loads (Quinton et al. 2016). The various time integration schemes are discussed further in section 1.4.1.1.

Choice of element type is an important aspect of NFEA. Depending on the type of load scenario specific elements may perform better than others. DNV (2013) outlines that in general using a higher order element (more nodes per elements) will give more accurate results, but will increase the computational time. For NFEM structural analysis it is usually advised to use shell elements with a minimum of 5 through thickness integration

points (LSTC 2017). Another important aspect of element choice is whether the elements use a full or reduced integration scheme for the in-plane integration points. For NFEM, using full integration elements can cause the elements to exhibit unnatural material behaviour such as volumetric and shear locking (LSTC 2017). These behaviours are artificial and are due to the simplifications within the element formulations. Using reduced integration elements mitigates these locking issues but enables a new issue, hourglassing (LSTC 2017). These issues are discussed in detail in Chapter 3 but in general reduced integration elements are more robust, reduce computational time and, with proper modeling techniques, the negative effects of hourglassing are less than those associated with element locking (Det Norske Veritas 2013).

The mesh size and shape is very important for NFEA. The mesh must be small enough to capture the behaviour of the structure and avoid issues like locking or hourglassing but not too small to avoid violating size restriction for shell elements (element side length cannot be less than the element thickness) (LSTC 2017) and increasing the computational time. In general, it is suggested that the mesh in areas of interest, such as the structure surrounding the load and supporting structure be finer to capture all of the important behaviour (Quinton et al 2016). It is also suggested by both DNV (2013) and Quinton et al. (2016) that a mesh convergence study be carried out to find the point where the results converge (becoming mesh independent), that all essential structural behaviours are captured and the computational time can be minimized without sacrificing accuracy (Quinton et al. 2016).

As with any FE model an appropriate material model must be used. As the IACS rules design point involves a plastic structural response (IACS 2007), a plastic material model is required. If possible material test data for the steel being used in construction would give the most accurate results. As a minimum a bilinear model is required for plastic analysis. This requires values for the yield strength, Poisson's ratio, Young's Modulus (slope of elastic portion) and the Tangent Modulus (Slope of the plastic portion) (LSTC 2017). Depending on the loading scenario (loading and unloading, static, dynamic, etc.) the material model may also require definition of a hardening term. This will give the material isotropic or kinematic material properties with regards to loading (Det Norske Veritas 2013). In certain cases, it may also be appropriate to add material imperfections or impurities to more accurately model reality. Another important time dependant material property is strain rate hardening. The yield strength of shipbuilding steels depends on how quickly it is being loaded. The faster the strain rate the higher the yield strength. If a ship will be expected to see high strain rates (such as a blast scenario in naval ships) it would be important to include strain rate hardening in the material model to ensure accuracy (Det Norske Veritas 2013).

One other aspect of a finite element model that must be considered is the boundary conditions. The choice of boundary conditions is very dependent on the loading scenario and the object being modeled. In general, it is recommended to model the boundary conditions to be as close to reality as possible (Daley et al. 2005).

1.2.2 Polar Class Transverse Structure Research

Pearson et al. (2015) of Lloyd's Register (LR) developed an acceptance criteria that a grillage must meet when being analyzed using NFEA. They assessed different overload capacities and behaviours by analyzing the characteristic stiffness curve (load deflection curve) for a grillage, well into the plastic range. They used this stiffness curve to study how a specific structural arrangement can affect both the elastic and plastic response ranges. By understanding how different design decisions affect the overall response, the structure can be better optimized to reduce the weight of the ship without sacrificing strength (Pearson et al. 2015). This is especially important for ice class vessels as it allows the designers to ensure the grillage can perform well in overload scenarios without causing an instability or rupture in the grillage. In order to better understand how the stiffness curve could be used as a criterion to determine if a design is sufficient, the authors studied several different icebreaker structural grillages and their respective stiffness curves using NFEA. For all of the structural arrangements an implicit solver capable of highly nonlinear geometry and material models was used. All models used shell elements only and included all structural components and details such as brackets and any cutouts/penetrations (Pearson et al. 2015). Due to their implicit FE code choice, they experienced convergence issues at larger loads due to stiffener buckling/instability. As Quinton et al. (2016) discussed, for large overload scenarios it is generally beneficial to use an explicit solver due to convergence issues with implicit solvers for NFEA.

In order to determine criteria for deciding if a design is structurally sound Pearson et al. (2015) used stiffness curves in conjunction with plastic strain data. Specifically, they proposed that at a plastic strain level of 2.5% on the characteristic stiffness curve must coincide with a force level of approximately 150% of the design/rule force to be considered sufficient. There are advantages and disadvantages to this method. One advantage is plastic strain is easily calculated by FE codes and simple to plot, making it attractive for designers. However, strain in a FE mesh is always a mesh dependant as it will always increase with decreasing element size in the vicinity of stress concentrations. By decreasing the mesh to ensure the correct behaviour is captured the strain may become artificially high. This is especially true around cutouts/penetrations where the load may be concentrated. Due to this issue, plastic strain is not an ideal acceptance criterion. However, in general, using a characteristic stiffness curve with some other easily determined criteria would be very useful for future rule/guideline development.

1.3 Unified Polar Class Rules

Many northern countries that share a border with the North Atlantic, Pacific or Arctic Ocean created individual sets of rules that vessels traveling through their national waters have to follow. Countries such as Canada, Russia, Finland & Sweden have a set of rules that are specific to the ice and environmental conditions that would govern design and operations in their own waters. In addition to countries having a specific set of rules, the various classification societies also have rules that govern polar class ship design. In the 2000s a major push was made to unify these rules to ensure the safety of the crew and vessels working in ice infested waters, and improve the regulatory process for ships that

routinely travel between different national waterways. This unification was partially achieved when the Polar Class Rules produced by IACS came into effect in 2007. These rules prescribe different criteria for specific structural and mechanical details for a given polar class.

Depending on the mission or operational profile of a vessel, the structure and mechanical equipment will vary greatly. Some ships simply need additional strengthening as they will only operate in first-year ice conditions such as in the Baltic Sea, while others will be performing icebreaking operations in much heavier ice conditions. Within the Polar Class Rules there exist different PC classes depending on the vessels operational profile. The Polar Class designations range from PC7 (low) to PC1 (high). Please see Figure 1-1 below which outlines the different polar classes and their respective ice operational constraints.

Polar Class	Ice Description (based on WMO Sea Ice Nomenclature)
PC 1	Year-round operation in all Polar waters
PC 2	Year-round operation in moderate multi-year ice conditions
PC 3	Year-round operation in second-year ice which may include multi-year ice inclusions.
PC 4	Year-round operation in thick first-year ice which may include old ice inclusions
PC 5	Year-round operation in medium first-year ice which may include old ice inclusions
PC 6	Summer/autumn operation in medium first-year ice which may include old ice inclusions
PC 7	Summer/autumn operation in thin first-year ice which may include old ice inclusions

Figure 1-1: Polar Class Designation (IACS 2011)

Within the IACS Polar Class rules the load is determined for two different locations, the bow area, and any other area besides the bow. For design and analysis the load is applied as a static patch load with an average pressure, P_{avg}, based on the ships PC designation and displacement. See Chapter 3.6 for the load patch size and magnitude equations. Using this average pressure the minimum structural requirements can be determined and used for the ship's design. As noted before, the current IACS Polar Class Rules do not prescribe the design of transverse web frames (i.e. large transverse members). The rules state that the web frame or structural member should be able to withstand the applied load and that an appropriate method of analysis be completed to ensure that the web frame can withstand the load (IACS 2011).

1.4 The Finite Element Method

The finite element method is a numerical tool to assist in solving complex or advanced problems that cannot be solved using an empirical or analytical solution. The numerical tool works by first discretizing the domain of interest into small elements. Each element uses simplified physics and mathematics to approximate the response of a small portion of the domain. The sum of the responses from all elements approximates the total response of the domain (Cook et al. 2002). The finite element method can be used for many different applications including both static and dynamic structural analysis.

1.4.1 Finite Element Codes

Although the finite element method is a general method for many types of analysis, different codes have been created for different applications. Depending on the load case/problem the user is trying to solve, a specific code will be able to solve the problem more accurately and with fewer resources. The biggest reason for the differences between individual FEA codes is due to the time integration scheme that code uses. The two main time integration schemes are implicit and explicit. The differences between the two time integration schemes are discussed in the next section.

1.4.1.1 Implicit vs Explicit Time Integration

As mentioned in the previous section the time integration scheme used by a specific FE code will have an impact on how efficient the code will be at solving different problems. One of the simple implicit time integration schemes is the Backwards Euler method (Cook et al. 2002). This method allows for a variable to be solved in the next time step by knowing the value of the derivative of the variable at the next time step and the value of the variable at the current time step. See the equation below for a simple representation of the backwards Euler method. In order to solve for a variable at the next time step knowledge of both the current time step and next time step is required. This means that the code must assume a value for the next time step and iterate until the solution converges to a specified tolerance.

$$X_{n+1} = (\Delta t \cdot \dot{X}_{n+1}) + X_n$$

Where X is any variable being solved for and Δt is the time step. This iteration scheme allows large time steps to be used, making implicit solvers "unconditionally stable", in

the sense that the results computed by the code will not be completely unbounded but not necessarily accurate. This makes implicit solvers more suitable for long-duration problems, where the response of the structure does not occur quickly. In order to solve the models, many iterations may be required for a single time step, to reach convergence, significantly increasing the computational time of the simulation.

If a problem is static, then there is no time dependency and the Backwards Euler Method is unnecessary. For static cases it is often the case that the load must be divided into steps to ensure that the implicit solver can reach convergence (i.e. for a solution to be found). In some cases a structural instability may occur and special solutions methods may be required to capture them (LSTC 2017).

An explicit solver uses a different method of time integration, such as the forward Euler method. For explicit solvers only values for the current time step are required to solve for the next timestep. See below for the forward Euler equation.

$$X_{n+1} = (\Delta t \cdot \dot{X}_n) + X_n$$

Where X is any variable being solved for and Δt is the time step. For explicit solvers very small timesteps are required as the time scheme will become unbounded if the timestep is too large. For explicit analysis the time step is governed by the size of the elements within the model. The largest time step in an explicit model is the amount of time it takes for a single sound wave to travel through the shortest path of the smallest element (Cook et al.

2002). See below for the maximum theoretical timestep used by explicit solvers employing the central difference time integration scheme (Cook et al. 2002). Depending on element size this can make some models very computationally expensive. The more elements a model has, the longer it will take to solve.

$$\Delta t_{max} = \frac{l_{min}}{c}$$

Where l_{min} is the shortest path through the element and c is the speed of sound in the element, which is dependent on the material associated with the element. Since time must be considered and the time step will be small, explicit solvers can handle short-duration structural response much more efficiently than implicit solvers.

The type of solver that would suit the needs of the analyst depends highly on the type of loading that will be applied. Static loading is generally better for implicit while dynamic cases are better suited for explicit solvers. For this thesis an explicit solver was used for all simulations. Due to the nonlinear behaviour expected (highly deformed structures and possible instabilities) which could cause convergence issues for an implicit solver, an explicit solver was used for this research.

1.4.2 Reasons for non-linearity

One other aspect that must be considered when selecting the type of solver to use is if the model will be linear or non-linear. There are three different factors that influence the linearity of a simulation: geometric, material and boundary condition nonlinearities. Geometric nonlinearities are related to large changes in geometry due to the applied

loads. This is due to the strain-displacement relationship of the material. At very small strains the displacement follows a linear path for most materials. As the strain increases this relationship tends to become non-linear. Material nonlinearities exist when the plastic portion of a material stress strain curve has been modeled. Boundary condition nonlinearities exist due to gaps in the mesh, contact between different parts within the model or from nodes that are tied but have certain conditions that can allow them to break.

Each source of nonlinearity can significantly increase the amount of time required to solve a simulation, depending on the severity of the nonlinearity. A material that exhibits highly nonlinear behaviour with strain rate effects can take significantly longer to solve than an elastic material model. The larger the change in geometry the more computationally expensive a simulation will become, especially for implicit solvers due to a significant increase in the number of iterations within time steps or load steps required to capture the behaviour and reach convergence. When there is contact between different elements within a model the code must first be able to detect and recognize that there is contact, artificially create an interface force to stop the contact while also calculating contact forces which may become computational expensive. Different types of contact also exist, such as edge to edge, surface to surface, surface to edge, etc. which can have different computational costs.

Chapter 2 Methodology

2.1 Initial Model Development

Different structures react very differently to applied loads based on their size and spacing. In order to understand transverse web frame response in Polar Class ships it was decided to create two initial models of different structures. One model was a PC7 class design (low ice class) and the other a PC3 design (high ice class). This allowed for experience to be gained in modelling and analyzing structures, along with determining which design details should be incorporated to ensure the models are accurate. As these structures will differ greatly in size and arrangement their responses will be different. These models were then analyzed using NFEA. Initial results were used to lead further research and develop specific response criteria to determine when a web frame design is suitable. The structural arrangements for both PC7 and PC3 model were developed using the IACS (2011) rules and industry experience. See sections 3.1.1 and 3.1.2 for the PC3 and PC7 models respectively.

The various components of the numerical models used in this thesis can be found in section 3.2 through 3.8. The boundary conditions were set as fully fixed along all model boundaries. The structure at the boundaries was assumed to be very large and stiff in comparison (bulkheads, main decks, etc.). To ensure the boundary conditions did not influence the results the model was made very large to ensure no plasticity would occur at the boundaries. The applied load patch size and magnitude was determined using the

IACS rules (2011) and applied to the center of the model. Specifically the load was applied as a uniform patch load to the outer shell, centered vertically and horizontally to the center of the model. The middle of the load patch lined up with the central web frame in both polar class models. By centering the load over the web frame the largest stresses and deflections will occur in the web frame, while also allowing the surrounding structure to influence the response. This allowed for the grillage to be studied together with an investigation of how the different design factors influence the response. This was especially true when investigating the influence of design details (penetrations, cutouts, lugs) and their influence on the web frames response.

2.2 Initial DOE Study

From the initial PC7 and PC3 results a DOE experiment was setup and run. This experiment studied the factors determined during initial model development stage (structural sizing and spacing, cutout sizing) and specific responses to better understand how the factors influence the responses. This also allowed for an opportunity to develop numerical equations that could possibly be used to govern transverse web frame design. A uniform design was used for the DOE experiment. This type of experimental design is appropriate for numerical simulations as it can fill the design space in cases where there is no random or experimental error. Eight factors, each with three levels (low, medium, high) were studied. The responses studied were the force to cause in-plane plasticity, force to cause an out of plane instability and the force to cause a plastic strain of 2.5%. See section 3.9 for more details regarding the DOE study.

2.3 Web Frame Stiffening Using DOE Models

After investigating the DOE models in Section 2.2 and finding the lowest capacity structure, different stiffening arrangements, applied directly to the web frame, were developed and studied. These web frame stiffening arrangements were determined using results from the initial models in Section 2.1 and 2.2, along with industry experience and previous icebreaking designs. These arrangements ranged in size from small structural details located in the penetrations or cutouts to full span and depth flat bar stiffening arrangements. In total 7 different arrangements were studied. For each of these arrangements, the responses developed in the initial model development and DOE experiment were used to evaluate which arrangements increased the web frames capacity. See section 4.2 for details on the various web frame stiffening arrangements and their influence on the in and out of plane characteristic response curves.

2.4 Web Frame Stiffening For PC7

Although the numerical results from the DOE web frame stiffening arrangement study showed several trends the DOE structure itself is not a "real" structure. That is to say that an actual ship would never have the structural sizing and spacing as in the DOE model. The results from the web frame stiffening study using the DOE structure were applied to the PC7 structure. Three different web frame stiffening arrangements were studied using the PC7 structure. The responses were analyzed and compared. See section 4.3 for more details regarding the web frame stiffening arrangements and their influence on the various responses for a "real" polar class structure.

Chapter 3 Numerical Model

3.1 Geometric Model

In order to perform an FE analysis an initial geometry must be created. The geometry can be made up of many different parts/components that can be connected or independent of other parts/components. The geometry can be made up of points (0 dimensional), lines (1 dimensional), planes (2 dimensional) or solid bodies (3 dimensional). The geometry is then discretized into many small elements that create the mesh. For the numerical models below, all components have been modeled as 2 dimensional bodies, also referred to as shells. This is a common practice for marine and ship applications as the computational power required to perform the calculations is reduced when compared to modelling components with solid elements; without reducing the accuracy of the results. These different parts are represented by *PART cards within LS-DYNA. This allows for the parts to have different element and material properties assigned to them through the use of *SECTION and *MAT cards within LS-DYNA respectively.

For all of the geometric models outlined below it is important to note the presence of different cutouts through the web frames. The cutout, also referred to as a penetration, on the left of the figure allows the longitudinals to span the whole length of the model. The access hole cut towards the centre of the web frames to allow crew access in between frames. These design details take a significant amount of time to model and have a major

impact on the response of the structure. Please see Figure 3-1 below outlining the different types of cutouts in the web frames for both structures.

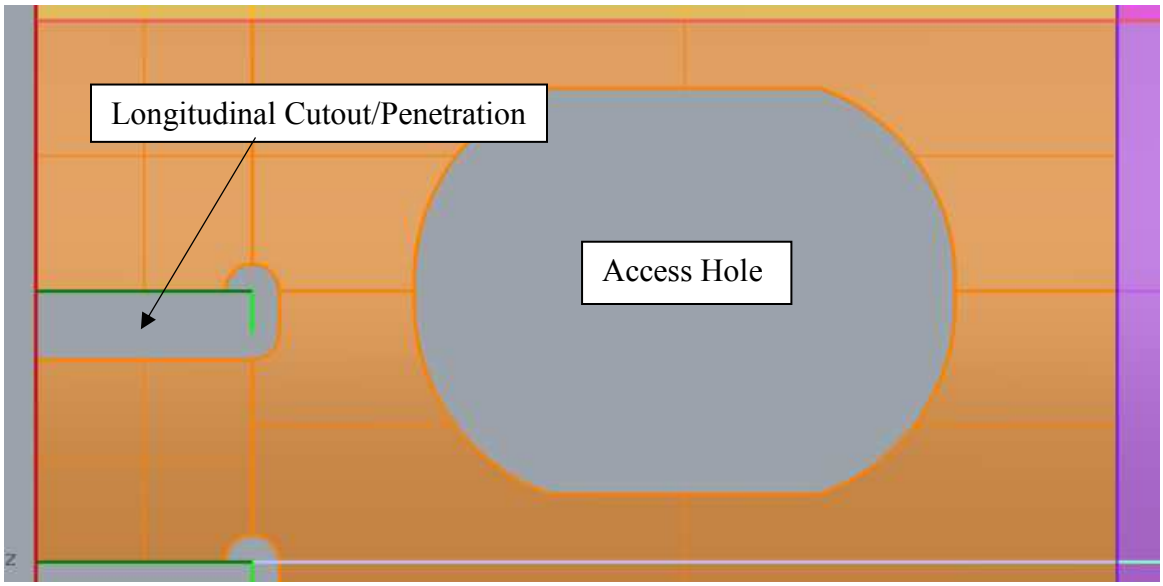

Figure 3-1 Schematic View of Cutouts through Web Frames

3.1.1 PC3 Structural Arrangement

Several geometric models were created to study how different design factors influence the response of the transverse structure. One of the models created was that of a PC3 icebreaking side shell structure. The structural arrangement and sizing was created based upon the polar class rules. This model consists of three web frames (spaced 1.5m apart) of the side shell, at the ships waterline. Along the outer and inner shell there are longitudinal stringers along the length of the entire model.

The model consists of 14 separate parts. The parts, a short description and their dimensions are outlined in Table 3-1 and Figure 3-2 below. Note that all of the parts in

the initial geometry have been modeled as shells for two reasons; shell elements are relatively easy to use (compared with solid elements) and are very computational efficient.

Table 3-1 PC3 Part Description and Sizing

Part Number	Description	Dimensions (L x W x t)
1	Inner Shell Long. Web	6000mm x 120mm x 7mm
2	Outer Shell Long. Web	6000mm x 240mm x 12mm
3	Inner Shell	6000mm x 6200mm x 9mm
4	Inner BHD	6000mm x 6200mm x 20mm
5	Outer Shell	6000mm x 6200mm x 20mm
6	Outer Shell Long. Flange	6000mm x 46mm x 25mm
7	Inner Shell Long. Flange	6000mm x 24mm x 12.35mm
8	Outer Lower Web Frame	2400mm x 1200mm x 12mm
9	Inner Lower Web Frame	2400mm x 500mm x 12mm
10	Flat Bar Transverse Stiffener	960mm x 100mm x 10mm
11	Lower Decks (2 Total)	1 - 6000mm x 1200mm x 8mm 2 – 6000mm x 1700mm x 8mm
12	Top Deck	6000mm x 1200mm x 8mm
13	Inner Upper Web Frame	3800mm x 500mm x 12mm
14	Outer Upper Web Frame	3800mm x 1200mm x 12mm

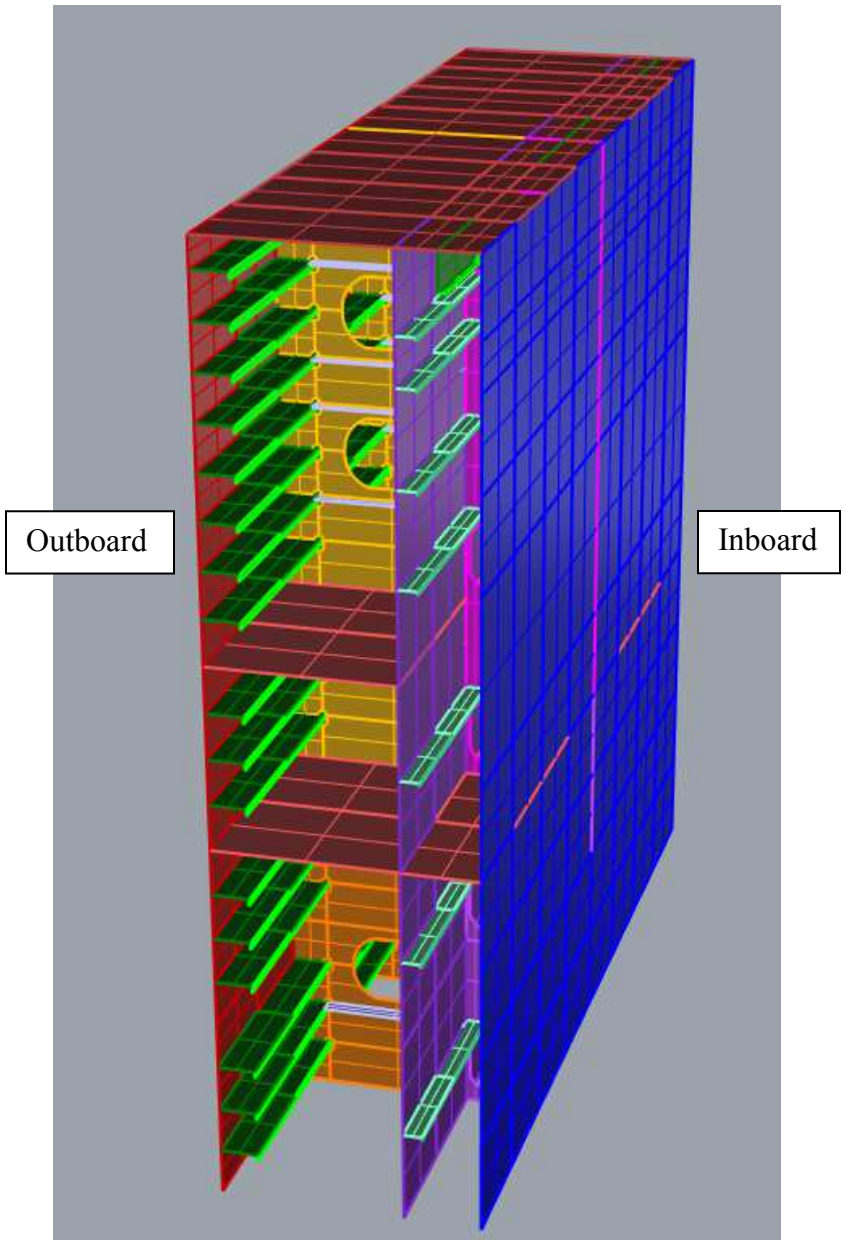

Figure 3-2 PC3 Icebreaking Side Shell Structure

3.1.2 PC7 Structural Arrangement

The PC7 structure used for this research was based on an offshore supply vessel that would encounter only very light ice conditions. As such the structural scantlings are much lighter than that of the PC3 model. The structural arrangement and sizing was created

based upon the polar class rules. As before the model consist of three web frames (1.5m apart) around the waterline of the supply vessel. There are longitudinal members along the inner and outer shell that are the same size. The model consists of 7 individual parts. The parts, a short description and their dimensions are outlined in Table 3-2 and Figure 3-3 below. Note that all of the parts in the initial geometry have been modeled as shells similar to the PC3 model. For a sample k-file, the file format used as the input file for an LS-DYNA simulation, please see Appendix A.

Table 3-2 PC7 Structure Description and Sizing

Part Number	**Description**	**Dimensions (L x W x t)**
1	Shell Long. Web	6000mm x 200mm x 10mm
2	Shell Long. Flange	6000mm x 25mm x 22.58mm
3	Inner Shell	6000mm x 4950mm x 10mm
4	Flat bar Stiffener	6000mm x 100mm x 8mm
5	Outer Shell	6000mm x 4950mm x 12mm
6	Decks	6000mm x 1000mm x 10mm
7	Web Frame	4950mm x 1000mm x 8mm

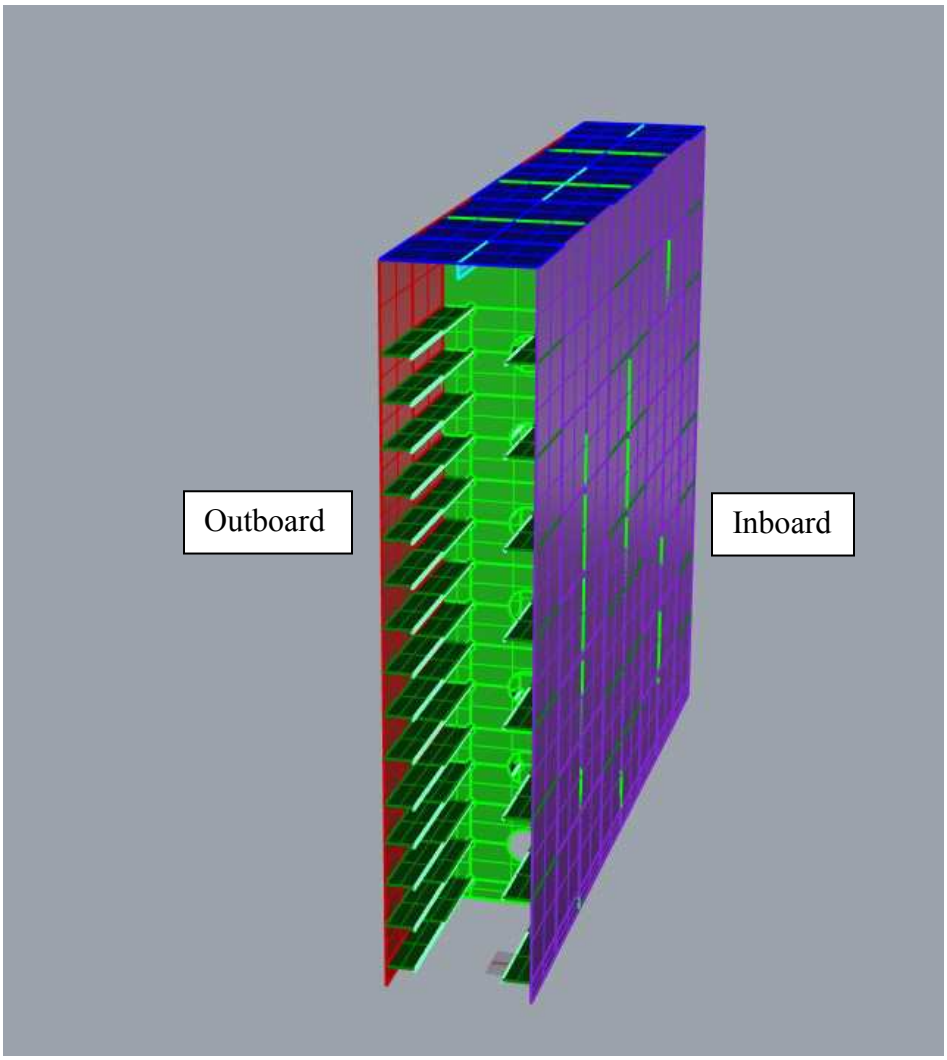

Figure 3-3 PC7 OSV Side Shell Structure

3.2 Element Type and Formulation

As mentioned above all components of the structural arrangements were modeled using shell elements. In general shell elements are very useful for modelling geometries where one dimension is significantly smaller than the other two dimensions. This becomes extremely useful when modelling steel plates on a ship. Generally the plates are much longer and wider than they are thick, making them prime candidates for being modeled

with shell elements. At higher load levels, large deformations within the web frame are expected. With large deformation in mind, it is more beneficial to use reduced integration elements over fully integrated elements. At higher deformations shear locking and volumetric locking may become an issue due to the elements inability to deform properly from bending stresses. For fully integrated elements this becomes a major issue. In order to counteract the locking issues a reduced integration element can be used. This reduces the number of in-plane integration points used by the element, thereby reducing the number of "constraints" that cause the element to lock; however this creates a new issue, hourglassing, which will be discussed further down in section 3.3.2.

Separate from the integration points discussed above, is the number of through thickness integration points for shell elements. This is due to the parameterization of one or more dimensions (i.e. thickness for shell elements) to allow for specific assumptions to be true. In a real structure, the strains/stresses would change through the thickness, but due to the parameterization of the thickness for shell elements, it becomes zero. In order to determine the bending stresses of shell elements, integration points are introduced through the thickness. For shell elements it is suggested (LSTC 2017) to use five through thickness integration points for each shell element; this was done for all elements used in this research.

As it was decided that a reduced integration element would be most beneficial, several formulation options were available. Two of the popular shell element formulations for non-linear FE analysis are the Hughes-Liu (H-L) and Belytscho-Tsay (B-T) element formulations (LSTC 2017). The H-L element formulation is good for non-linear analysis and large elemental deformations. It also takes into consideration warping of elements and an optional hourglassing control. It is computationally efficient but more expensive than the B-T element formulation. The B-T formulation is also used for non-linear analysis but the formulation is better suited for small elemental deformations. It also does not directly address warping or hourglassing; but both of these options can be enabled by the user. For this analysis H-L shell elements were used due to their robustness, even though they come at a greater computational cost. The elements used in this research are first order elements, meaning that nodes only exist at the corners of an element. Since there are only straight lines connecting between the nodes, which must remain straight during loading (the nodes can move but the lines connecting nodes must stay linear) first order elements cannot take on curved shapes. For explicit FE codes, the computational cost is generally higher for higher-order elements, than it is for using more, smaller elements to achieve appropriate deformed shapes.

A shear correction factor was employed for all shell elements used for this research. This is required due to the assumption that the shear through the thickness of an element is linear, when in reality it is quadratic. The shear calculation is made accurate by including a correction factor for second order effects. Depending on the cross-sectional shape of an

element a different shear factor should be applied. For shell elements with rectangular cross-section, a correction factor of 5/6 (0.8333333) (LSTC 2017) should be used and was applied to all shell elements used for this research.

3.3 Mesh Convergence Analysis

With any FE analysis a mesh convergence study must be carried out. This process involves changing the size of the elements within a numerical model from large (coarse) to small (fine) and comparing the results from these analyses until the results converge to a certain value. This must be completed for any change in geometry or load. In general the smaller the mesh, the more accurate the results and the closer to reality the numerical model is. This is however computational inefficient. As the mesh becomes smaller, the number of elements increases significantly, which in turn increases the amount of computational time. By finding the point where the size of the mesh no longer has an effect on the accuracy of the results, the most efficient computational time is identified. It is also important to ensure that the mesh is fine enough to capture the expected behaviour of the structure being analyzed. If the mesh is too coarse the mesh will not be able to take on certain shapes. This is especially important when large strains/deformations are expected, such as elastic and plastic buckling, or when membrane behaviour in thin plates dominates (Quinton et al. 2016).

It is important to note that not all of the output variables from the FE analysis can be used for a mesh convergence analysis. Stress and strain should not be used as the convergence

criteria when conducting a mesh convergence analysis, if there are any geometric discontinuities in the mesh. This is due to the way that stress and strain is calculated through an element. As the mesh is made smaller the strain through an element will increase, except for the case where there are no stress risers. Since stress and strain are mesh dependant it should not be used for mesh convergence. Many other variables can be used such as the in or out of plane displacement.

3.3.1 Element Size

For all of the different geometric models used in this research a mesh convergence analysis was completed. If any changes were made to the geometry or the load was modified, a new convergence analysis was completed. In all cases the resultant displacement of the web frames was used to determine when the mesh had converged. If the resultant displacement changed less than 5%, the mesh was considered converged. For the PC3 mesh, further mesh reduction was done due to larger than expected hourglassing energy in the highly deformed areas around the longitudinal cutouts/penetrations. The PC7 model had an element edge length of 30mm while the PC3 model had an element edge length of 25mm. In some models the mesh directly around a cutout was reduced in size to more accurately model the deformed shape at higher load levels. This led to approximate model sizes between 150 000 – 250 000 elements per model.

3.3.2 Hourglassing

As mentioned above the use of reduced integration elements gives rise to the potential for hourglassing within the mesh. Hourglassing leads to energy losses due to unconstrained spurious vibrations of the hourglassing elements. When hourglassing occurs it allows the

effected elements to change shape regardless of the loading, using energy that would normally be used to resist loads or moments. If hourglassing is an issue the mesh can be refined or the hourglassing controls can be refined to counteract these issues. Generally an hourglassing energy of 5% or less of the internal energy is deemed appropriate for FE analysis. If the mesh can no longer be refined due to element size restrictions, hourglass controls for specific element formulations may be used which introduce an extra stiffness to an element to help resist hourglassing. For the numerical models presented in this thesis hourglassing became an issue for higher load levels in the PC3 model. The hourglassing energy approached 10% of the total energy for a mesh with an element edge length of 30 mm. To reduce the hourglassing within the models the mesh was reduced in size to 25mm. This reduced the hourglassing energy to 3.1% of the total energy of the system.

3.4 Boundary Conditions

In order to perform an FE analysis the model must have some form of boundary conditions so the model does not arbitrarily travel through space in responses to an applied load. Boundary condition are applied to nodes within a numerical model, which can limit or allow motion in the six DOF (degrees of freedom) (Dx, Dy, Dz, Rx, Ry, Rz) where D stands for displacement in the direction of an axis denoted by the lower case adjacent consonant, and R stands for rotation about the axis. Special care must be taken when performing an FE analysis to ensure that the boundary conditions closely model those of reality and that they will not negatively affect the results. All of the numerical models created for this research had the same boundary conditions. All free edge nodes at

the terminating ends of the mesh along the sides, top and bottom of the models were fixed in all degrees of freedom. All interior nodes within the mesh had no boundary conditions applied to them. During the initial model development stage, the model extent was increased to ensure that having fixed edge boundary conditions would not cause any plastic strain at the boundaries. If plastic strain is present in the elements on the edge of the model the boundary conditions are not valid. For all simulations there was no plastic strain in any of the boundary elements. The boundary conditions were applied through the *BOUNBDARY_SPC_NODE_SET card within LS-DYNA. This card first created a *SET_NODE card of all the outer free nodes and then applied the *BOUNDARY_SPC card to create the displacement and rotation restrictions mentioned above. This process was used for all numerical models created for this research. Please see Figure 3-4 which shows the boundary conditions applied to the PC3 numerical model. Note that all of the white markers along the boundary of the mesh are the nodes with boundary conditions.

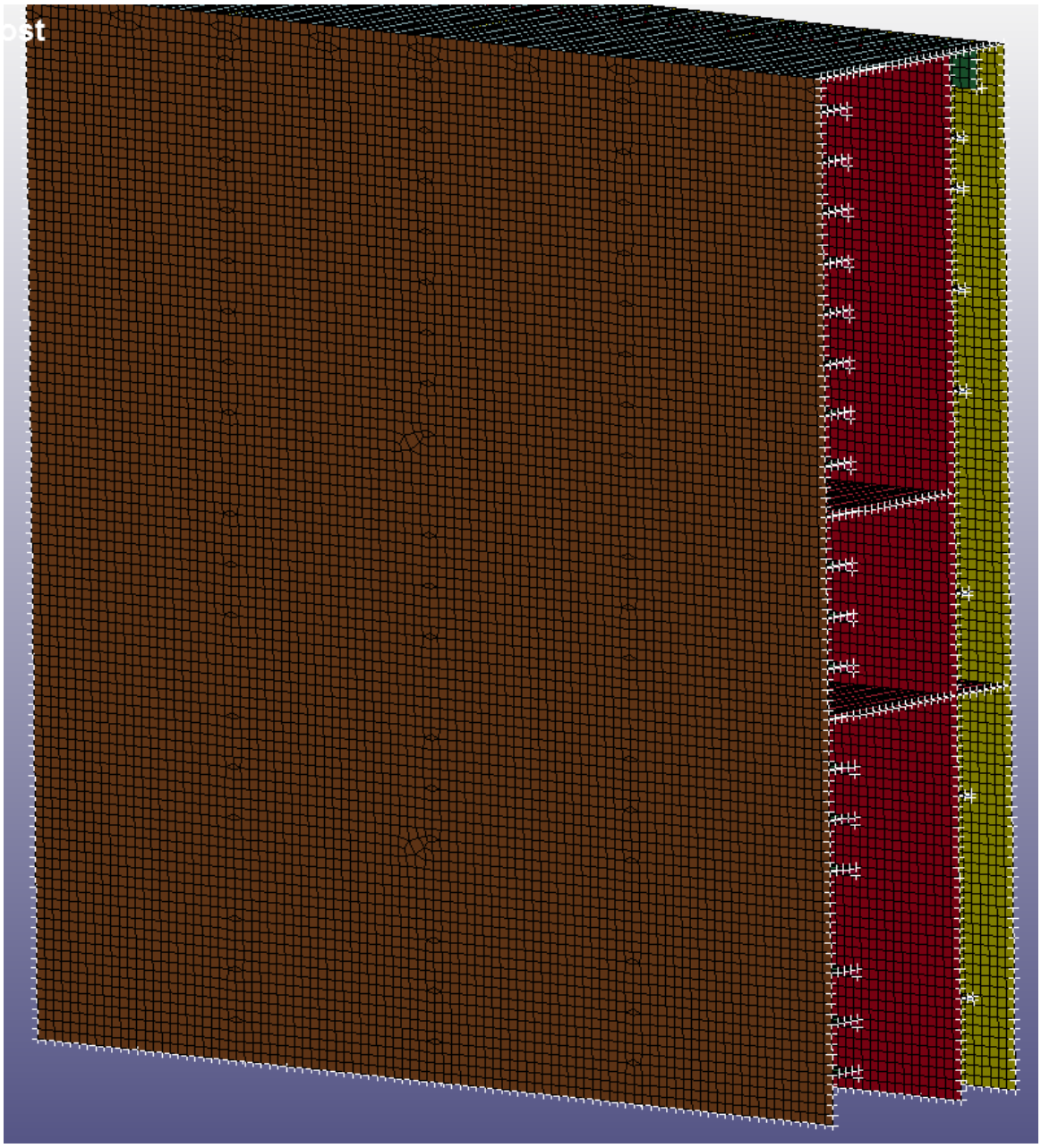

Figure 3-4 Boundary Conditions for PC3 Model, Fixed in all DOF

3.5 Material Model

A material model is required to solve any finite element model. Depending on the type of analysis, different material models can be used. As this research was focused on the overload capacity, which falls into the plastic range for ship structures, an elastic-plastic material model was used. Note that no actual material test data was available. As such a bilinear material model using standard ice class steel properties was used for all of the simulations. Specifically material model

*MAT_024_PIECEWISE_LINEAR_PLASTICITY was employed. This material model has the capability to have a true material stress strain curve (from a material test) that includes plasticity, strain rate effects, and isotropic or kinematic hardening. The values for the different material properties can be found in Table 3-3 below.

Table 3-3 Bilinear Material Model Properties

Mass Density (kg/m^3)	7850
Yield Stress (MPa)	350
Young's Modulus (GPa)	200
Poisson's Ratio	0.3
Tangent Modulus (GPa)	1
Failure Strain	N/A

The yield stress is the stress when the material transitions from a linear elastic response to a plastic response. The Young's Modulus is the slope of the elastic portion of the material curve. As this model is bilinear the plastic portion is represented by a linear line with a

slope equal to the tangent modulus that starts at a stress equal to the yield stress and a strain of the yield stress divided by the Young's Modulus. As no failure strain was included in the model there is no cap on how high the stress or strain can go within the model. This requires good judgement and engineering knowledge from the user to know when a stress or strain is abnormally high and not achievable in reality.

3.6 Load

For polar class ships the design load is prescribed in the IACS rules based on the location along the hull, the ships principal particulars, and the specific polar class. As this thesis only focused on midbody design, this section will only discuss the calculated loads for a midbody side shell section for a polar class ship. To determine a design load for any polar class ship midbody section, the following equation is used:

$$F_{nonbow} = 0.36 * CF_c * DF$$

Where CF_c = the crushing force class factor based upon the ice class
DF = ship displacement factor
= $D^{0.64}$ if D ≤C F_{dis}
= $CF_{dis}^{0.64}$ + 0.1*(D-CF_{dis})
D = ship displacement in kilotonnes and not taken less than 10kt
CF_{dis}= Displacement class factor based upon the ice class

From this initial design load calculation a design line load can be calculated using the follow equation:

$$Q_{nonbow} = 0.639 * F_{nonbow}^{0.61} * CF_D$$

Where CF_D = load patch dimensions class factor based upon the ice class

After determining the design load, the load patch dimensions (the width, w_{nonbow} and height, b_{nonbow}) can be determined from the following equations:

$$w_{nonbow} = \frac{F_{nonbow}}{Q_{nonbow}}$$

$$b_{nonbow} = \frac{w_{nonbow}}{3.6}$$

As the load is applied as a uniform pressure patch, as prescribed in the IACS Polar Class rules (IACS 2011), finally the average pressure must be calculated. The average pressure is calculated using the equation below.

$$P_{avg} = \frac{F_{nonbow}}{(b_{nonbow} * w_{nonbow})}$$

After calculating the average pressure a hull area factor must be applied, depending on the polar class of the ship and the location for the load. This factor has to do with the expected loading for that particular part of a ship in ice conditions. This hull area factor is multiplied by the design load to obtain the design force, average pressure and patch dimensions that must be applied to a model during the design stage to verify the structures capabilities. See Table 3-4 and Table 3-5 for the class factors and hull area factors discussed in the equations above.

Table 3-4 Class Factors (IACS 2011)

Polar Class	Crushing Failure Class Factor (CF_C)	Flexural Failure Class Factor (CF_F)	Load Patch Dimensions Class Factor (CF_D)	Displacement Class Factor (CF_{DIS})	Longitudinal Strength Class Factor (CF_L)
PC1	17.69	68.60	2.01	250	7.46
PC2	9.89	46.80	1.75	210	5.46
PC3	6.06	21.17	1.53	180	4.17
PC4	4.50	13.48	1.42	130	3.15
PC5	3.10	9.00	1.31	70	2.50
PC6	2.40	5.49	1.17	40	2.37
PC7	1.80	4.06	1.11	22	1.81

Table 3-5 Hull Area Factors (IACS 2011)

Hull Area		Area	Polar Class						
			PC1	PC2	PC3	PC4	PC5	PC6	PC7
Bow (B)	All	B	1.00	1.00	1.00	1.00	1.00	1.00	1.00
Bow Intermediate (BI)	Icebelt	BI_I	0.90	0.85	0.85	0.80	0.80	1.00*	1.00*
	Lower	BI_I	0.70	0.65	0.65	0.60	0.55	0.55	0.50
	Bottom	BI_b	0.55	0.50	0.45	0.40	0.35	0.30	0.25
Midbody (M)	Icebelt	M_I	0.70	0.65	0.55	0.55	0.50	0.45	0.45
	Lower	M_I	0.50	0.45	0.40	0.35	0.30	0.25	0.25
	Bottom	M_b	0.30	0.30	0.25	**	**	**	**
Stern (S)	Icebelt	S_I	0.75	0.70	0.65	0.60	0.50	0.40	0.35
	Lower	S_I	0.45	0.40	0.35	0.30	0.25	0.25	0.25
	Bottom	S_b	0.35	0.30	0.30	0.25	0.15	**	**

** Indicates that strengthening for ice loads is not necessary.

The design load for the PC3 model had a load patch with dimensions of 2.46m wide x 0.68m high, with a uniform pressure of 5.65 MPa over the design load patch, which corresponds to a total load of 9.52 MN. The design load for the PC7 model had a load patch with dimensions of 1.54m wide x 0.43m high, with a uniform pressure of 4.24 MPa over the design load patch, which corresponds to a total load of 1.27MN.

The load was applied in the center of the model directly over the central web frame as well as being applied at the ships design waterline. The load is applied to the outer shell

of the hull only. In this analysis the load was applied as a uniform pressure over the shell elements in the patch load, always directed opposite to the elements normal direction. This was done using the *LOAD_SHELL_SET card in LS-DYNA. This load card first creates a set of elements selected by the user and then applies a uniform pressure to all the elements within the set. The rate and magnitude of the load is set by the user using the *DEFINE_CURVE card. This card creates a curve which can be linear, cyclical, transient, etc. which can describe the load over the length of time of the simulation. Please see Figure 3-5 below outlining the location of the load patch for the PC3 model. The load patch for the PC7 model is located similarly to the PC3 model, directly centered over the central web frame and half way between the bottom and top of the model. In both structural arrangements the load patch is also centered on a longitudinal as seen in the figure below. Note that the structure in the figure is on a slight angle instead of directly perpendicular to the web frame to allow the reader to better visualize the load in relation to the internal structure.

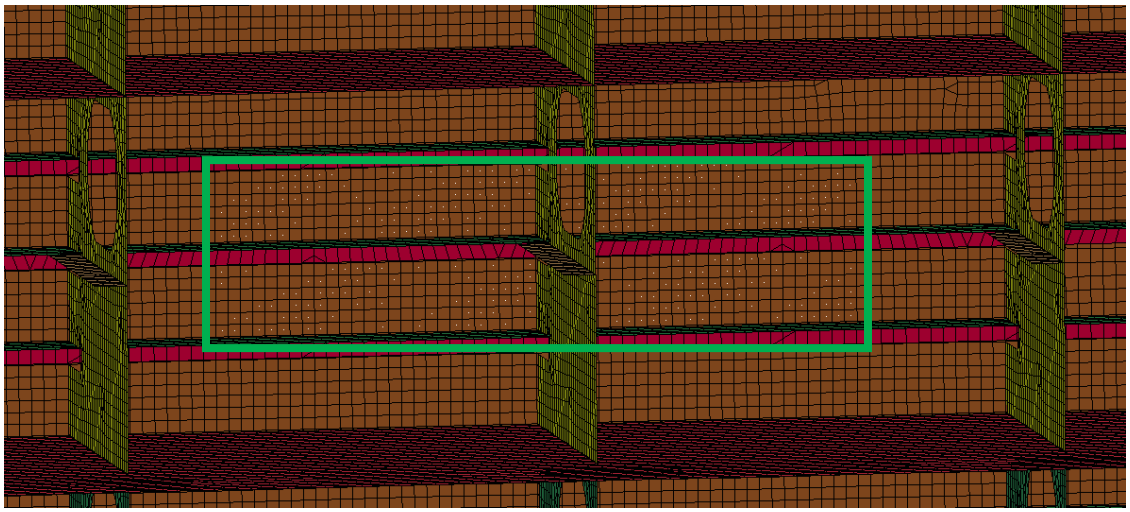

Figure 3-5 PC3 Load Patch Location

In this analysis two different load levels were used, the initial design load found above using the IACS rules, and 1.5 times the design load. For each of these load levels a mesh convergence analysis was done. For this analysis strain rate effects were not considered. As such the uniform pressure was applied by linearly increasing the pressure from 0 at time 0s to full pressure at time 1s. The total model simulation time was 1s for all of the different runs.

3.7 Contact

Due to the large overload being placed on the structures, large deformations form in the outer shell, shell longitudinals and the web frames. Due to these large deformations some of the structure underneath the load patch comes in contact with different parts. This involves special consideration to ensure that the contact is captured to obtain an accurate solution. There are several different types of contact. Contact can be a node from one element passing through another elements edge or through a segment of that element. Contact can also occur as an element edge passes through another element's edge or through a segment. Depending on the mesh and part alignment, one or both of these types of contact may occur. It is also possible for a single part to contact itself. Depending on the type of contact, different methods can be employed to capture the contact.

This research used the penalty contact method. This method involves an algorithm that checks to see if a node or edge from one element has entered through another elements edge or segment for each time step. If the algorithm does find one of the scenarios

mentioned above it adds a force to the invading node or edge to push it out of the element edge or segment it has invaded. The amount of force is calculated using material properties of the two elements involved.

3.8 Solution Controls

In order for a simulation to give accurate results special care must be taken by the user to ensure proper solution controls have been applied. This includes setting the simulation time, resolution and type of data outputs, and specific controls like added stiffness to combat hourglassing. For the research described in this thesis many different controls were added and are described in this section below.

The first solution control added to the simulation was a termination time. This was done in LS-DYNA through a *CONTROL_TERMINATION card. As discussed in a previous section all simulations ran for 1 second of simulation time. At this rate of loading no significant dynamic effects are present. In order to capture hourglassing energy in the total energy of the system a *CONTROL_ENERGY card was applied, as hourglassing energy is not part of the standard energy balance calculation. The hourglassing energy can then be checked and used to ensure that it has not significantly impacted the results.

A major part of any FE analysis is checking the results from the simulation are valid. This is done in LS-DYNA by activating different database cards which inform the solver to output the requested data into different files, depending on the type of data, user input and

processer type being used. The main output file for an LS-DYNA simulation is the d3plot binary file. These binary files are very large and have a large amount of element and nodal data including stresses, strains and deformations. These binary files also contain a render of the structure at specific time steps set by the user. As these files are very large, the resolution is generally poor. For an entire simulation it is generally suggested to have between 40 and 50 d3plot binary files. All of the simulations done for this thesis had 50 d3plot binary files with a frequency of 0.02s between writing of d3plot files. The card *DATABASE_BINARY_D3PLOT is used to inform the solver to output d3plot files based on the users input.

For higher resolution data the different ASCII database files in LS-DYNA are used. These types of simple text files are very small in comparison to the binary d3plot files discussed above. There are many different ASCII databases but only those selected by the user are output at a user defined frequency. For the simulations done for this thesis the following ASCII databases were output at a frequency of 0.0001s: *DATABASE_ASCII_ELOUT was used to collect higher resolution data for specified elements, specifically element strains and deformations. *DATABASE_ASCII_GLSTAT for looking at global model statistical properties like energy balances which can be used for model checking. *DATABASE_ASCII_MATSUM to look at material properties over the simulation which again is generally used for model checking purposes. *DATABASE_ASCII_NCFORC to measure the contact forces between different nodes. This is especially useful for crash analysis commonly used in the automotive industry.

*DATABASE_ASCII_NODOUT to output nodal data such as forces, displacements, velocity and accelerations. *DATABASE_ASCII_SLEOUT to measure the sliding or frictional forces between different elements, and finally *DATABASE_ASCII_SPCFORC which measures the reaction forces at the boundary nodes. This card is especially useful as it can quickly show if there are contact issues, and can be used to plot different values against forces such as the characteristic force displacement curves mentioned in the introduction section.

3.9 DOE Project

In order to investigate some of the specific effects of several design factors on the response of the web frames a numerical experiment was designed and undertaken using the Design of Experiments (DOE) statistical approach. This approach allows for a reduced number of experiments to be run while having the ability to study each individual factor's effect on a given response as well as the interaction effects between factors and their effect on a given response. This approach also allows for mathematical/regression equations for each response to be made using the statistically significant factors based on a user defined level of confidence. For this research, a uniform design was used. This type of DOE design has specific points that must be met within the design space (specific levels/values for specific combination of factors) which allows it to be used for experiments when there is no random error term, making it a very useful tool for a numerical simulation experiment. The different factors studied and the level associated with each factor can be found in Table 3-6 below.

The levels for each factor were based on industry experience or a range determined from various rules such as IACS (2011) or the Finish and Swedish Maritime Association (2010). These ranges also allowed for the DOE experiment to range across multiple polar classes. The premise of this was that multiple polar classes could be studied at the same time. If time were available separate studies for each polar class would be conducted instead of one overarching study.

Table 3-6 DOE Factors and Levels

Factor	Level 1	Level 2	Level 3
Shell Thickness (mm)	15	25	35
Web Thickness (mm)	9	12	15
Web Depth (mm)	1000	1800	2600
Cutout Width as a % of Depth	30%	40%	50%
Span (mm)	1200	2400	3600
Deck Thickness (mm)	10	15	20
Shell Longitudinal Height (mm)	200	300	400
Shell Longitudinal Thickness (mm)	12	16	20

The responses being studied for this DOE analysis are the force to cause first yield/force to cause plastic deformation in the plane of the web frame, the force to cause an out of plane instability/buckle in the web frame and the force to cause 2.5% plastic strain. In order to have a high level of confidence in the results from the experiment a 51 run uniform design was used. Please see Table 3-7 below outlining the different factors and their values for each of the 51 runs.

Table 3-7 Specific DOE Factors and Levels for each Run

Run	Shell Thickness (mm)	Web Thickness (mm)	Web Depth (mm)	Cutout Width (mm)	Span (mm)	Deck Thickness (mm)	Shell Longitudinal Height (mm)	Shell Longitudinal thickness (mm)
1	15	9	1800	540	3600	10	400	12
2	35	15	1800	900	1200	10	400	16
3	15	15	1000	400	3600	20	200	20
4	25	15	1000	500	2400	15	400	20
5	25	12	2600	1300	3600	10	400	20
6	15	9	1000	400	2400	20	300	12
7	15	9	2600	1040	1200	20	400	16
8	35	12	1000	500	3600	20	300	20
9	35	12	2600	780	2400	10	400	12
10	25	12	1000	300	3600	10	200	16
11	35	9	1000	400	2400	10	400	20
12	35	12	1800	720	1200	20	300	12
13	35	15	1800	540	2400	20	200	16
14	35	15	2600	780	1200	15	200	20
15	35	12	1000	300	1200	15	400	16
16	25	12	1800	720	2400	15	300	16
17	15	12	1800	540	1200	15	200	12
18	25	15	2600	1040	3600	15	300	12
19	35	9	1800	900	2400	20	300	16
20	25	15	1000	300	1200	20	400	12
21	35	15	1800	540	3600	10	300	20
22	15	12	1000	500	1200	20	200	16
23	35	9	2600	1300	1200	15	400	12
24	25	15	1800	720	2400	15	300	16
25	35	15	1000	500	2400	10	200	12
26	25	15	2600	1300	1200	20	300	20
27	25	12	2600	1300	3600	20	200	12
28	15	15	1000	300	2400	10	300	16
29	15	15	1800	900	3600	15	200	16
30	15	9	2600	1300	2400	10	200	20
31	35	9	1800	720	1200	20	200	20
32	35	12	2600	1040	2400	15	300	20
33	25	9	1000	500	1200	10	300	12
34	25	9	1800	540	3600	20	400	20
35	15	12	1800	900	3600	10	300	12

Run	Shell Thickness (mm)	Web Thickness (mm)	Web Depth (mm)	Cutout Width (mm)	Span (mm)	Deck Thickness (mm)	Shell Longitudinal Height (mm)	Shell Longitudinal thickness (mm)
36	35	15	2600	1040	3600	20	400	16
37	15	15	2600	1040	1200	10	200	12
38	25	9	2600	780	2400	20	200	12
39	25	12	1000	400	1200	10	200	20
40	15	15	1800	900	2400	20	400	12
41	15	12	2600	780	3600	20	300	16
42	15	9	1000	300	1200	15	300	20
43	25	9	2600	780	1200	10	300	16
44	15	9	1000	500	3600	15	400	16
45	25	12	1000	400	3600	15	400	12
46	25	9	1800	900	2400	15	200	20
47	25	12	1800	720	2400	15	300	16
48	15	15	2600	780	2400	15	400	20
49	15	12	1800	720	1200	10	400	20
50	35	9	2600	1040	3600	10	200	16
51	35	9	1000	300	3600	15	200	12

Each of the numerical models created for the DOE experiment had their geometric models, consisting of 4 parts, created in the 3D modelling software Rhinoceros®. These models were then exported to LS-PREPOST where the remaining components of the model were created. Each of the components mentioned in the previous sections in Chapter 2 were added to each numerical model in the DOE analysis with one major difference; the applied load was set at 10 MN for every run. Since the DOE analysis requires a large range of structural sizes a “design load” could not be explicitly calculated, as a unique Polar Class could not be established due to time constraints. The load patch dimensions were also held constant for each run with a size of 2.4m wide by 0.6m high. The load was applied to the outer shell centered on the middle web frame as

well as being centered vertically between the top and bottom of the model. Please see Figure 3-6 and Figure 3-7 below showing the load patch location on the outer shell.

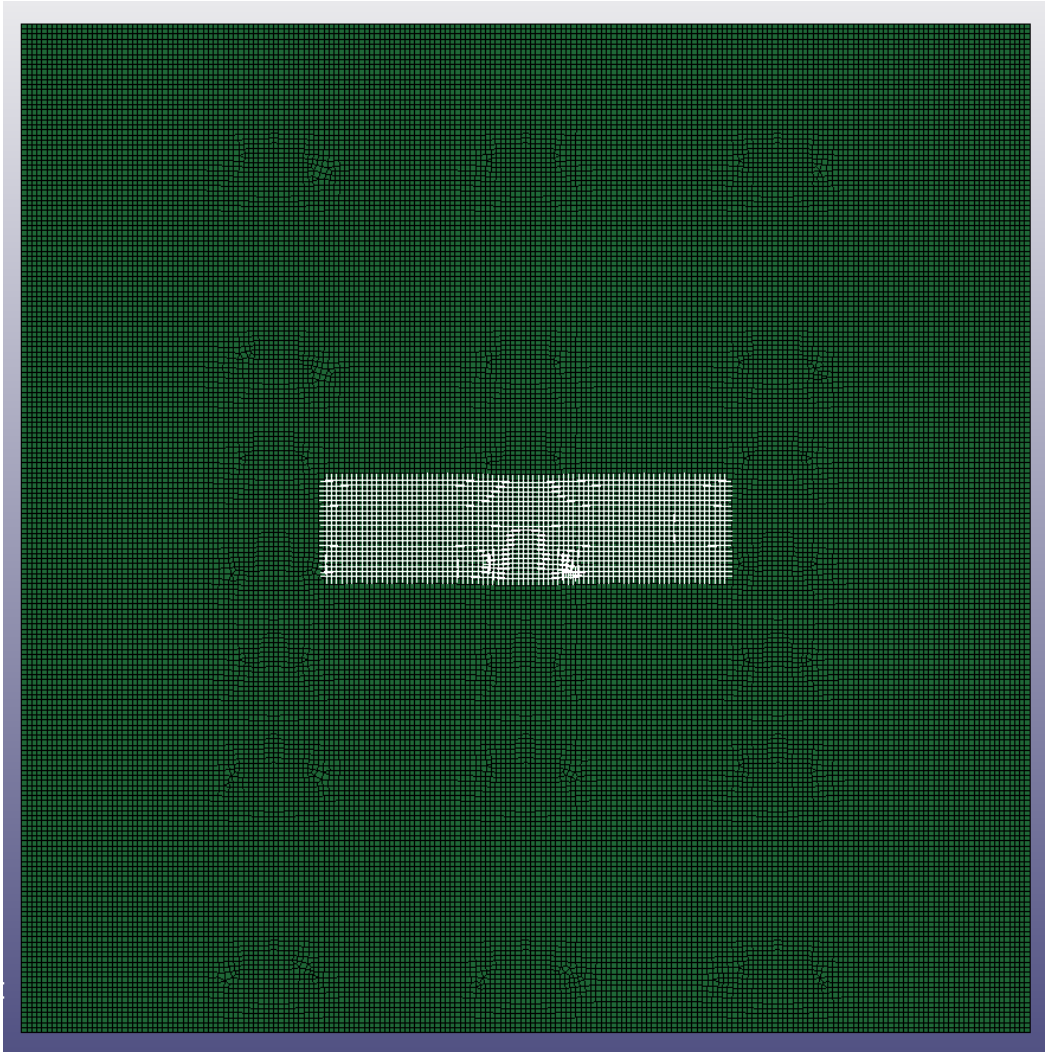

Figure 3-6 DOE Load Patch Location, Front View

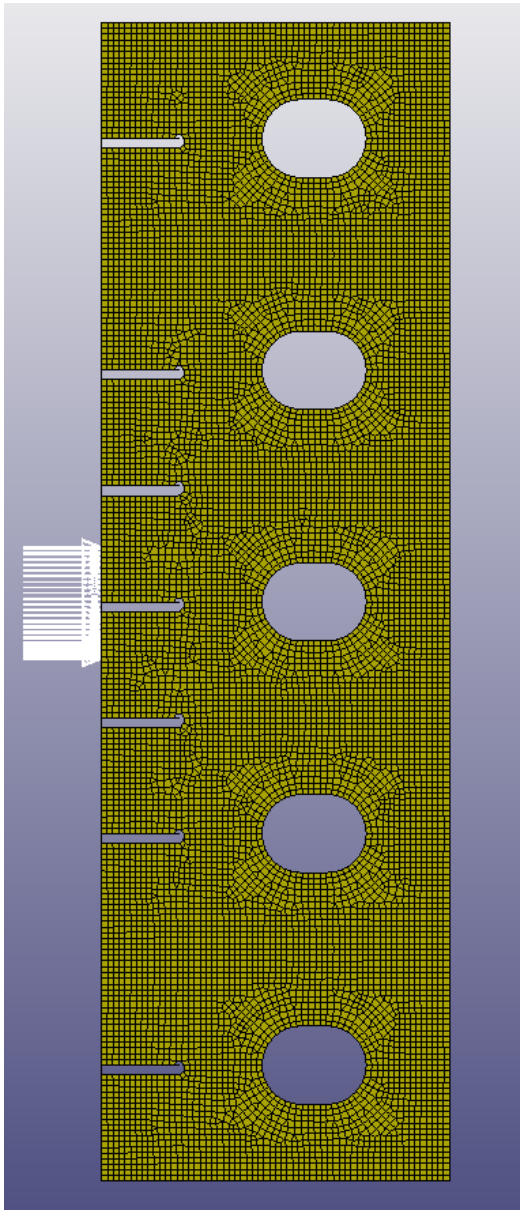

Figure 3-7 DOE Load Patch Location, Side View

Some simplifications were made to the geometric model structure to allow for quick model creation. For all models it was decided to have 3 web frames, spaced 1.5m apart. The longitudinals were spaced 600mm apart unless in way of a deck. All longitudinals are

modeled as flat bars (so as to reduce the number of factors by not including a flange). All access holes are equally spaced 1200mm except when in way of a deck. All of the penetrations/cutouts for the longitudinals through the web frames have the same dimensions. Each model is 6m in height and width to ensure no plasticity occurred at the boundaries. Please see Figure 3-8 below for an isometric view showing each of the 4 parts. The red part is the outer and inner shell (assumed the same thickness), the green part is the deck, the blue part is the longitudinals and the purple part is the web frames.

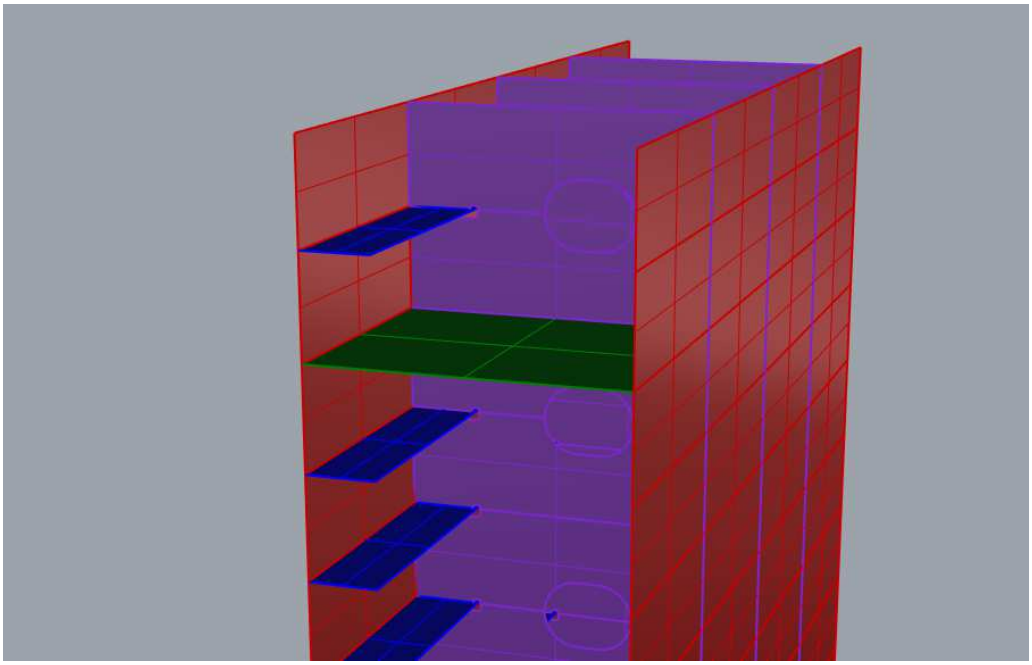

Figure 3-8 DOE Isometric Part View

The material model used for the DOE analysis was the same used for both PC3 and PC7 models. The boundary conditions were also kept the same as the PC3 and PC7 models, fixing all of the outer nodes of the model in all degrees of freedom. For the results of the DOE experiment please see Appendix B.

Chapter 4 Numerical Results

After initial model development a significant amount of time was spent building different structural models for both the PC3 and PC7 arrangements. This initial research focused on determining the different design factors that are often overlooked or not included in FE models during the design phase. Often small details like access holes, penetrations and lugs are not modelled to save time and resources. Please see Figure 3-1 and Figure 4-1 for an example of the design details mentioned above. Please note that in Figure 4-1 the white and pink parts are one continuous lug in reality, but have been modeled as separate parts for all FE models in this thesis. This was done for two reasons: the first being the complexity of modelling the contact between the lug and web frame (especially at higher load levels); and the second is due to the different thicknesses from the overlap of the lug and web frame compared to the lug in the open penetration. Thus, the pink part has a combined thickness of the lug (10mm) and web frame (12mm) whereas the white part has a thickness of 10mm.

Access holes are placed throughout the ship for two reasons; to reduce the weight of the structure and to allow workers access to different parts of the ship. The longitudinal cutouts/penetrations in transverse members allow the longitudinals to extend the length of the hull which increases the bending capacity of the ship. Lugs are placed on the bottom of the longitudinals and welded to the web frames on one side (forward or aft). These different design details were modeled for both PC3 and PC7 structural arrangements and the characteristic force displacement curves were analyzed for the in and out of plane

responses. This was done to estimate the effect that each of the design details have on the overall strength of a web frame in an overload capacity.

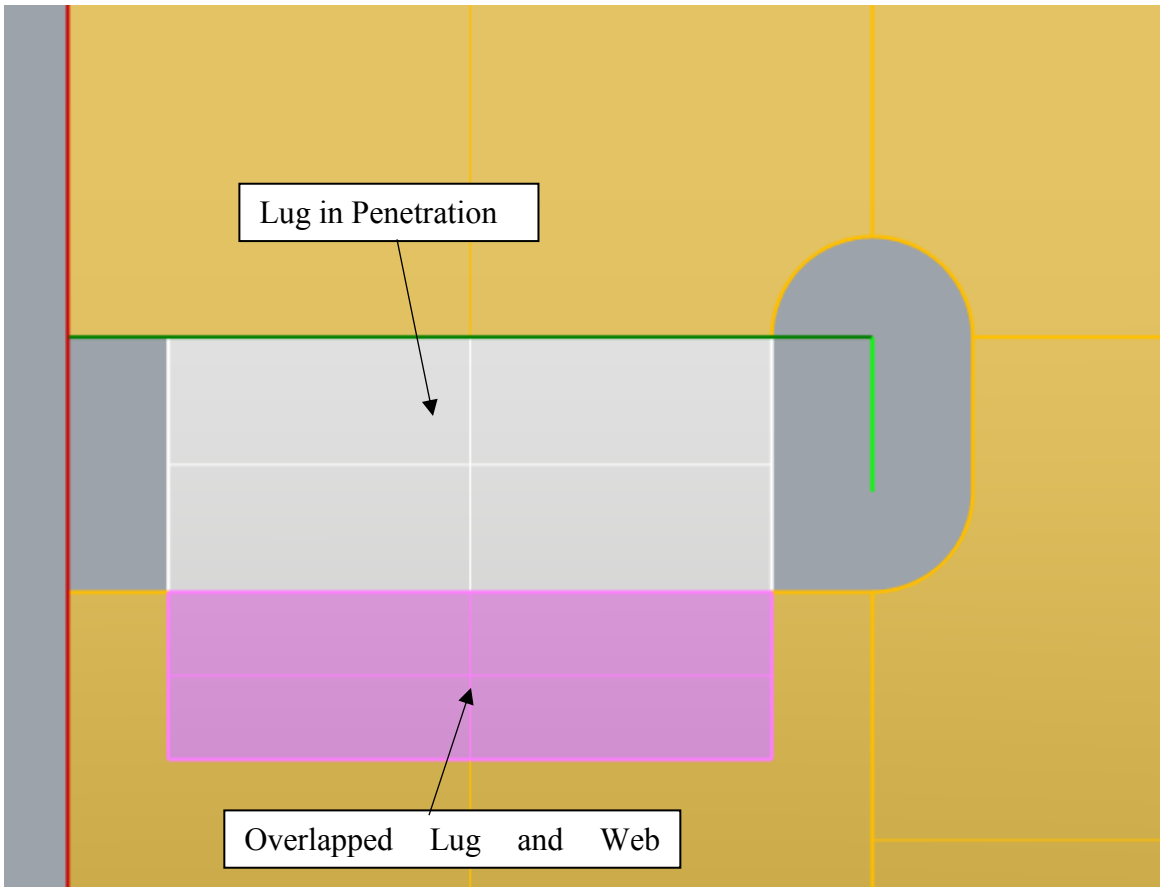

Figure 4-1 Lug Placement and Arrangement for PC3 Model

The design force for each polar class was added to the plots to compare how the different design features/details affected the response of the overall structure. The in and out of plane deformations are taken with respect to the plane of the web frame, which exists in a global x and y plane. In-plane refers to deformations in the global y direction whereas out of plane refers to the deformations in the global x direction. Please see Figure 4-2 and

Figure 4-3 below for the PC7 and PC3 characteristic in-plane force displacement curves respectively. Note that what appears to be a vibration of the web frame in Figure 4-2 and Figure 4-3 is actually caused by contact between the web frame and the longitudinals. There is no major vibrational response from this type of loading. This vibration due to contact has no bearing on the results of this research.

For the PC7 arrangements, the basic case, which has no cutouts or lugs, gave the stiffest response and more reserve capacity/greater force to cause plasticity past the design force. This is an expected result as there are no discontinuous design features modeled (cutouts) thus there are no added stress concentrations to the web frame and more material is available to withstand the load. When the access holes are modeled there is a slight decrease in the structure's stiffness and a very slight drop in overload capacity. Although it appears that including these access holes has very little effect for the PC7 model in plane displacement, it significantly changes how the load builds up in the web frame. For the basic case the load builds up between the outer shell plate, web frame and longitudinal until yield is reached. The outer shell plate, web frame and longitudinal then deform plastically, the load continues to flow through the depth of the web frame until an out of plane instability (buckling) occurs. For the case with the access hole the load initially builds the same as the basic case until yield is reached. As the web frame deforms plastically the elements around the access hole quickly become plastic due to the load concentrating around the cutout. This load concentration caused buckling to occur around the cutout instead of closer to the outer side shell plating.

When only the longitudinal penetrations are modeled the stiffness and overload capacity are significantly decreased. As the penetrations remove material from the web frames, directly in way of the load being applied to the side shell, the stress becomes concentrated within the penetration. Due to this stress concentration, the web frame quickly yields and the out of plane instability occurs closer to the penetration. With both cutouts being modeled there is again a drop in stiffness and overload capacity. This is likely due to there being two sources of discontinuities through the web frame where the stress can concentrate. By including the lugs along with all cutouts the stiffness and overall capacity is increased significantly when compared to the all cutouts case. The lug allows for more of the load to transfer into the web frame, away from the penetrations causing it to act similarly to the access hole case but with a slightly reduced stiffness and capacity.

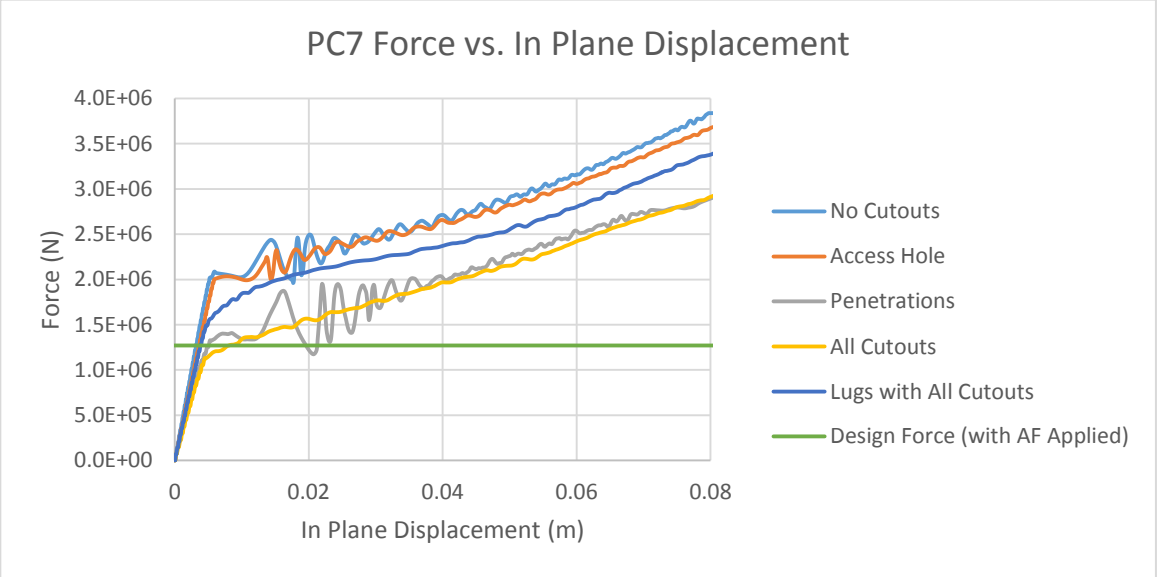

Figure 4-2 PC7 Characteristic Force In-Plane Displacement Curve

The PC3 arrangements follow the same trends as the PC7 case; the stiffest and highest capacity case occurred when no details were modeled, the least stiff and lowest capacity case occurred when both cutouts were included in the model. By including lugs a significant increase in the capacity and an increase in stiffness was observed.

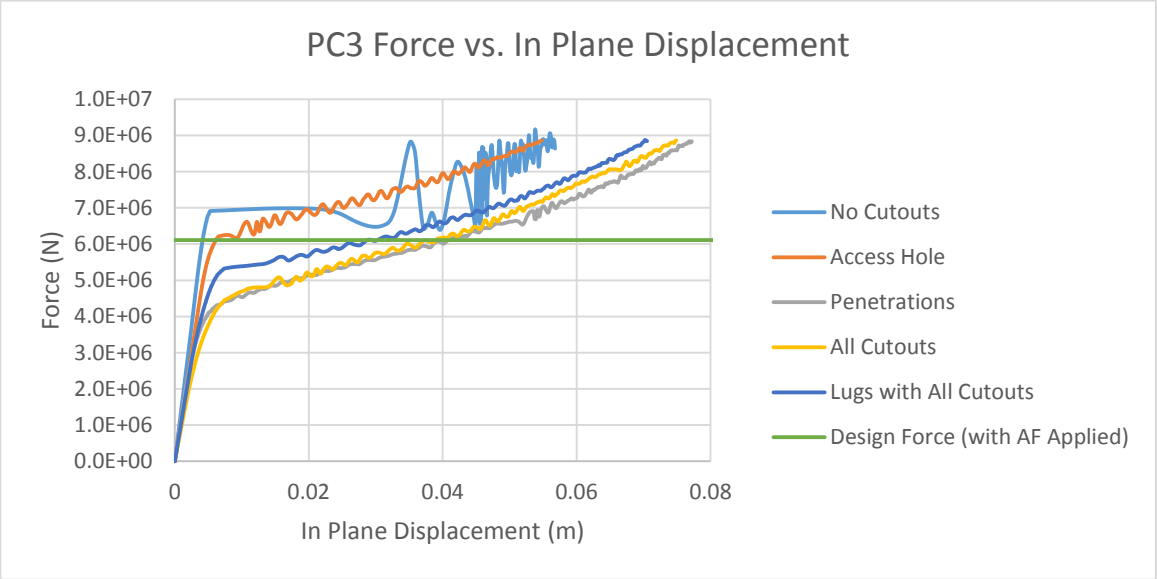

Figure 4-3 PC3 Characteristic Force In-Plane Displacement Curve

From analyzing the in-plane results it becomes apparent that design details such as cutouts, lugs and other small structural details that are near the applied load should be modeled as close to the real design as possible to ensure more accurate results. It was mentioned previously that in conjunction with analyzing the in-plane displacements, the out of plane displacements were also investigated for the various arrangements for both the PC7 and PC3 models. Out of plane failures generally happen rapidly at a specific load level, depending on the size of the structure. This includes failure modes like buckling

which often lead to catastrophic failure unless specifically designed for. As shown in Figure 4-4 and Figure 4-5 below for the PC7 and PC3 characteristic out of plane force displacement curves, once a specific load level is reached an instability occurs causing large out of plane deformations. For the PC7 model it appears that the instability is a shear buckle (buckled "waves" are at an angle to the load), while for the PC3 model it appears to be a normal buckling pattern.

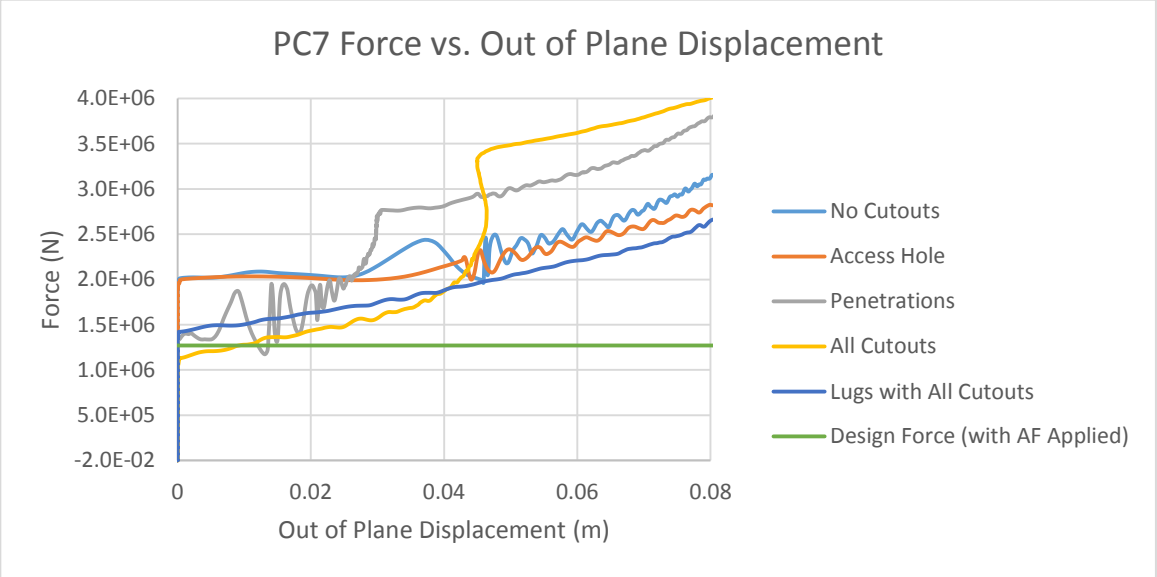

Figure 4-4 PC7 Characteristic Force Out-of-Plane Displacement Curve

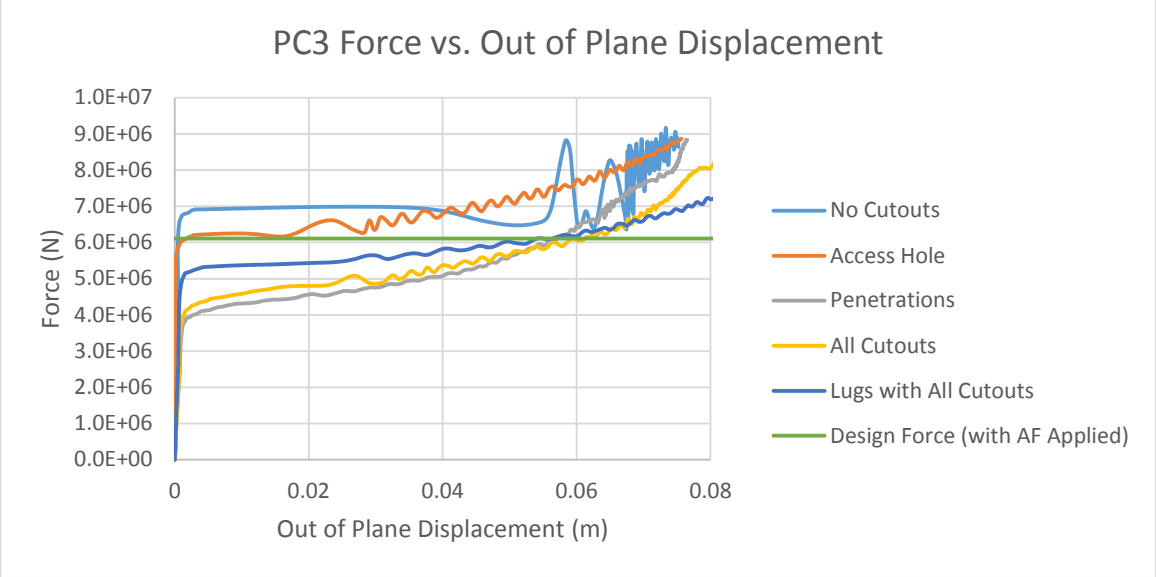

Figure 4-5 PC3 Characteristic Force Out-of-Plane Displacement Curve

From the figures above it is observed that none of the studied design features effect the slope of the linear elastic portion (see Figures 3-2 and 3-3) of the curves. There was, however a large impact on the force to cause the out of plane instability (see Figures 3-4 and 3-5). For the PC7 case in Figure 4-4 there was virtually no change in the force to cause the instability between the basic "no cutouts" case and the case where the access hole is modeled. This is likely due to the relatively low design force as the PC7 ice designation has very low ice capabilities and the structure is relatively thick for that ice class. The addition of the penetrations significantly decreased the force to cause an instability. This is likely due to the force being concentrated so heavily around the penetrations, similar to the in plane behaviour. When all cutouts are modeled the force decreases further. By including the lugs in the penetrations there is a slight increase in capacity to withstand the out of plane instability.

The results for the PC3 out of plane displacements were similar to the PC7 case. The basic no cutouts case had the highest capacity followed by the access hole only case, followed by the lug case and the all cutout case which had very similar capacities. Note that it appears the penetration only case actually fared worse than the "all cutouts" case for the PC3 model which was an unexpected result. This is likely due to a small contact or mesh issue in way of the load. The penetration only case should perform better than the "all cutouts" case, just as it did for the PC7 case. Just as with the in-plane characteristic curves, it has been shown that for the out of plane response all cutouts should be modeled as well as design details like lugs that are close to the members being loaded. The out of plane response should be considered for future rule development due to the catastrophic nature of the failure.

It is also important to note that the PC3 in and out of plane characteristics curves have a relatively high design force of approximately 6 MN. From these curves only two of the models are still in the elastic response region when the design force is reached, the basic and access hole only cases, which are missing some key design features that have been shown above to affect the response of web frames significantly. This in general would be considered a failed design if it were to be built in reality. Some plastic deformation is appropriate as the polar class rules are designed about the three hinge plastic mechanism; however it is not suggested to allow an out of plane mechanism to form. The PC3

structure used for this research should be altered in future revisions to avoid this mechanism but due to time constraints could not be completed at this time.

4.1 DOE Results

After the initial development for both the PC7 and PC3 models and the investigation into the effect that the design features (penetrations, cutouts and lugs) had on the results of a nonlinear finite element simulation, a numerical experiment was setup to study some of the effects more closely. The experiment used a DOE approach, specifically a uniform design, as discussed in Chapter 3.9. Please refer to Table 3-6 for the factors being studied and their respective values for each numerical model. It is important to note that lugs were not modeled for this numerical experiment for two reasons. The first reason; the experiment took a substantial amount of time to model all of the different geometries and to prepare all of the remaining components of the numerical models. If the lugs were included it would have significantly increased the time for the models to be prepared due to their geometry, which changes depending on the other factors for that specific run. The second reason is that the lugs themselves were not part of this numerical study, it focused more on the web frame geometry, surrounding structure and the effect of the cutouts on the capacity of the web frames. With these two things considered it was decided that the best course of action was to neglect modelling lugs even though they had been proven to be important in the overall response of the web frames. For future work the lugs would be included in all numerical models.

The results from each of the 51 numerical models were analyzed and the responses were extracted and presented in a graphical format using Microsoft Excel. This made it easier to determine the force to cause plasticity for the in plane response and the force to cause an out of plane instability for the out of plane response. For the 2.5% plastic strain response a search function was used to find the force that corresponds to 0.025 strain. As discussed previously the 2.5% plastic strain limit is not an ideal design point for finite element models due to the strain being dependant on the size of the mesh, however for comparison purposes it was chosen as one of the responses for the DOE analysis. Please see Figure 4-6 through Figure 4-8 below outlining a single numerical model's responses. Note for Figure 4-6 and Figure 4-8 the gradual change in slope of the curves whereas for Figure 4-7 it is a very sudden change in slope. This out of plane displacement (instability) can cause catastrophic failures to a ship's structure or operational profile. This makes the out of plane displacement, or force to cause an out of plane instability, a prime candidate as an acceptance criterion.

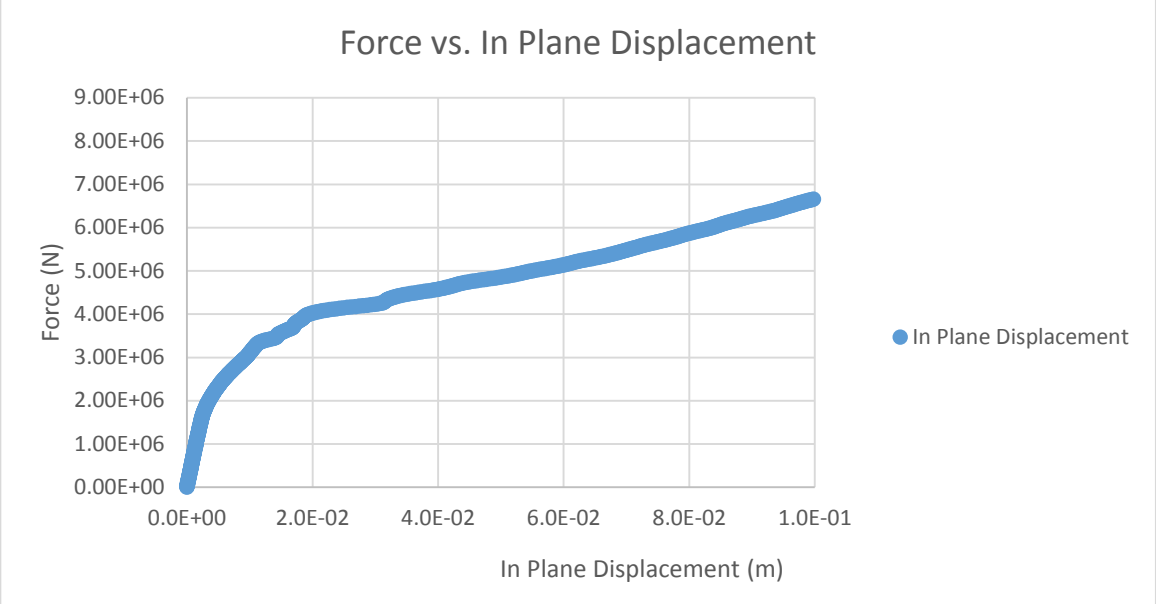

Figure 4-6 Characteristic Force In Plane Displacement Curve – Run 29

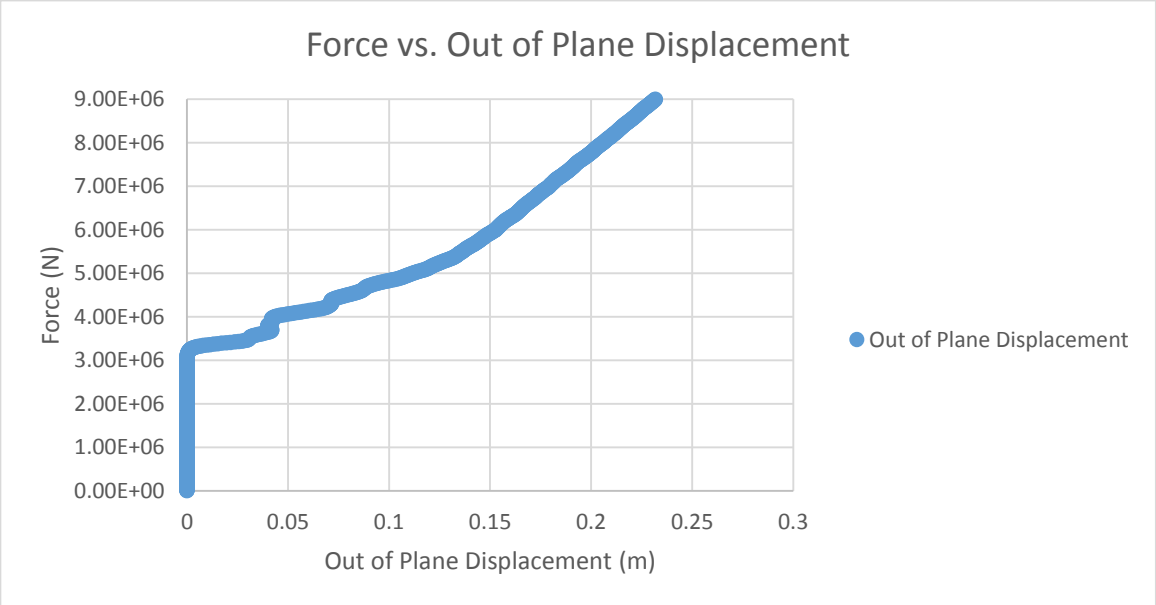

Figure 4-7 Characteristic Out of Plane Displacement Curve – Run 29

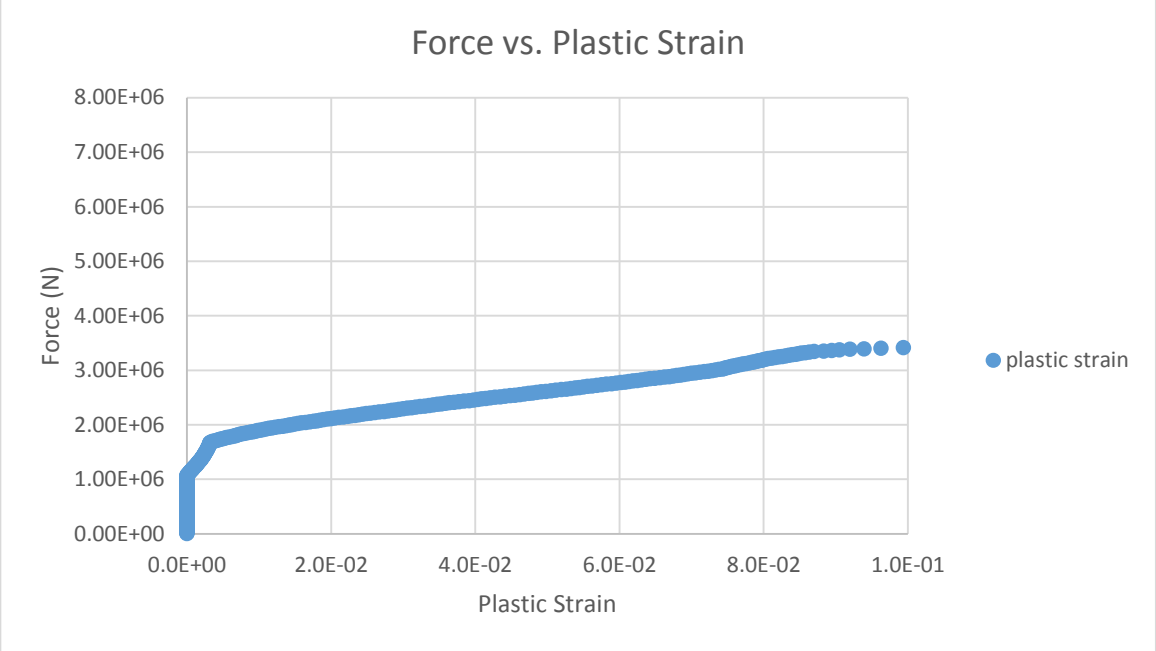

Figure 4-8 Force vs Plastic Strain – Run 29

For each run the responses were recorded and analyzed using the DOE software Design Expert®. This software can help develop the experimental setup and test procedure for many different types of DOE analysis. Although Design Expert does not have a specific format for a Uniform Design, a custom format was used which can create the response surfaces and optimization functions along with performing the statistical analysis and creating the model equations. The results from the DOE analysis for their respective runs can be found in Table 4-1 below. In general, it was noticed that the force to cause plasticity in the plane of the web frame was significantly lower than the force to cause an out of plane instability. In general, it was also noticed that the force to cause 2.5% plastic strain was generally close to the force to cause an out of plane instability but as mentioned should not be used due to being mesh dependant.

Table 4-1 Response results from DOE Analysis

Run	Response 1: Force to Cause In Plane Plasticity (MN)	Response 2: Force to Cause Out of Plane Instability (MN)	Response 3: Force to Cause 2.5% Plastic Strain (MN)
1	1	2	2.09
2	2.2	8.4	6.09
3	1	3.2	2.17
4	1.6	5.5	4.71
5	1.6	3	3.71
6	0.8	1.8	1.9
7	0.8	3	2.61
8	1.6	3.6	3.83
9	1.4	3.4	3.79
10	1	4	3.1
11	1.4	2.5	2.66
12	1.4	6	4.72
13	1.4	4.5	5.32
14	1.4	8.5	6.3
15	1.6	6.5	5.2
16	1.4	2.75	3.36
17	0.8	1.4	2
18	1.4	3.7	4.07
19	1.4	2.7	2.76
20	1.6	7.5	4.69
21	1.8	5.2	5.39
22	1	3	1.85
23	1.4	4	4.09
24	1.6	4.5	3.95
25	2	5.8	6.05
26	1.6	8	3.97
27	1.2	2	2.89
28	1.2	5.5	3.01
29	1.2	3.1	2.2
30	0.6	1.4	1.5
31	1.2	3.5	3.39
32	1.4	3.9	3.98
33	1.2	2.7	2.77
34	1.2	2.1	2.65
35	1.2	2.4	2.53

Run	Response 1: Force to Cause In Plane Plasticity (MN)	Response 2: Force to Cause Out of Plane Instability (MN)	Response 3: Force to Cause 2.5% Plastic Strain (MN)
36	1.8	6	4.79
37	1	3	2.51
38	1	1.8	2.09
39	1.2	3.9	3.09
40	1.6	4	3.95
41	1	3	2.48
42	0.8	2.5	2.02
43	1	2.8	2.77
44	0.6	3	2.13
45	1.4	4.2	4.1
46	1	1.8	2.17
47	1.4	2.7	3.36
48	1.4	5	4.06
49	1.2	5.8	3.38
50	1	2	2.39
51	1.2	2.1	2.43

The responses and factor levels were statistically analyzed using Design Expert, which uses Analysis of Variance (ANOVA), a statistical technique which compares the differences between means and their variances for different factors and their responses and interactions. An algorithm was used to determine if a factor or factor interaction effects have a statistically significant impact on a response. Specifically, the backwards method with a confidence of 90% or alpha value of 0.1 was used. This was employed due to a very large number of factors and their interactions which would have taken a significant amount of time if done manually for each response.

For each of the three responses the significant factors and their interactions were found and outlined in ANOVA tables, which show each factor's individual significance in the overall model equation. Please see Table 4-2 through Table 4-4 for the ANOVA tables for each of the three responses respectively. The Sum of Squares column is the sum of the square of the deviation between the response and its mean. The df column is the degrees of freedom a factor possesses; which in general is 1 degree of freedom per term. The Mean Square column is the division of the Sum of Squares by the degrees of freedom for a given factor/term. The F value is calculated from dividing the Mean Square by the Mean Square of the residual. This F value is then compared to the F distribution and allows for the p-value to be calculated. As long as the p-value is below the chosen alpha/confidence value the factor is considered significant. Some of the factors in the ANOVA tables have p-values above the chosen alpha/confidence value of 0.1. This is because even though the factor itself may not be significant in the overall response model, its interaction with another factor is significant. In order to ensure the model is hierarchical the insignificant main factors that are part of higher order interaction terms must be included in the model.

Table 4-2 ANOVA Table for Response 1 – Force to Cause In-Plane Plasticity

ANOVA for Response Surface Reduced Quadratic model					
	Sum of		**Mean**	**F**	**p-value**
Source	**Squares**	**df**	**Square**	**Value**	**Prob > F**
Model	5.13	10	0.51	43.24	< 0.0001
A-Shell Thickness	*2.02*	*1*	*2.02*	*170.61*	*< 0.0001*
B-Web Thickness	*1.84*	*1*	*1.84*	*155.39*	*< 0.0001*
C-Web Depth	*0.16*	*1*	*0.16*	*13.81*	*0.0006*
D-Cutout Radius	*0.14*	*1*	*0.14*	*12.02*	*0.0013*

E-Span	*9.547E-004*	*1*	*9.547E-004*	*0.080*	*0.7781*
G-Shell Longitudinal Height	*0.67*	*1*	*0.67*	*56.26*	*< 0.0001*
AC	*0.12*	*1*	*0.12*	*9.70*	*0.0034*
CE	*0.070*	*1*	*0.070*	*5.90*	*0.0197*
DG	*0.060*	*1*	*0.060*	*5.06*	*0.0300*
C^2	*0.073*	*1*	*0.073*	*6.13*	*0.0176*
Residual	0.47	40	0.012		
Lack of Fit	*0.47*	*39*	*0.012*		

Table 4-3 ANOVA Table for Response 2 – Force to Cause an Out of Plane Instability

ANOVA for Response Surface Reduced Quadratic model					
	Sum of		**Mean**	**F**	**p-value**
Source	**Squares**	**df**	**Square**	**Value**	**Prob > F**
Model	9.80	13	0.75	38.60	< 0.0001
A-Shell Thickness	*1.13*	*1*	*1.13*	*57.95*	*< 0.0001*
B-Web Thickness	*5.50*	*1*	*5.50*	*281.55*	*< 0.0001*
C-Web Depth	*5.817E-004*	*1*	*5.817E-004*	*0.030*	*0.8639*
D-Cutout Radius	*6.256E-003*	*1*	*6.256E-003*	*0.32*	*0.5748*
E-Span	*1.26*	*1*	*1.26*	*64.37*	*< 0.0001*
G-Shell Longitudinal Height	*0.94*	*1*	*0.94*	*47.92*	*< 0.0001*
H-Shell Logitudinal Thickness	*0.14*	*1*	*0.14*	*7.21*	*0.0108*
AE	*0.24*	*1*	*0.24*	*12.39*	*0.0012*
AG	*0.49*	*1*	*0.49*	*25.09*	*< 0.0001*
CD	*0.16*	*1*	*0.16*	*8.36*	*0.0064*
DE	*0.099*	*1*	*0.099*	*5.05*	*0.0307*

E^2	*0.25*	*1*	*0.25*	*12.82*	*0.0010*
H^2	*0.15*	*1*	*0.15*	*7.60*	*0.0090*
Residual	0.72	37	0.020		
Lack of Fit	*0.72*	*36*	*0.020*	*119.19*	*0.0725*

Table 4-4 – ANOVA Table for Response 3 – Force to Cause 2.5% Plastic Strain

ANOVA for Response Surface Reduced Quadratic model					
	Sum of		**Mean**	**F**	**p-value**
Source	**Squares**	**df**	**Square**	**Value**	**Prob > F**
Model	6.14	15	0.41	128.07	< 0.0001
A-Shell Thickness	*2.37*	*1*	*2.37*	*743.08*	*< 0.0001*
B-Web Thickness	*2.49*	*1*	*2.49*	*780.26*	*< 0.0001*
D-Cutout Radius	*2.978E-003*	*1*	*2.978E-003*	*0.93*	*0.3409*
E-Span	*0.19*	*1*	*0.19*	*60.71*	*< 0.0001*
F-Deck Thickness	*7.554E-003*	*1*	*7.554E-003*	*2.37*	*0.1330*
G-Shell Longitudinal Height	*0.58*	*1*	*0.58*	*180.22*	*< 0.0001*
AB	*0.040*	*1*	*0.040*	*12.41*	*0.0012*
AE	*0.083*	*1*	*0.083*	*25.85*	*< 0.0001*
AG	*0.39*	*1*	*0.39*	*121.66*	*< 0.0001*
BE	*0.066*	*1*	*0.066*	*20.80*	*< 0.0001*
BF	*0.031*	*1*	*0.031*	*9.63*	*0.0038*

FG	*0.019*	*1*	*0.019*	*6.06*	*0.0189*
A^2	*0.020*	*1*	*0.020*	*6.17*	*0.0179*
B^2	*0.065*	*1*	*0.065*	*20.47*	*< 0.0001*
D^2	*0.015*	*1*	*0.015*	*4.61*	*0.0389*
Residual	0.11	35	3.194E-003		
Lack of Fit	*0.11*	*34*	*3.288E-003*		

The model equations for each of the responses are outlined in two different forms; coded or actual values. The coded values use a place holder variable to represent the factors. This is done as the constant in front of the variable can easily show which factors have the largest impact on the model as the p-value can sometimes be misleading. If the constant in front of the coded variable is very large it has a large effect on the response. The same is true if the constant is very negative, just that it has a negative effect on the response. The coded equation however does not take in the actual factor values and is not practical for use outside of the ANOVA software. The actual value equations can be used for practical purposes but the constants in front of the variables cannot be used as a measure of significance or as a measure to their impact on the model equation. Care must also be taken to ensure proper units are used exactly as they were setup during the statistical analysis or the actual value equations will be highly inaccurate. Please see below for the coded and actual value model equations for each of the three responses. For the following equations A is the shell thickness, B is the web frame thickness, C is the web frame depth, D is the cutout width, E is the web frame span between decks/stringers, F is the deck thickness, G is the shell longitudinal height and H is the shell longitudinal thickness.

Response 1 – Force to In Plane Plasticity

Coded:

$$F_{ip} = 1.36 + 0.25A + 0.23B - 0.13C + 0.17D - 5.31210^{-3}E + 0.14G - 0.074AC + 0.055CE + 0.07DG - 0.08C^2$$

Real Value:

$$F_{ip} = -0.82666 + 0.041298A + 0.078277B + 3.78142 * 10^{-4}C - 7.774833 * 10^{-5}D - 1.08102 * 10^{-4}E + 3.27083 * 10^{-6}G - 9.2833910^{-6}AC + 5.75974 * 10^{-8}CE + 1.40222 * 10^{-6}DG - 1.25653 * 10^{-7}C^2$$

Response 2- Force to cause an Out of Plane Instability

Coded:

$$\ln F_{oop} = 1.13 + 0.18A + 0.41B - 9.261 * 10^{-3}C - 0.039D - 0.2E + 0.17G + 0.065H - 0.11AE - 0.15AG + 0.17CD - 0.085DE + 0.15E^2 - 0.12H^2$$

Real Value:

$$\ln F_{oop} = -3.83791 + 0.08533A + 0.13605B - 3.45846 * 10^{-4}C - 4.89946 * 10^{-4}D$$
$$- 3.40401 * 10^{-4}E + 5.46074 * 10^{-3}G + 0.25016H - 8.942 * 10^{-6}AE$$
$$- 1.5161 * 10^{-4}AG + 4.17837 * 10^{-7}CD - 1.42040 * 10^{-7}DE$$
$$+ 1.06342 * 10^{-7}E^2 - 7.31029 * 10^{-3}H^2$$

Response 3 – Force to Cause 2.5% Plastic Strain

Coded:

$$\ln F_{2.5\%} = 1.22 + 0.27A + 0.28B + 0.013D - 0.077E - 0.015F + 0.13G + 0.041AB$$
$$- 0.063AE - 0.14AG + 0.059BE - 0.038BF + 0.031FG - 0.043A^2$$
$$- 0.08B^2 + 0.05D^2$$

Real Value:

$$\ln F_{2.5\%} = -2.85724 + 0.086873A + 0.26929B - 2.92156 * 10^{-4}D - 1.291 * 10^{-4}E$$
$$+ 8.4332 * 10^{-3}F + 3.94911 * 10^{-3}G + 1.38062 * 10^{-3}AB$$
$$- \ 5.27374 * 10^{-6}AE - 1.42661 * 10^{-4}AG + 1.64178 * 10^{-5}BE$$
$$- 2.51907 * 10^{-3}BF + 6.25903 * 10^{-5}FG - 4.28194 * 10^{-4}A^2$$
$$- 8.87607 * 10^{-3}B^2 + 1.99152 * 10^{-7}D^2$$

At first glance it appears that the model equations for each of the three responses are very complicated. Although they have many terms some conclusions can still be drawn from the equations that can shape future work. For response 1 the shell and web frame thickness terms, cutout size and the frame depth, span as well as the longitudinal height were all found significant as well as the interactions between the shell thickness and web depth, web frame depth and span, cutout width and longitudinal height as well as the web frame depth squared term. The thickness terms had a positive effect on the model, meaning that an increase in thickness increases the structures capacity to resist the load. This result is intuitive as increasing the amount of material would lead to an increase in capacity. The web frame depth had a negative effect on the frames capacity. Even though there is more material to resist the load in the plane of the web frame, the increase in depth can lead to an out of plane instability at a decreased load if the thickness is not also increased. The cutout width also had a positive effect on the in plane response which similar to the depth is counter intuitive. As the web frame cutout size increases that must also mean the depth of the web frame is large enough to accommodate the cutout. As long as the web frame thickness is also increased the size of the cutout should not decrease the structures capacity. An increase in the span had a negative effect on the capacity which is expected. This causes the frame to have less support from the decks/stringers reducing its capacity. The longitudinal height had a positive effect on the web frames ability to resist the load. This is intuitive as it adds more structure/material to reduce the load with only a small increase in the cutout size required to fit the larger longitudinal.

If the interaction effects are more closely examined the first response model equations becomes much easier to understand. The interaction effects somewhat reflect beam slenderness ratios for the web frame in both the in and out of plane directions. As the beam becomes more slender (large span:depth ratio and span:thickness ratio) the frame loses capacity. If we reduce the slenderness of the beam we can create a stronger structure. As before with the web frame cutout size factor, the interaction between the cutout size and the longitudinal height had a positive effect. This again is likely due to the frame being larger to accommodate the larger cutouts which gives more material overall to resist the load. The model equation for the first response is small enough that it could be used as a first estimate to calculate the force required to cause plasticity in the plane of the web frame.

A similar process was done for the remaining two responses, looking at each factor's significance to the overall model equation. However due to the very large increase in complexity and number of terms in the model equations it has been omitted from this thesis. It was noticed that for the out of plane response to be studied further it would require significant time that was not available to the author. If more time was available a second DOE analysis with more pointed factors would be done to further investigate the significant factors found from the initial broader DOE analysis. The plastic strain response was not considered any further in the research within this thesis. As discussed in previous sections strain is mesh dependant, especially around cutouts/discontinuities and should not be used as an acceptance criterion.

4.2 Web Frame Stiffening

As the DOE analysis did not shed much light on the out of plane instability response a separate study was done. In real ship designs for polar class vessels the web frames usually have some form of stiffening on the fore or aft side that adds stiffness and capacity against plasticity as well as out of plane instabilities. This study focused on different web frame stiffening arrangements and their impact on the in and out of plane response of the web frames. The case that had the lowest capacity (run 30) for both the in and out of plane response from the DOE analysis was used as the base case for investigating the different web frame stiffening arrangements. Seven different arrangements were tested and compared. The seven arrangements were the 'x' arrangement, the 'bridge' arrangement, the 'penetration ring' arrangement, the 'access hole ring' arrangement, both the penetration and access hole rings in a single model, the bridge with both penetration and access rings and finally the x arrangement with an access ring. Please see Figure 4-9 through Figure 4-15 to better visualize each of the seven arrangements. In all of the web frame stiffening arrangements the additional structures are modeled as shell elements with a thickness of 10mm. All other parts of the model were kept identical to the original model used in the DOE analysis. The same material model was used for the web frame stiffening as for the main structural members. Blue circles and arrows have been added to the figures below to point out the penetration and access hole rings respectively.

The ‘x’ arrangements consists of diagonal flat bars that form an X, the first half spanning between the corner of the upper deck and outer shell to the corner of the lower deck and inner shell. The other half of the X spans from the corner of the lower deck and outer shell to the corner of the upper deck and inner shell. Both halves of the X terminate at the central access hole in the web frame. The ‘bridge’ arrangement has a flat bar vertically oriented between the upper and lower deck with two transverse members from the inner shell to the vertical web stiffening, one above and below the access hole. The ‘penetration ring’ case is a steel ring that would be welded to the web frame inside the penetrations which protrudes both fore and aft of the web frame in which it was fitted. In reality these rings would take considerable time and effort to build and weld into the penetrations. This made the penetration rings an unattractive option but was used for comparison to the other arrangements. The ‘access hole rings’ are similar to the penetration rings but placed within the access holes. The remaining three cases are combinations of the different arrangements discussed above.

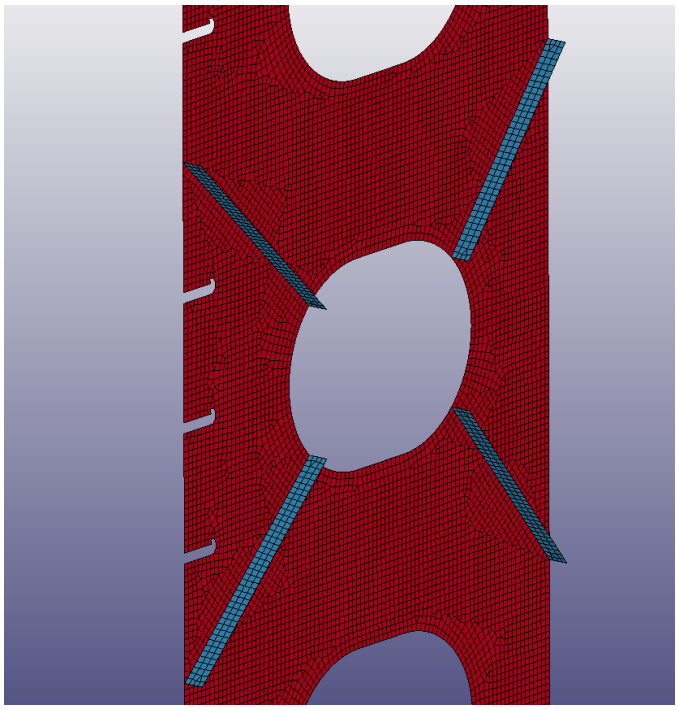

Figure 4-9 ‘X’ Web Frame Stiffening Arrangement

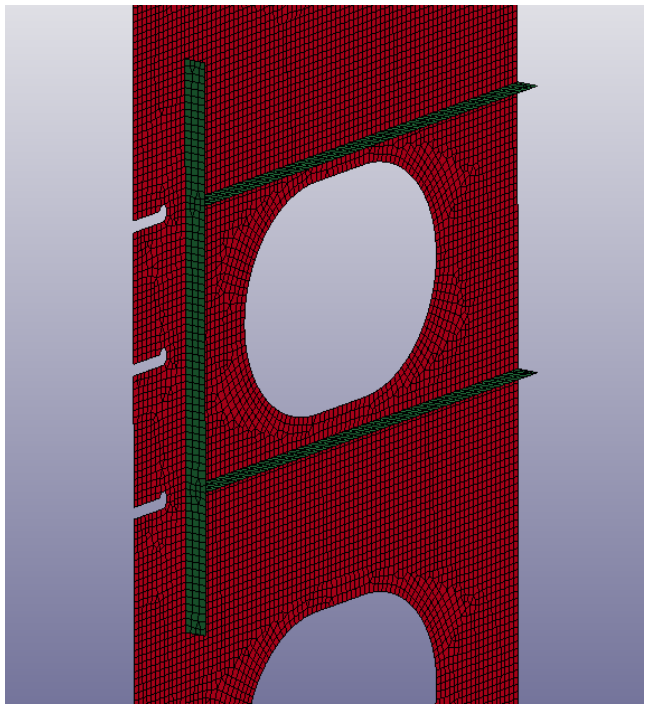

Figure 4-10 ‘Bridge’ Web Frame Stiffening Arrangement

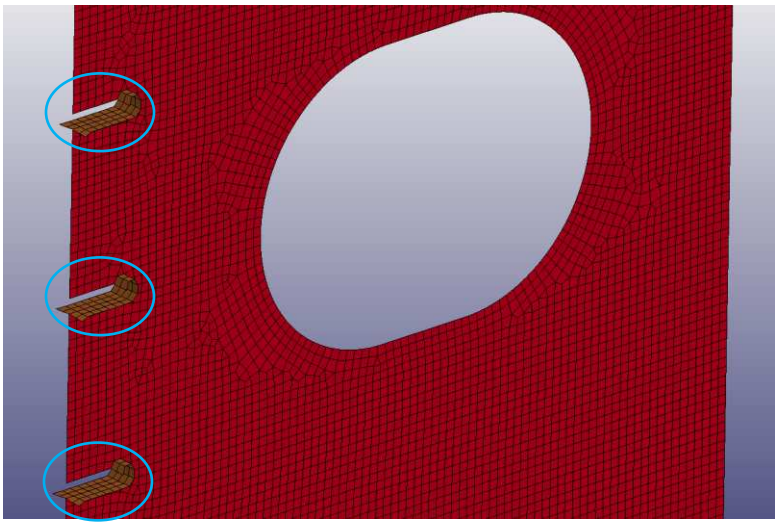

Figure 4-11 ‘Penetration Ring’ Web Frame Stiffening Arrangement

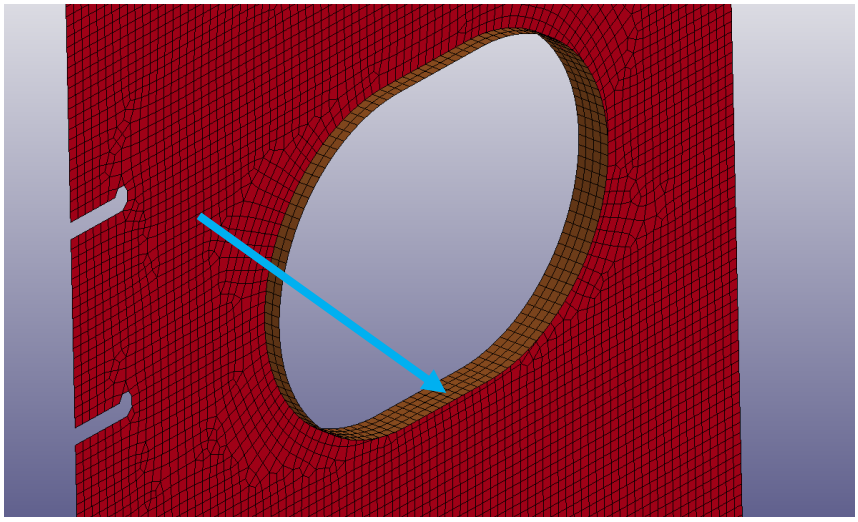

Figure 4-12 ‘Access Hole Ring’ Web Frame Stiffening Arrangement

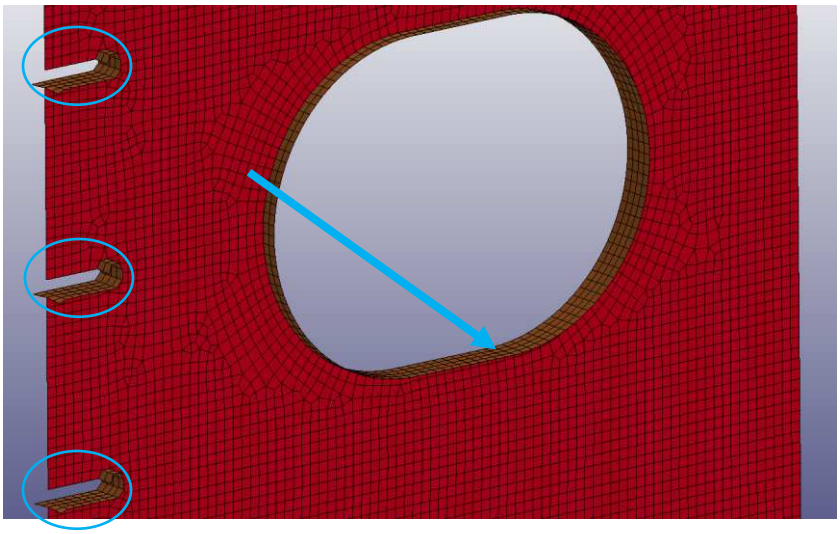

Figure 4-13 ‘Penetration and Access Hole Rings’ Web Frame Stiffening Arrangements

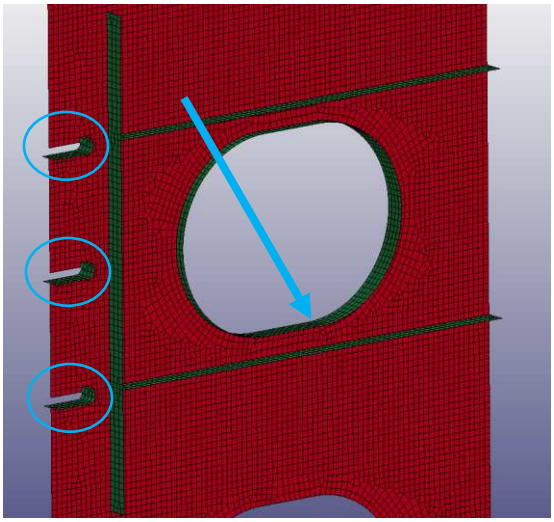

Figure 4-14 ‘Penetration Rings, Access Hole Rings and Bridge’ Web Frame Stiffening Arrangement

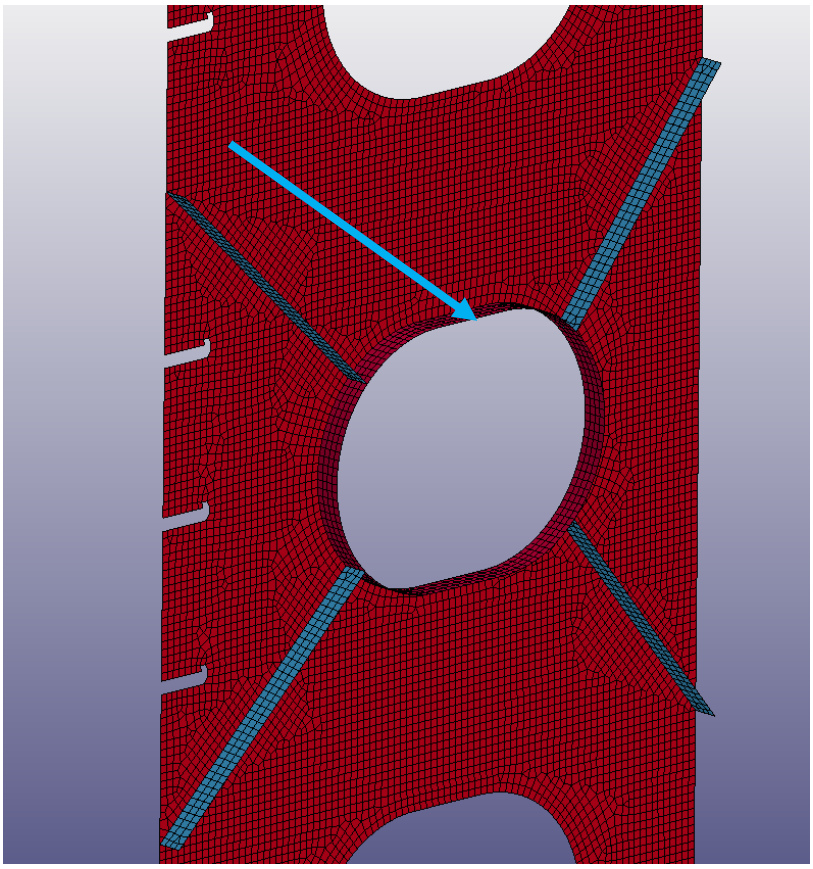

Figure 4-15 ‘Access Hole Ring and X’ Web Frame Stiffening Arrangement

It was found that the different web frame arrangements had a very large influence on the response of the web frames. The in and out of plane characteristic force displacement curves can be found in Figure 4-16 and Figure 4-17 below. The figures have each of the seven different arrangements as well as the basic no additional stiffening case. Several observations were made when analyzing the results. For the in plane response the bridge plus penetration and access rings arrangement, penetration and access hole ring arrangement and finally the access hole case gave a stiffer response than the other arrangements. As discussed previously the penetration rings are not practical and would

require a significant amount of time to prepare and install in reality. It was decided to not investigate numerical models with penetration rings any further except for comparison purposes. The remaining four arrangements have a less stiff elastic response and overload capacity but as discussed are more comparable and appropriate for ship design. The bridge arrangement had slightly more overload capacity than the access hole and the x arrangements. This is likely due to the way the stress transfers through the web stiffening and the web frame. This stress transfer becomes an issue with the X arrangements as it causes significant load concentrations. This will be discussed in greater detail below. The access hole ring arrangement did increase the overall capacity of the web frame and could be easily installed within the ice belt of a real ship. In general for the in plane response any additional stiffening added to the web frame would lead to an increase in capacity before going plastic, as long as the arrangement does not cause stress concentrations. All stiffening arrangements followed the same trend but had different yield points with slight changes in stiffness for the penetration ring cases.

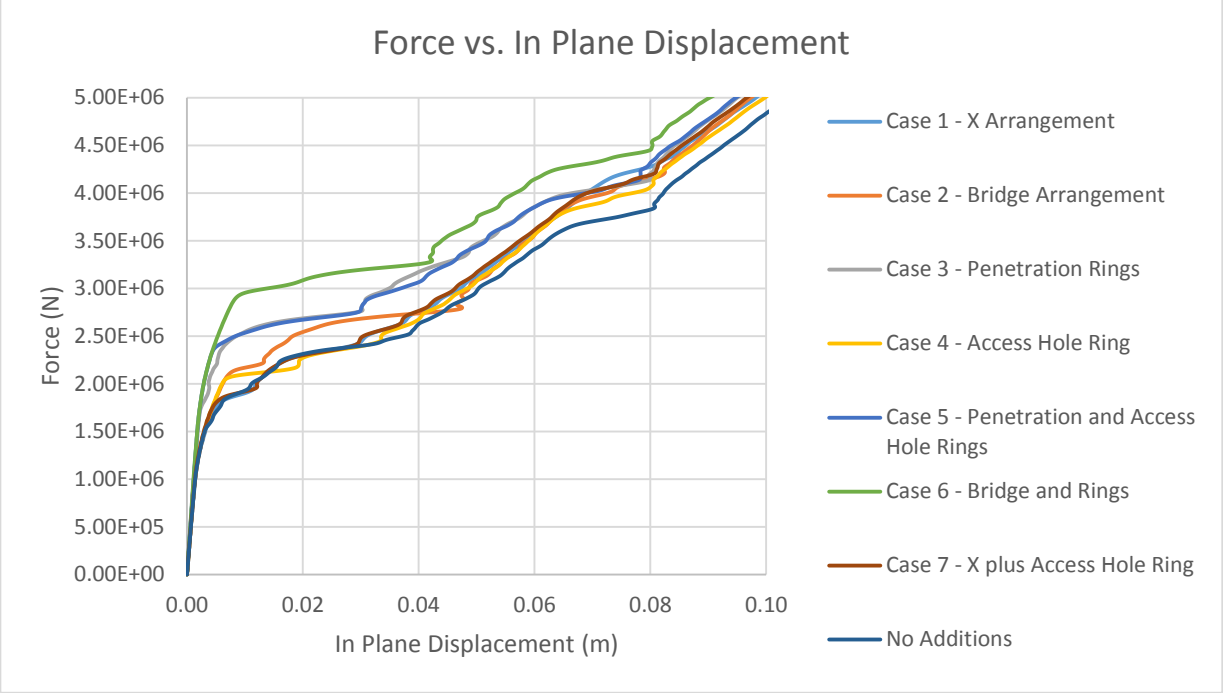

Figure 4-16 Characteristic In Plane Force Displacement Curves for the Various Web Stiffening Arrangements

In general the out of plane response has an elastic portion up until some limit followed by a rapid loss of capacity in the form of some instability as discussed in previous sections. This appears to be caused by the load concentrating in the cutouts/discontinuities. This caused the out of plane response to differ greatly for the different stiffening arrangements. However, similar to the in plane response, some of the arrangements that had penetration rings had an increase in stiffness when compared to the arrangements that did not have them, excluding the access hole ring arrangement which also exhibited the increase in stiffness. As discussed above this is likely due to the stress concentrated in the cutouts/discontinuities being redistributed through the web frame. The X-arrangement performed very poorly for the out of plane response. This is the same behaviour exhibited

for the in plane response. The web frame stiffening concentrates the load between the two diagonal stiffeners that terminate at the access hole, causing the instability to form at a lower force compared to the other stiffening arrangements. The X-arrangement performed worse than the no stiffening case. Please see Figure 4-18 below showing how the load is concentrated between the outer diagonal members of the web frame X-arrangement. By placing a ring within the access hole the load can be distributed to the other side of the cutout, significantly increasing the web frames capacity. This can be seen in Figure 4-17 as the red characteristic curve. For that arrangement, no out of plane instability occurred unlike all other structural arrangements. It may appear that the results are promising as it gives the highest capacity with no out of plane instability; however the response was incredibly stiff. In the model the stresses reached approximately 2000 MPa. This amount of stress is not possible meaning that the structure would likely fracture in an overload scenario. A designer would need to use this type of arrangement with caution; if large peak loads could be expected to occur for that location along the midbody, fracture could occur leading to catastrophic failure. If the loads are not expected to be very large and mainly in the elastic or early onset of plasticity, the X and access hole ring arrangement can perform very well. As this research is focused on overload capacity for polar class ships it is advised to not use the X-stiffening arrangement with or without an access hole ring.

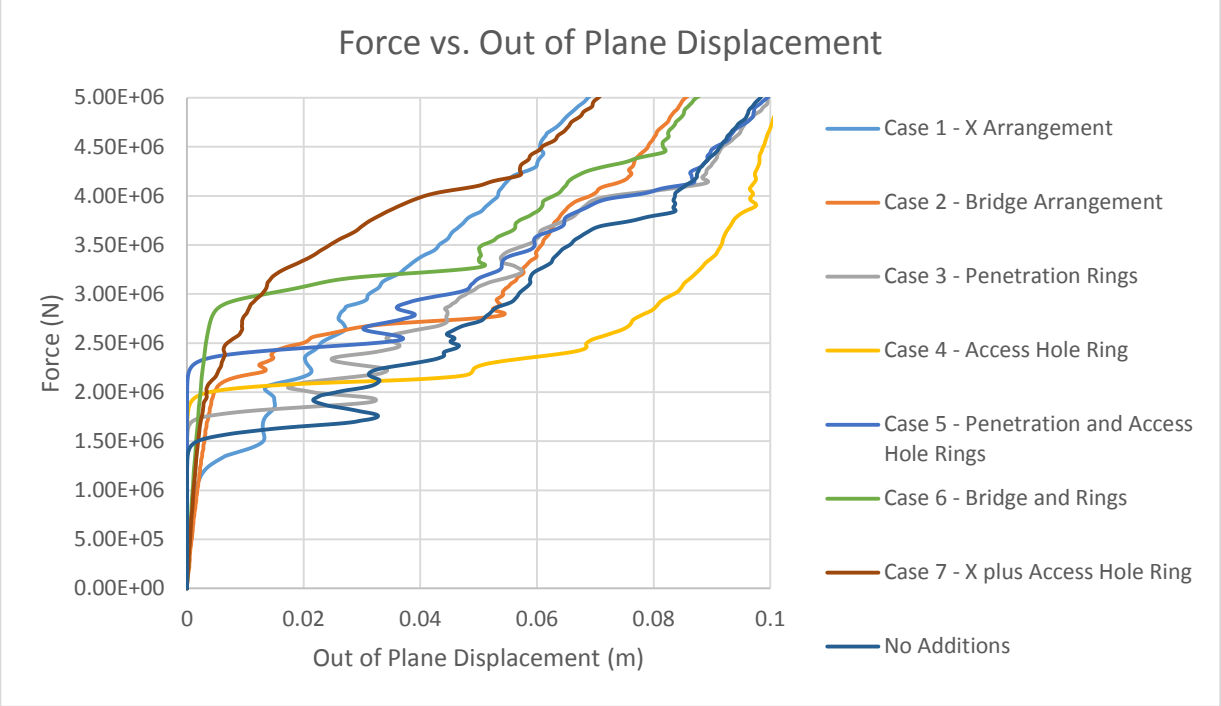

Figure 4-17 Characteristic Out of Plane Force Displacement Curves for the Various Web Stiffening Arrangements

The bridge arrangements, with and without cutout/penetration rings performed very well. There is a slight decrease in stiffness as discussed previously but a significant increase in the force to cause an out of plane instability. It was also observed that the slope of the plastic portion of the characteristic curve is stiffer than all of the other arrangements, excluding the overly stiff X-arrangement. This lead to overall less deformation after the instability occurred. It is best to reduce the overall deformations to ensure no major loss of structural capacity and that the vessel will still remain operational. The bridge arrangement blocks the stress from flowing through the web frame towards the inner shell. The stress continues to build until the vertical member of the web stiffening yields,

at which point the load is able to transfer through the web frame and the horizontal members allowing for the instability to occur. It may be the horizontal members that span from the vertical member to the inner shell that allow for the increase in stiffness in the plastic region of the characteristic curve. More work would be required to investigate if it is the horizontal members are the cause for this increase in plastic stiffness.

This study has shown that if the web frame is considered as a beam, both in and out the plane of the web frame, the beam can be made less slender which should increase the load required to cause plasticity. For the out of plane response some form of web stiffening, preferably made up of horizontal and longitudinal members that can resist and transfer the load through the web frame past any cutouts or discontinuities, can be used to significantly increase the web frames capacity to resist out of plane instabilities. It appears that the out of plane instability is the limiting mechanism for the web frames studied within this research. For this study the bridge with access hole ring arrangement performed the best. Although the web frame had a slightly less stiff response in the elastic region when compared to other arrangements, it increased the required load to cause in plane plastic behaviour, as well as the force to cause an out of plane instability. Furthermore, even after the load has caused an instability, the bridge and ring arrangement increased the stiffness of the plastic response region.

It is important to note that for this study the geometry from the lowest capacity model from the DOE study was used, meaning there was not a specific polar class being studied. The factors and their levels along with the load, was setup to ensure a large range of polar classes could be studied. It would be the responsibility of the designer to ensure their design is checked against a specific polar class load level as dictated in the IACS rules. For future work, it would be beneficial to analyze each of the runs against the rules which prescribe the thickness, spans, etc. to approximate which polar class each run was and then analyze the response of the web frame for that polar class load.

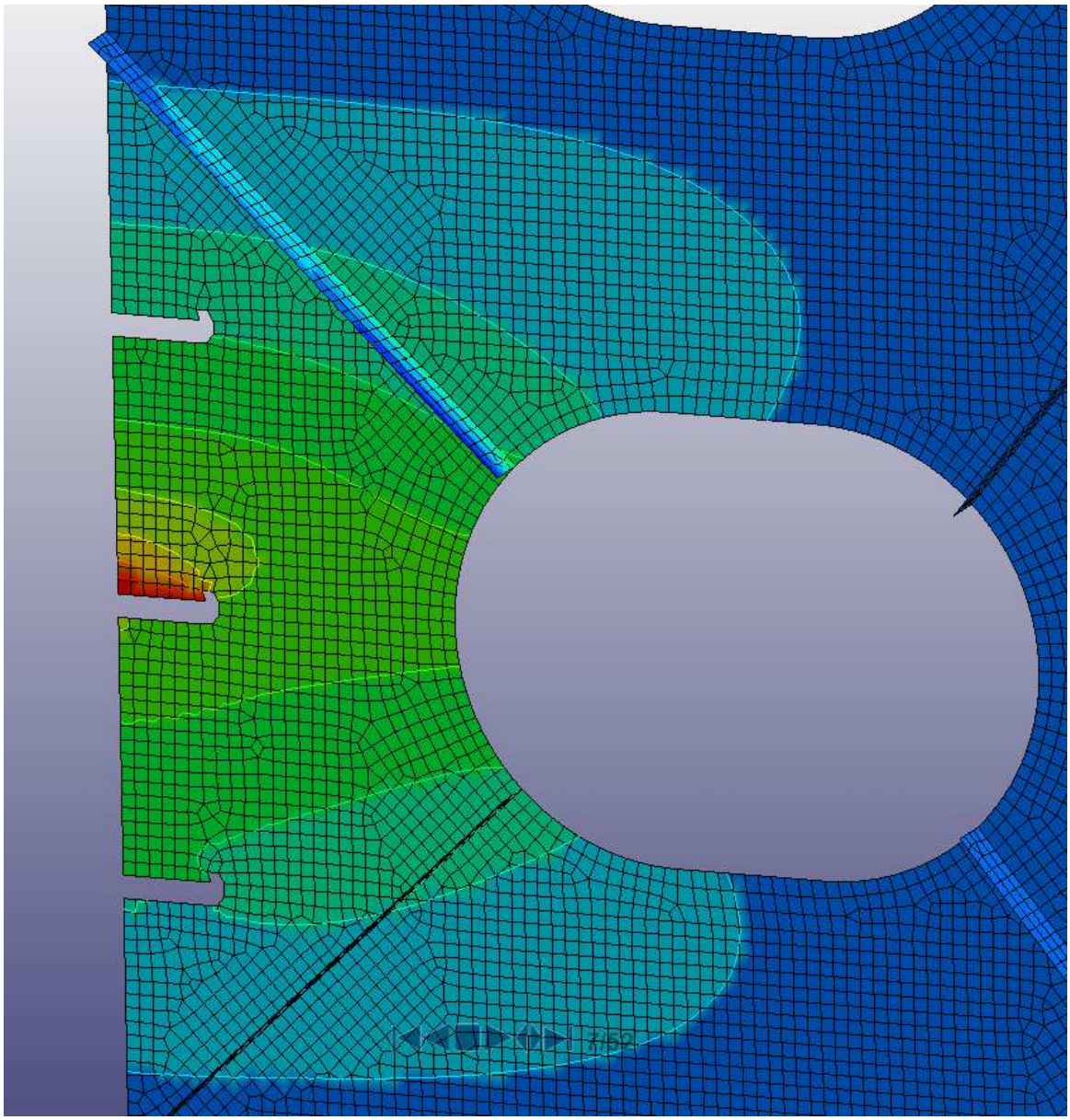

Figure 4-18 Load Concentration for X Web Frame Stiffening Arrangement

4.3 Web Frame Stiffening for PC7

The results and lessons learned from the DOE analysis were applied to the PC7 structure which was discussed earlier in Chapter 3. Four different arrangements were prepared and analyzed. The four arrangements were a basic no added stiffening case, access hole ring

arrangement, penetration ring arrangement and a similar bridge stiffening arrangement to the previous study in section 4.2. There are several differences that should be noted between the DOE structures analyzed and the PC7 structures used in this research. The DOE structures had decks spaced maximum 3.6m apart, the PC7 structure has a much larger span of 6m. This causes the buckling to go from an in plane regular buckle to a shear buckle. Another important difference is the shape of the access holes. The DOE structures had an oval/ellipsoid shape whereas the PC7 structure has circular cutouts. This can cause the structure to respond differently due to the stress not being as concentrated in the circular access holes compared to the oval/ellipsoid access holes. The size of the structure (thickness, depth, longitudinal size, etc.) is in general smaller for the PC7 model than for the DOE structures, however the design load is also smaller. Finally, the bridge arrangement differs from that of the study done in section 4.2. As the decks were spaced much closer for the DOE geometry only 2 horizontal stiffening members were used. The PC7 case has very large spacing between decks so several more horizontal stiffening members have been added in between the access holes, extending from the vertical member to the inner shell longitudinals. Please see Figure 4-19 below showing the PC7 web frame stiffening arrangement. The thickness of the web frame stiffening is 10mm with a height of 100mm, the same stiffening used for the section 4.2 web frame stiffening models.

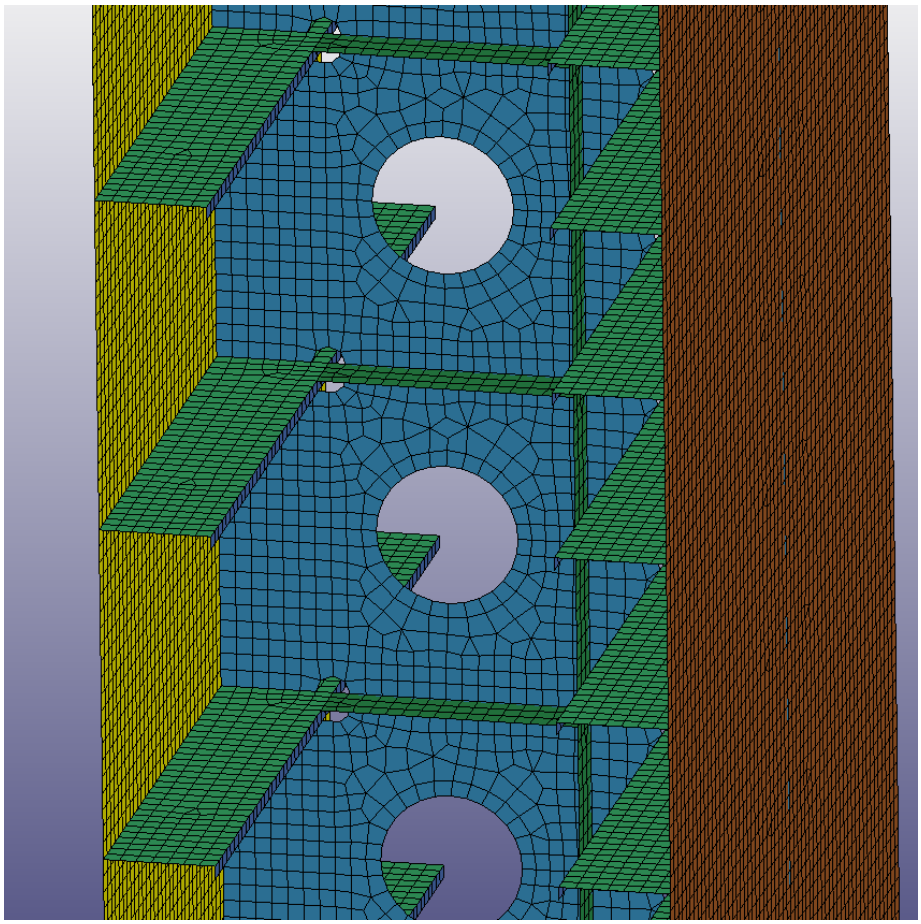

Figure 4-19 PC7 Web Frame Stiffening Arrangement

The in and out of plane responses were extracted from the numerical models and the characteristic force displacement curves were plotted. As the initial structure was designed to a specific polar class load level, the design load as well as 1.5 and 2 times the design load were also added to the plots. Please see Figure 4-20 and Figure 4-21 for the in and out of plane characteristic force displacement curves for the PC7 web frame stiffening arrangements.

When analyzing the in-plane results the four arrangements performed nearly identically in the elastic response region with yield occurring after the design force has been reached. This means that the initial structural design of the shell plating, longitudinals and web frames was done sufficiently well. After the yield point some of the arrangements begin to increase the stiffness of the plastic portion and allow for a greater overload capacity. The no-stiffening case, case 1 in both characteristic curves, has a greater stiffness and more capacity than the penetration ring case. As discussed in the previous section the penetration rings, case 3 in the plots below, would not work in reality due to their complexity and potential difficulties during installation. In the case of the PC7 web frame stiffening study they actually concentrated the load into the cutouts/penetrations for the longitudinals, causing them to have a reduced capacity when compared to the other stiffening arrangements. This was true for both the in and out of plane response. This makes the penetration rings undesirable for any potential design.

The access hole ring case, case 2, provided a significant increase in the capacity and stiffness of the web frame for both the in and out of plane response. For the in plane response it compares to the bridge arrangement in terms of stiffness and capacity. This result is in line with the way the load builds through the web frame for the PC7 structure. The load initially transfers from the side shell where the load patch is applied, into the longitudinals and web frames. In the web frame the load initially concentrates in the penetrations. As the load is increased it begins to concentrate at the access holes in the middle of the web frame. When the elastic limit is reached the web frame first goes

plastic around the access hole, which is the location the out of plane instability occurs. By adding the access rings the load is redistributed around the access holes delaying the out of plane instability. The bridge arrangement works similarly, except instead of redistributing the load around the access hole it redistributes the load into the web frame, above and below the load patch, until the load causes the web frame stiffening to yield, after which an out of plane instability occurs. It is important to note that the access ring out of plane response went out of plane in one direction initially but as the load continued to increase the web frame came back in the opposite direction. This is likely due to the added stiffness from the access hole ring in the cutout.

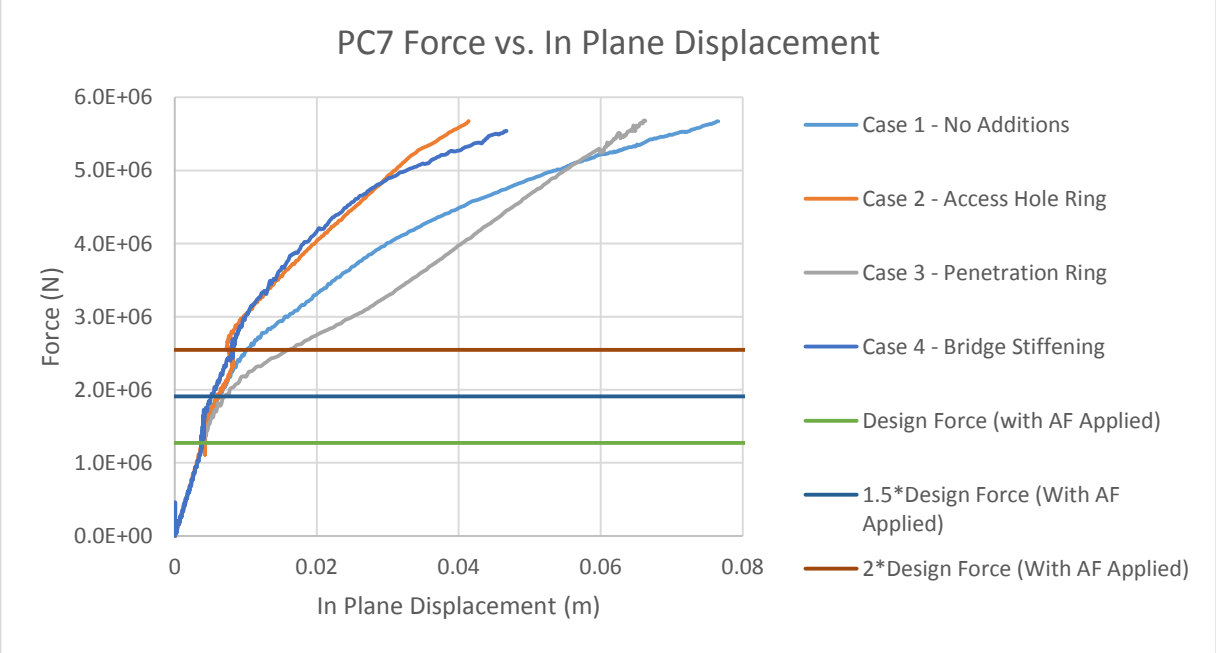

Figure 4-20 Characteristic Force In Plane Displacement Curve for PC7 Web Frame Stiffening Arrangements

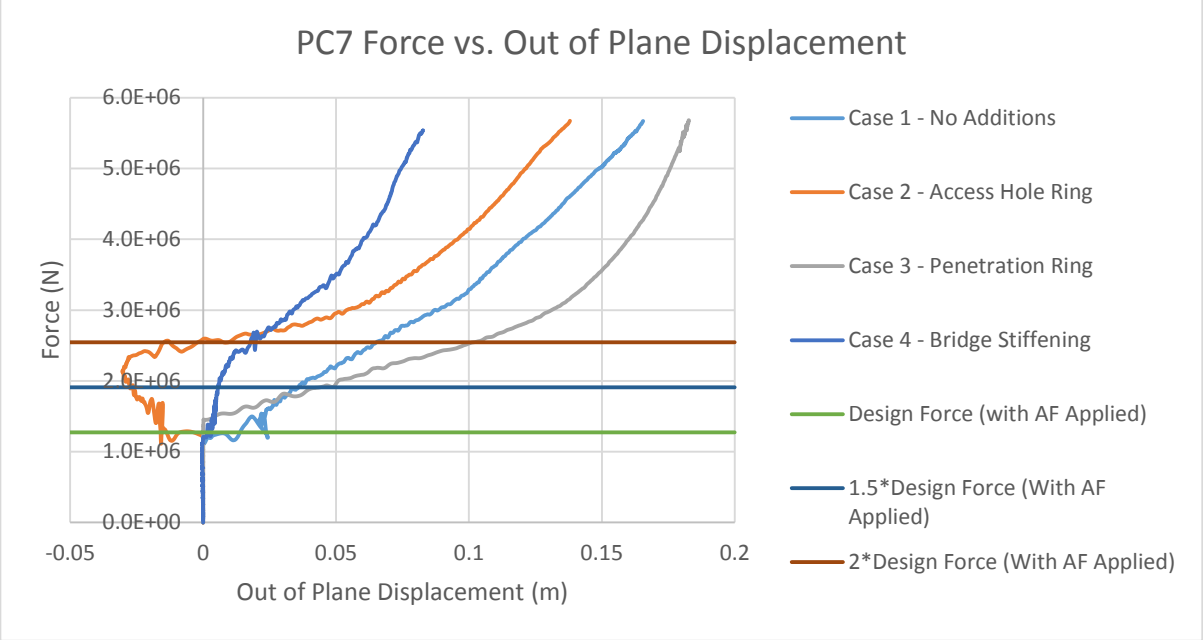

Figure 4-21 Characteristic Force Out of Plane Displacement Curve for PC7 Web Frame Stiffening Arrangements

Note that for the access hole ring case in Figure 4-21, the web frame initially deforms in the negative direction. This is due to the circular shape of the access hole ring redistributing the load through the web frame. As more force is applied and the access ring yields and the web frame deforms similar to the other arrangements. The bridge arrangement gave the best response for the PC7 structure. It provided an increase in stiffness in the plastic region, to the point where there is almost no out of plane instability and just normal plasticity. The bridge arrangement also caused most of the plastic deflection to be concentrated between the vertical stiffening member and the side shell structural components. The results from this PC7 study are in line with the DOE analysis. Access hole rings can increase the stiffness and capacity of a web frame for both the in

and out of plane response. The bridge arrangements, or some form of web frame stiffening that combines vertical and horizontal members around cutouts or other discontinuities, increases the stiffness both in and out of plane. In the PC7 case, it nearly stopped the out of plane instability from forming at twice the design load.

Chapter 5 Conclusions and Recommendations

5.1 Conclusions

This research focused on developing general guidelines for conducting a NFEA for polar class ship design as well as some design considerations that should be taken into account to ensure the design will be sufficient in accidental overload scenarios. Many designers overlook the importance of choosing a solver capable of completing NFEA. For most overload scenarios, the solver will require both material and geometric nonlinear capabilities. Depending on how the load is modelled, an indenter may be used which requires nonlinear boundary capabilities in the form of contact. These nonlinearities come with a significant computational cost but are required for highly deformed structures due to overload.

There are many important other considerations that must be included in a model such as a material model that is at minimum a bilinear model to ensure the plastic behaviour is captured. If possible, material test data should be used for a material model. An elastic perfectly plastic model can be used to be conservative but can lead to numerical solution issues due to the larger deformations. The boundary conditions applied to the model must be as close to reality as possible. If that is not possible the model must be large enough to ensure that the boundary conditions do not have an effect on the results of the analysis. The geometry must be modeled large enough to ensure there are no boundary effects but not too large that the computational time becomes prohibitive. It is also important that all

of the important structural components have been modeled as well as some finer design details such as lugs.

The applied load is prescribed in the IACS rules, as a uniform patch load. This type of load only covers a single load scenario, depending on the operational profile of a vessel more scenarios may be required to be analyzed with different load conditions. Consideration must also be given to the type of elements that will be used. It is also important to consider the element formulation used for the FE analysis. If computing power is plentiful it is best to use a more robust formulation, such as H-L for shell elements compared to the less robust but more computationally efficient B-T formulation. Another important aspect of any FE model is the mesh. The mesh must be fine enough to capture all of the behaviours, especially in highly nonlinear cases, but large enough that the computational time is not prohibitively high. A mesh convergence analysis should be done to find the point at which the element size no longer has an effect on the results of the simulation. It is also important to ensure that the elements in the mesh are properly formed; specifically the majority of the elements for a shell mesh should be square with an aspect ratio of one. Degenerate elements such as triangular elements for shell meshes should only be used in transitional areas between different components. As part of the mesh convergence analysis it is also important to ensure that the hourglassing energy of the model is below 5% of the total energy if reduced integration elements have been used. If fully integrated elements have been used shear locking or volumetric locking may occur. It is suggested that reduced integration elements be used for all NFEA as the

effects of hourglassing are less than those from shear or volumetric locking, as well as reducing the computational time of the model. In short, the finite element code being used to solve the numerical models should have nonlinear finite element capabilities, specifically nonlinear material and geometric capabilities. The designer/analyst must also take appropriate action to ensure the model is as accurate as possible through the use of proper geometric model techniques, element type and formulation selection. This combined with proper model checking for things such as hourglassing and locking will allow for an accurate solution to be reached.

As shown from the research done within this thesis all structural members in way of the load should be modeled as they influence the overall response of the structure. This is especially true for design details such as cutouts/penetrations as well as lugs which directly affect the web frames capacity. It was shown that as more cutouts are included a frame's elastic capacity decreases significantly. The inclusion of the longitudinal penetrations also reduces the stiffness of the elastic response. By adding lugs to the numerical model the elastic stiffness increases as well as the web frames elastic capacity. This was true for both low ice class, the PC7 structure in this thesis and high ice class, the PC3 structure in this thesis. As such it is suggested that for any ice class being analyzed with NFEA, all structural members that will absorb energy from the applied load should be modelled. As a minimum structural details that remove material, such as cutouts and penetrations should be modeled in the way of the load, i.e. in the span between the decks where the load. If the load is applied over multiple spans the cutout details should be

modeled in both spans. Preferably, cutout details should be modeled in the entire model but this can be a very time consuming process. Structural details such as lugs should also be modeled in way of the load. Even though excluding them would lead to a more conservative structure it was shown in this thesis that including these details can change both the stiffness and capacity of the web frame.

It is difficult to determine exact criteria to prescribe when a web frame's design has passed or failed when considering overload scenarios. It was shown in this thesis that the characteristic force displacement curve is an excellent tool for studying the response of a web frame. The stiffness and capacity are very easily obtained from the characteristic force displacement curve for both the elastic and plastic portions of the response curves. Two main responses were studied in this thesis, the in and out of plane response of the web frames using characteristic force displacement curves. These were chosen instead of the resultant characteristic curve as it was noticed that the out of plane response was usually the limiting factor that drove the failure of the web frames. This was usually in the form of an out of plane instability such as buckling. By designing the frames to withstand the out of plane instabilities a ship gains considerable overload capacity.

The DOE experiment showed that the in plane response could be improved by treating the web frame as a beam in each of its principal directions. By ensuring the beam is not slender, considerable overload capacity can be obtained but this comes with a weight

penalty. A somewhat complex equation can be used as a first estimate of the force a web frame can sustain until it exhibits plastic behaviour for the in plane response. The out of plane response equation determined from the DOE analysis was too complex to use in a design or first estimate capacity. In order to investigate the out of plane response and how it could be improved, different web frame stiffening arrangements were analyzed and compared against the baseline no stiffening case for the lowest capacity frame from the DOE analysis. It was found that any addition of structure increases the capacity for both in and out of plane response. The penetration rings were shown to add very little to the frames in and out of plane capacity and are not practical in reality. The X stiffening arrangement as described above was shown to concentrate the load into the access hole or produce an overly stiff response, to the point that stresses were approaching 2000 MPa, an unobtainable high stress. The inclusion of access hole rings lead to an increase in both the in and out of plane capacity and stiffness of the web frame. The access hole rings are easily modeled in most FEA commercial codes and would be relatively cheap and easy to install in reality. The arrangement that gave the biggest improvement to the in and out of plane response, almost to the point that the out of plane instability would become normal plastic deformation, was the bridge arrangement. The horizontal and vertical stiffening placed around the access hole and penetrations allowed the load to spread through the web frame and inner shell instead of concentrating in the discontinuous cutouts. By combining the bridge web frame stiffening and the access hole rings the web frame increased in capacity significantly.

The downside of the DOE analysis is the structure is not based on a real design or to a specific polar class. In order to better understand how the stiffening arrangements effect a more reality based design, the web frame stiffening arrangements were added to the PC7 model and the in and out of plane responses were analyzed. The results were consistent with the DOE experiment, the penetration rings added very little to the capacity of the web frames, while the access rings and bridge arrangements added a significant amount of capacity and stiffness to the in and out of plane response for the web frames. As before, the bridge arrangement added enough stiffness to the out of plane response that the instability almost did not form.

To conclude, the following criteria are suggested when using nonlinear finite element analysis to determine if a design is acceptable: For PC5 and lower polar class apply 1.5 times the design load determined from the IACS rules to a properly prepared finite element model. If the characteristic force displacement curves for the web frames under load have the elastic capacity at or above the design load both in and out of plane and that the out of plane instability has not occurred until after 1.5 times the load, the web frame design should be considered sufficient. For PC4 and above the same criteria applies but only for 1.25 times the design load. This is due to the higher polar classes having significantly higher design loads than lower polar classes. See Table 5-1 below outlining the load that should be applied based on the polar class of the design. These values have been chosen based on the previous research done by Pearson et al. (2015), which used 1.5 times the design load and the plastic strain as an acceptance criterion. Further work

should be done, specifically determining an overload factor that the instability has not occurred at or before, for each polar class. The factors described above serve as a starting point for future researchers.

Table 5-1: Load Factors for Specific Polar Classes

Polar Class	Applied Load Factor
PC1	1.25
PC2	1.25
PC3	1.25
PC4	1.25
PC5	1.50
PC6	1.50
PC7	1.50

5.2 Recommendations & Future Work

Several areas could be expanded upon to extend the research in this thesis. The first would be to model other polar class hull structures, preferably all remaining polar classes. This would allow for better understanding of the web frames in and out of plane responses at low, intermediate and high polar class. This would also allow for more investigations into different stiffening arrangements and optimizing them around specific polar class load levels to reduce the weight of the additional structure without sacrificing strength. It would also be beneficial to test different structural additions such as brackets that are welded from the longitudinal to the web frame or from the underside of the

longitudinal to the side shell, for the various polar classes, to determine which have the greatest impact on the web frame's response. It is important to note that the PC3 structure should have been initially redesigned due to poor web frame performance before the design force has been reached. In future iterations, the PC3 structural arrangement would be changed to ensure there was no early failure. In general, the models were still useful and gave insight into how the web frames in polar class ships responds under load for different arrangements.

One of the main goals of the DOE analysis was to create simple equations that could be used to determine a web frames in and out of plane capacity based on simple design factors. There proved to be many interacting factors making this goal incredibly difficult to achieve. A subsequent DOE analysis could be done to better understand the interacting factors and their impact on the in and out of plane response. A DOE analysis could also have been used to quantify the differences between the different web frame stiffening arrangements. The same thing could have been done to better understand and quantify the effects of cutouts and penetrations on the web frame's capacity and stiffness. Due to time restrictions lugs were not added to the DOE analysis numerical models. It was shown earlier in the thesis that the lugs changed the response enough to include in most numerical studies. If more time was available the DOE models would be rerun with lugs included in every model. It would also be beneficial to complete a study to determine and quantify which members of the bridge arrangement web frame stiffening cases cause the increase in capacity for both the in and out of plane responses. It is recommended to

check each of the DOE numerical models against the IACS rules to determine which polar class each model is, making it easier to compare the results from different numerical models and even other designs. Finally, load multiplication factors should be determined for all polar classes, instead of the broad PC7-PC5 and PC4-PC1 having a load factor of 1.5 and 1.25 respectively. Higher polar classes have incredibly large, stiff structures and likely do not need a multiplication factor, but work would need to be done to confirm this.

Chapter 6 References

Cook, R. D., Malkus, D. S., Plesha, M. E. and Witt, R. J. 2002. "*Concepts and Applications of Finite Element Analysis. Fourth Edition"*. John Wiley & Sons, Inc.

Daley, C. G. and A. Kendrick. 2002. *"Framing Design in the Unified Requirements for Polar Class Ships"*.

Daley, C. G. and Hermanski, G. 2005. "*Ship Frame/Grillage Research Program Investigation of Finite Element Analysis Boundary Conditions".* National Research Council.

Daley, C. G. and Hussein, A. 2007. "*Ultimate Strength of Frames and Grillages Subject to Lateral Loads - an Experimental Study"*. Practical Design of Ships and Floating Structures, Houston, Texas, USA.

Daley, C. G. 2002. "Derivation of Plastic Framing Requirements for Polar Ships." *Marine Structures* 15: 543.

Det Norske Veritas. 2013. *Determination of Structural Capacity by Non-Linear FE Analysis Methods*: Det Norske Veritas AS.

Finnish and Swedish Ice Class Rules, 2010. *The Structural Design and Engine Output Required of Ships For Navigation in Ice.* Finnish and Swedish Maritime Associations.

IACS. 2011. *Requirements Concerning POLAR CLASS*: International Association of Classification Societies.

LSTC, 2017. *LS-DYNA Keyword User's Manual, Volume 1.* Livermore Software Technology Corporation.

Pearson, D., R. Hindley, and J. Crocker. 2015. "*Icebreaker Grillage Structural Interaction and the Characteristic Stiffness Curve"*. Providence, Rhode Island, USA.

Quinton, B., C. G. Daley, R. Gagnon, and B. Colbourne. 2016. *"Guidelines for the Nonlinear Finite Element Analysis of Hull Response to Moving Loads on Ships and Offshore Structures."* Ships and Offshore Structures.

Appendix A Sample K-File, PC7 Structure

```
$# LS-DYNA Keyword file created by LS-PrePost 4.1 - 08Mar2014(14:00)
$# Created on Feb-28-2017 (13:56:01)
*KEYWORD
*TITLE
$# title
LS-DYNA keyword deck by LS-PrePost
*CONTROL_ENERGY
$#    hgen      rwen    slnten     rylen
         2         2         1         1
*CONTROL_MPP_IO_NODUMP
*CONTROL_TERMINATION
$#  endtim    endcyc     dtmin    endeng    endmas
  1.000000         0     0.000     0.000     0.000
*DATABASE_ELOUT
$#      dt    binary      lcur     ioopt   option1   option2   option3   option4
 1.0000E-3         0         0         1         0         0         0         0
*DATABASE_GLSTAT
$#      dt    binary      lcur     ioopt
 1.0000E-3         0         0         1
*DATABASE_MATSUM
$#      dt    binary      lcur     ioopt
 1.0000E-3         0         0         1
*DATABASE_NCFORC
$#      dt    binary      lcur     ioopt
 1.0000E-3         0         0         1
*DATABASE_NODOUT
$#      dt    binary      lcur     ioopt   option1   option2
 1.0000E-3         0         0         1     0.000         0
*DATABASE_RCFORC
$#      dt    binary      lcur     ioopt
 1.0000E-3         0         0         1
*DATABASE_SLEOUT
$#      dt    binary      lcur     ioopt
 1.0000E-3         0         0         1
*DATABASE_SPCFORC
$#      dt    binary      lcur     ioopt
 1.0000E-3         0         0         1
*DATABASE_BINARY_D3PLOT
$#      dt      lcdt      beam     npltc    psetid
 2.0000E-2         0         0         0         0
$#   ioopt
         0
*BOUNDARY_SPC_SET
$#    nsid       cid      dofx      dofy      dofz     dofrx     dofry     dofrz
         1         0         1         1         1         1         1         1
*SET_NODE_LIST_TITLE
NODESET(SPC) 1
$#     sid       da1       da2       da3       da4    solver
         1     0.000     0.000     0.000     0.000MECH
$#    nid1      nid2      nid3      nid4      nid5      nid6      nid7      nid8
      4485      4491      4492      4493      4494      4495      4496      4497
      4498      4499      4500      4501      4502      4503      4504      4505
      4506      4507      4508      4509      4510      4511      4512      4513
      4514      4515      4516      4517      4518      4519      4520      4521
```

4522	4523	4524	4525	4526	4527	4528	4529
4530	4531	4532	4533	4534	4535	4536	4537
4538	4539	4796	4801	4802	4803	4804	4805
4806	4807	4808	4809	4810	4811	4812	4813
4814	4815	4816	4817	4818	4819	4820	4821
4822	4823	4824	4825	4826	4827	4828	4829
4830	4831	4832	4833	4834	4835	4836	4837
4838	4839	4840	4841	4842	4843	4844	4845
4846	4847	4848	4849	5107	5112	5113	5114
5115	5116	5117	5118	5119	5120	5121	5122
5123	5124	5125	5126	5127	5128	5129	5130
5131	5132	5133	5134	5135	5136	5137	5138
5139	5140	5141	5142	5143	5144	5145	5146
5147	5148	5149	5150	5151	5152	5153	5154
5155	5156	5157	5158	5159	5160	5419	5423
5424	5425	5426	5427	5428	5429	5430	5431
5432	5433	5434	5435	5436	5437	5438	5439
5440	5441	5442	5443	5444	5445	5446	5447
5448	5449	5450	5451	5452	5453	5454	5455
5456	5457	5458	5459	5460	5461	5462	5463
5464	5465	5466	5467	5468	5469	5470	5471
5472	37200	37206	37207	37208	37209	37210	37211
37212	37213	37214	37215	37216	37217	37218	37219
37220	37221	37222	37223	37224	37225	37226	37227
37228	37229	37230	37231	37232	37233	37234	37235
37236	37237	37238	37239	37240	37241	37242	37243
37244	37245	37246	37247	37248	37249	37250	37251
37252	37253	37254	37511	37515	37516	37517	37518
37519	37520	37521	37522	37523	37524	37525	37526
37527	37528	37529	37530	37531	37532	37533	37534
37535	37536	37537	37538	37539	37540	37541	37542
37543	37544	37545	37546	37547	37548	37549	37550
37551	37552	37553	37554	37555	37556	37557	37558
37559	37560	37561	37562	37563	37564	37827	37828
37829	37830	37831	37832	37833	37834	37835	37836
37837	37838	37839	37840	37841	37842	37843	37844
37845	37846	37847	37848	37849	37850	37851	37852
37853	37854	37855	37856	37857	37858	37859	37860
37861	37862	37863	37864	37865	37866	37867	37868
37869	37870	37871	37872	37873	37874	37875	38134
38138	38139	38140	38141	38142	38143	38144	38145
38146	38147	38148	38149	38150	38151	38152	38153
38154	38155	38156	38157	38158	38159	38160	38161
38162	38163	38164	38165	38166	38167	38168	38169
38170	38171	38172	38173	38174	38175	38176	38177
38178	38179	38180	38181	38182	38183	38184	38185
38186	38187	82057	82058	82059	82060	82061	82062
82109	82114	82115	82116	82117	82118	82119	82120
82121	82122	82123	82124	82125	82126	82127	82128
82129	82130	82131	82132	82133	82219	82224	82225
82226	82227	82228	82229	82267	82268	82269	82270
82271	82272	82283	82289	82290	82291	82292	82293
82294	82295	82296	82297	82298	82299	82300	82301
82302	82303	82304	82305	82306	82307	82308	82428

82433	82434	82435	82436	82437	82438	94258	94262
94263	94264	94265	94266	94267	94268	94269	94270
94271	94272	94273	94274	94275	94276	94277	94278
94279	94280	94281	94282	94383	94384	94385	94386
94387	94388	94416	94417	94418	94419	94420	94421
4434	4486	4487	4488	4489	27850	27875	27876
27877	27878	27879	27880	27881	27882	27883	27884
27885	27886	27887	27888	27889	27890	27891	27892
27893	27894	28421	28422	28423	28424	28425	28426
28427	28428	28429	28430	28431	28432	28433	28434
28435	28436	28437	28438	28439	28440	28968	28969
28970	28971	28972	28973	28974	28975	28976	28977
28978	28979	28980	28981	28982	28983	28984	28985
28986	29488	29514	29515	29516	29517	29518	29519
29520	29521	29522	29523	29524	29525	29526	29527
29528	29529	29530	29531	29532	30035	30061	30062
30063	30064	30065	30066	30067	30068	30069	30070
30071	30072	30073	30074	30075	30076	30077	30078
30079	30080	30605	30630	30631	30632	30633	30634
30635	30636	30637	30638	30639	30640	30641	30642
30643	30644	30645	30646	30647	30648	31152	31153
31154	31155	31156	31157	31158	31159	31160	31161
31162	31163	31164	31165	31166	31167	31168	31169
31170	31672	31698	31699	31700	31701	31702	31703
31704	31705	31706	31707	31708	31709	31710	31711
31712	31713	31714	31715	31716	37150	37201	37202
37203	37204	65642	65667	65668	65669	65670	65671
65672	65673	65674	65675	65893	65928	65953	65954
65955	65956	65957	65958	65959	65960	65961	66179
66239	66240	66241	66242	66243	66244	66245	66246
66247	66465	66500	66525	66526	66527	66528	66529
66530	66531	66532	66533	66751	66811	66812	66813
66814	66815	66816	66817	66818	66819	67037	67097
67098	67099	67100	67101	67102	67103	67104	67105
67323	67383	67384	67385	67386	67387	67388	67389
67390	67391	67609	67669	67670	67671	67672	67673
67674	67675	67676	67677	67895	67956	67957	67958
67959	67960	67961	67962	67963	67964	67965	68207
68266	68267	68268	68269	68270	68271	68272	68273
68467	68527	68528	68529	68530	68531	68532	68533
68534	68535	68753	68813	68814	68815	68816	68817
68818	68819	68820	68821	69099	69100	69101	69102
69103	69104	69105	69106	69107	69370	69395	69396
69397	69398	69399	69400	69401	69402	69403	69404
69405	69406	69407	69408	69409	69410	69411	69412
69413	69931	69932	69933	69934	69935	69936	69937
69938	69939	124756	124757	124758	124759	124760	124761
124762	124964	124965	124966	124967	124968	124969	124970
125172	125173	125174	125175	125176	125177	125178	125380
125381	125382	125383	125384	125385	125386	125588	125589
125590	125591	125592	125593	125594	125796	125797	125798
125799	125800	125801	125802	126004	126005	126006	126007
126008	126009	126010	126212	126213	126214	126215	126216
126217	126218	126420	126421	126422	126423	126424	126425

126426	126628	126629	126630	126631	126632	126633	126634
126836	126837	126838	126839	126840	126841	126842	127044
127045	127046	127047	127048	127049	127050	127252	127253
127254	127255	127256	127257	127258	127460	127461	127462
127463	127464	127465	127466	127668	127669	127670	127671
127672	127673	127674	127876	127877	127878	127879	127880
127881	127882	128084	128085	128086	128087	128088	128089
128090	128292	128293	128294	128295	128296	128297	128298
128500	128501	128502	128503	128504	128505	128506	128708
128709	128710	128711	128712	128713	128714	128916	128917
128918	128919	128920	128921	128922	129124	129125	129126
129127	129128	129129	129130	129332	129333	129334	129335
129336	129337	129338	141494	141546	141598	141650	141702
141754	141806	141858	141910	141962	142014	142066	142118
142170	142222	142274	142326	142378	142430	142482	142534
142586	142638	149519	149520	149521	149522	149523	149524
149525	149526	149527	149528	149529	149530	149531	149532
149533	149534	149986	149987	149988	149989	149990	149991
149992	149993	149994	149995	149996	149997	149998	149999
150000	150001	150002	152037	152038	152039	152040	5392
5473	5474	5475	5476	32198	32268	32269	32270
32271	32272	32273	32274	32275	32276	32277	32278
32279	32280	32281	32282	32283	32284	32285	32286
32814	32815	32816	32817	32818	32819	32820	32821
32822	32823	32824	32825	32826	32827	32828	32829
32830	32831	32832	33290	33334	33359	33360	33361
33362	33363	33364	33365	33366	33367	33368	33369
33370	33371	33372	33373	33374	33375	33376	33810
33881	33882	33883	33884	33885	33886	33887	33888
33889	33890	33891	33892	33893	33894	33895	33896
33897	33898	33899	33900	34452	34453	34454	34455
34456	34457	34458	34459	34460	34461	34462	34463
34464	34465	34466	34467	34468	34469	34470	34973
34998	34999	35000	35001	35002	35003	35004	35005
35006	35007	35008	35009	35010	35011	35012	35013
35014	35015	35016	35474	35519	35544	35545	35546
35547	35548	35549	35550	35551	35552	35553	35554
35555	35556	35557	35558	35559	35560	35561	35562
36020	36090	36091	36092	36093	36094	36095	36096
36097	36098	36099	36100	36101	36102	36103	36104
36105	36106	36107	36108	38107	38188	38189	38190
38191	70192	70193	70194	70195	70196	70197	70198
70199	70200	70201	70453	70478	70479	70480	70481
70482	70483	70484	70485	70486	70487	70765	70766
70767	70768	70769	70770	70771	70772	70773	71025
71050	71051	71052	71053	71054	71055	71056	71057
71058	71059	71337	71338	71339	71340	71341	71342
71343	71344	71345	71597	71622	71623	71624	71625
71626	71627	71628	71629	71630	71631	71883	71909
71910	71911	71912	71913	71914	71915	71916	71917
72195	72196	72197	72198	72199	72200	72201	72202
72203	72480	72481	72482	72483	72484	72485	72486
72487	72488	72489	72767	72768	72769	72770	72771
72772	72773	72774	72775	72776	72777	73077	73078

```
     73079     73080     73081     73082     73083     73084     73085     73338
     73339     73340     73341     73342     73343     73344     73345     73346
     73347     73599     73624     73625     73626     73627     73628     73629
     73630     73631     73632     73633     73911     73912     73913     73914
     73915     73916     73917     73918     73919     74206     74207     74208
     74209     74210     74211     74212     74213     74214     74215     74216
     74217     74218     74219     74220     74221     74222     74223     74224
     74225    129540    129565    129566    129567    129568    129569    129570
    129748    129773    129774    129775    129776    129777    129778    129956
    129981    129982    129983    129984    129985    129986    130164    130189
    130190    130191    130192    130193    130194    130372    130397    130398
    130399    130400    130401    130402    130580    130605    130606    130607
    130608    130609    130610    130788    130813    130814    130815    130816
    130817    130818    130996    131021    131022    131023    131024    131025
    131026    131204    131229    131230    131231    131232    131233    131234
    131412    131437    131438    131439    131440    131441    131442    131620
    131645    131646    131647    131648    131649    131650    131828    131853
    131854    131855    131856    131857    131858    132036    132061    132062
    132063    132064    132065    132066    132244    132269    132270    132271
    132272    132273    132274    132452    132477    132478    132479    132480
    132481    132482    132660    132685    132686    132687    132688    132689
    132690    132868    132893    132894    132895    132896    132897    132898
    133076    133101    133102    133103    133104    133105    133106    133284
    133309    133310    133311    133312    133313    133314    133492    133517
    133518    133519    133520    133521    133522    133700    133725    133726
    133727    133728    133729    133730    133908    133933    133934    133935
    133936    133937    133938    134116    134141    134142    134143    134144
    134145    134146    142690    142742    142794    142846    142898    142950
    143002    143054    143106    143158    143210    143262    143314    143366
    143418    143470    143522    143574    143626    143678    143730    143782
    143834    150479    150480    150481    150482    150483    150484    150485
    150486    150487    150488    150489    150490    150491    150492    150493
    150494    150922    150947    150948    150949    150950    150951    150952
    150953    150954    150955    150956    150957    150958    150959    150960
    150961    150962    152147    152172    152173    152174         0         0
*LOAD_SHELL_SET_ID
$#      id                                                                heading
         1
$#    esid      lcid        sf        at
         1         1 6.3600E+6     0.000
*CONTACT_AUTOMATIC_GENERAL
$#     cid                                                                title
$#    ssid      msid     sstyp     mstyp    sboxid    mboxid       spr       mpr
         0         0         0         0         0         0         0         0
$#      fs        fd        dc        vc       vdc    penchk        bt        dt
     0.000     0.000     0.000     0.000     0.000         0     0.0001.0000E+20
$#     sfs       sfm       sst       mst      sfst      sfmt       fsf       vsf
  1.000000  1.000000     0.000     0.000  1.000000  1.000000  1.000000  1.000000
*PART
$# title
LSHELL1
$#     pid     secid       mid     eosid      hgid      grav    adpopt      tmid
         1         1         1         0         0         0         0         0
*SECTION_SHELL_TITLE
```

```
Inner Shell
$#   secid    elform      shrf       nip     propt   qr/irid     icomp     setyp
         1         1  0.833333         5         1         0         0         1
$#      t1        t2        t3        t4      nloc     marea      idof    edgset
 1.0000E-2 1.0000E-2 1.0000E-2 1.0000E-2     0.000     0.000     0.000         0
*MAT_PIECEWISE_LINEAR_PLASTICITY
$#     mid        ro         e        pr      sigy      etan      fail      tdel
         1 7850.00002.0000E+11  0.300000 3.5000E+8 2.0000E+9     0.000     0.000
$#       c         p      lcss      lcsr        vp
     0.000     0.000         0         0     0.000
$#    eps1      eps2      eps3      eps4      eps5      eps6      eps7      eps8
     0.000     0.000     0.000     0.000     0.000     0.000     0.000     0.000
$#     es1       es2       es3       es4       es5       es6       es7       es8
     0.000     0.000     0.000     0.000     0.000     0.000     0.000     0.000
*PART
$# title
LSHELL2
$#     pid     secid       mid     eosid      hgid      grav    adpopt      tmid
         2         2         1         0         0         0         0         0
*SECTION_SHELL_TITLE
Outer Shell
$#   secid    elform      shrf       nip     propt   qr/irid     icomp     setyp
         2         1  0.833333         5         1         0         0         1
$#      t1        t2        t3        t4      nloc     marea      idof    edgset
 1.5000E-2 1.5000E-2 1.5000E-2 1.5000E-2     0.000     0.000     0.000         0
*PART
$# title
LSHELL3
$#     pid     secid       mid     eosid      hgid      grav    adpopt      tmid
         3         9         1         0         0         0         0         0
*SECTION_SHELL_TITLE
lug overlap
$#   secid    elform      shrf       nip     propt   qr/irid     icomp     setyp
         9         1  0.833333         5         1         0         0         1
$#      t1        t2        t3        t4      nloc     marea      idof    edgset
 8.0000E-3 8.0000E-3 8.0000E-3 8.0000E-3     0.000     0.000     0.000         0
*PART
$# title
LSHELL4
$#     pid     secid       mid     eosid      hgid      grav    adpopt      tmid
         4         7         1         0         0         0         0         0
*SECTION_SHELL_TITLE
web frames
$#   secid    elform      shrf       nip     propt   qr/irid     icomp     setyp
         7         1  0.833333         5         1         0         0         1
$#      t1        t2        t3        t4      nloc     marea      idof    edgset
 8.0000E-3 8.0000E-3 8.0000E-3 8.0000E-3     0.000     0.000     0.000         0
*PART
$# title
LSHELL6
$#     pid     secid       mid     eosid      hgid      grav    adpopt      tmid
         6         5         1         0         0         0         0         0
*SECTION_SHELL_TITLE
long web
```

```
$#   secid    elform      shrf       nip     propt   qr/irid     icomp     setyp
         5         1  0.833333         5         1         0         0         1
$#      t1        t2        t3        t4      nloc     marea      idof    edgset
 1.0000E-2 1.0000E-2 1.0000E-2 1.0000E-2     0.000     0.000     0.000         0
*PART
$# title
LSHELL7
$#     pid     secid       mid     eosid      hgid      grav    adpopt      tmid
         7         6         1         0         0         0         0         0
*SECTION_SHELL_TITLE
long flange
$#   secid    elform      shrf       nip     propt   qr/irid     icomp     setyp
         6         1  0.833333         5         1         0         0         1
$#      t1        t2        t3        t4      nloc     marea      idof    edgset
 2.2580E-2 2.2580E-2 2.2580E-2 2.2580E-2     0.000     0.000     0.000         0
*PART
$# title
LSHELL8
$#     pid     secid       mid     eosid      hgid      grav    adpopt      tmid
         8         3         1         0         0         0         0         0
*SECTION_SHELL_TITLE
FB
$#   secid    elform      shrf       nip     propt   qr/irid     icomp     setyp
         3         1  0.833333         5         1         0         0         1
$#      t1        t2        t3        t4      nloc     marea      idof    edgset
 8.0000E-3 8.0000E-3 8.0000E-3 8.0000E-3     0.000     0.000     0.000         0
*PART
$# title
LSHELL9
$#     pid     secid       mid     eosid      hgid      grav    adpopt      tmid
         9         4         1         0         0         0         0         0
*SECTION_SHELL_TITLE
FB
$#   secid    elform      shrf       nip     propt   qr/irid     icomp     setyp
         4         1  0.833333         5         1         0         0         1
$#      t1        t2        t3        t4      nloc     marea      idof    edgset
 8.0000E-3 8.0000E-3 8.0000E-3 8.0000E-3     0.000     0.000     0.000         0
*DEFINE_CURVE
$#    lcid      sidr       sfa       sfo      offa      offo    dattyp
         1         0  1.000000  1.000000     0.000     0.000         0
$#              a1                  o1
             0.000               0.000
          1.000000            1.000000
          1.100000            1.000000
*SET_SHELL_LIST
$#     sid       da1       da2       da3       da4
         1     0.000     0.000     0.000     0.000
$#    eid1      eid2      eid3      eid4      eid5      eid6      eid7      eid8
     36846     36847     36849     36850     36851     36852     36853     36854
     36855     36857     36861     36862     36866     36869     36870     36873
     36874     36877     36878     36881     36882     36885     36887     36888
     36889     36891     36892     36897     36898     36902     36903     36904
     36905     36906     36907     36908     36909     36910     36911     36912
     36913     36915     36916     36917     36918     36919     36920     36921
```

36923	36924	36925	36926	36927	36928	36929	36930
36931	36932	36933	36934	36935	36936	36951	36952
36953	36954	36955	36956	36957	36965	36966	36967
36968	36969	36970	36971	36972	36973	36974	36975
36976	36977	36978	36979	36980	36981	36982	36983
36984	36985	36986	36987	36988	36989	36990	36991
36992	36993	36994	36995	36996	36997	36998	36999
37000	37001	37002	37003	37004	37005	37006	37007
37008	37009	37010	37011	37012	37013	37014	37015
37016	37017	37018	37019	37020	37021	37022	37023
37024	37025	37026	37027	37028	37029	37030	37031
37032	37033	37034	37035	37036	37037	37038	37039
37040	37041	37042	37043	37044	37045	37046	37047
37048	37049	37050	37051	37052	37053	37054	37055
37056	37057	37058	37059	37060	37061	37062	37063
37064	37065	37066	37067	37068	37069	37070	37071
37072	37073	37074	37075	37076	37077	37078	37079
37080	37081	37082	37083	37084	37085	37086	37087
37088	37089	37090	37091	37092	37093	37094	37095
37096	37097	37098	37099	37100	37101	37104	37105
37106	37107	37108	37109	37110	37111	37112	37114
37115	37116	37117	37120	37121	37122	37123	37124
37125	37128	37129	37130	37131	37132	37133	37136
37137	37138	37139	37140	37142	37143	37144	37149
37150	37151	37152	37155	37156	37157	37170	37171
37172	37173	37174	37175	37176	37177	37178	37179
37180	37181	37182	37183	37184	37193	37194	37195
37196	37197	37198	37199	37200	37201	37202	37203
37204	37205	37206	37214	37215	37216	37217	37218
37219	37220	37228	37229	37230	37231	37232	37233
37234	37235	37236	37237	37238	37239	37240	37241
37242	37243	37244	37245	37246	37247	37248	37249
37250	37251	37252	37253	37254	37255	37256	37257
37258	37259	37260	37261	37262	37263	37264	37265
37266	37267	37268	37269	37270	37271	37272	37273
37274	37275	37276	37277	37278	37279	37280	37281
37282	37283	37284	37285	37286	37287	37288	37289
37290	37291	37292	37293	37294	37295	37296	37297
37298	37299	37300	37301	37302	37303	37304	37305
37306	37307	37308	37309	37310	37311	37312	37313
37314	37315	37316	37317	37318	37319	37320	37321
37322	37323	37324	37325	37326	37327	37328	37329
37330	37331	37332	37333	37334	37335	37336	37337
37338	37339	37340	37341	37342	37343	37344	37345
37346	37347	37348	37349	37350	37351	37352	37353
37354	37355	37356	37357	41173	41174	41176	41177
41178	41179	41180	41181	41182	41184	41186	41188
41189	41190	41194	41195	41196	41197	41198	41201
41202	41203	41204	41205	41208	41209	41210	41211
41216	41217	41218	41219	41224	41225	41226	41230
41231	41232	41233	41234	41240	41242	41243	41244
41245	41246	41247	41248	41250	41252	41253	41255
41257	41258	41259	41260	41261	41262	41266	41267
41268	41273	41274	41275	41276	41281	41282	41283

```
     41284     41286     41287     41288     41289     41290     41291     41292
     41299     41300     41301     41302     41303     41304     41305     41306
     41307     41308     41309     41310     41311     41312     41313     41314
     41315     41316     41317     41318     41319     41320     41321     41322
     41323     41324     41325     41326     41327     41328     41329     41330
     41331     41332     41333     41334     41335     41336     41337     41338
     41339     41340     41341     41342     41343     41344     41345     41346
     41347     41348     41349     41350     41351     41352     41353     41354
     41355     41356     41357     41358     41359     41360     41361     41362
     41363     41364     41365     41366     41367     41368     41369     41370
     41371     41372     41373     41374     41375     41376     41377     41378
     41379     41380     41381     41382     41383     41384     41385     41386
     41387     41388     41389     41390     41391     41392     41393     41394
     41395     41396     41397     41398     41399     41400     41401     41402
     41403     41404     41405     41406     41407     41408     41409     41410
     41411     41412     41413     41414     41415     41416     41417     41418
     41419     41420     41421     41422     41423     41424     41425     41426
     41427     41428     41431     41432     41433     41434     41435     41436
     41437     41438     41439     41441     41443     41445     41448     41449
     41450     41451     41452     41455     41456     41457     41458     41459
     41462     41463     41468     41469     41470     41471     41476     41477
     41478     41479     41483     41484     41485     41491     41492     41493
     41494     41495     41497     41498     41499     41500     41501     41502
     41503     41504     41505     41507     41508     41509     41511     41513
     41515     41516     41517     41518     41522     41523     41524     41525
     41530     41531     41532     41533     41538     41540     41541     41542
     41549     41550     41551     41552     41553     41554     41555     41556
     41557     41558     41559     41560     41561     41562     41563     41564
     41565     41566     41567     41568     41569     41570     41571     41572
     41573     41574     41575     41576     41577     41578     41579     41580
     41581     41582     41583     41584     41585     41586     41587     41588
     41589     41590     41591     41592     41593     41594     41595     41596
     41597     41598     41599     41600     41601     41602     41603     41604
     41605     41606     41607     41608     41609     41610     41611     41612
     41613     41614     41615     41616     41617     41618     41619     41620
     41621     41622     41623     41624     41625     41626     41627     41628
     41629     41630     41631     41632     41633     41634     41635     41636
     41637     41638     41639     41640     41641     41642     41643     41644
     41645     41646     41647     41648     41649     41650     41651     41652
     41653     41654     41655     41656     41657     41658     41659     41660
     41661     41662     41663     41664     41665     41666     41667     41668
     41669     41670     41671     41672     41673     41674     41675     41676
     41677     41678     41679     41680     41681     41682     41683     41684
     43220     43222     43223     43224     43225     43226     43227     43228
     43475     43477     43479     43480     43481     43482     43483     43484
     51643     51645     51652     51653     51660     51661     51668     51672
     51906     51913     51914     51921     51922     51927     51928     51929
         0         0         0         0         0         0         0         0
*END
```

Appendix B DOE Experimental Results

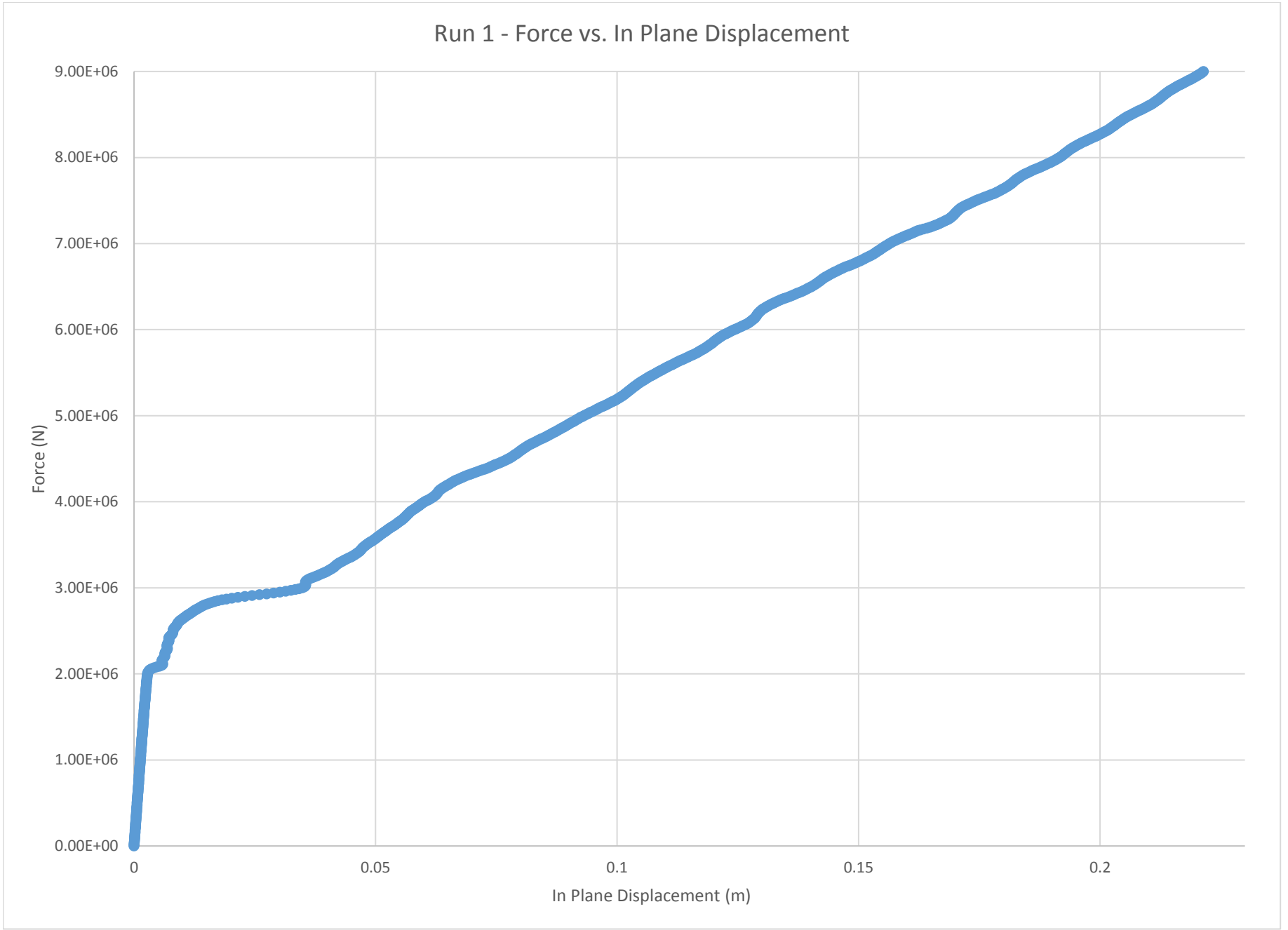
Run 1 - Force vs. In Plane Displacement
9.00E+06
8.00E+06
7.00E+06
6.00E+06
5.00E+06
4.00E+06
3.00E+06
2.00E+06
1.00E+06
0.00E+00
Force (N)
0
0.05
0.1
0.15
0.2
In Plane Displacement (m)

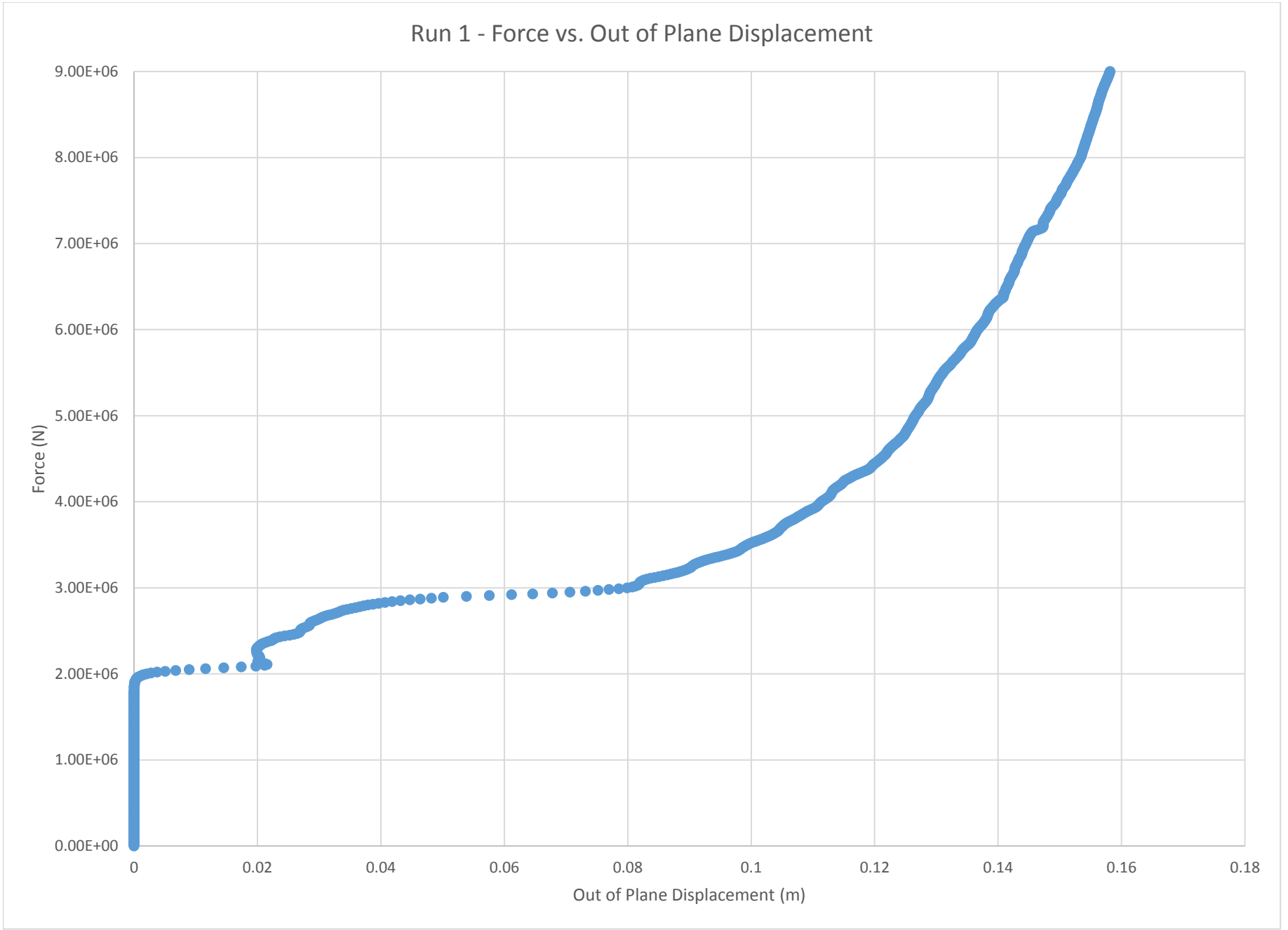
Run 1 - Force vs. Out of Plane Displacement
Force (N)
9.00E+06
8.00E+06
7.00E+06
6.00E+06
5.00E+06
4.00E+06
3.00E+06
2.00E+06
1.00E+06
0.00E+00
0
0.02
0.04
0.06
0.08
0.1
0.12
0.14
0.16
0.18
Out of Plane Displacement (m)

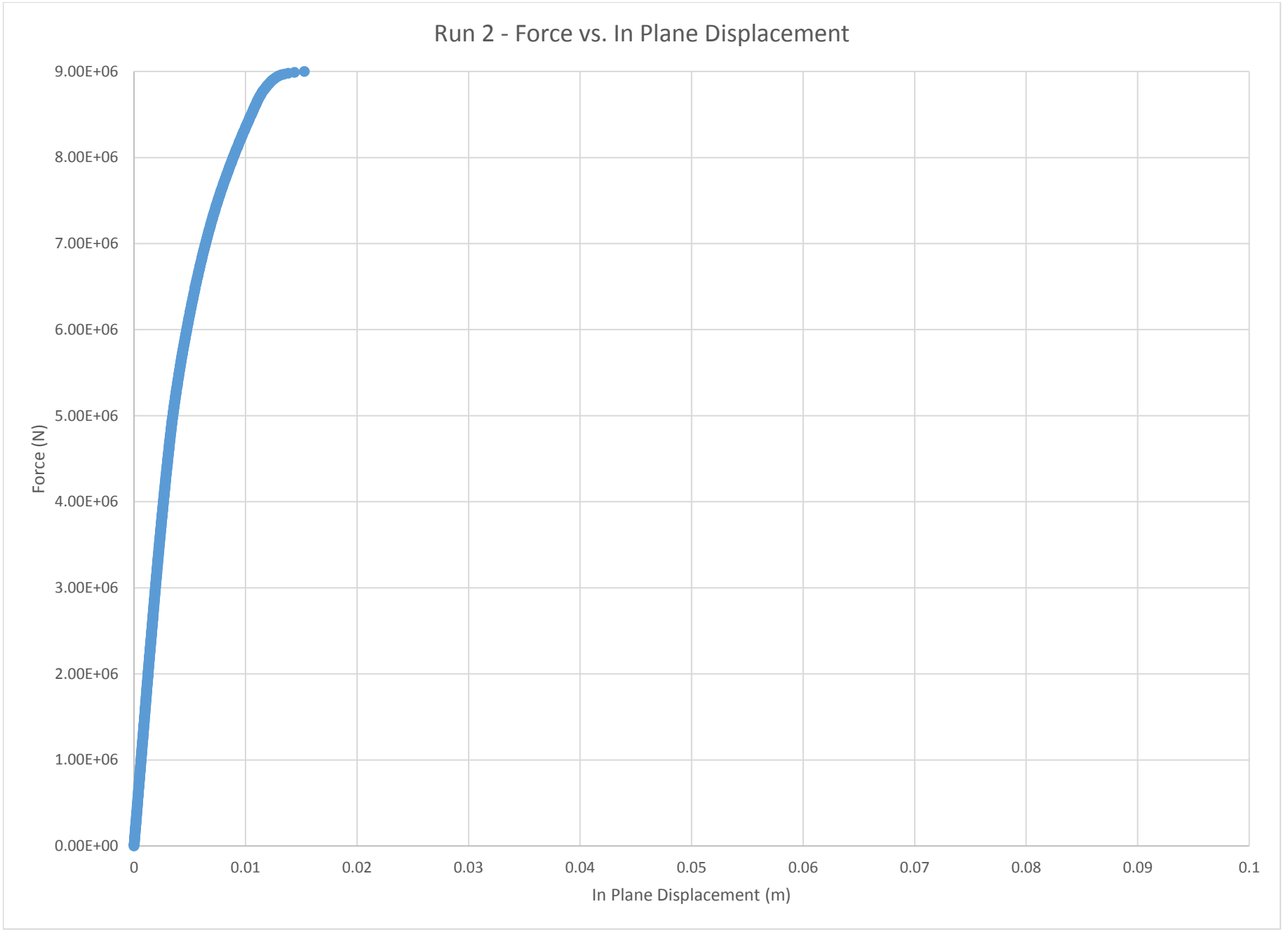
Run 2 - Force vs. In Plane Displacement
9.00E+06
8.00E+06
7.00E+06
6.00E+06
5.00E+06
4.00E+06
3.00E+06
2.00E+06
1.00E+06
0.00E+00
Force (N)
0
0.01
0.02
0.03
0.04
0.05
0.06
0.07
0.08
0.09
0.1
In Plane Displacement (m)

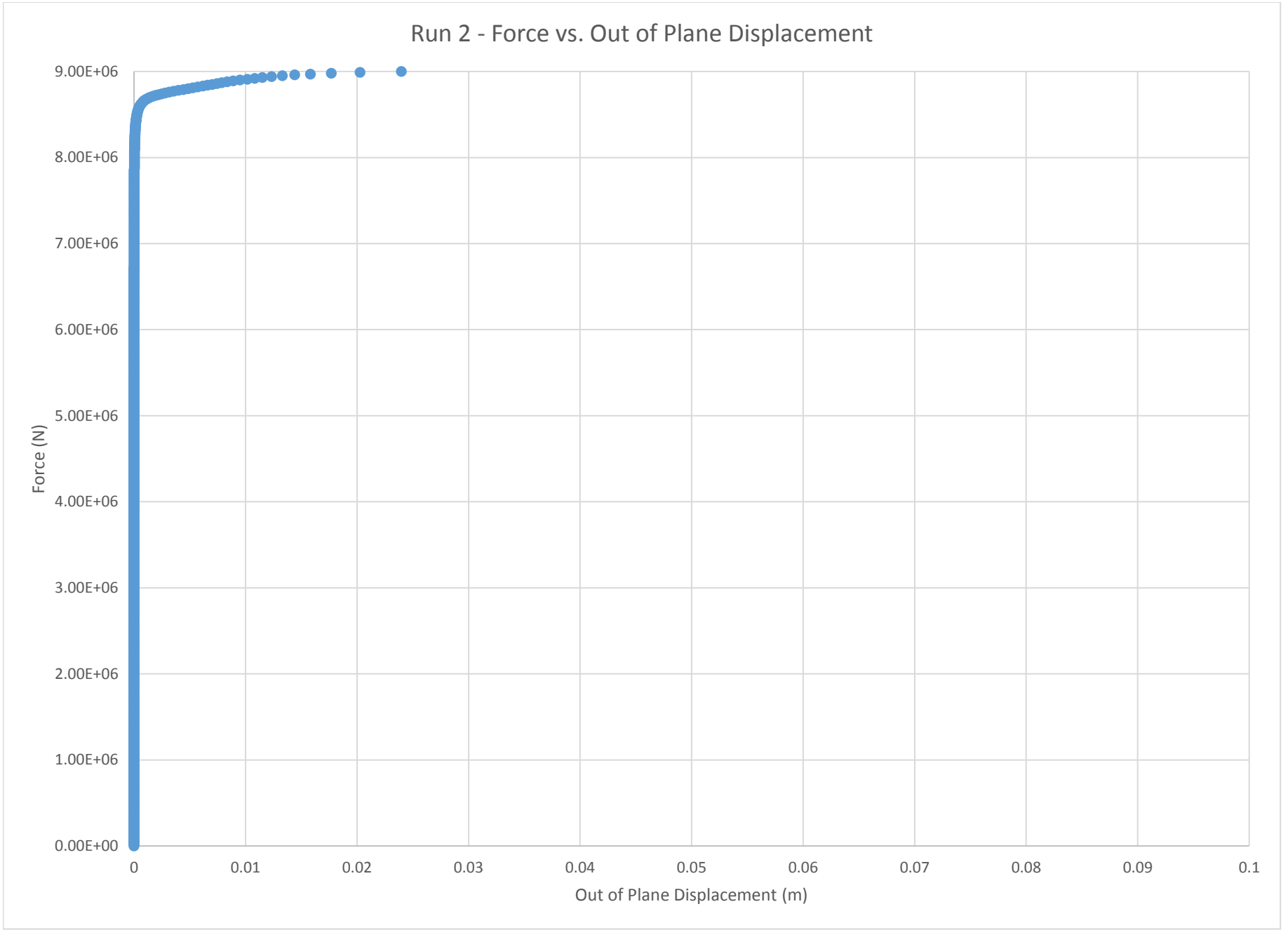
Run 2 - Force vs. Out of Plane Displacement
9.00E+06
8.00E+06
7.00E+06
6.00E+06
5.00E+06
4.00E+06
3.00E+06
2.00E+06
1.00E+06
0.00E+00
Force (N)
0
0.01
0.02
0.03
0.04
0.05
0.06
0.07
0.08
0.09
0.1
Out of Plane Displacement (m)

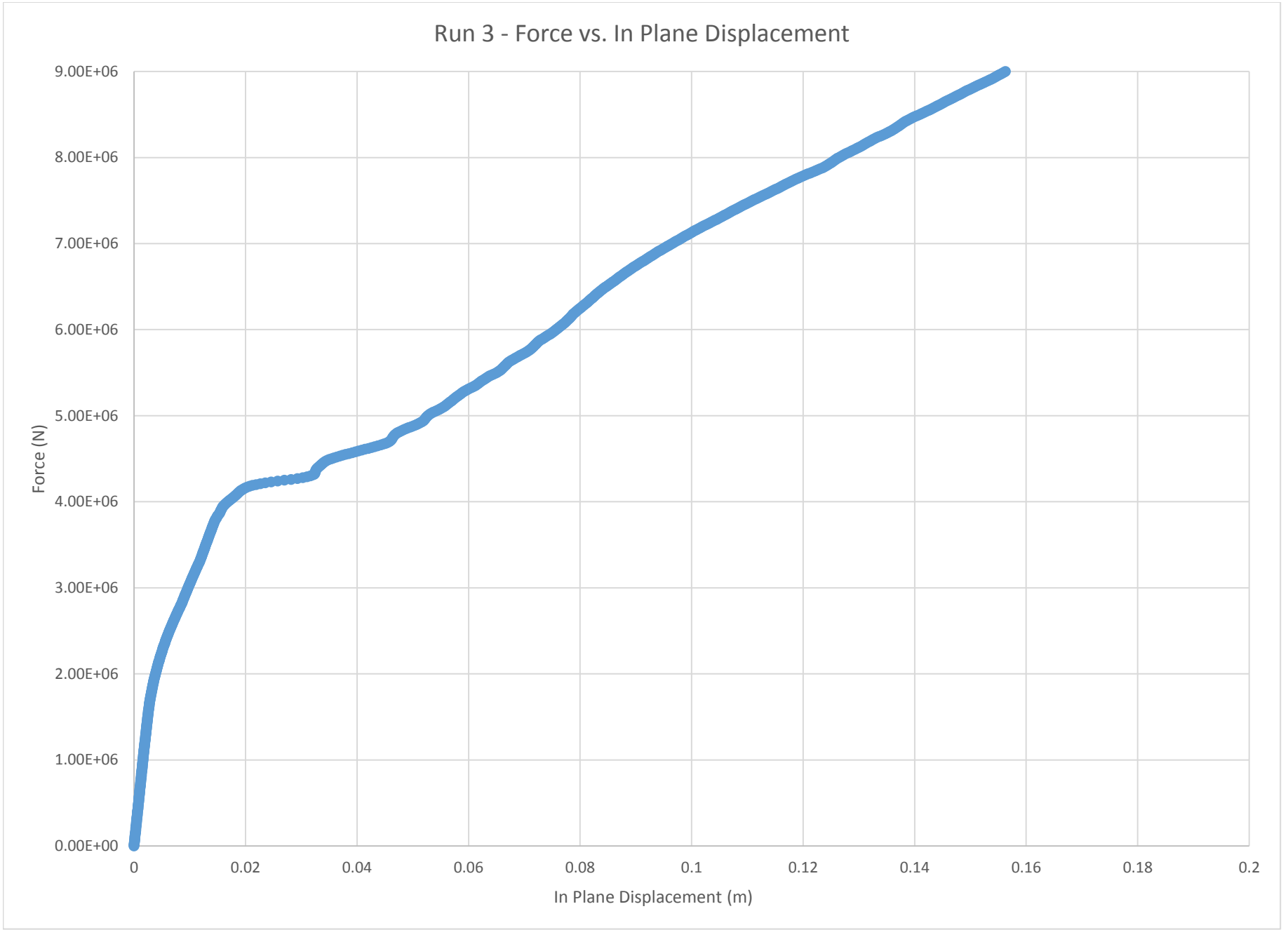
Run 3 - Force vs. In Plane Displacement
9.00E+06
8.00E+06
7.00E+06
6.00E+06
5.00E+06
4.00E+06
3.00E+06
2.00E+06
1.00E+06
0.00E+00
Force (N)
0
0.02
0.04
0.06
0.08
0.1
0.12
0.14
0.16
0.18
0.2
In Plane Displacement (m)

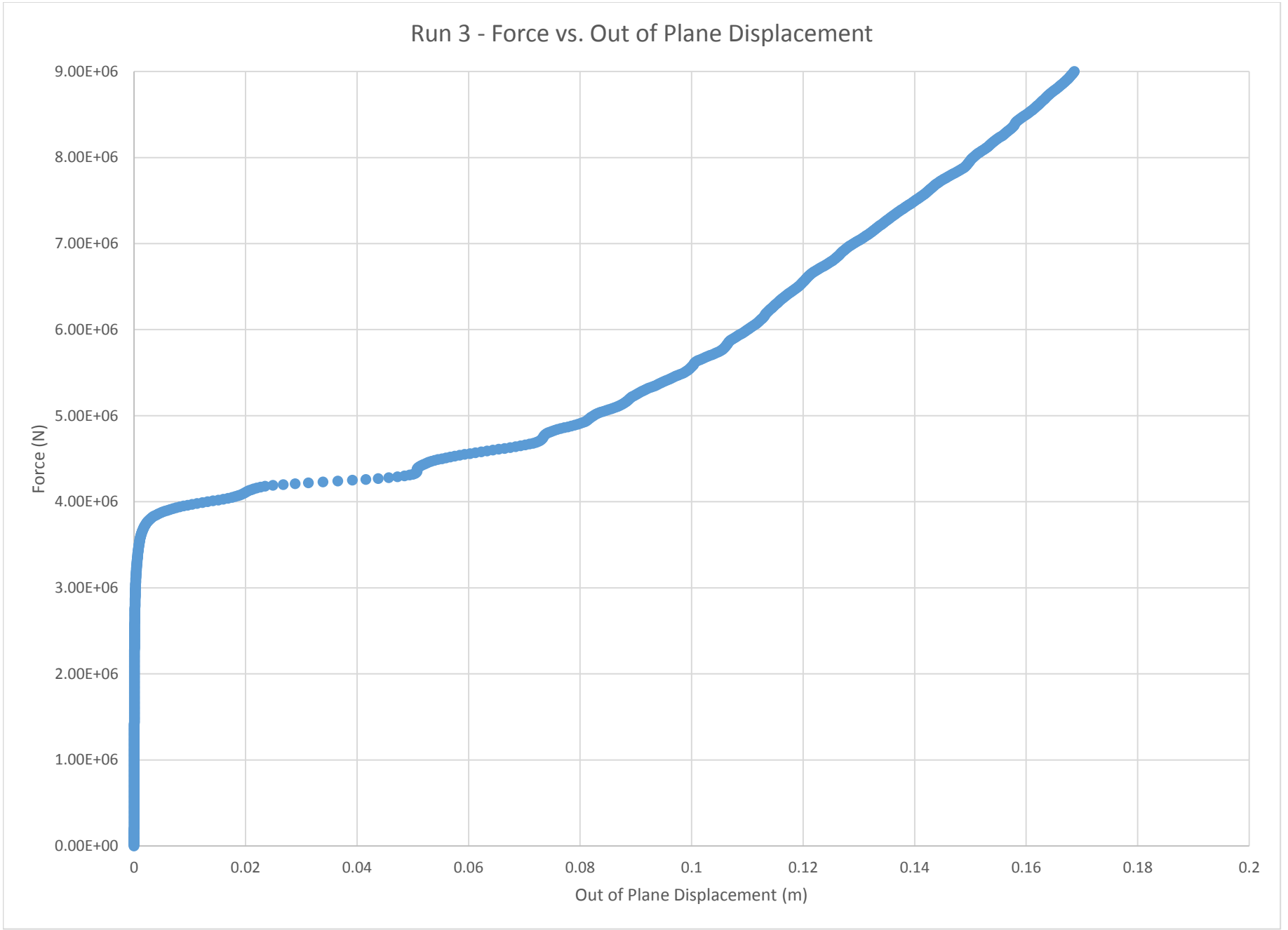
Run 3 - Force vs. Out of Plane Displacement
Force (N)
9.00E+06
8.00E+06
7.00E+06
6.00E+06
5.00E+06
4.00E+06
3.00E+06
2.00E+06
1.00E+06
0.00E+00
0
0.02
0.04
0.06
0.08
0.1
0.12
0.14
0.16
0.18
0.2
Out of Plane Displacement (m)

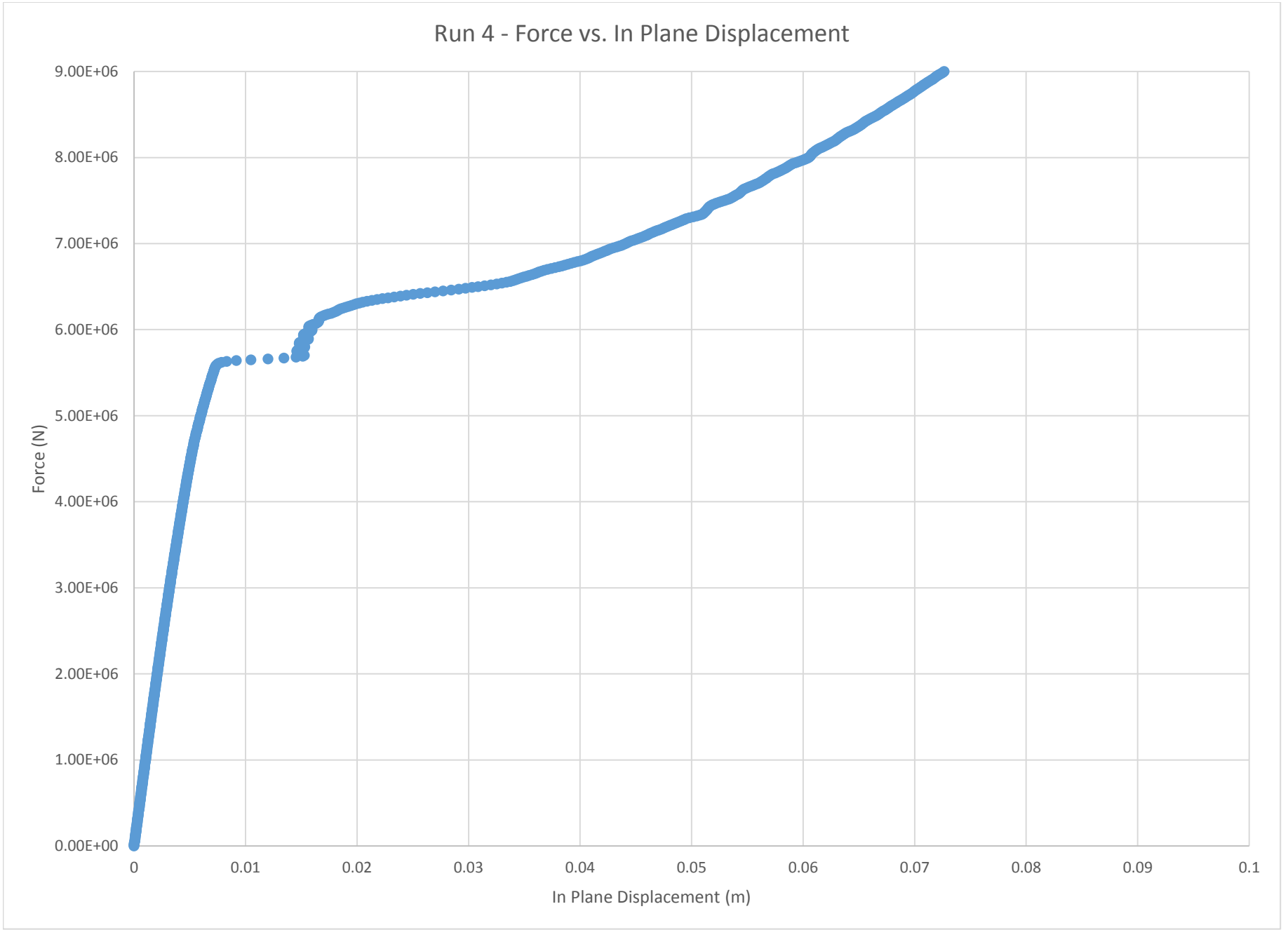
Run 4 - Force vs. In Plane Displacement
9.00E+06
8.00E+06
7.00E+06
6.00E+06
5.00E+06
4.00E+06
3.00E+06
2.00E+06
1.00E+06
0.00E+00
Force (N)
0
0.01
0.02
0.03
0.04
0.05
0.06
0.07
0.08
0.09
0.1
In Plane Displacement (m)

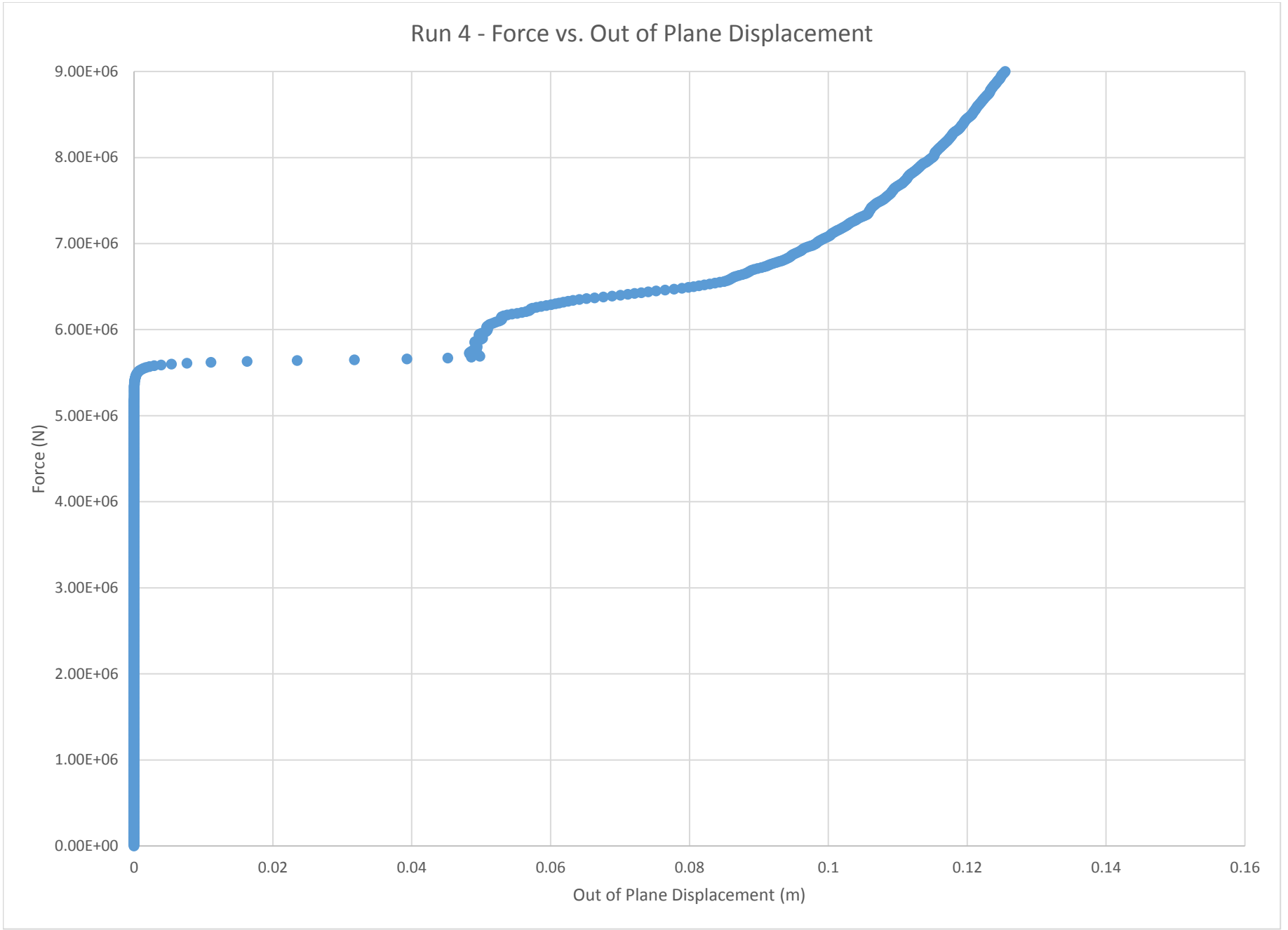
Run 4 - Force vs. Out of Plane Displacement
9.00E+06
8.00E+06
7.00E+06
6.00E+06
5.00E+06
4.00E+06
3.00E+06
2.00E+06
1.00E+06
0.00E+00
Force (N)
0
0.02
0.04
0.06
0.08
0.1
0.12
0.14
0.16
Out of Plane Displacement (m)

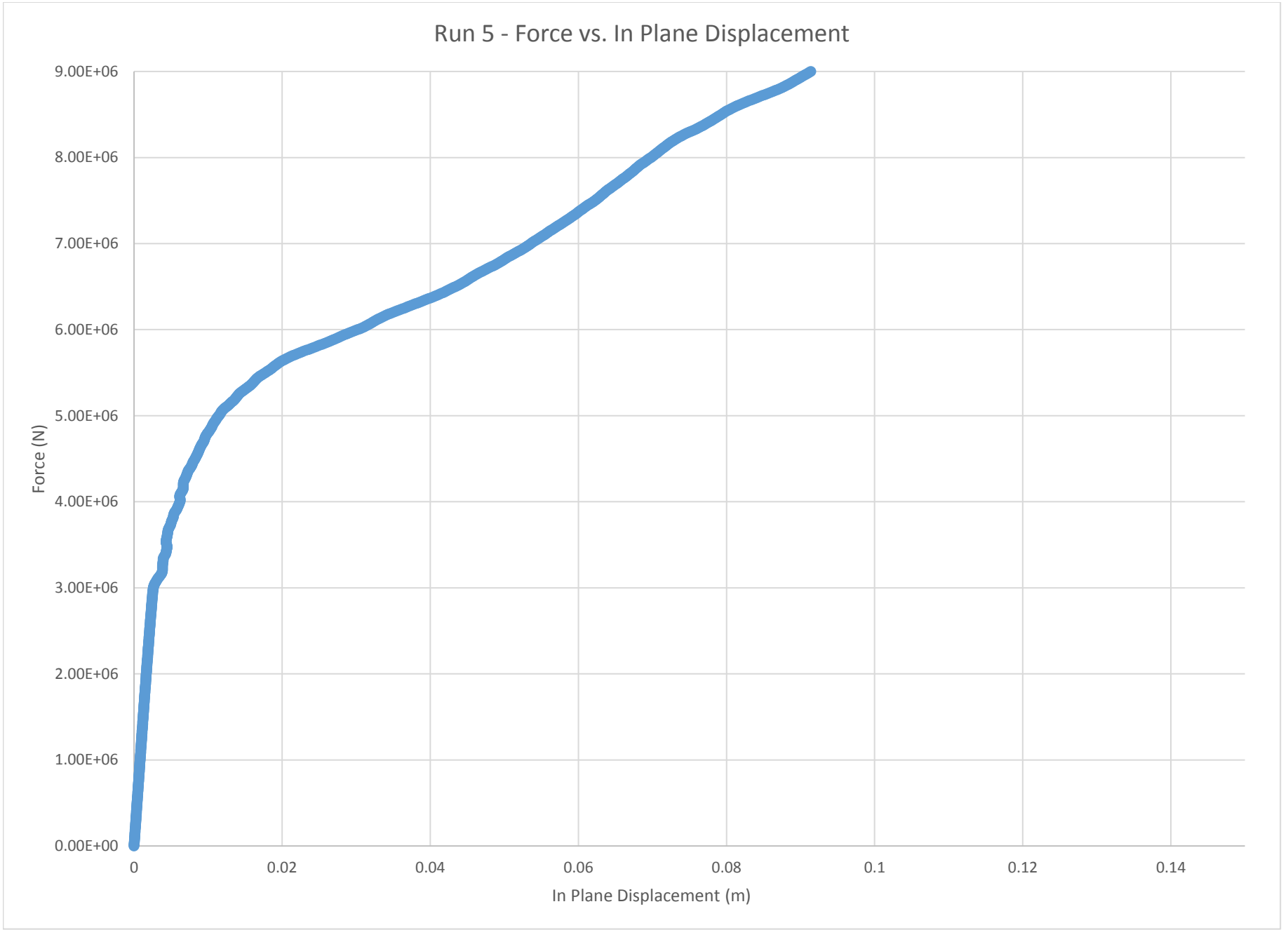
Run 5 - Force vs. In Plane Displacement
9.00E+06
8.00E+06
7.00E+06
6.00E+06
5.00E+06
4.00E+06
3.00E+06
2.00E+06
1.00E+06
0.00E+00
Force (N)
0
0.02
0.04
0.06
0.08
0.1
0.12
0.14
In Plane Displacement (m)

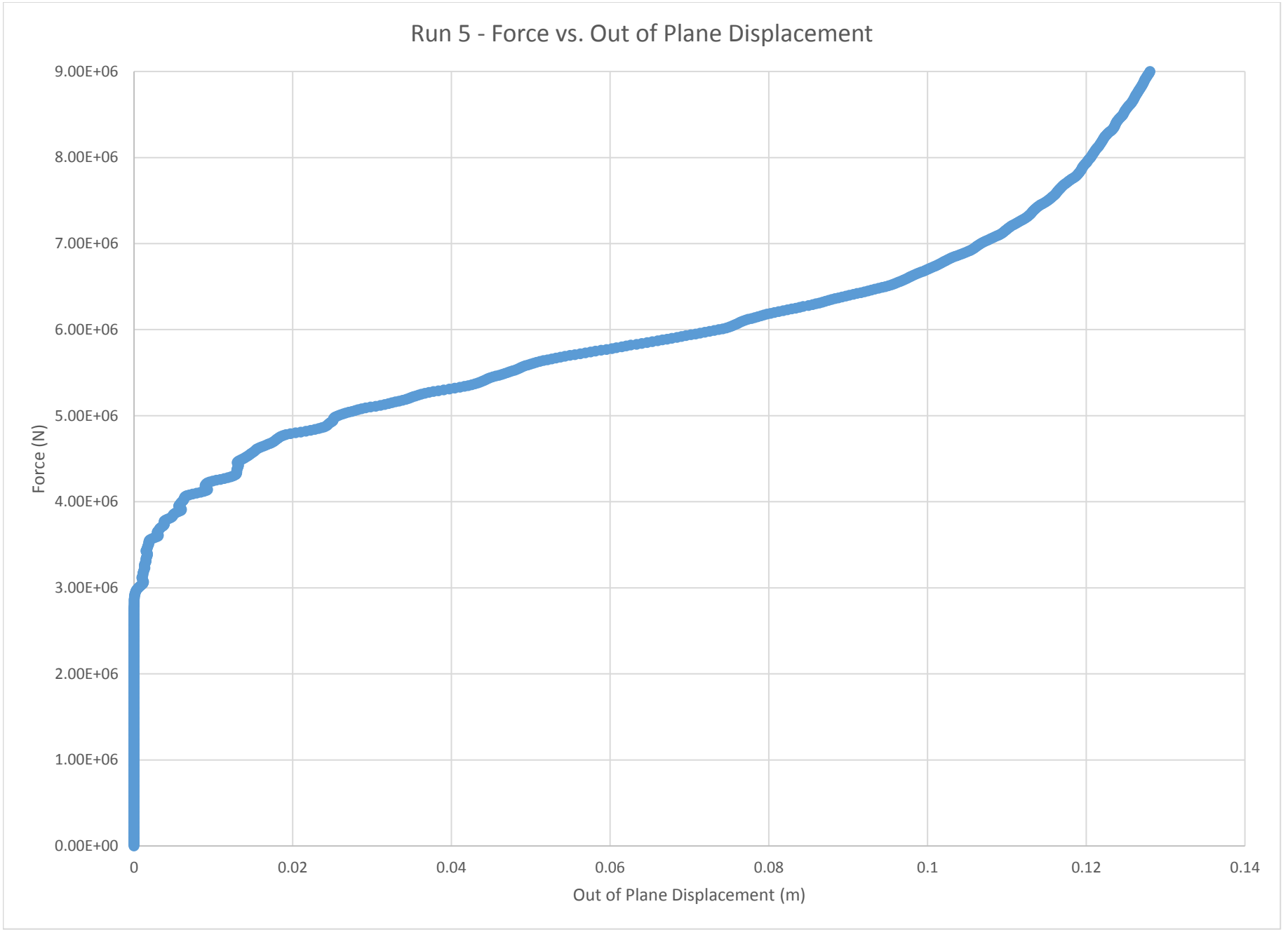
Run 5 - Force vs. Out of Plane Displacement
Force (N)
9.00E+06
8.00E+06
7.00E+06
6.00E+06
5.00E+06
4.00E+06
3.00E+06
2.00E+06
1.00E+06
0.00E+00
0
0.02
0.04
0.06
0.08
0.1
0.12
0.14
Out of Plane Displacement (m)

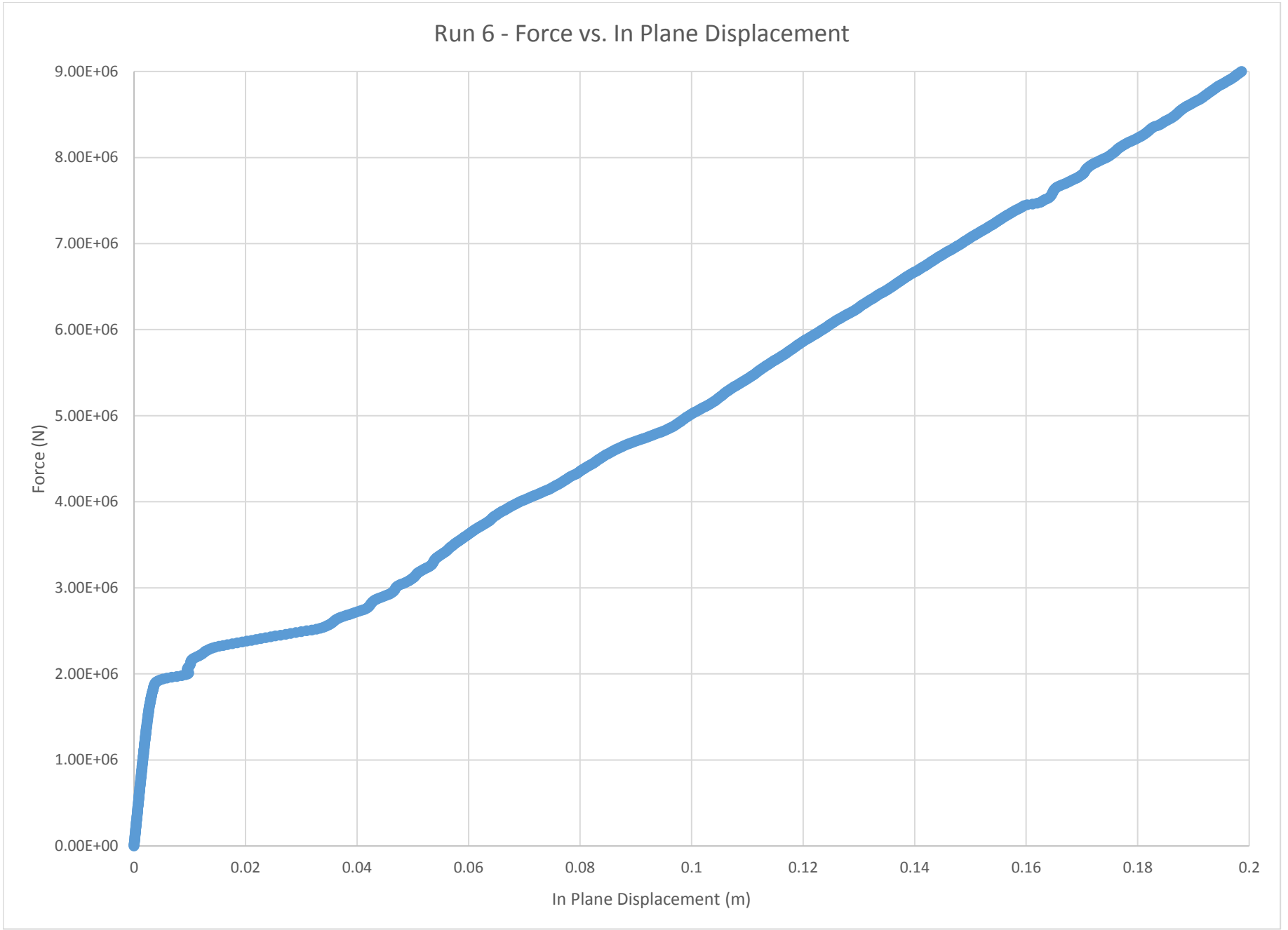
Run 6 - Force vs. In Plane Displacement
Force (N)
9.00E+06
8.00E+06
7.00E+06
6.00E+06
5.00E+06
4.00E+06
3.00E+06
2.00E+06
1.00E+06
0.00E+00
0
0.02
0.04
0.06
0.08
0.1
0.12
0.14
0.16
0.18
0.2
In Plane Displacement (m)

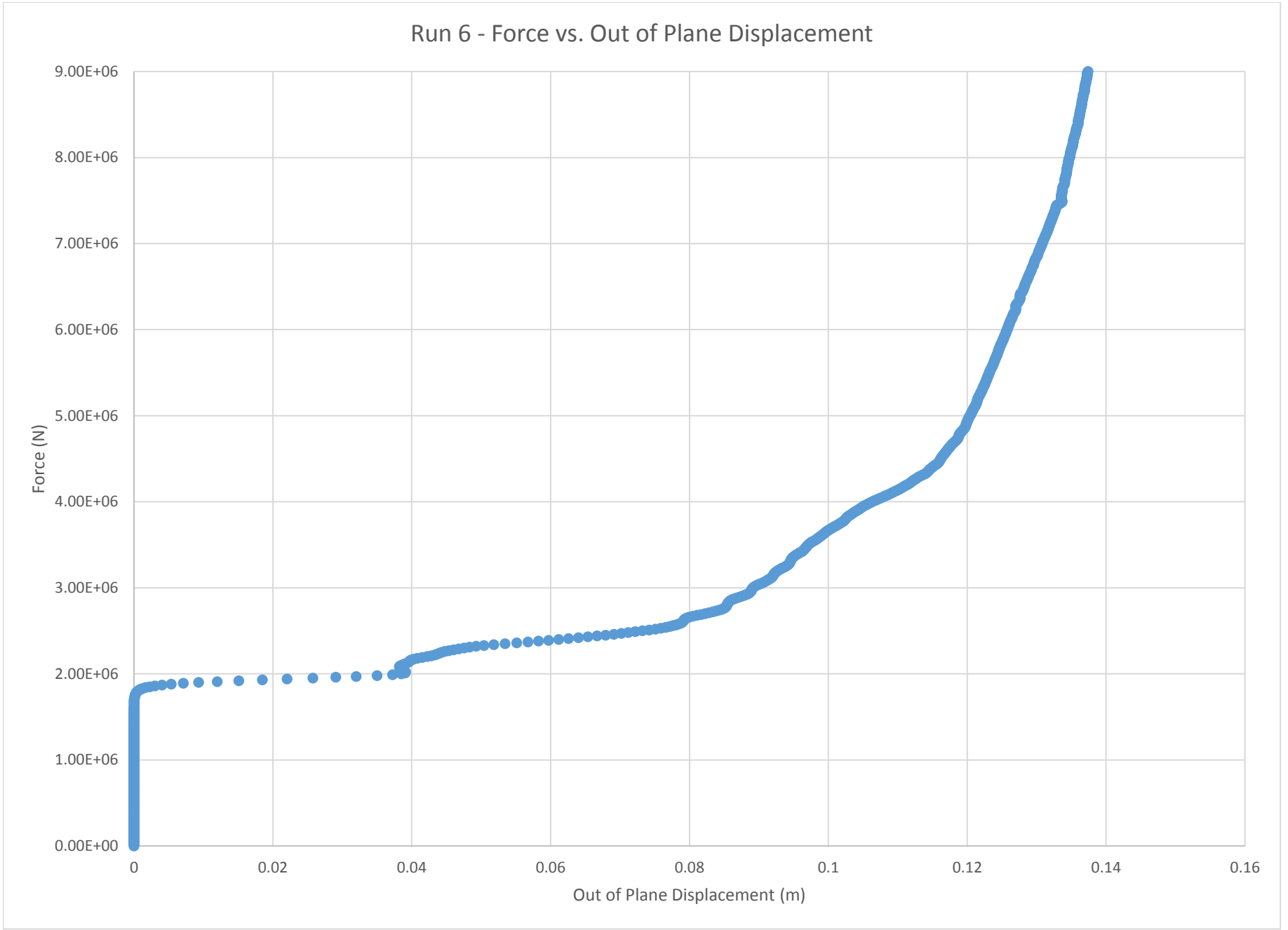
Run 6 - Force vs. Out of Plane Displacement
Force (N)
9.00E+06
8.00E+06
7.00E+06
6.00E+06
5.00E+06
4.00E+06
3.00E+06
2.00E+06
1.00E+06
0.00E+00
0
0.02
0.04
0.06
0.08
0.1
0.12
0.14
0.16
Out of Plane Displacement (m)

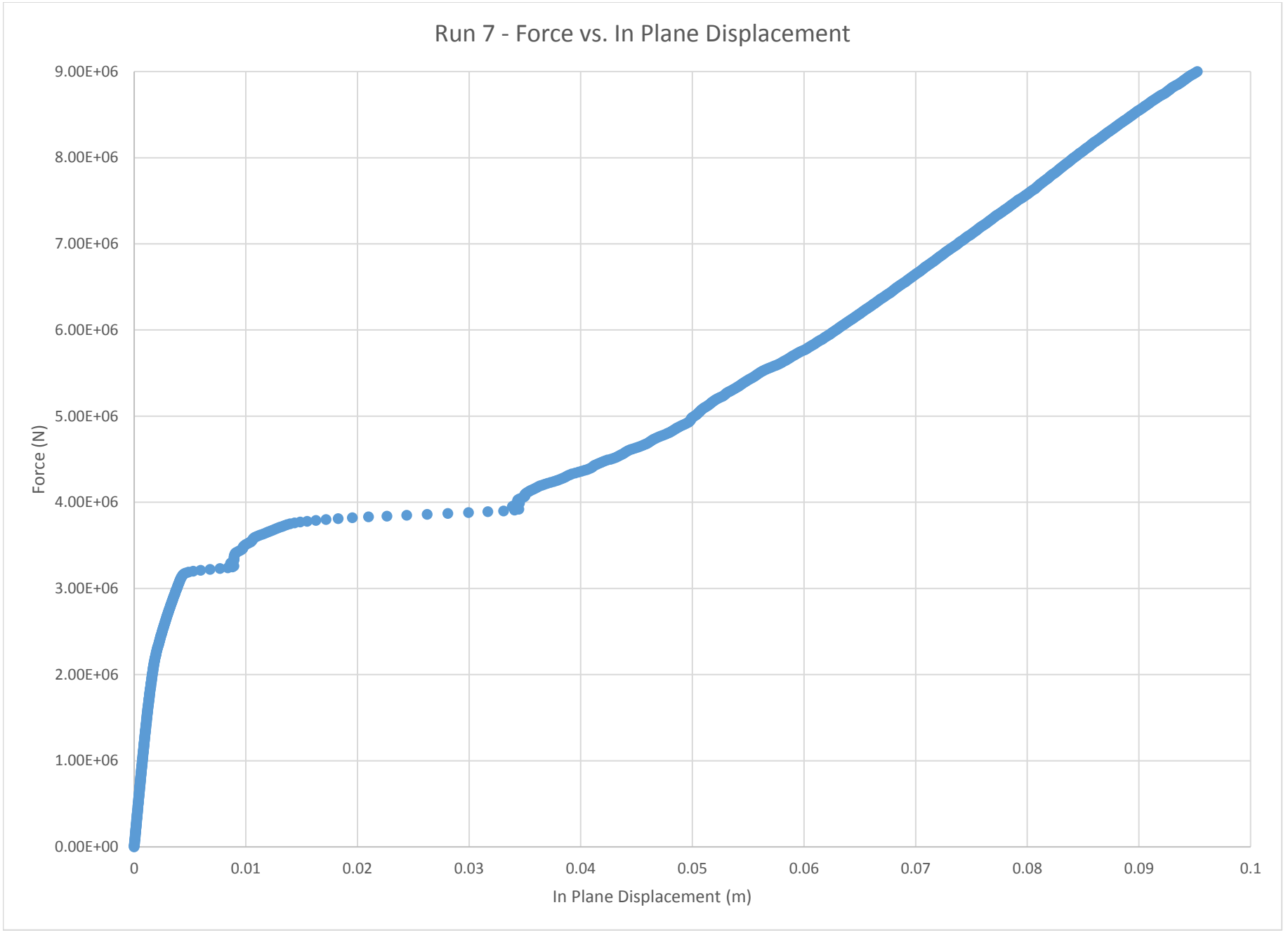
Run 7 - Force vs. In Plane Displacement
9.00E+06
8.00E+06
7.00E+06
6.00E+06
5.00E+06
4.00E+06
3.00E+06
2.00E+06
1.00E+06
0.00E+00
Force (N)
0
0.01
0.02
0.03
0.04
0.05
0.06
0.07
0.08
0.09
0.1
In Plane Displacement (m)

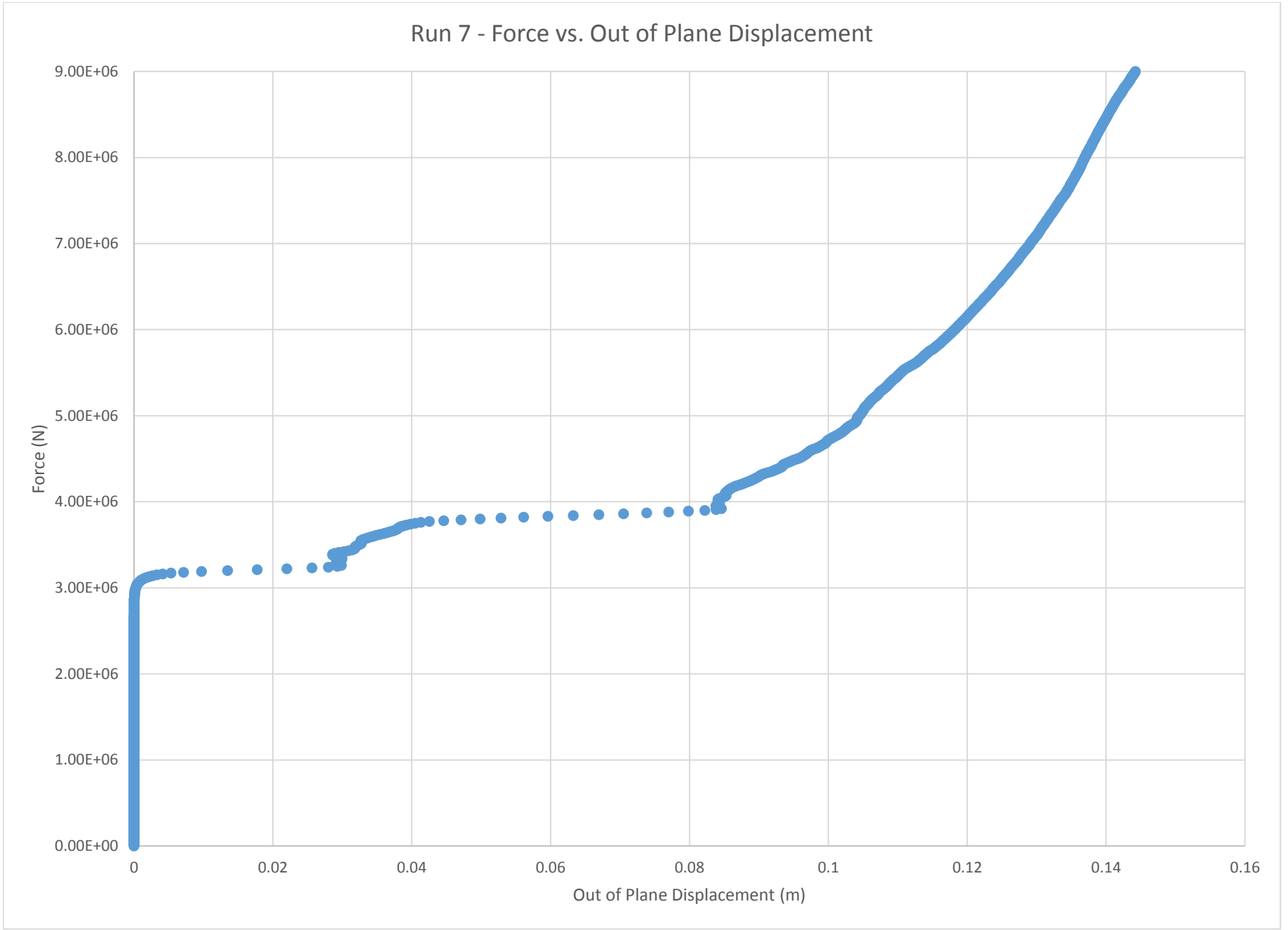
Run 7 - Force vs. Out of Plane Displacement
Force (N)
9.00E+06
8.00E+06
7.00E+06
6.00E+06
5.00E+06
4.00E+06
3.00E+06
2.00E+06
1.00E+06
0.00E+00
0
0.02
0.04
0.06
0.08
0.1
0.12
0.14
0.16
Out of Plane Displacement (m)

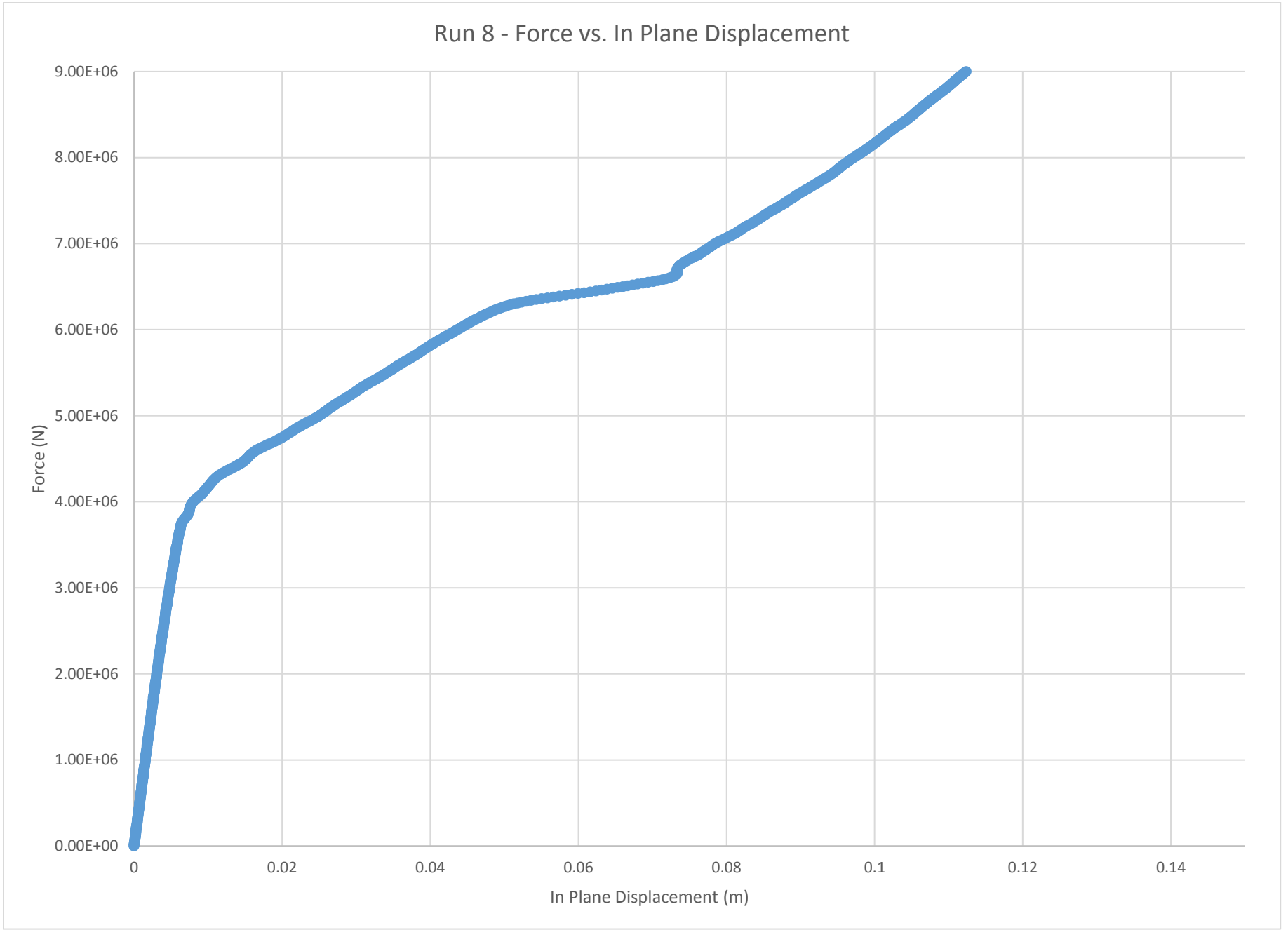
Run 8 - Force vs. In Plane Displacement
9.00E+06
8.00E+06
7.00E+06
6.00E+06
5.00E+06
4.00E+06
3.00E+06
2.00E+06
1.00E+06
0.00E+00
Force (N)
0
0.02
0.04
0.06
0.08
0.1
0.12
0.14
In Plane Displacement (m)

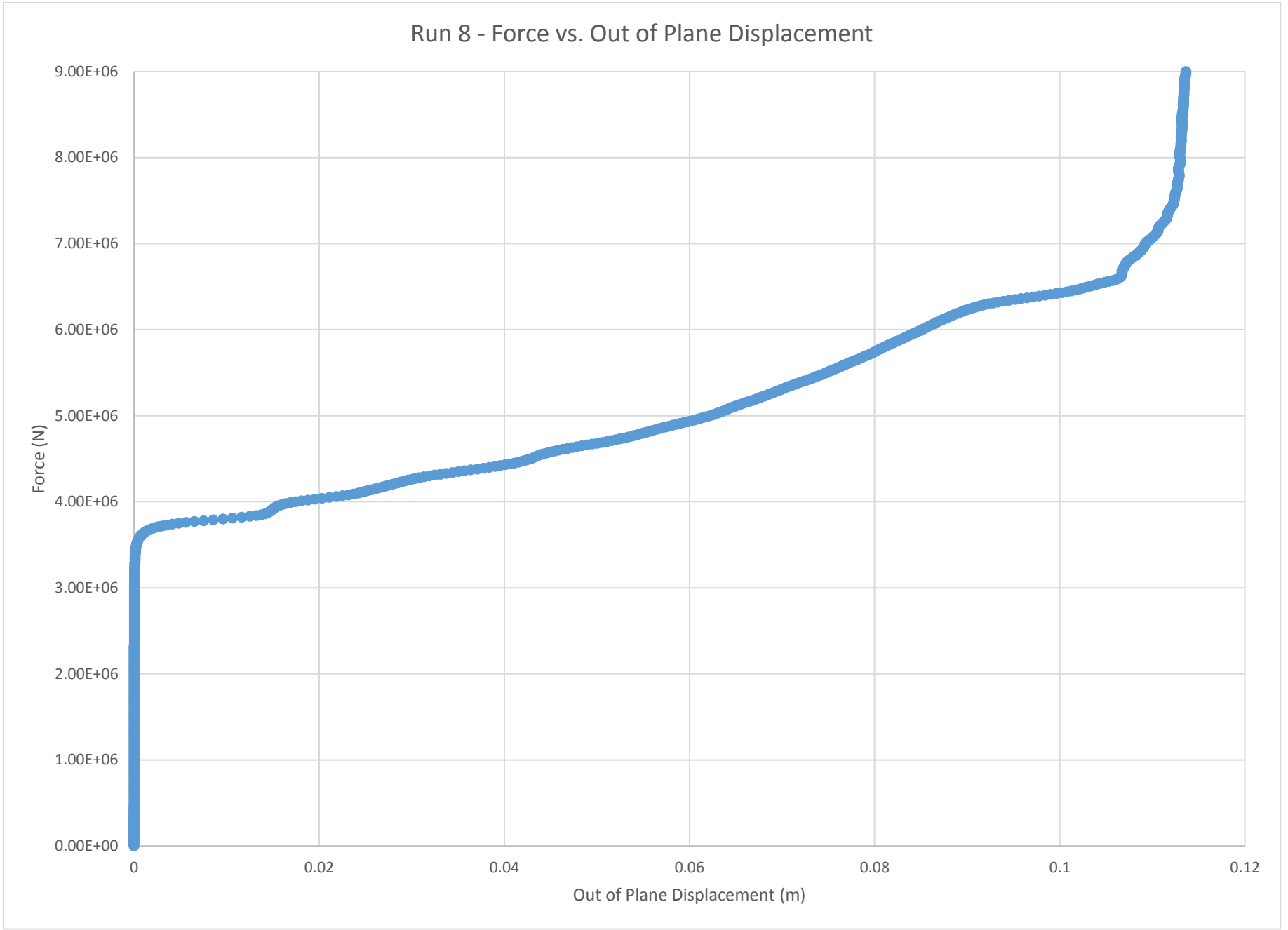
Run 8 - Force vs. Out of Plane Displacement
9.00E+06
8.00E+06
7.00E+06
6.00E+06
5.00E+06
4.00E+06
3.00E+06
2.00E+06
1.00E+06
0.00E+00
Force (N)
0
0.02
0.04
0.06
0.08
0.1
0.12
Out of Plane Displacement (m)

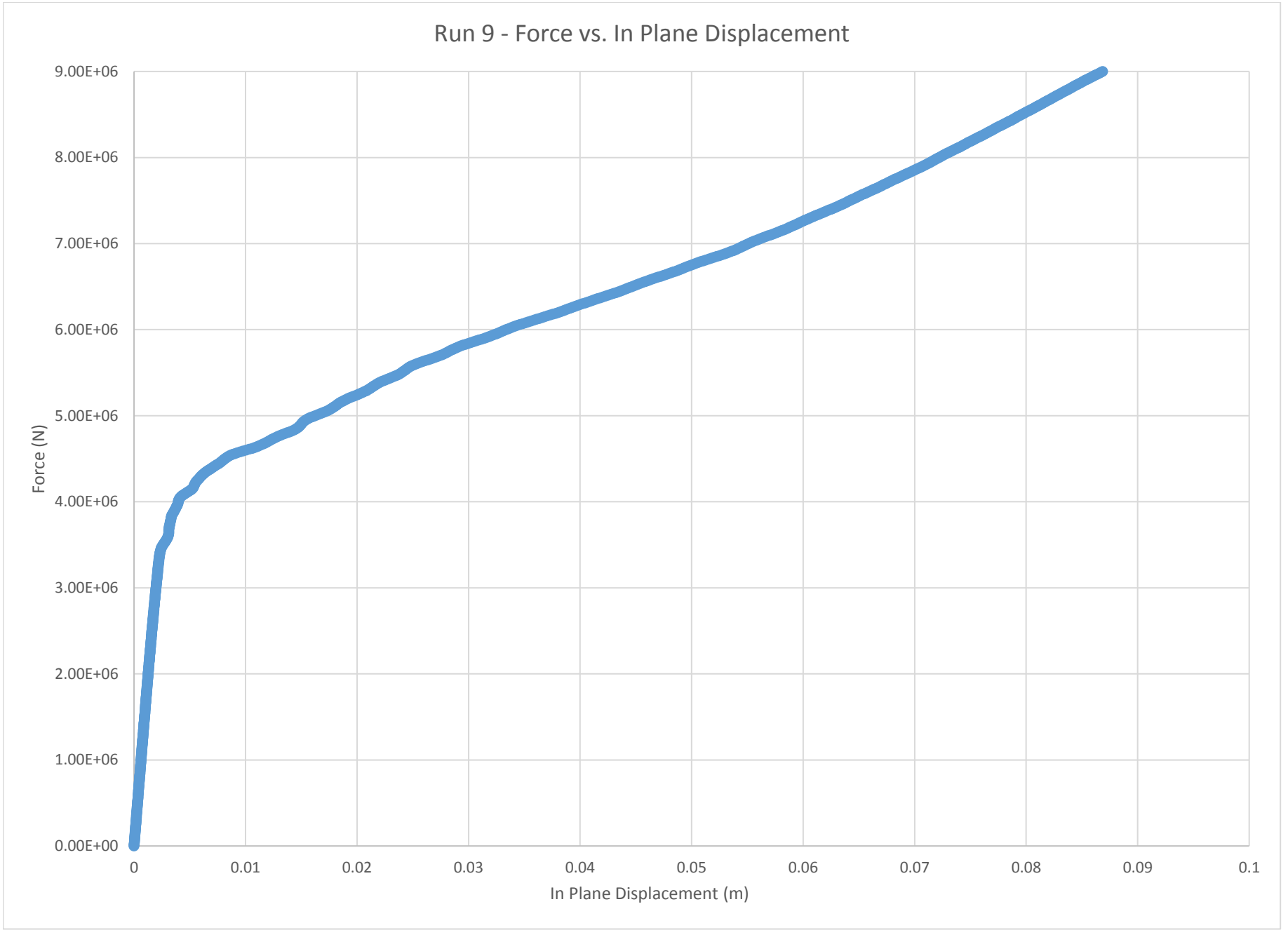
Run 9 - Force vs. In Plane Displacement
9.00E+06
8.00E+06
7.00E+06
6.00E+06
5.00E+06
4.00E+06
3.00E+06
2.00E+06
1.00E+06
0.00E+00
Force (N)
0
0.01
0.02
0.03
0.04
0.05
0.06
0.07
0.08
0.09
0.1
In Plane Displacement (m)

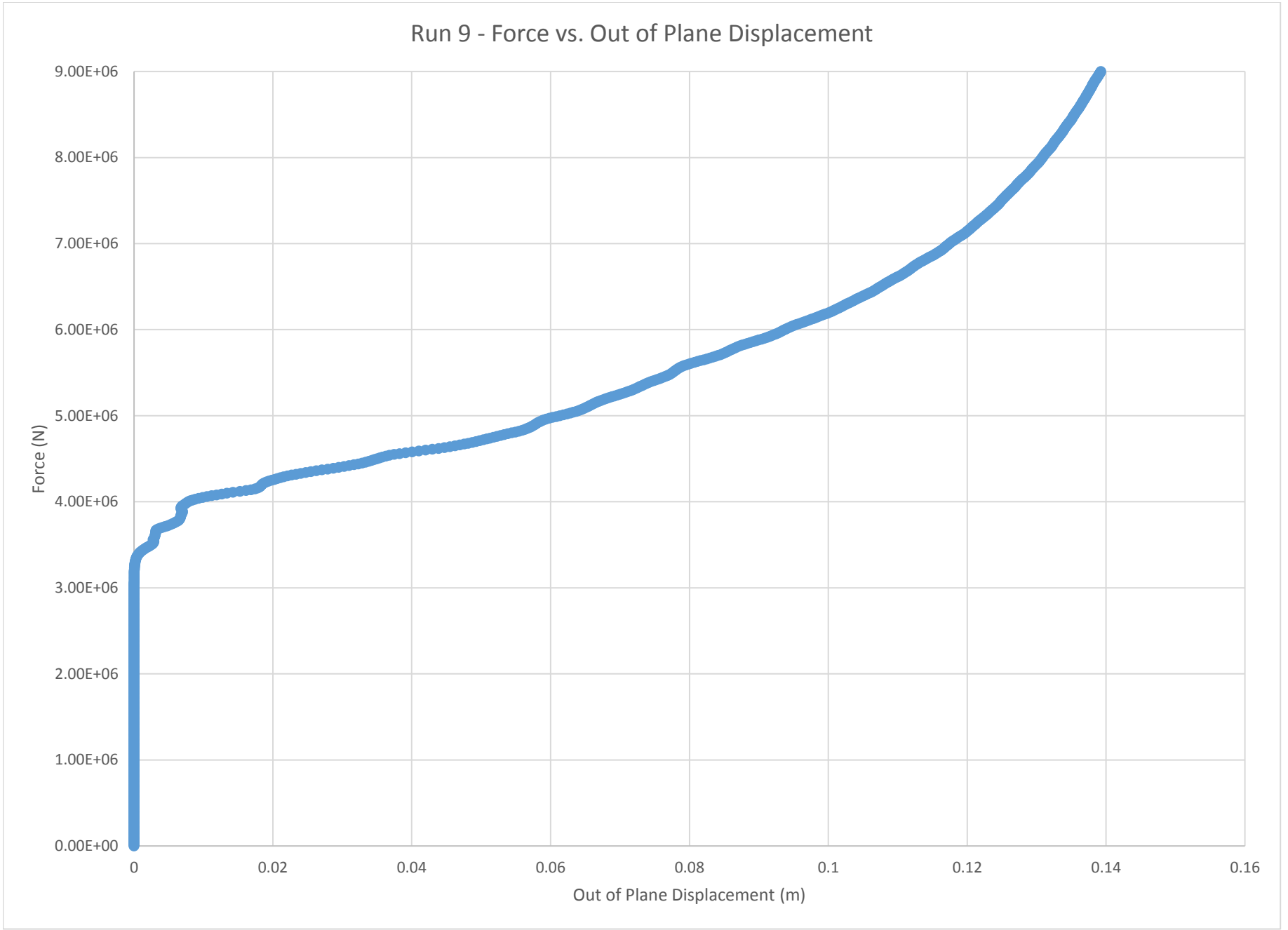
Run 9 - Force vs. Out of Plane Displacement
Force (N)
9.00E+06
8.00E+06
7.00E+06
6.00E+06
5.00E+06
4.00E+06
3.00E+06
2.00E+06
1.00E+06
0.00E+00
0
0.02
0.04
0.06
0.08
0.1
0.12
0.14
0.16
Out of Plane Displacement (m)

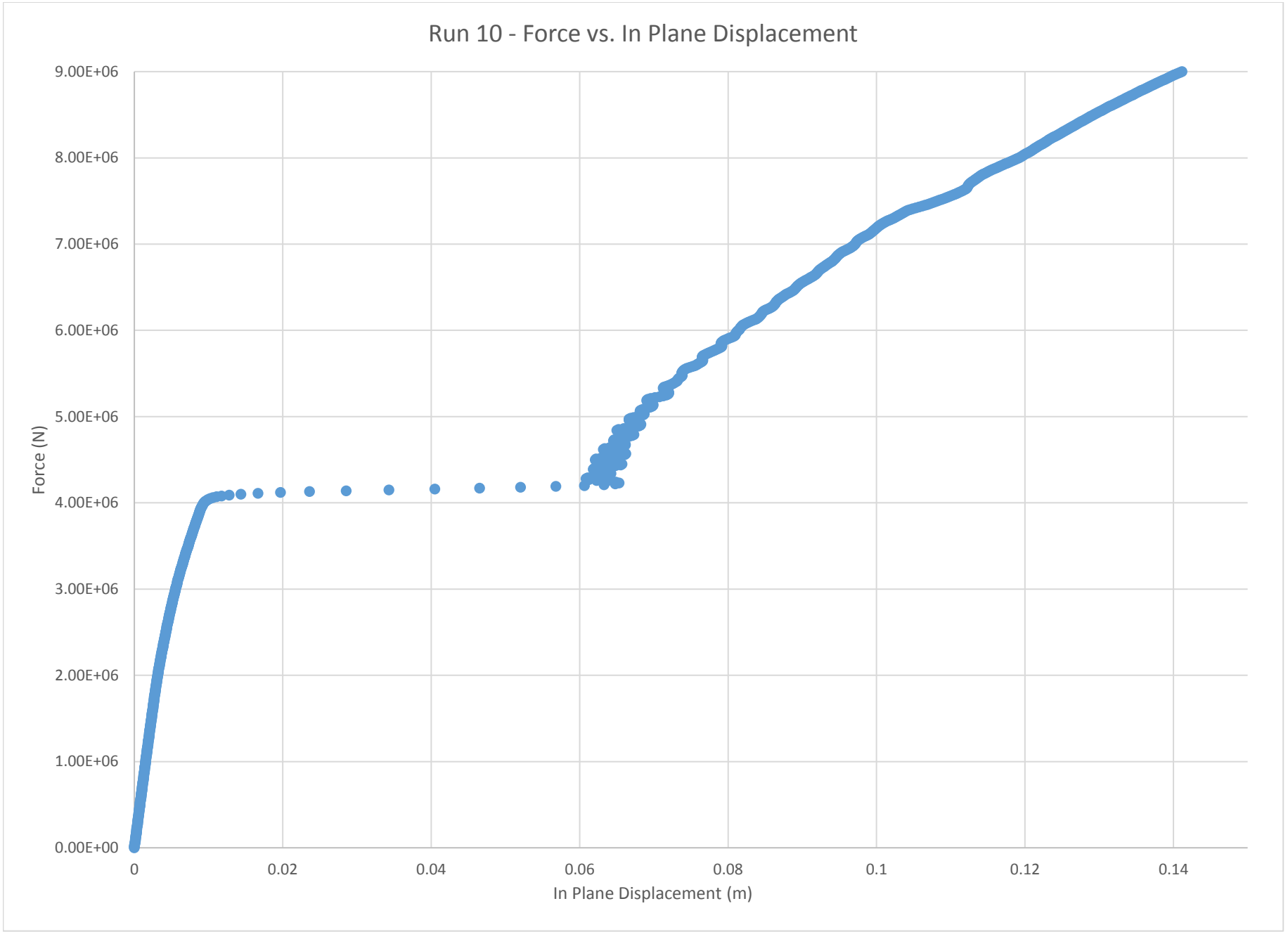
Run 10 - Force vs. In Plane Displacement
9.00E+06
8.00E+06
7.00E+06
6.00E+06
5.00E+06
4.00E+06
3.00E+06
2.00E+06
1.00E+06
0.00E+00
Force (N)
0
0.02
0.04
0.06
0.08
0.1
0.12
0.14
In Plane Displacement (m)

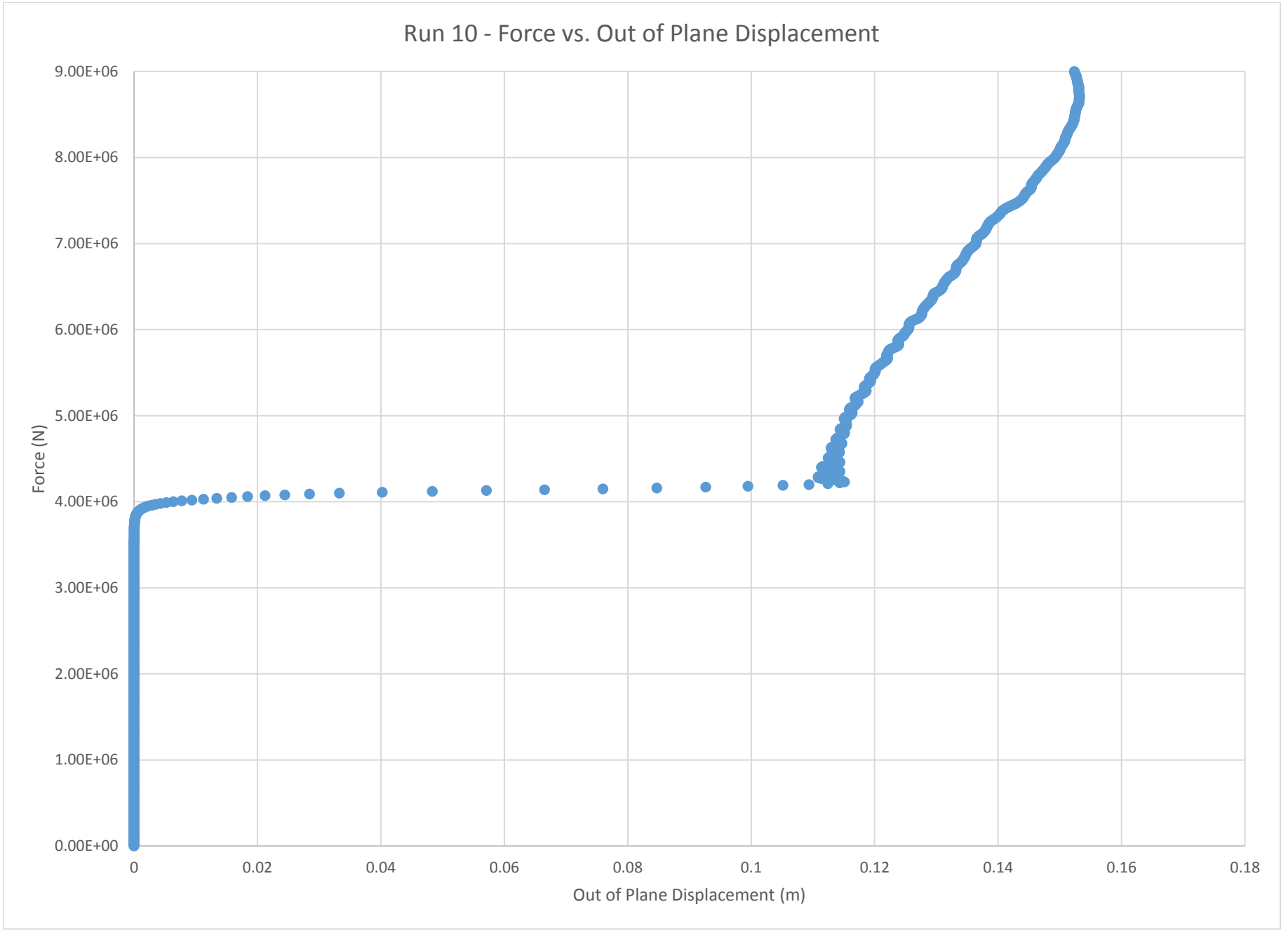
Run 10 - Force vs. Out of Plane Displacement
Force (N)
9.00E+06
8.00E+06
7.00E+06
6.00E+06
5.00E+06
4.00E+06
3.00E+06
2.00E+06
1.00E+06
0.00E+00
0
0.02
0.04
0.06
0.08
0.1
0.12
0.14
0.16
0.18
Out of Plane Displacement (m)

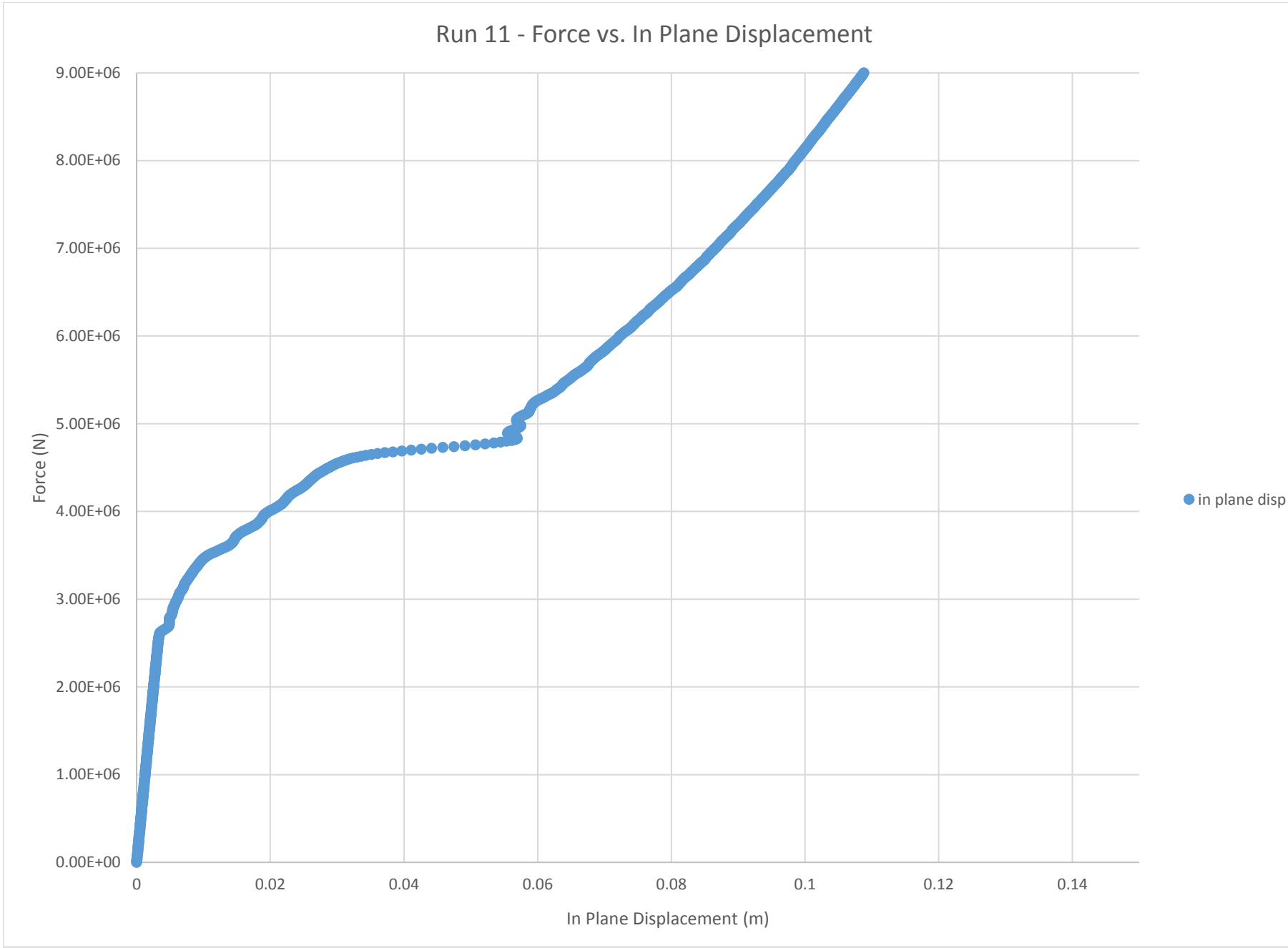
Run 11 - Force vs. In Plane Displacement
9.00E+06
8.00E+06
7.00E+06
6.00E+06
5.00E+06
4.00E+06
3.00E+06
2.00E+06
1.00E+06
0.00E+00
Force (N)
0
0.02
0.04
0.06
0.08
0.1
0.12
0.14
In Plane Displacement (m)
in plane disp

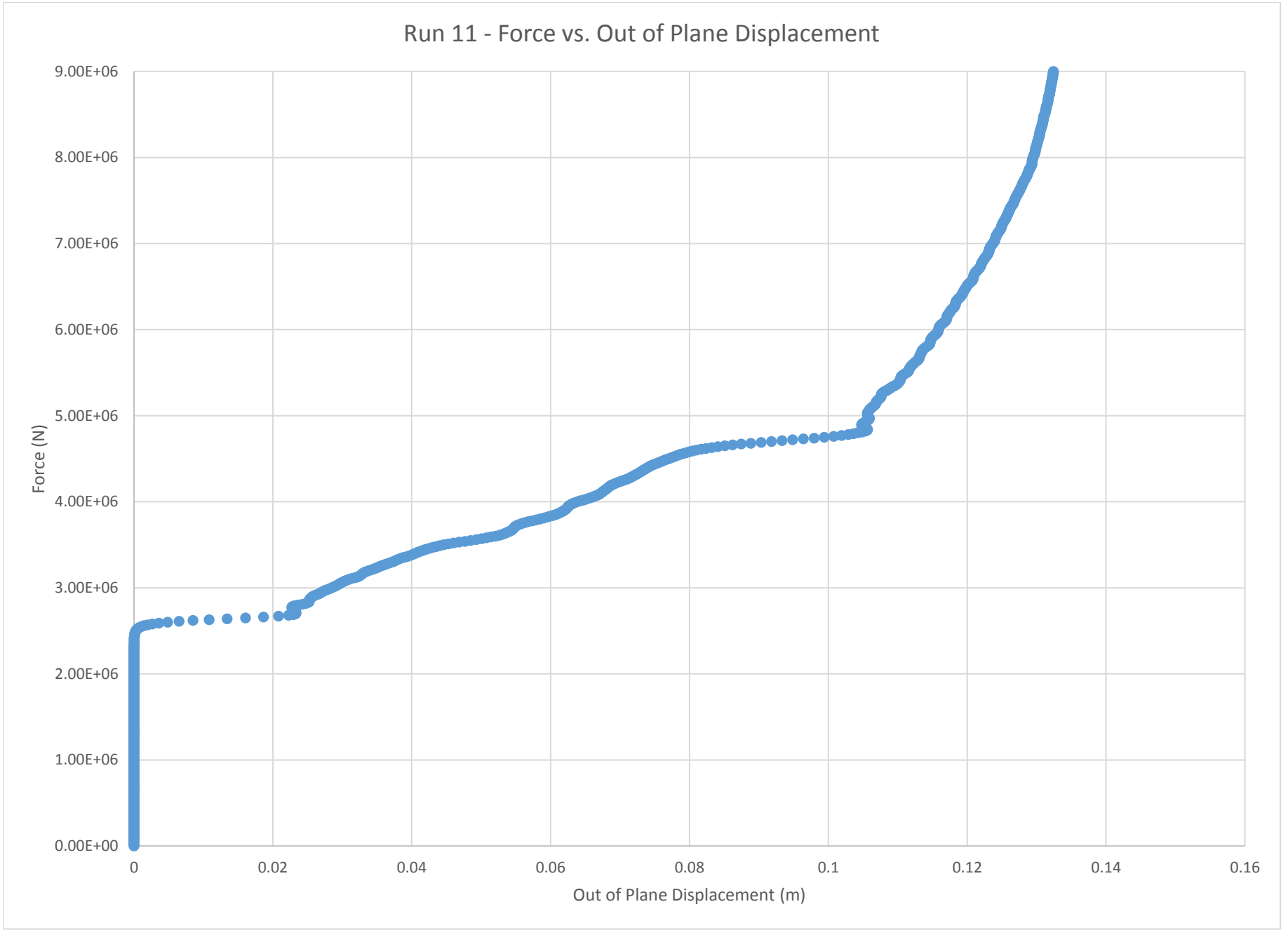
Run 11 - Force vs. Out of Plane Displacement
Force (N)
9.00E+06
8.00E+06
7.00E+06
6.00E+06
5.00E+06
4.00E+06
3.00E+06
2.00E+06
1.00E+06
0.00E+00
0
0.02
0.04
0.06
0.08
0.1
0.12
0.14
0.16
Out of Plane Displacement (m)

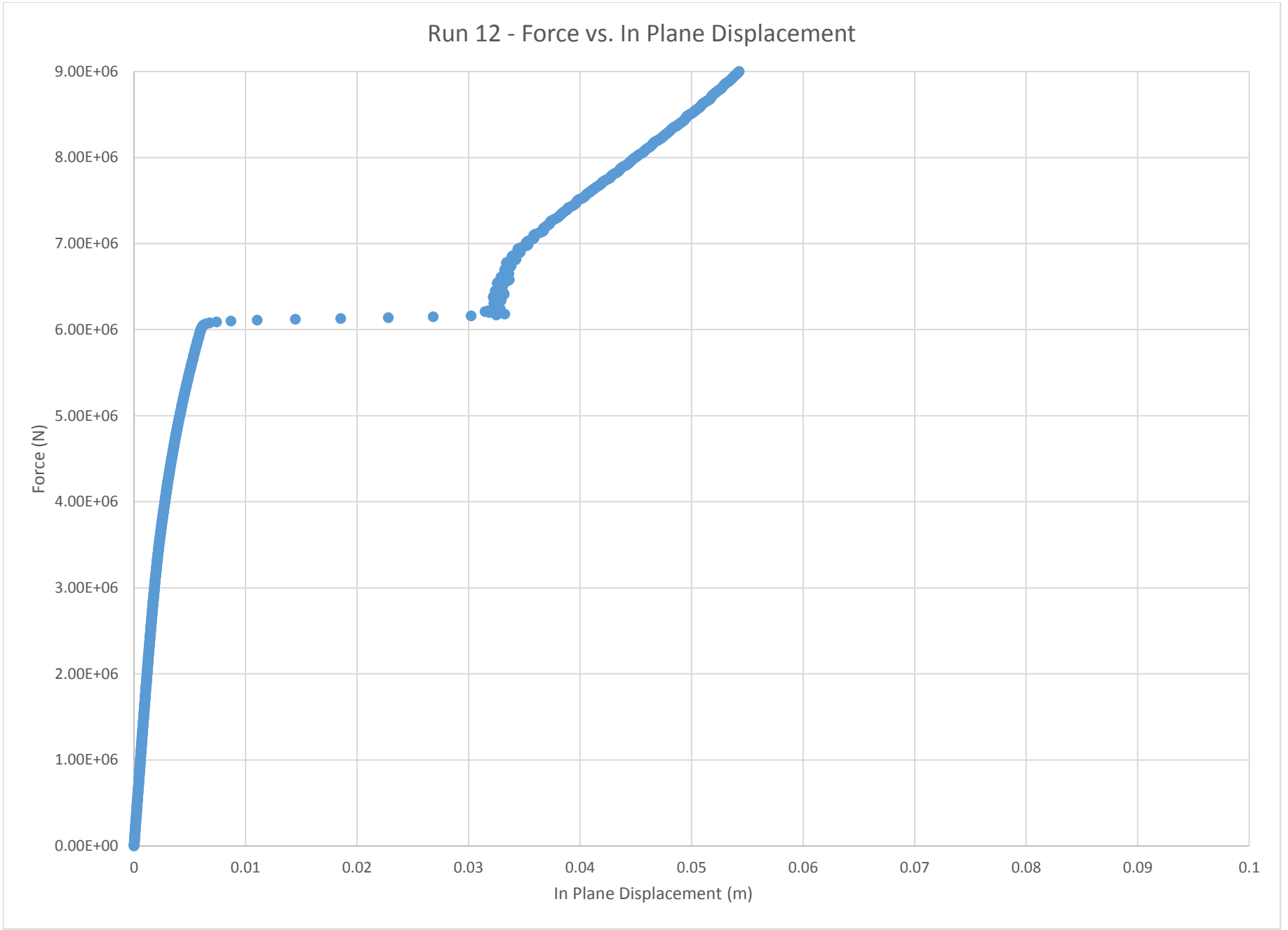
Run 12 - Force vs. In Plane Displacement
9.00E+06
8.00E+06
7.00E+06
6.00E+06
5.00E+06
4.00E+06
3.00E+06
2.00E+06
1.00E+06
0.00E+00
Force (N)
0
0.01
0.02
0.03
0.04
0.05
0.06
0.07
0.08
0.09
0.1
In Plane Displacement (m)

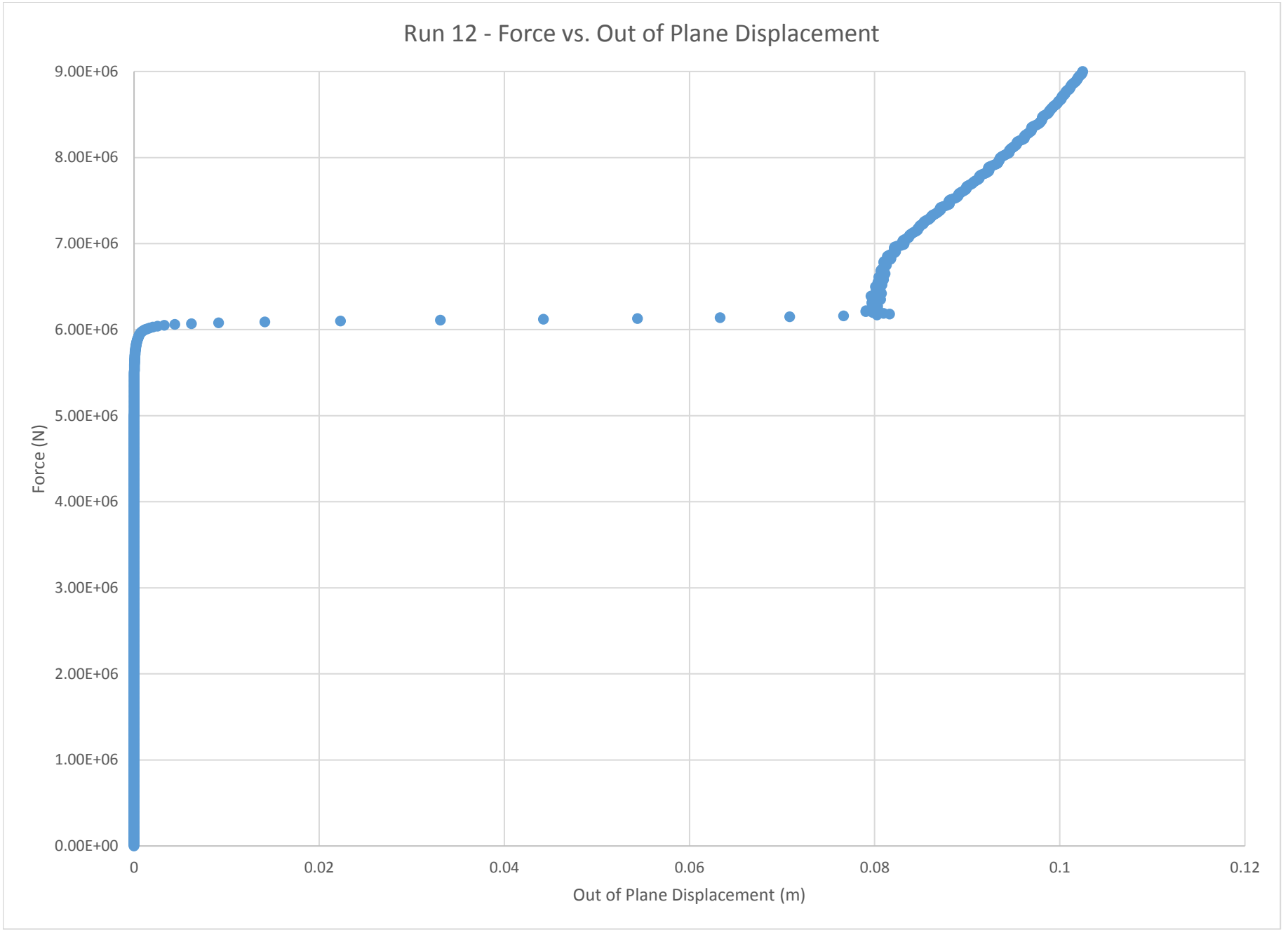
Run 12 - Force vs. Out of Plane Displacement
9.00E+06
8.00E+06
7.00E+06
6.00E+06
5.00E+06
4.00E+06
3.00E+06
2.00E+06
1.00E+06
0.00E+00
Force (N)
0
0.02
0.04
0.06
0.08
0.1
0.12
Out of Plane Displacement (m)

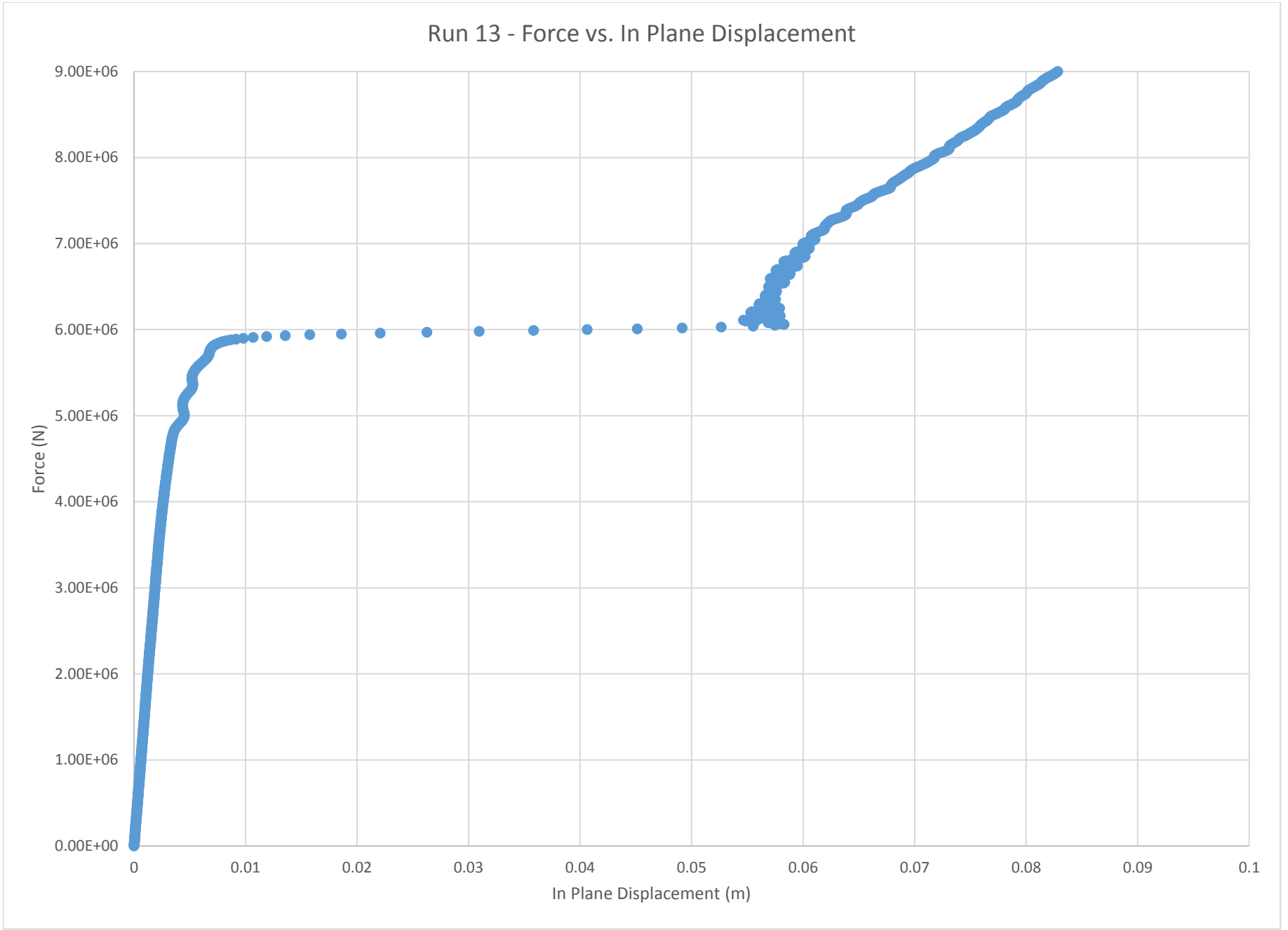
Run 13 - Force vs. In Plane Displacement
9.00E+06
8.00E+06
7.00E+06
6.00E+06
5.00E+06
4.00E+06
3.00E+06
2.00E+06
1.00E+06
0.00E+00
Force (N)
0
0.01
0.02
0.03
0.04
0.05
0.06
0.07
0.08
0.09
0.1
In Plane Displacement (m)

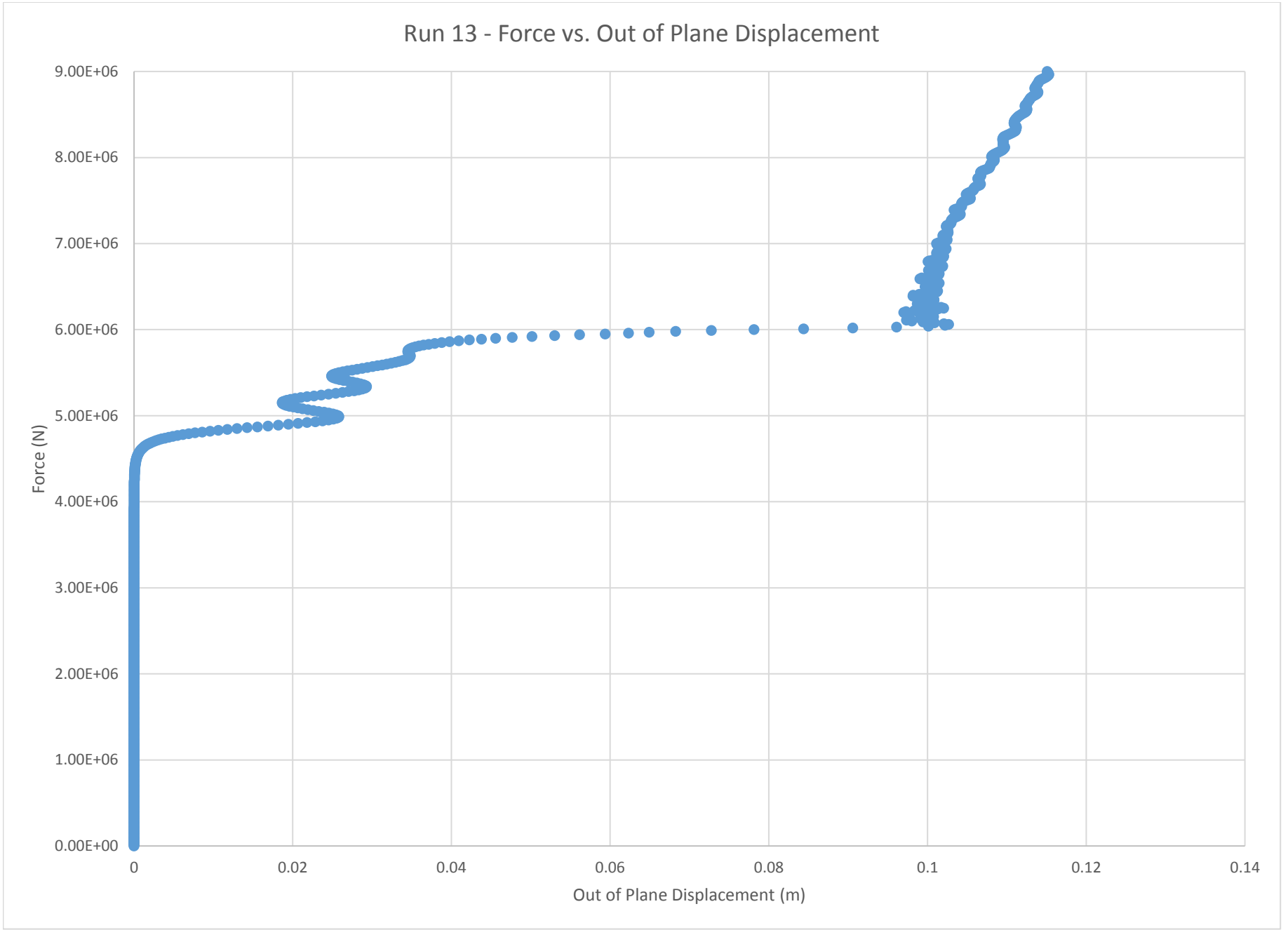
Run 13 - Force vs. Out of Plane Displacement
9.00E+06
8.00E+06
7.00E+06
6.00E+06
5.00E+06
4.00E+06
3.00E+06
2.00E+06
1.00E+06
0.00E+00
Force (N)
0
0.02
0.04
0.06
0.08
0.1
0.12
0.14
Out of Plane Displacement (m)

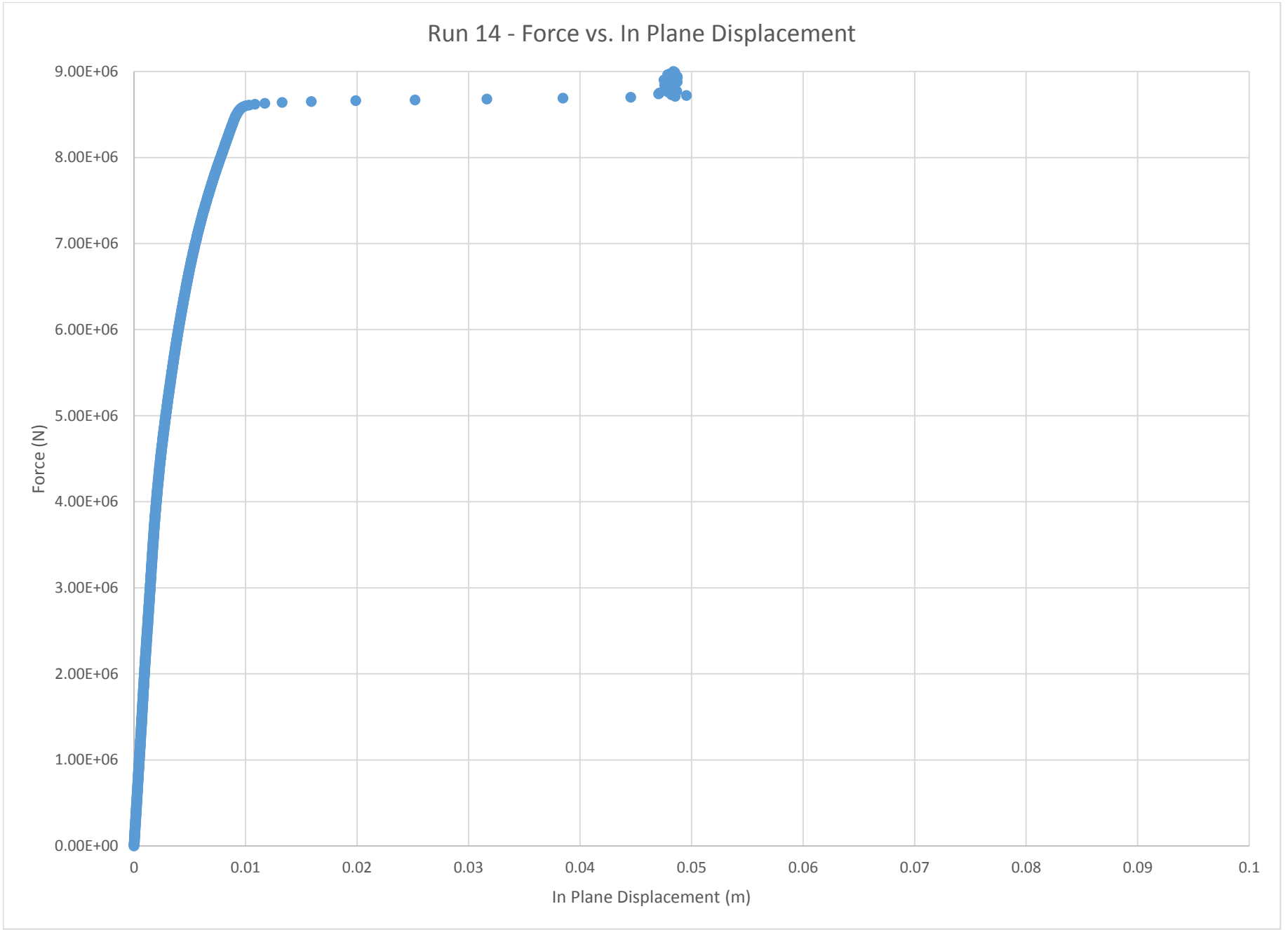
Run 14 - Force vs. In Plane Displacement
9.00E+06
8.00E+06
7.00E+06
6.00E+06
5.00E+06
4.00E+06
3.00E+06
2.00E+06
1.00E+06
0.00E+00
Force (N)
0
0.01
0.02
0.03
0.04
0.05
0.06
0.07
0.08
0.09
0.1
In Plane Displacement (m)

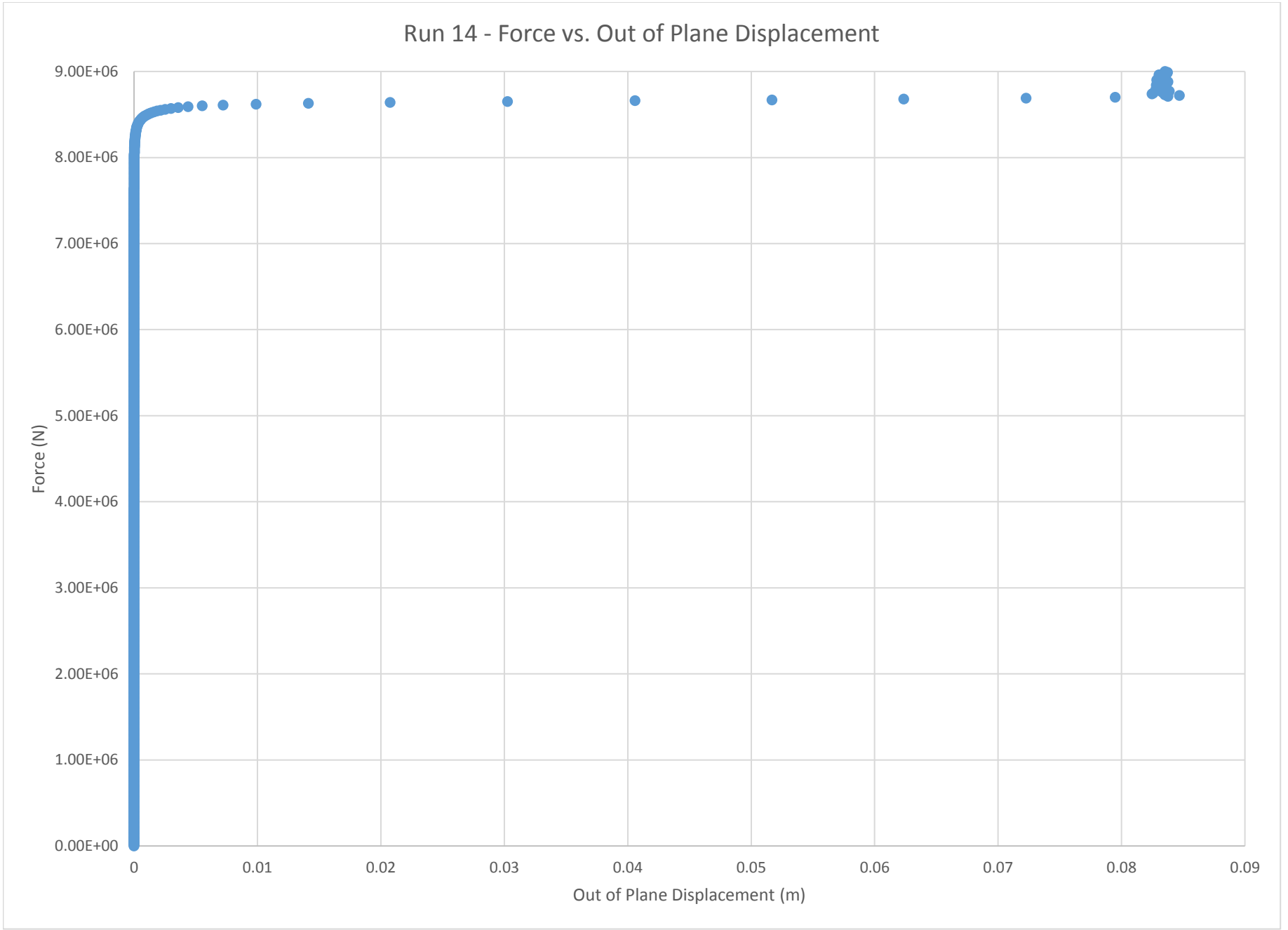
Run 14 - Force vs. Out of Plane Displacement
9.00E+06
8.00E+06
7.00E+06
6.00E+06
5.00E+06
4.00E+06
3.00E+06
2.00E+06
1.00E+06
0.00E+00
Force (N)
0
0.01
0.02
0.03
0.04
0.05
0.06
0.07
0.08
0.09
Out of Plane Displacement (m)


Run 15 - Force vs. In Plane Displacement
9.00E+06
8.00E+06
7.00E+06
6.00E+06
5.00E+06
4.00E+06
3.00E+06
2.00E+06
1.00E+06
0.00E+00
Force (N)
0
0.01
0.02
0.03
0.04
0.05
0.06
0.07
0.08
0.09
0.1
In Plane Displacement (m)

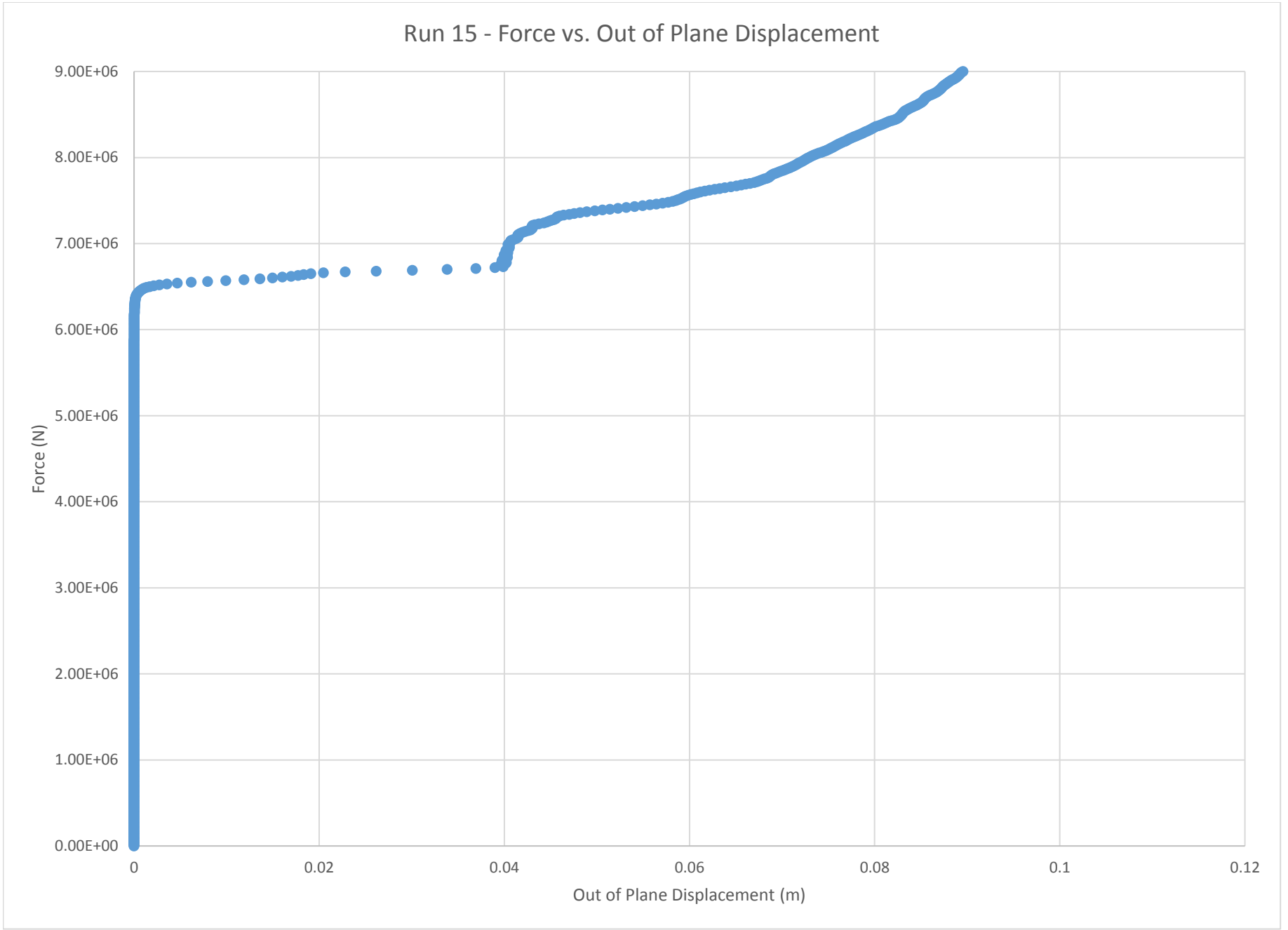
Run 15 - Force vs. Out of Plane Displacement
9.00E+06
8.00E+06
7.00E+06
6.00E+06
5.00E+06
4.00E+06
3.00E+06
2.00E+06
1.00E+06
0.00E+00
Force (N)
0
0.02
0.04
0.06
0.08
0.1
0.12
Out of Plane Displacement (m)

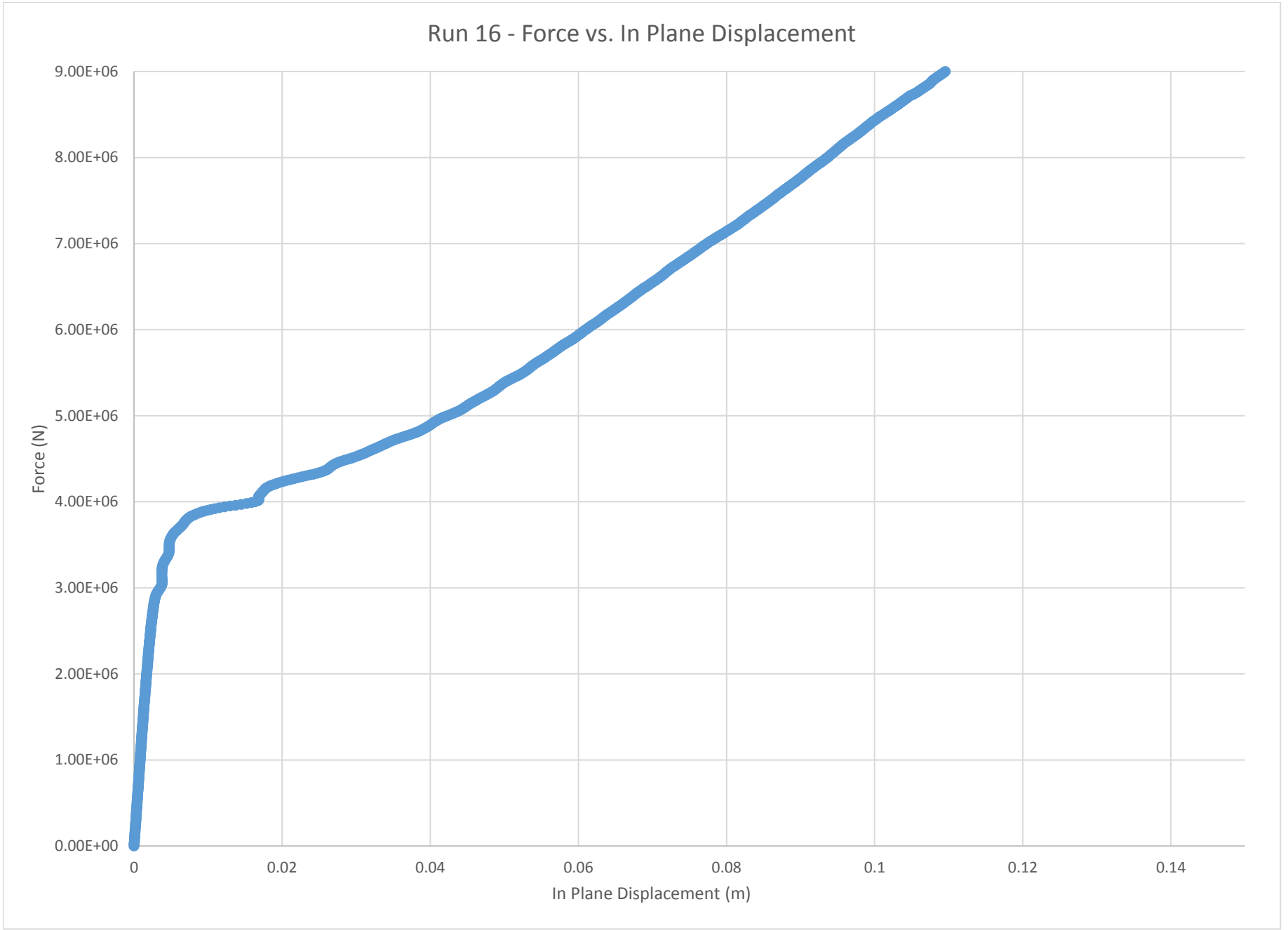
Run 16 - Force vs. In Plane Displacement
9.00E+06
8.00E+06
7.00E+06
6.00E+06
5.00E+06
4.00E+06
3.00E+06
2.00E+06
1.00E+06
0.00E+00
Force (N)
0
0.02
0.04
0.06
0.08
0.1
0.12
0.14
In Plane Displacement (m)

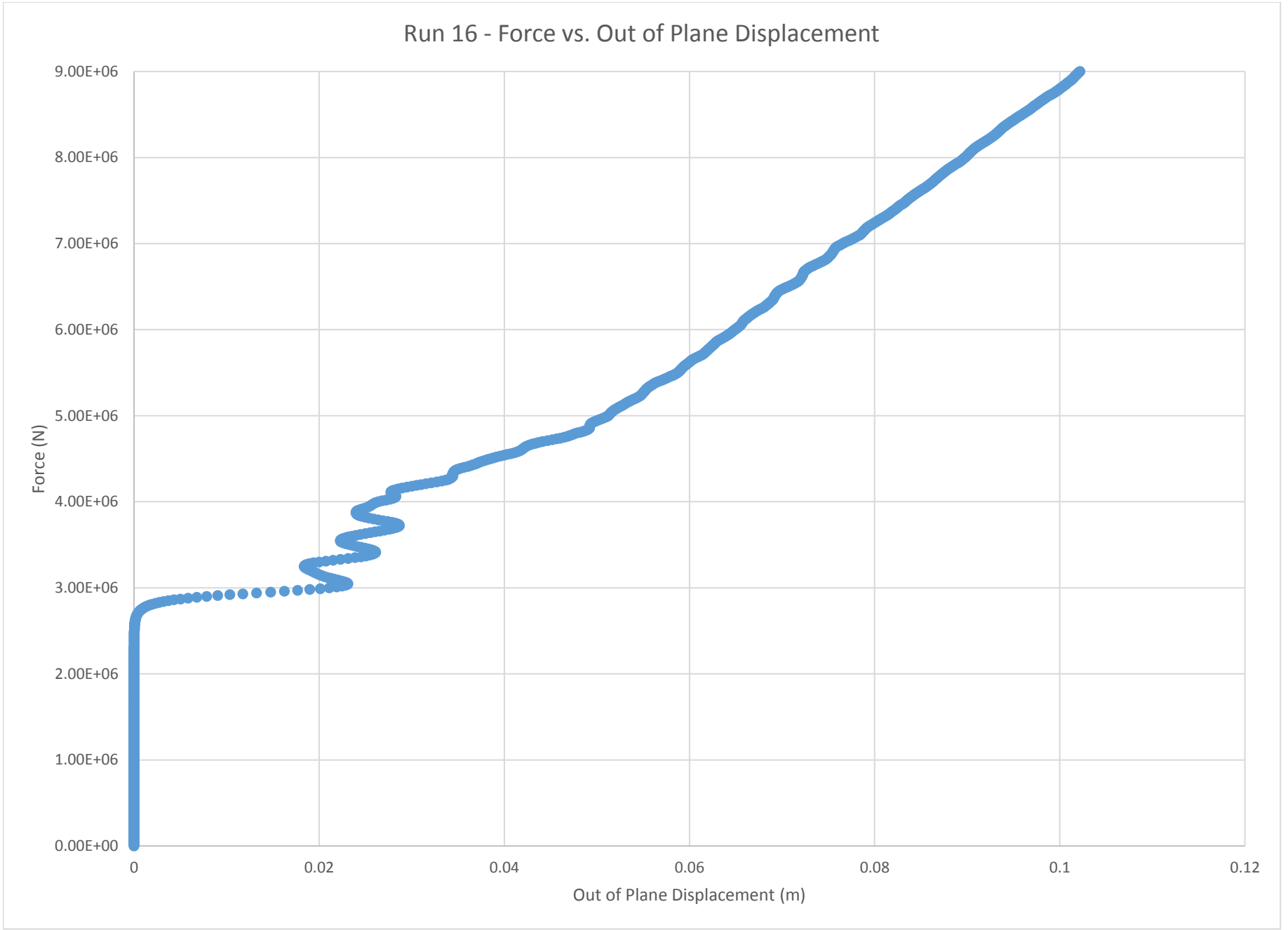
Run 16 - Force vs. Out of Plane Displacement
9.00E+06
8.00E+06
7.00E+06
6.00E+06
5.00E+06
4.00E+06
3.00E+06
2.00E+06
1.00E+06
0.00E+00
Force (N)
0
0.02
0.04
0.06
0.08
0.1
0.12
Out of Plane Displacement (m)

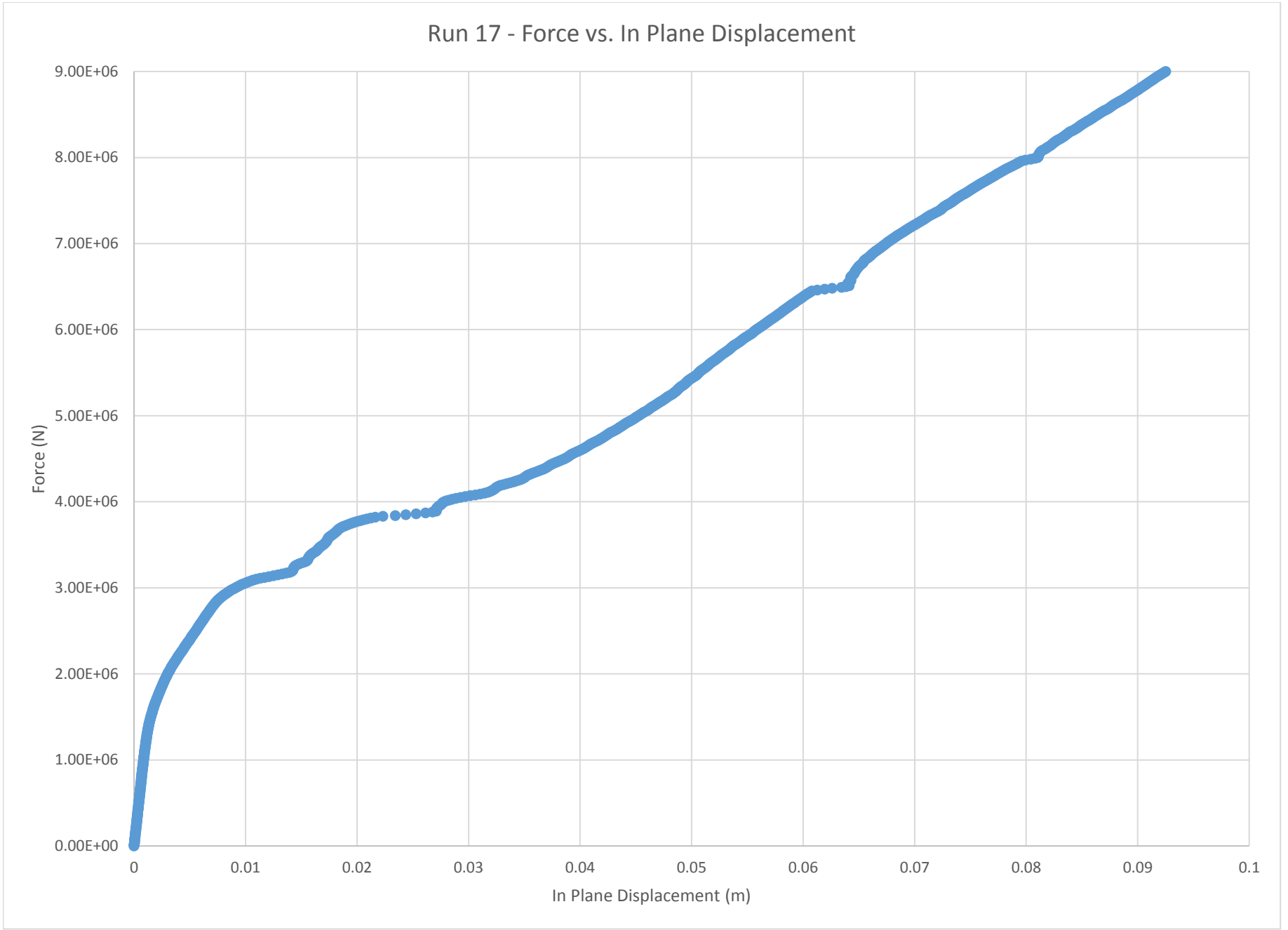
Run 17 - Force vs. In Plane Displacement
Force (N)
9.00E+06
8.00E+06
7.00E+06
6.00E+06
5.00E+06
4.00E+06
3.00E+06
2.00E+06
1.00E+06
0.00E+00
0
0.01
0.02
0.03
0.04
0.05
0.06
0.07
0.08
0.09
0.1
In Plane Displacement (m)

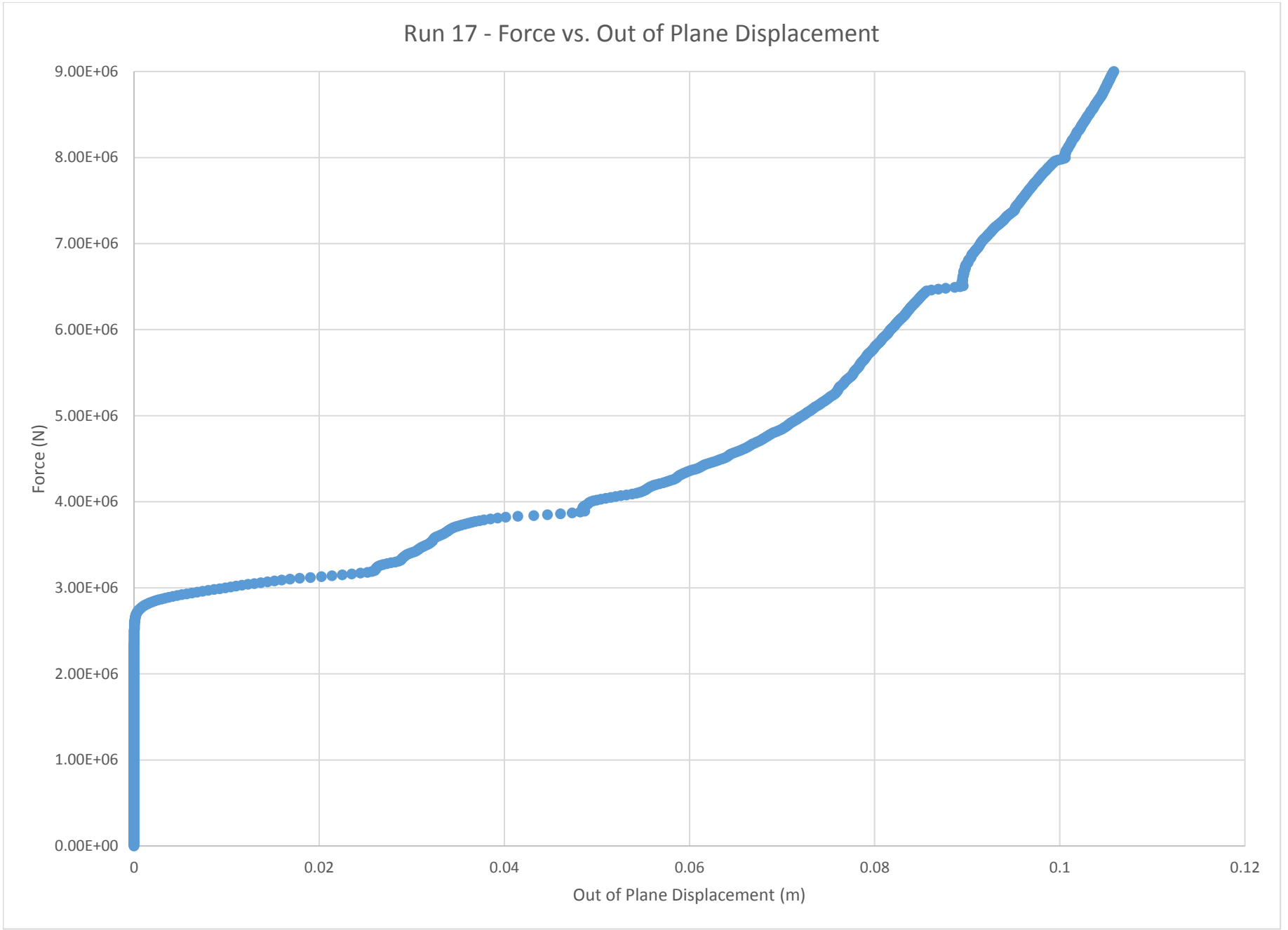
Run 17 - Force vs. Out of Plane Displacement
9.00E+06
8.00E+06
7.00E+06
6.00E+06
5.00E+06
4.00E+06
3.00E+06
2.00E+06
1.00E+06
0.00E+00
Force (N)
0
0.02
0.04
0.06
0.08
0.1
0.12
Out of Plane Displacement (m)

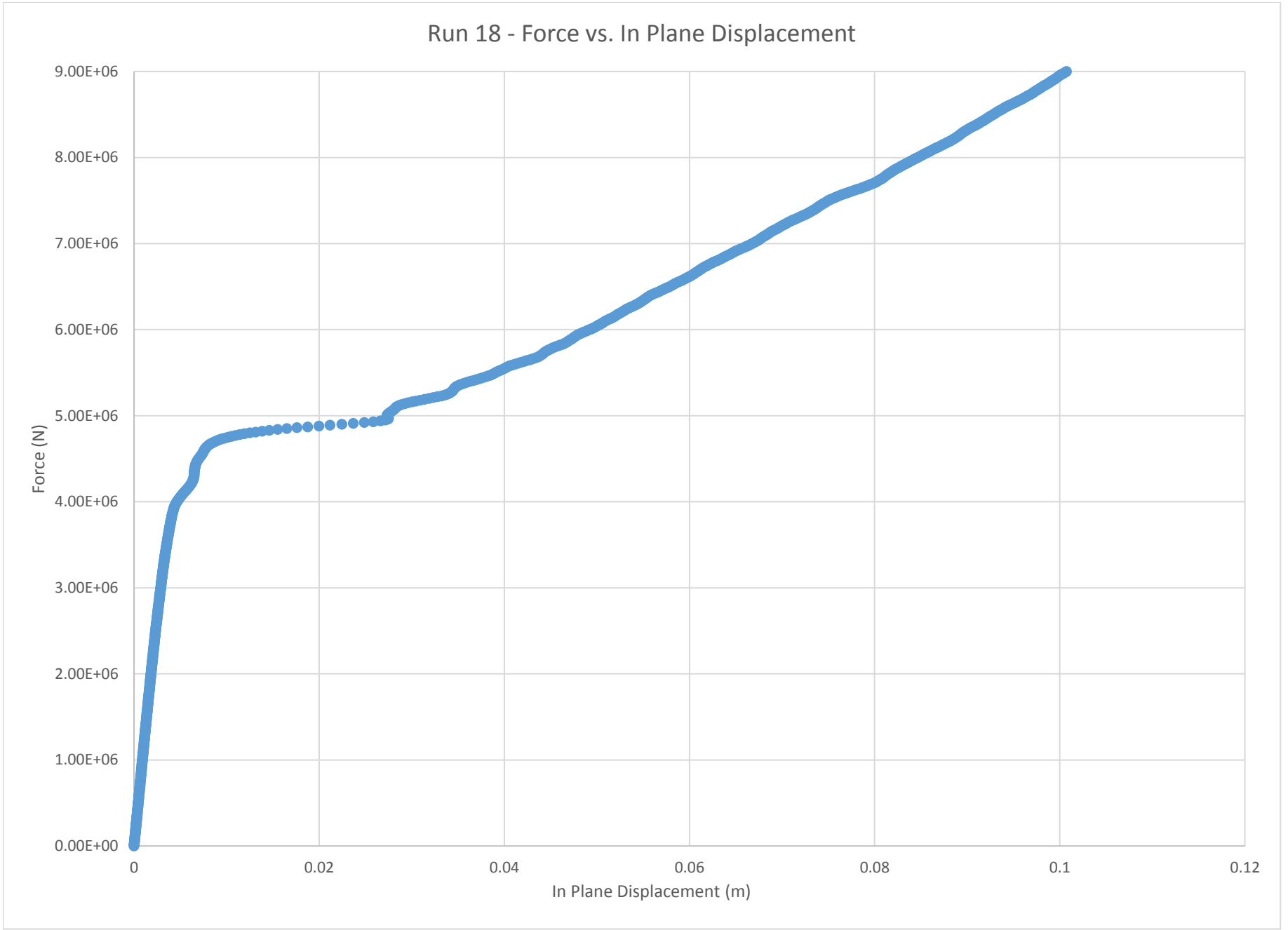
Run 18 - Force vs. In Plane Displacement
9.00E+06
8.00E+06
7.00E+06
6.00E+06
5.00E+06
4.00E+06
3.00E+06
2.00E+06
1.00E+06
0.00E+00
Force (N)
0
0.02
0.04
0.06
0.08
0.1
0.12
In Plane Displacement (m)

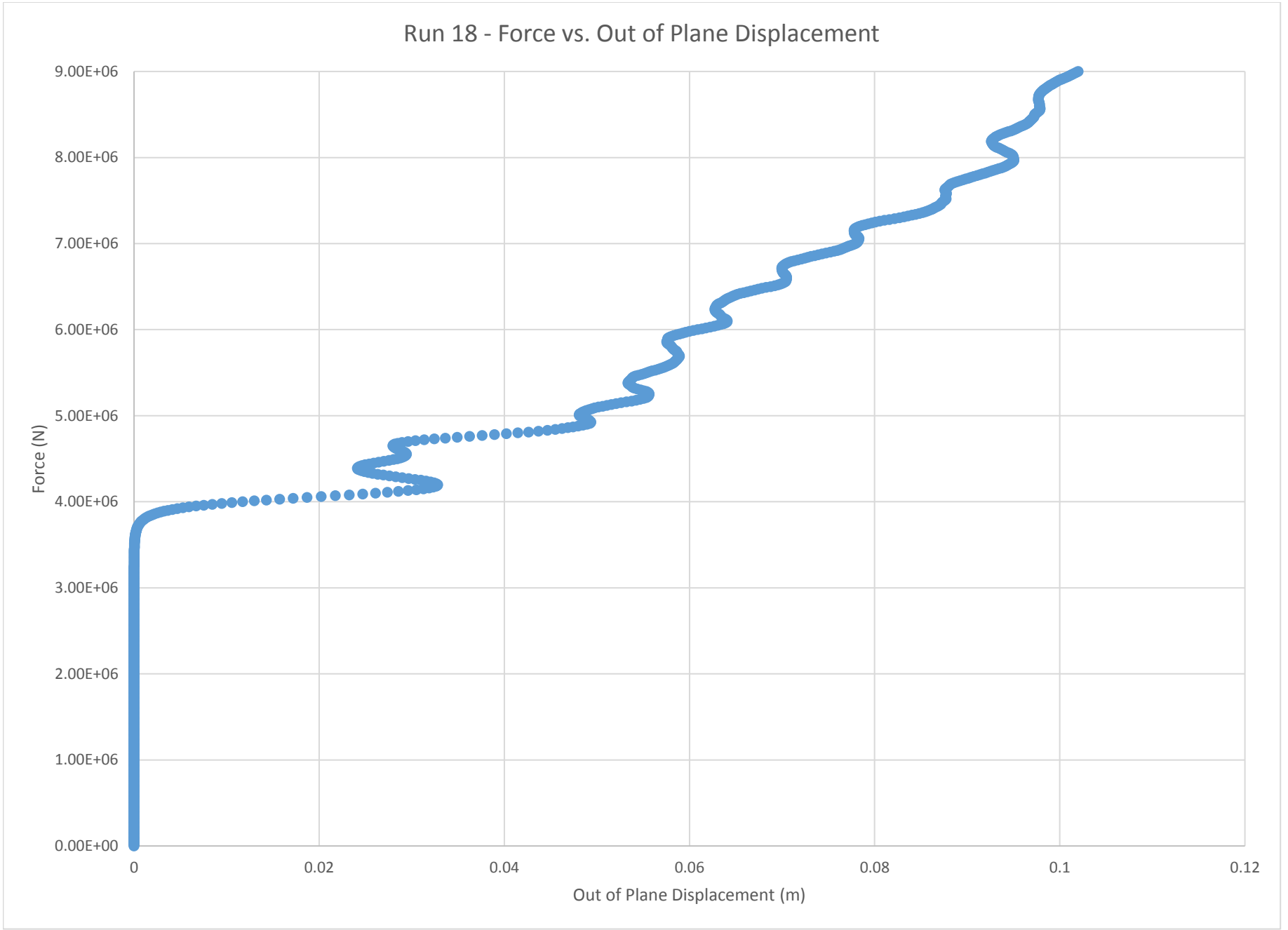
Run 18 - Force vs. Out of Plane Displacement
9.00E+06
8.00E+06
7.00E+06
6.00E+06
5.00E+06
4.00E+06
3.00E+06
2.00E+06
1.00E+06
0.00E+00
Force (N)
0
0.02
0.04
0.06
0.08
0.1
0.12
Out of Plane Displacement (m)

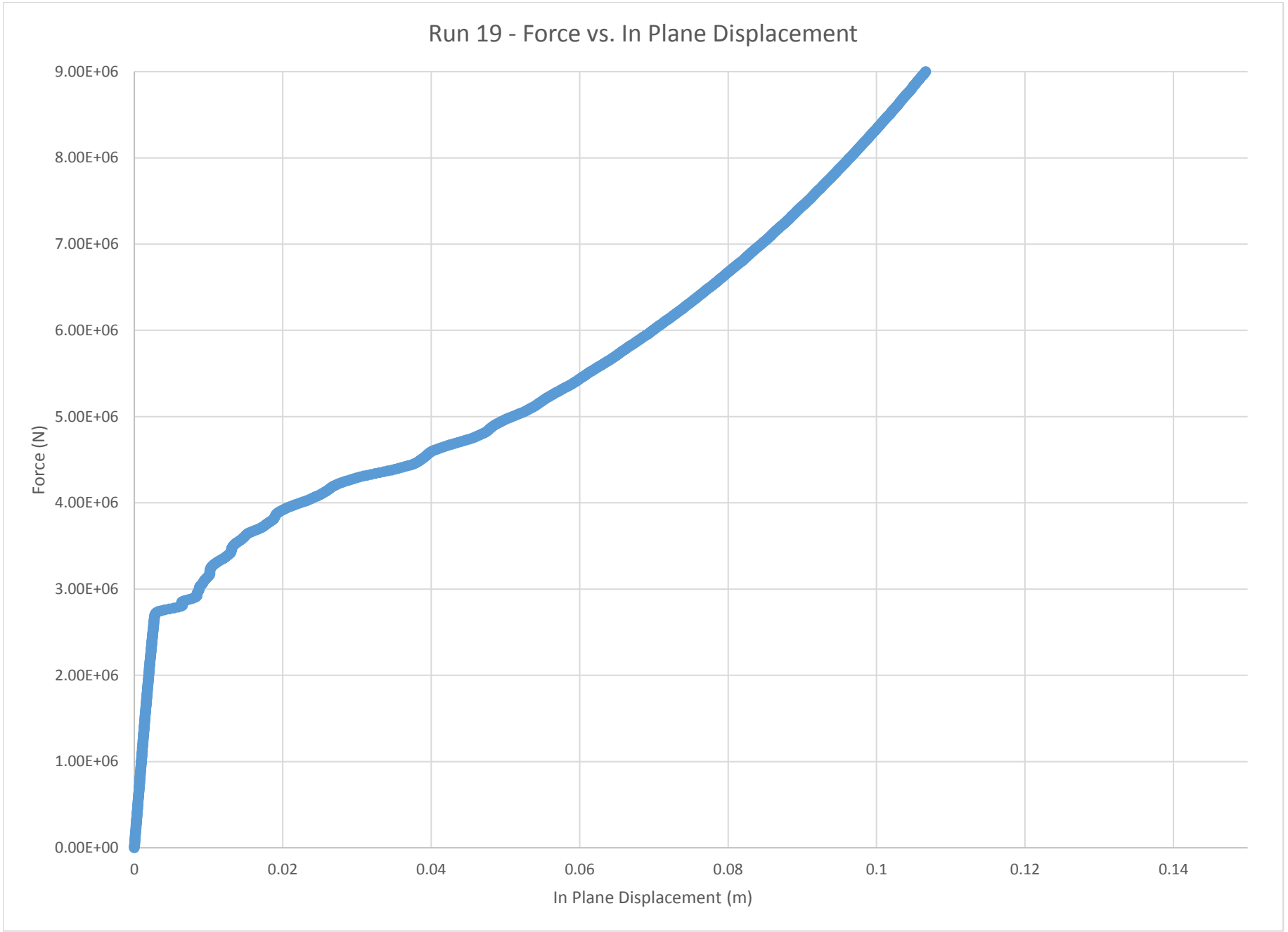
Run 19 - Force vs. In Plane Displacement
9.00E+06
8.00E+06
7.00E+06
6.00E+06
5.00E+06
4.00E+06
3.00E+06
2.00E+06
1.00E+06
0.00E+00
Force (N)
0
0.02
0.04
0.06
0.08
0.1
0.12
0.14
In Plane Displacement (m)

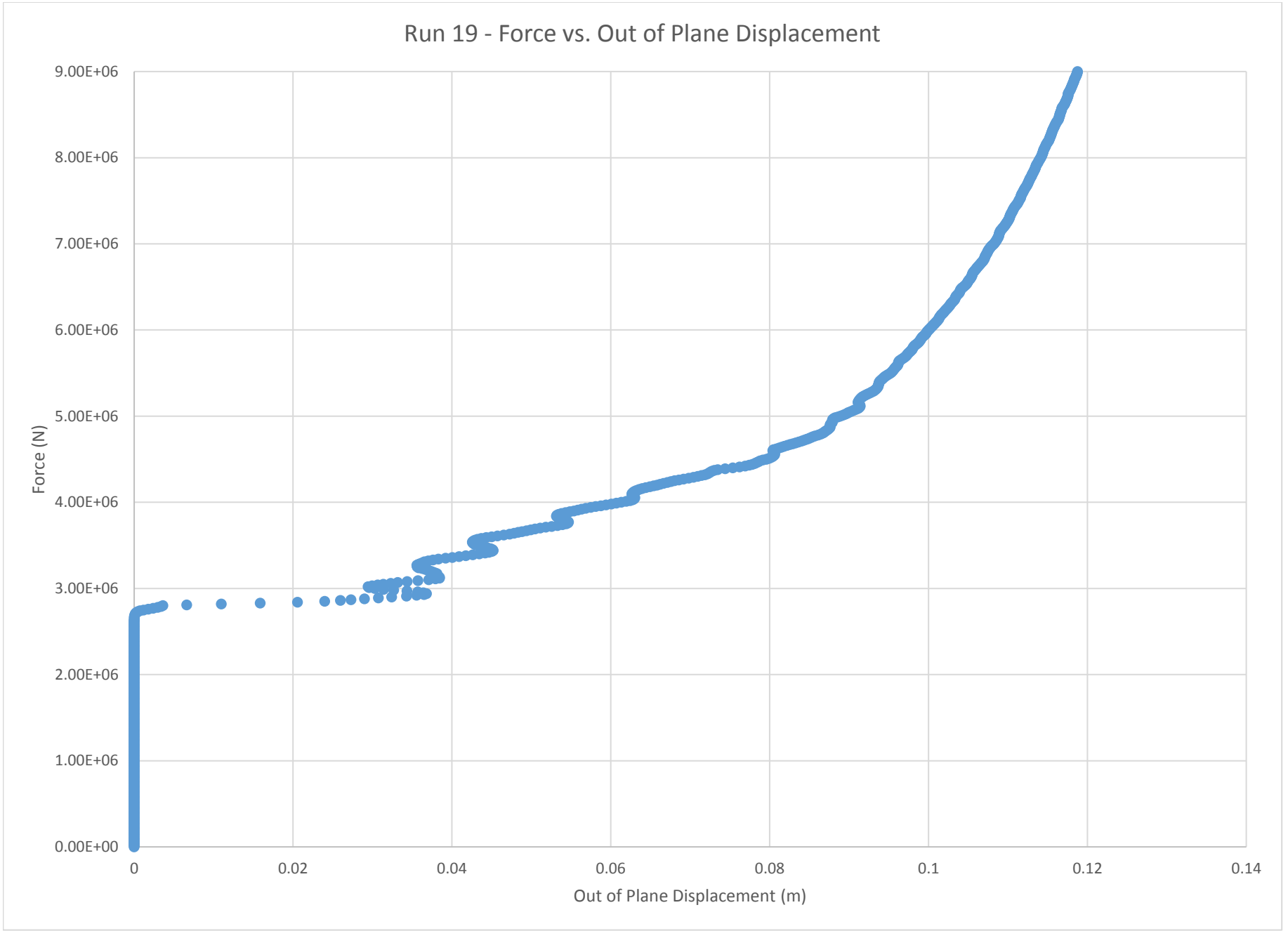
Run 19 - Force vs. Out of Plane Displacement
Force (N)
9.00E+06
8.00E+06
7.00E+06
6.00E+06
5.00E+06
4.00E+06
3.00E+06
2.00E+06
1.00E+06
0.00E+00
0
0.02
0.04
0.06
0.08
0.1
0.12
0.14
Out of Plane Displacement (m)

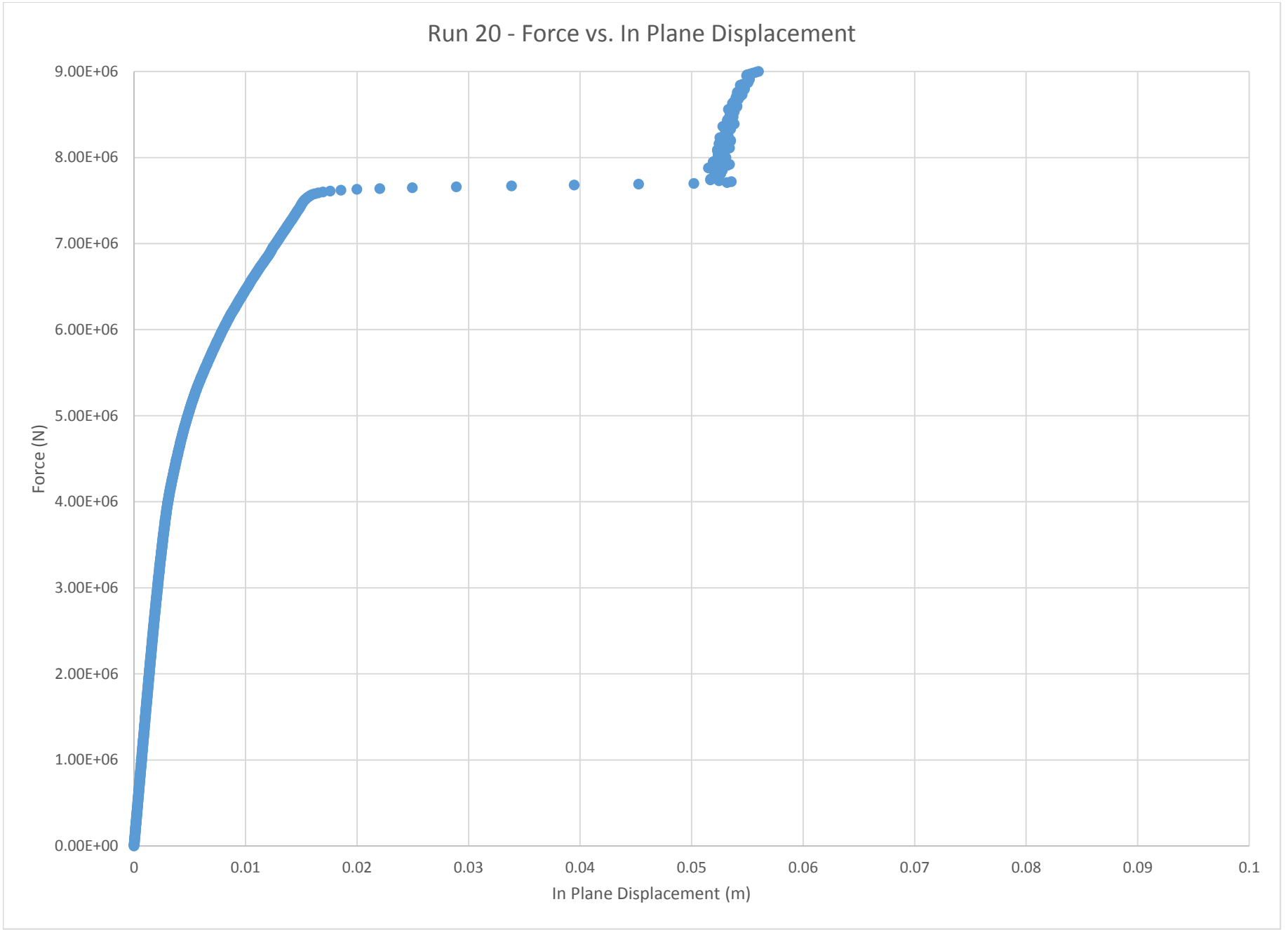
Run 20 - Force vs. In Plane Displacement
9.00E+06
8.00E+06
7.00E+06
6.00E+06
5.00E+06
4.00E+06
3.00E+06
2.00E+06
1.00E+06
0.00E+00
Force (N)
0
0.01
0.02
0.03
0.04
0.05
0.06
0.07
0.08
0.09
0.1
In Plane Displacement (m)

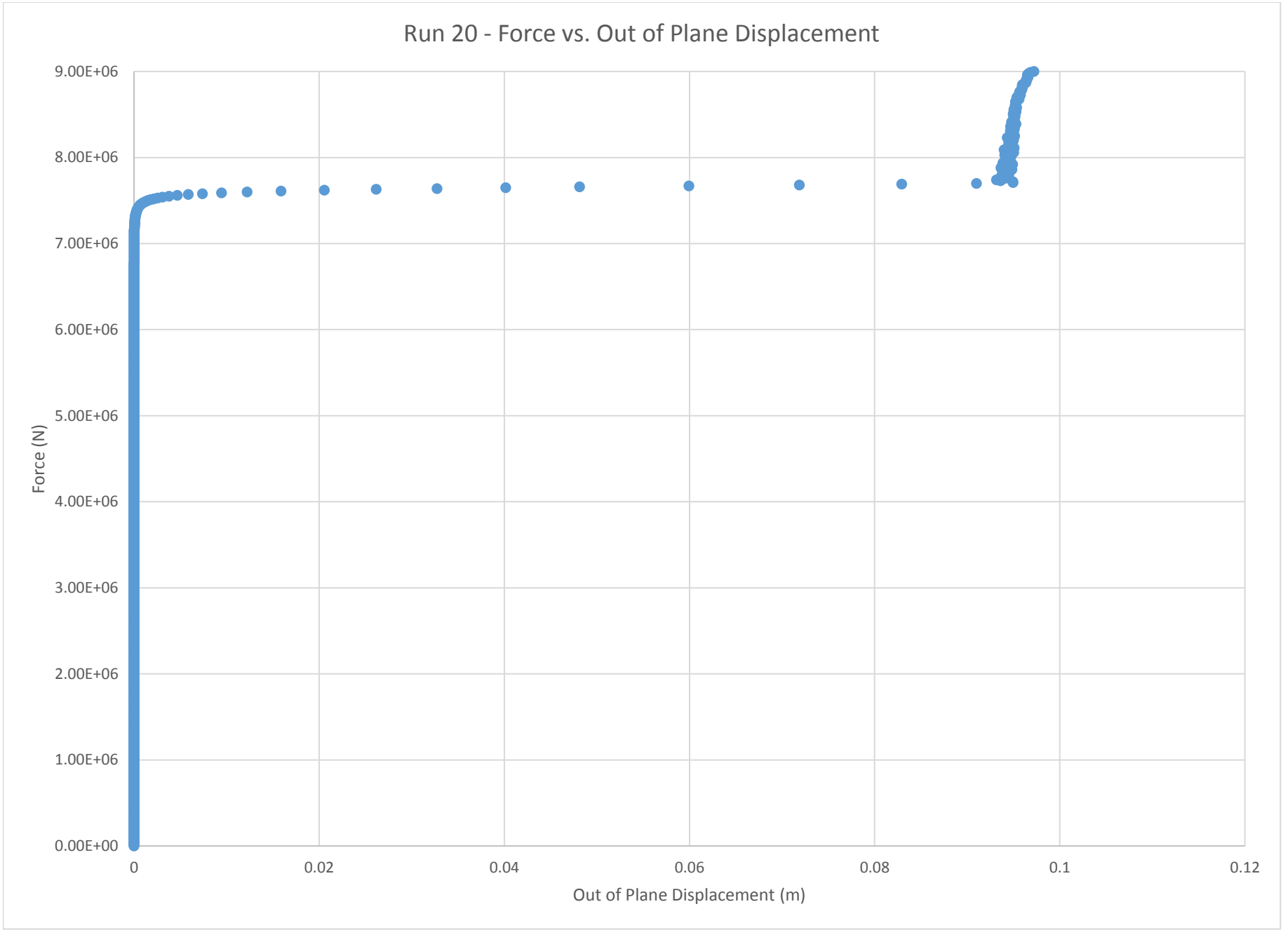
Run 20 - Force vs. Out of Plane Displacement
9.00E+06
8.00E+06
7.00E+06
6.00E+06
5.00E+06
4.00E+06
3.00E+06
2.00E+06
1.00E+06
0.00E+00
Force (N)
0
0.02
0.04
0.06
0.08
0.1
0.12
Out of Plane Displacement (m)

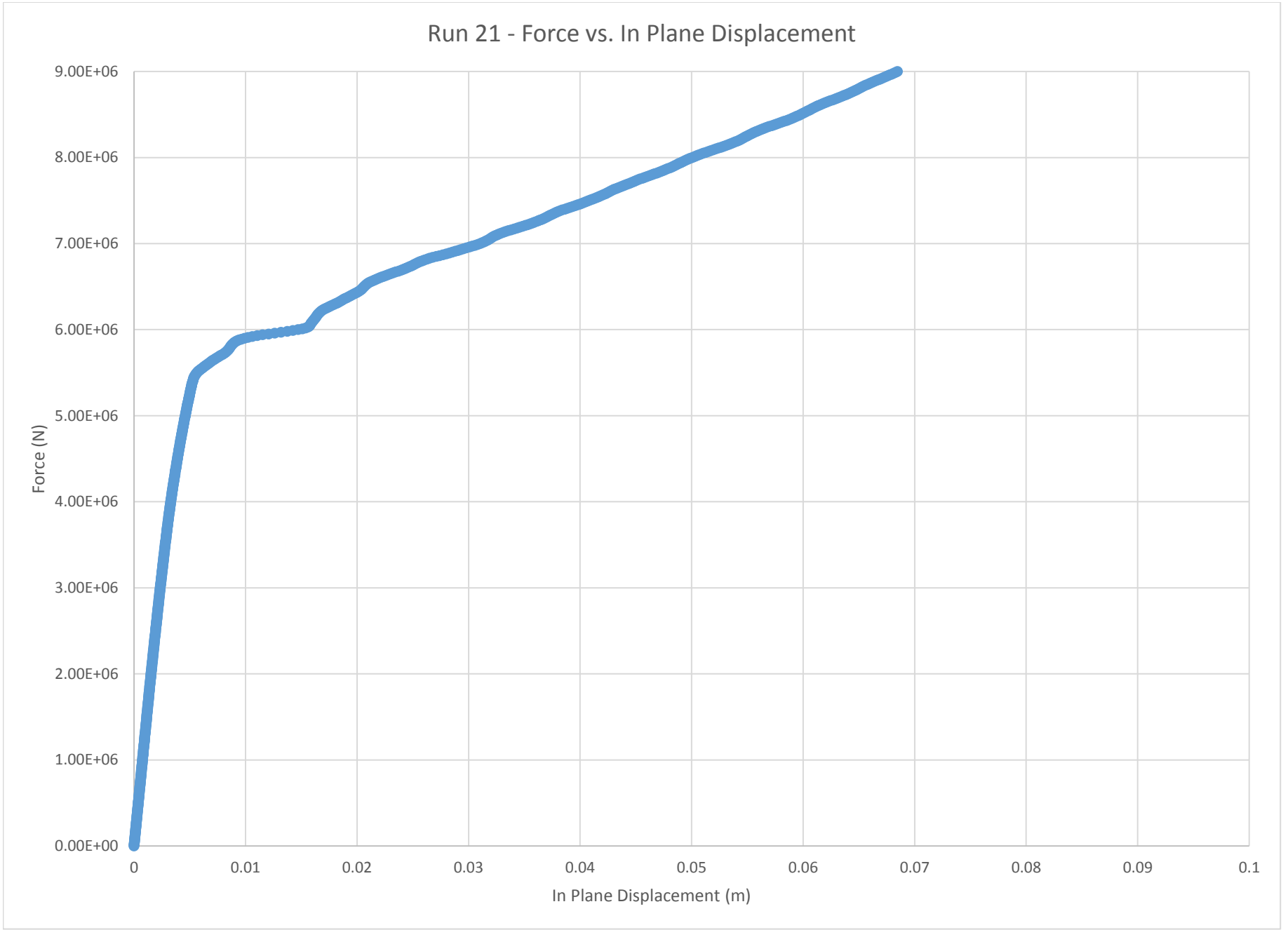
Run 21 - Force vs. In Plane Displacement
9.00E+06
8.00E+06
7.00E+06
6.00E+06
5.00E+06
4.00E+06
3.00E+06
2.00E+06
1.00E+06
0.00E+00
Force (N)
0
0.01
0.02
0.03
0.04
0.05
0.06
0.07
0.08
0.09
0.1
In Plane Displacement (m)

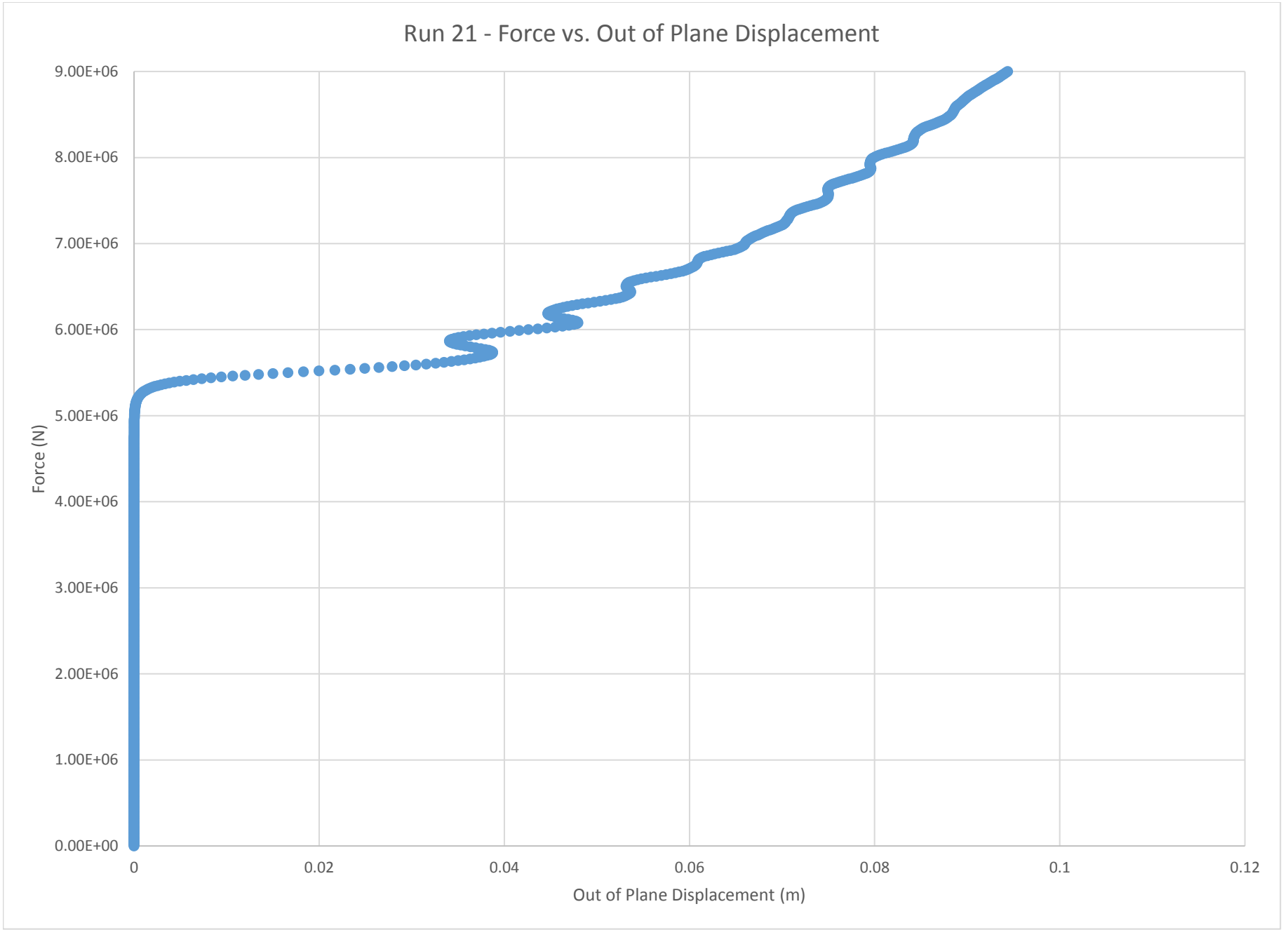
Run 21 - Force vs. Out of Plane Displacement
9.00E+06
8.00E+06
7.00E+06
6.00E+06
5.00E+06
4.00E+06
3.00E+06
2.00E+06
1.00E+06
0.00E+00
Force (N)
0
0.02
0.04
0.06
0.08
0.1
0.12
Out of Plane Displacement (m)

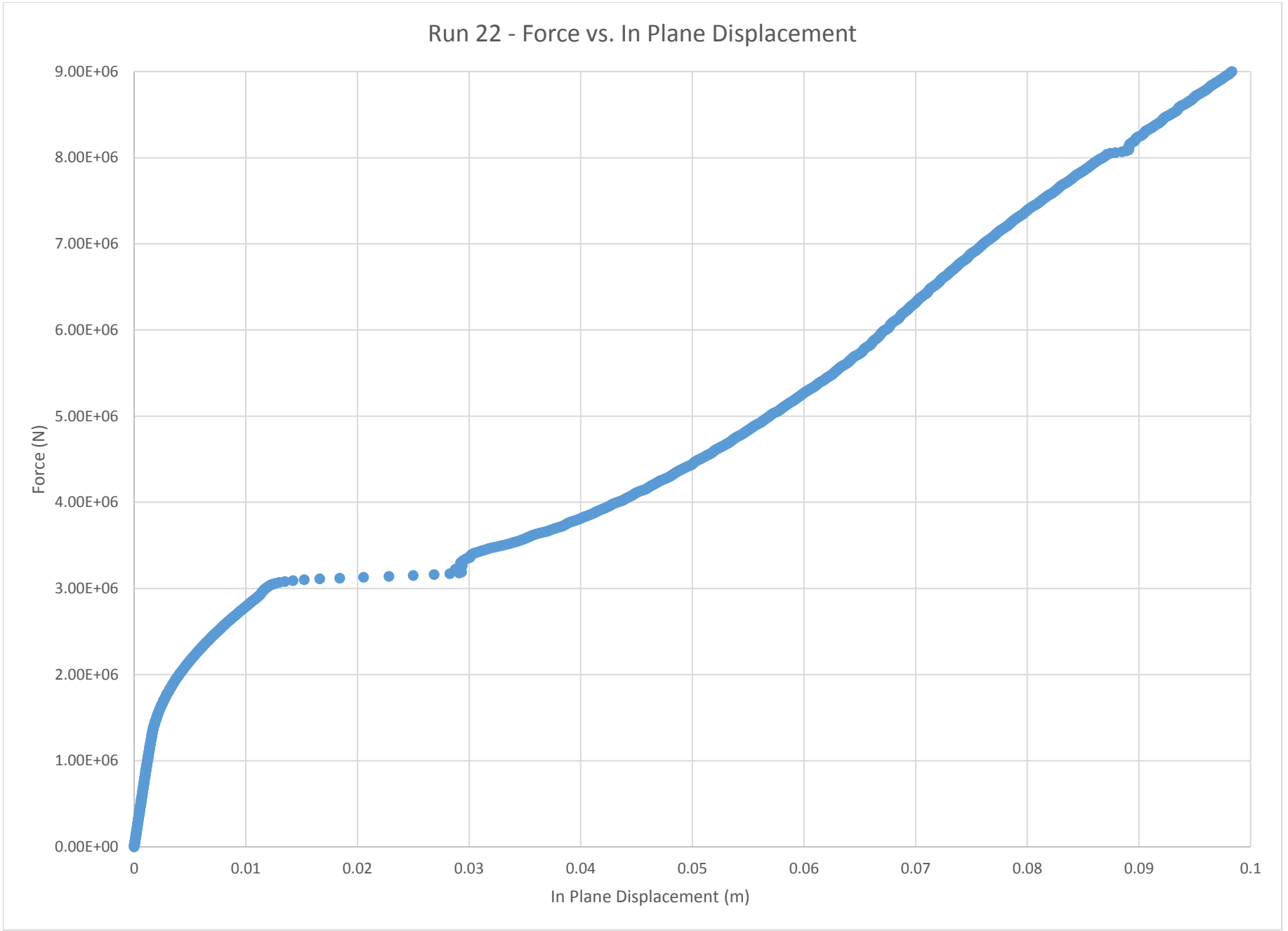
Run 22 - Force vs. In Plane Displacement
9.00E+06
8.00E+06
7.00E+06
6.00E+06
5.00E+06
4.00E+06
3.00E+06
2.00E+06
1.00E+06
0.00E+00
Force (N)
0
0.01
0.02
0.03
0.04
0.05
0.06
0.07
0.08
0.09
0.1
In Plane Displacement (m)

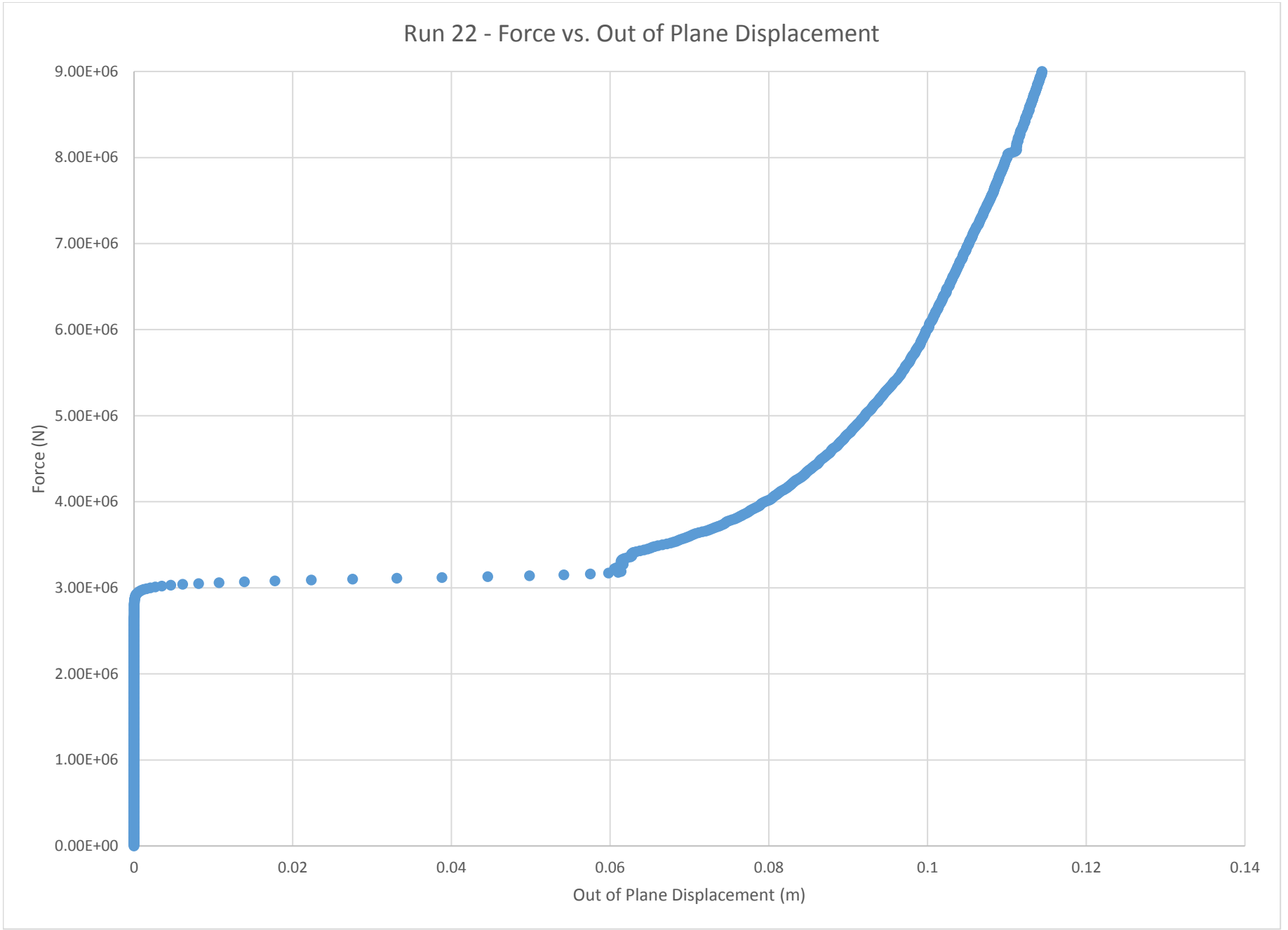
Run 22 - Force vs. Out of Plane Displacement
Force (N)
9.00E+06
8.00E+06
7.00E+06
6.00E+06
5.00E+06
4.00E+06
3.00E+06
2.00E+06
1.00E+06
0.00E+00
0
0.02
0.04
0.06
0.08
0.1
0.12
0.14
Out of Plane Displacement (m)

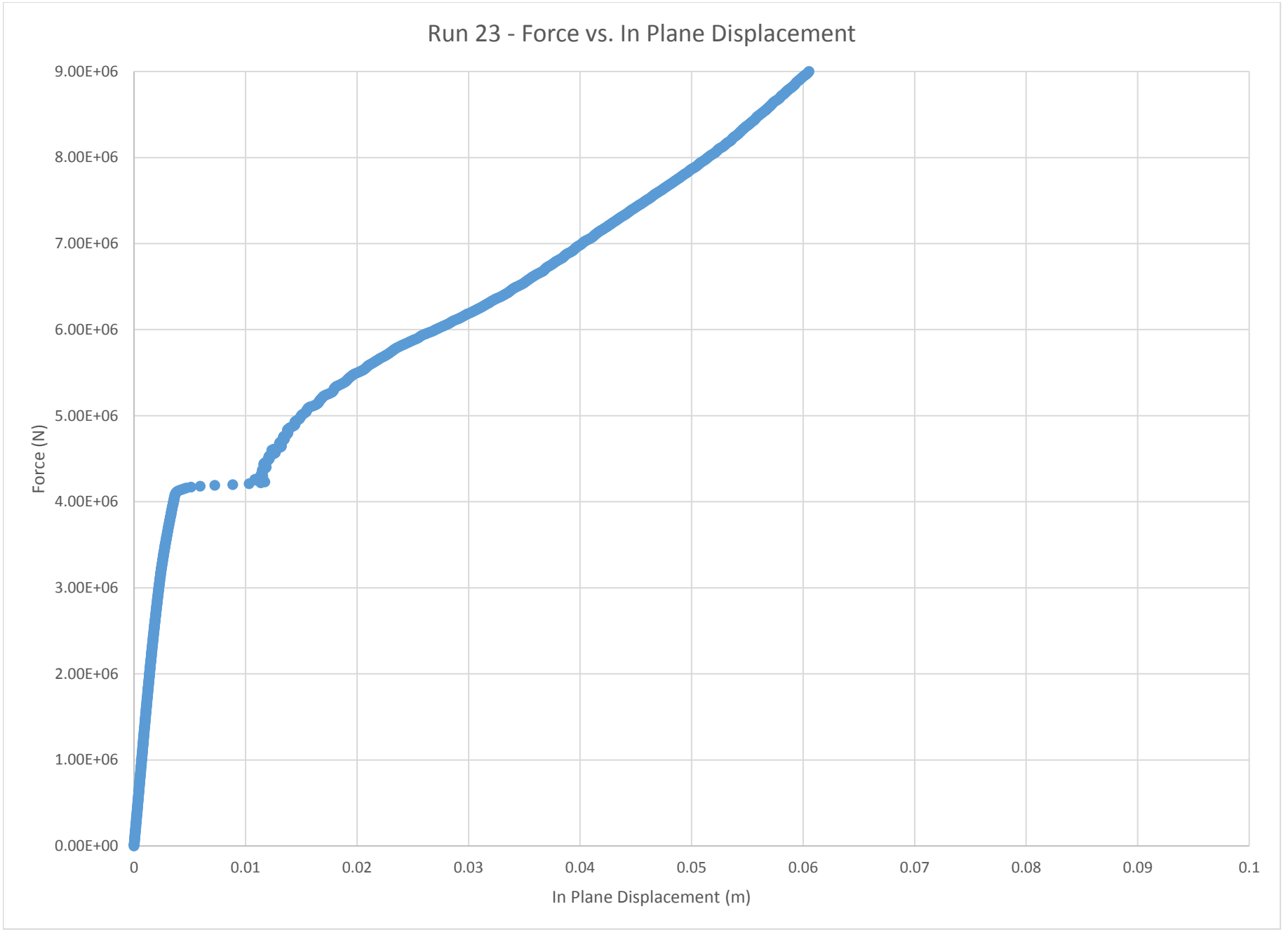
Run 23 - Force vs. In Plane Displacement
Force (N)
9.00E+06
8.00E+06
7.00E+06
6.00E+06
5.00E+06
4.00E+06
3.00E+06
2.00E+06
1.00E+06
0.00E+00
0
0.01
0.02
0.03
0.04
0.05
0.06
0.07
0.08
0.09
0.1
In Plane Displacement (m)

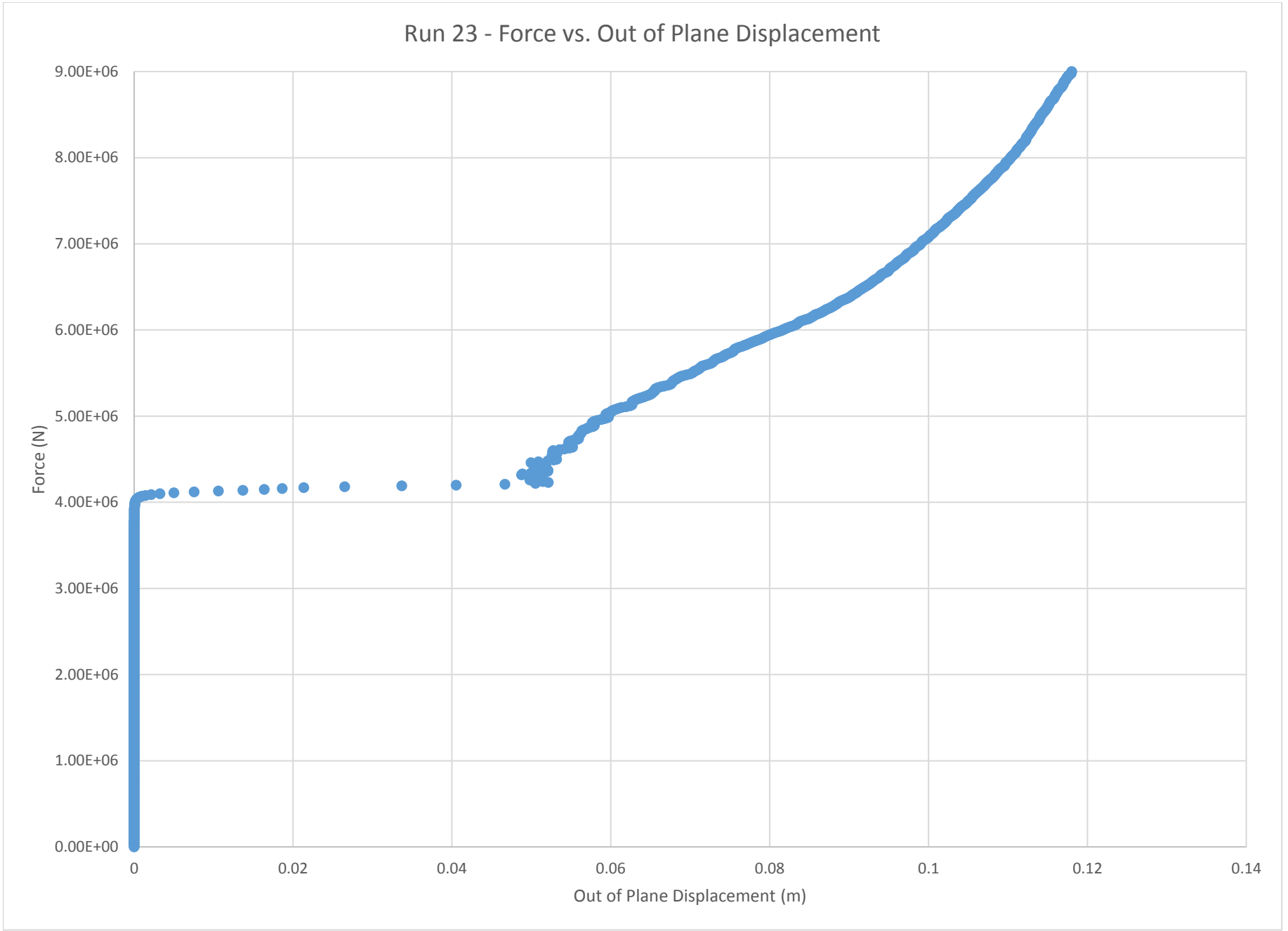
Run 23 - Force vs. Out of Plane Displacement
9.00E+06
8.00E+06
7.00E+06
6.00E+06
5.00E+06
4.00E+06
3.00E+06
2.00E+06
1.00E+06
0.00E+00
Force (N)
0
0.02
0.04
0.06
0.08
0.1
0.12
0.14
Out of Plane Displacement (m)

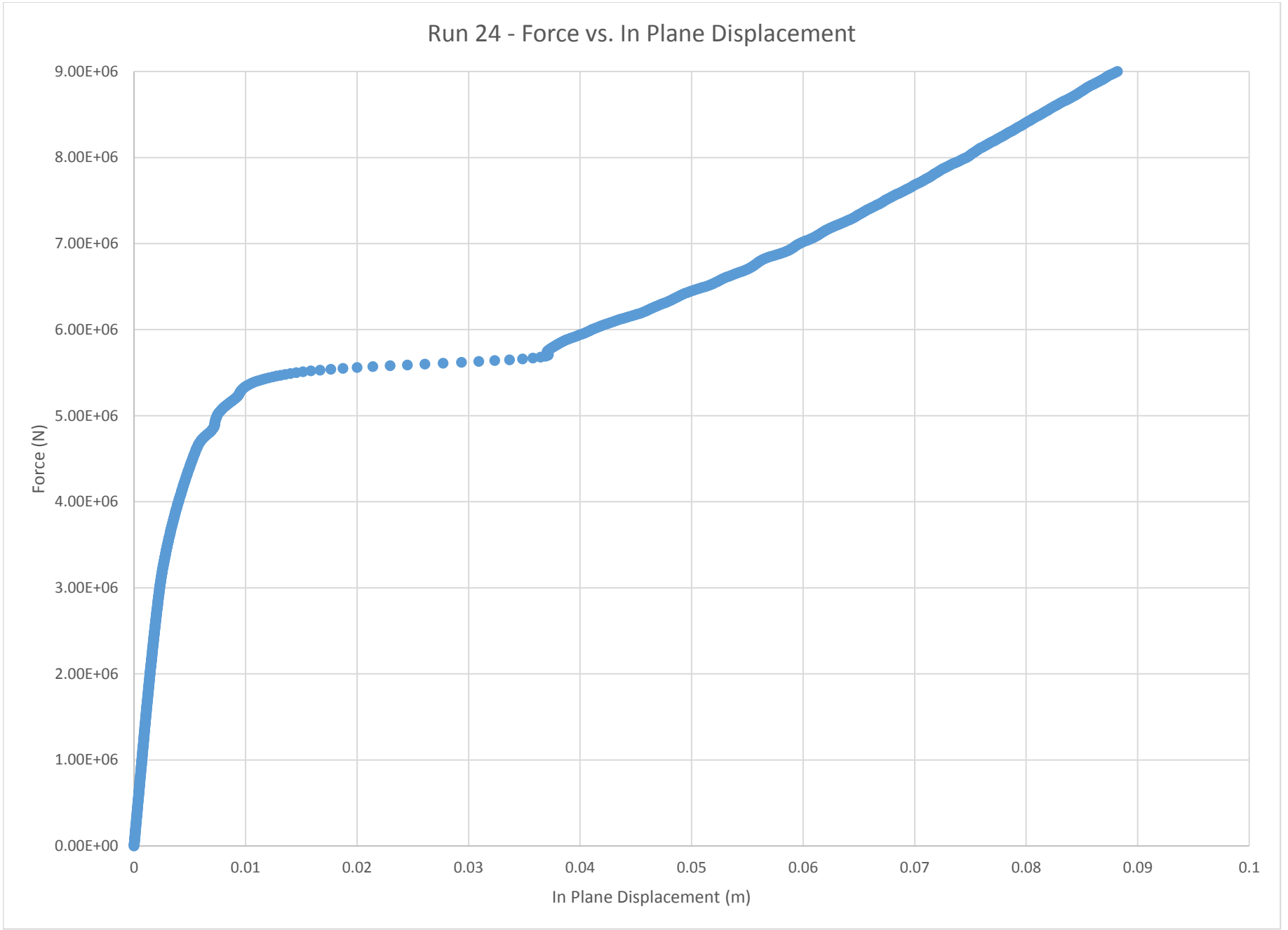
Run 24 - Force vs. In Plane Displacement
9.00E+06
8.00E+06
7.00E+06
6.00E+06
5.00E+06
4.00E+06
3.00E+06
2.00E+06
1.00E+06
0.00E+00
Force (N)
0
0.01
0.02
0.03
0.04
0.05
0.06
0.07
0.08
0.09
0.1
In Plane Displacement (m)

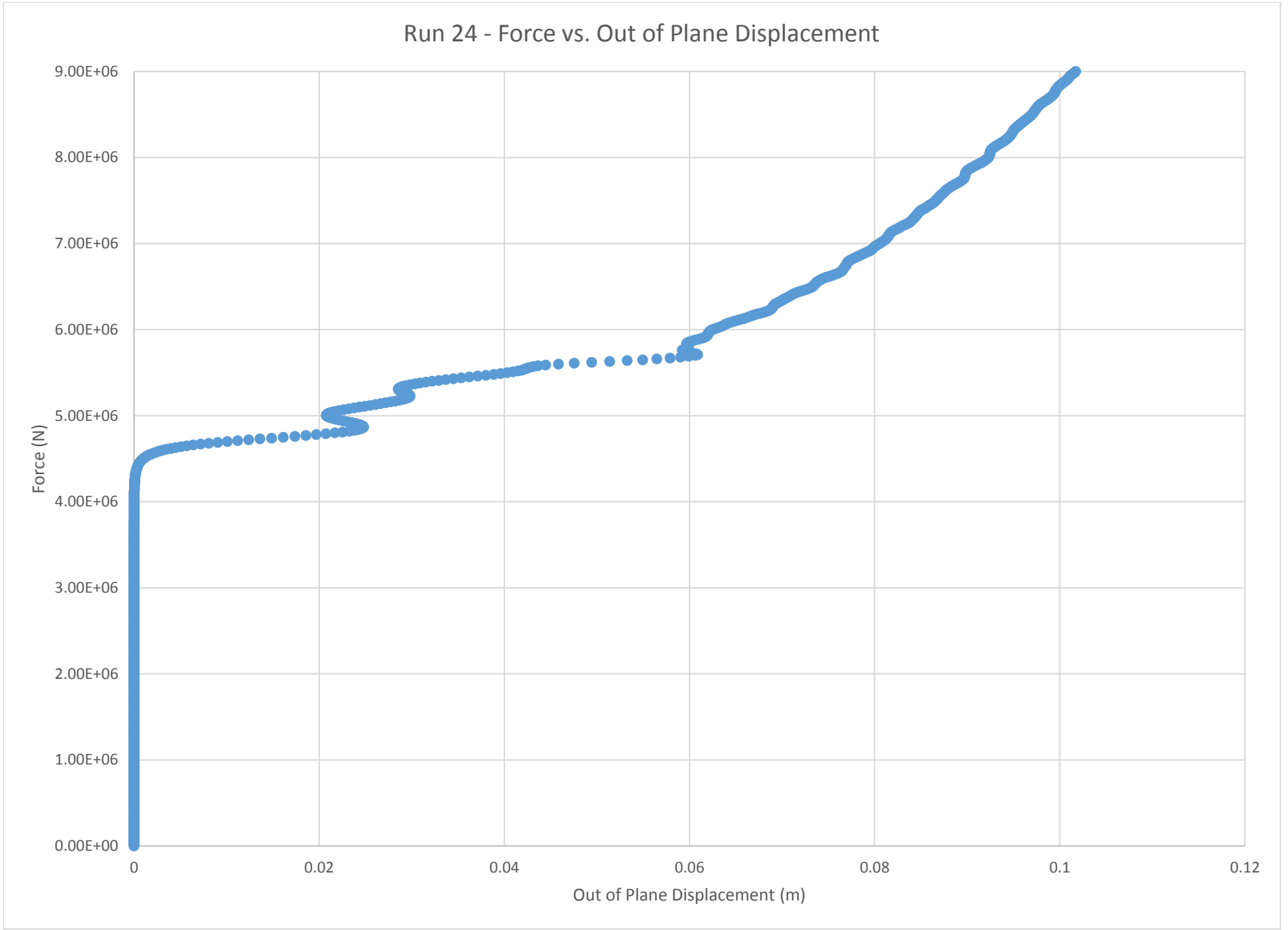
Run 24 - Force vs. Out of Plane Displacement
Force (N)
9.00E+06
8.00E+06
7.00E+06
6.00E+06
5.00E+06
4.00E+06
3.00E+06
2.00E+06
1.00E+06
0.00E+00
0
0.02
0.04
0.06
0.08
0.1
0.12
Out of Plane Displacement (m)

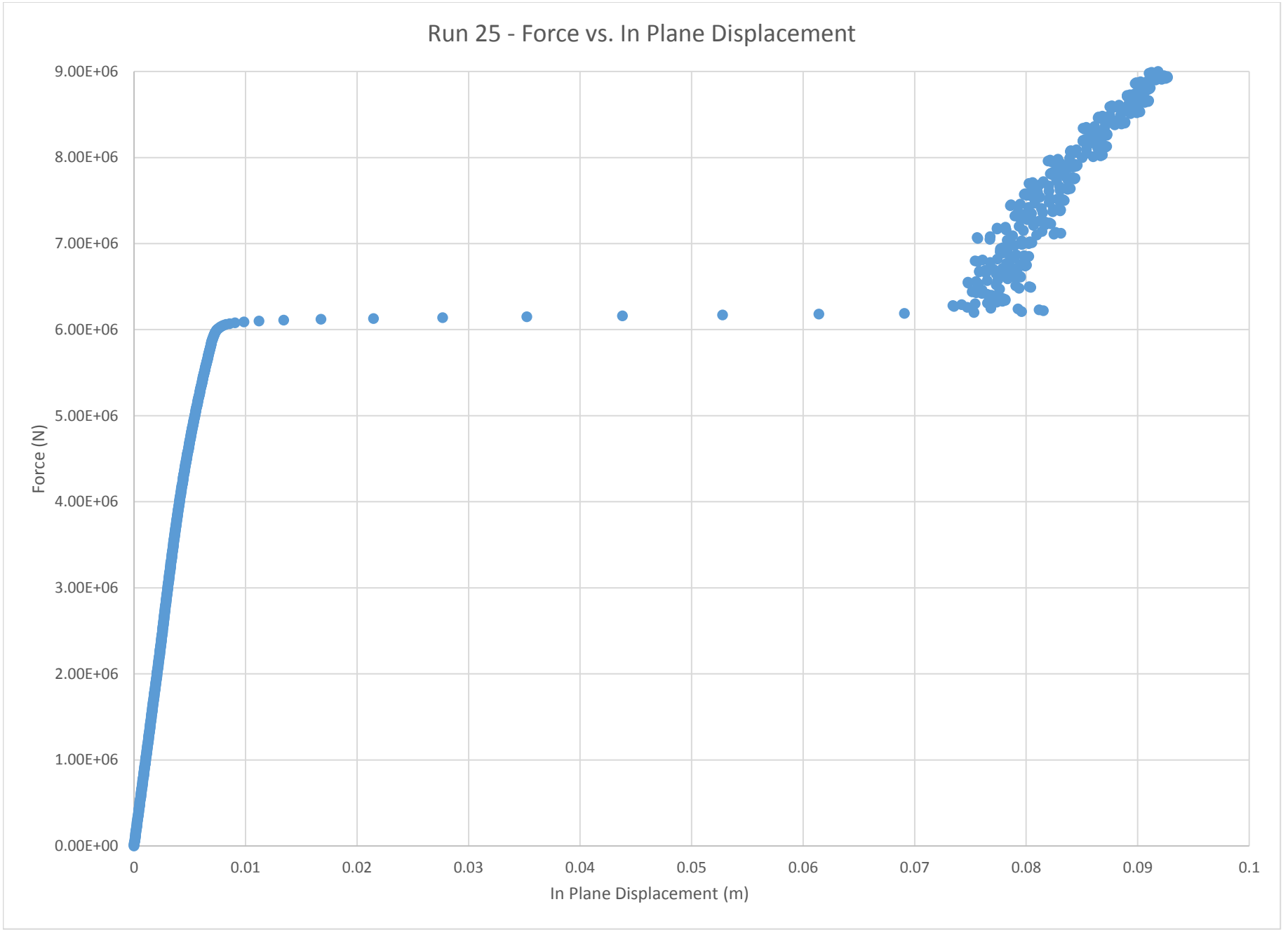
Run 25 - Force vs. In Plane Displacement
Force (N)
9.00E+06
8.00E+06
7.00E+06
6.00E+06
5.00E+06
4.00E+06
3.00E+06
2.00E+06
1.00E+06
0.00E+00
0
0.01
0.02
0.03
0.04
0.05
0.06
0.07
0.08
0.09
0.1
In Plane Displacement (m)

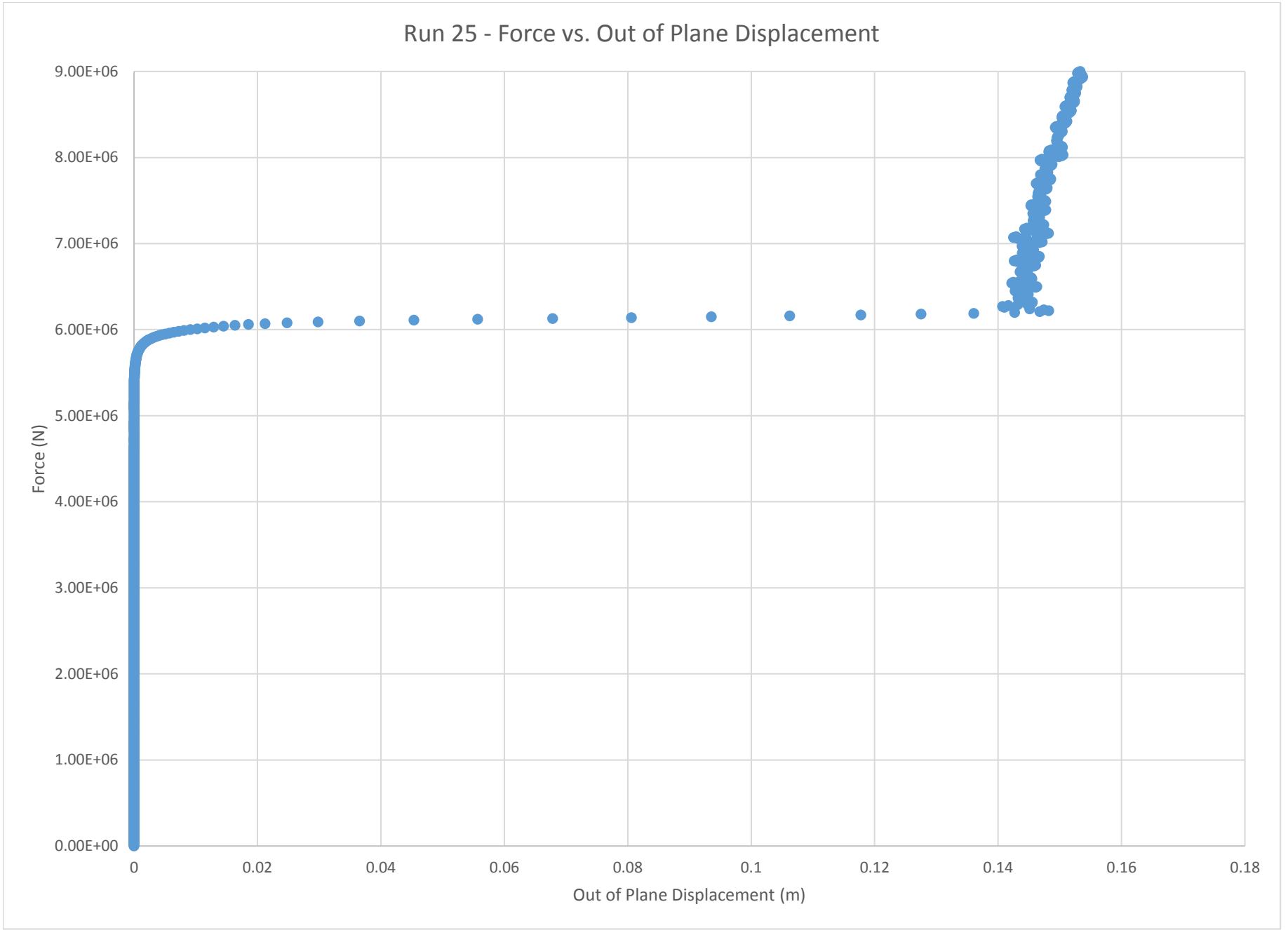
Run 25 - Force vs. Out of Plane Displacement
9.00E+06
8.00E+06
7.00E+06
6.00E+06
5.00E+06
4.00E+06
3.00E+06
2.00E+06
1.00E+06
0.00E+00
Force (N)
0
0.02
0.04
0.06
0.08
0.1
0.12
0.14
0.16
0.18
Out of Plane Displacement (m)

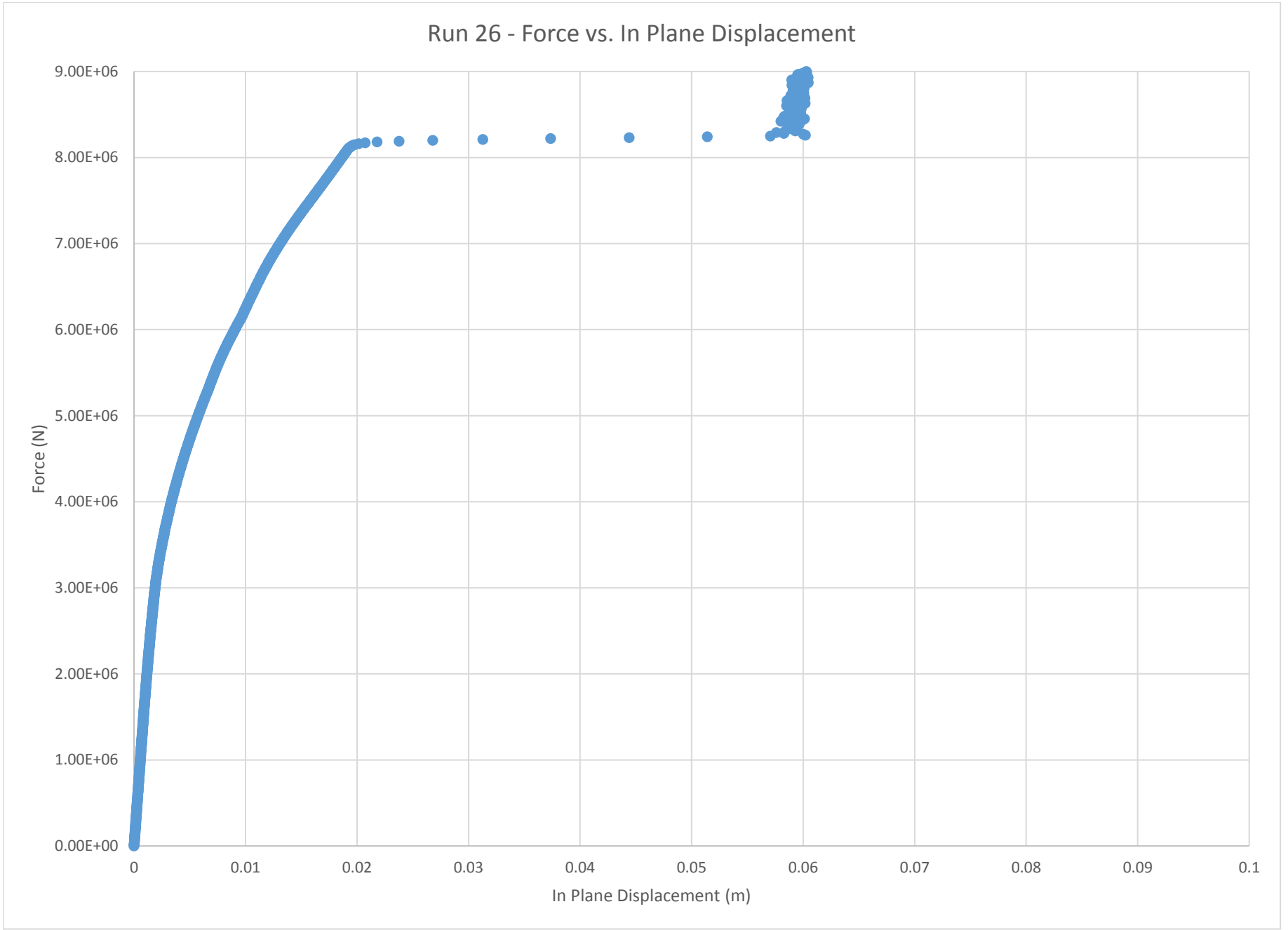
Run 26 - Force vs. In Plane Displacement
Force (N)
9.00E+06
8.00E+06
7.00E+06
6.00E+06
5.00E+06
4.00E+06
3.00E+06
2.00E+06
1.00E+06
0.00E+00
0
0.01
0.02
0.03
0.04
0.05
0.06
0.07
0.08
0.09
0.1
In Plane Displacement (m)

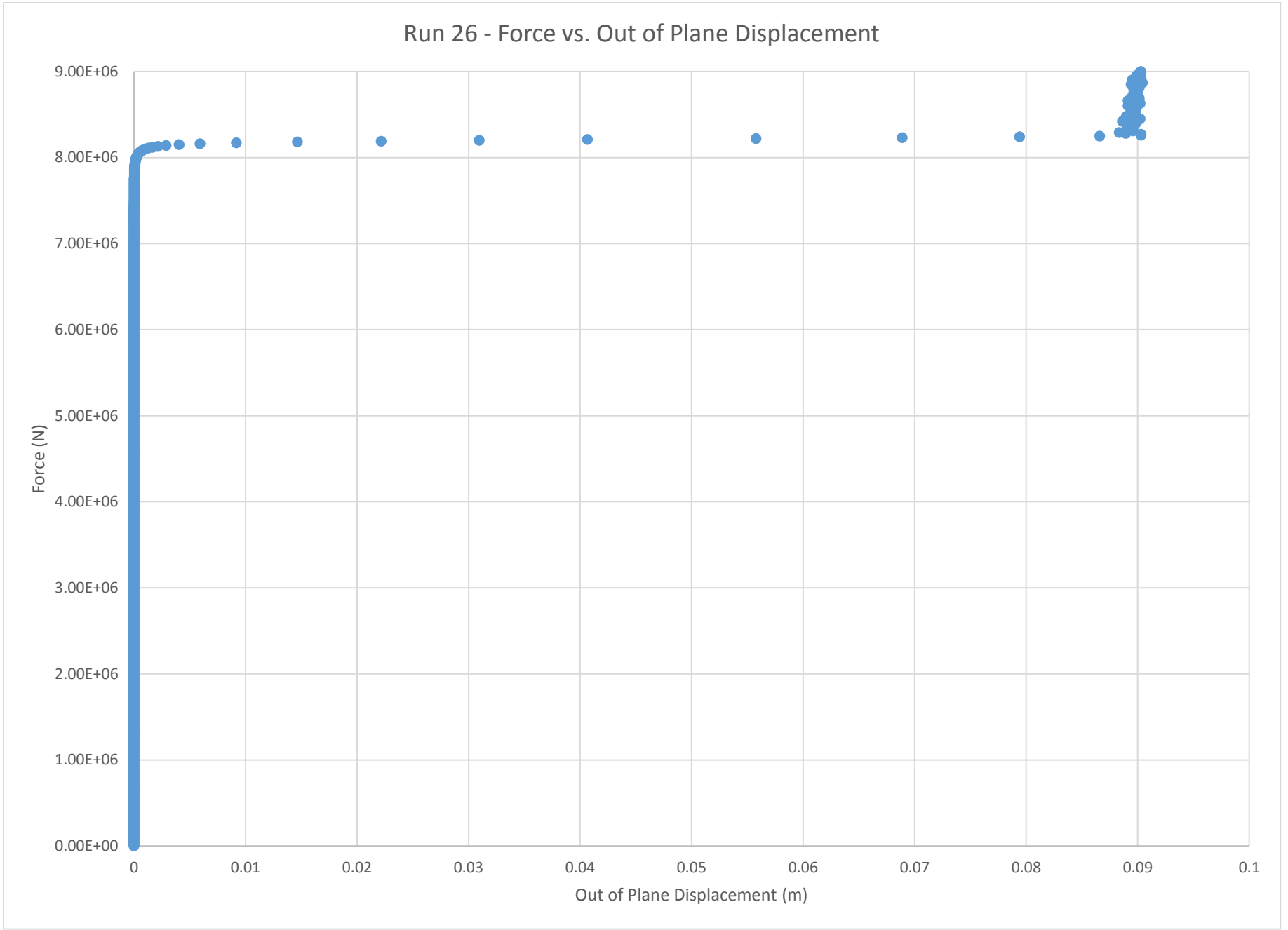
Run 26 - Force vs. Out of Plane Displacement
9.00E+06
8.00E+06
7.00E+06
6.00E+06
5.00E+06
4.00E+06
3.00E+06
2.00E+06
1.00E+06
0.00E+00
Force (N)
0
0.01
0.02
0.03
0.04
0.05
0.06
0.07
0.08
0.09
0.1
Out of Plane Displacement (m)

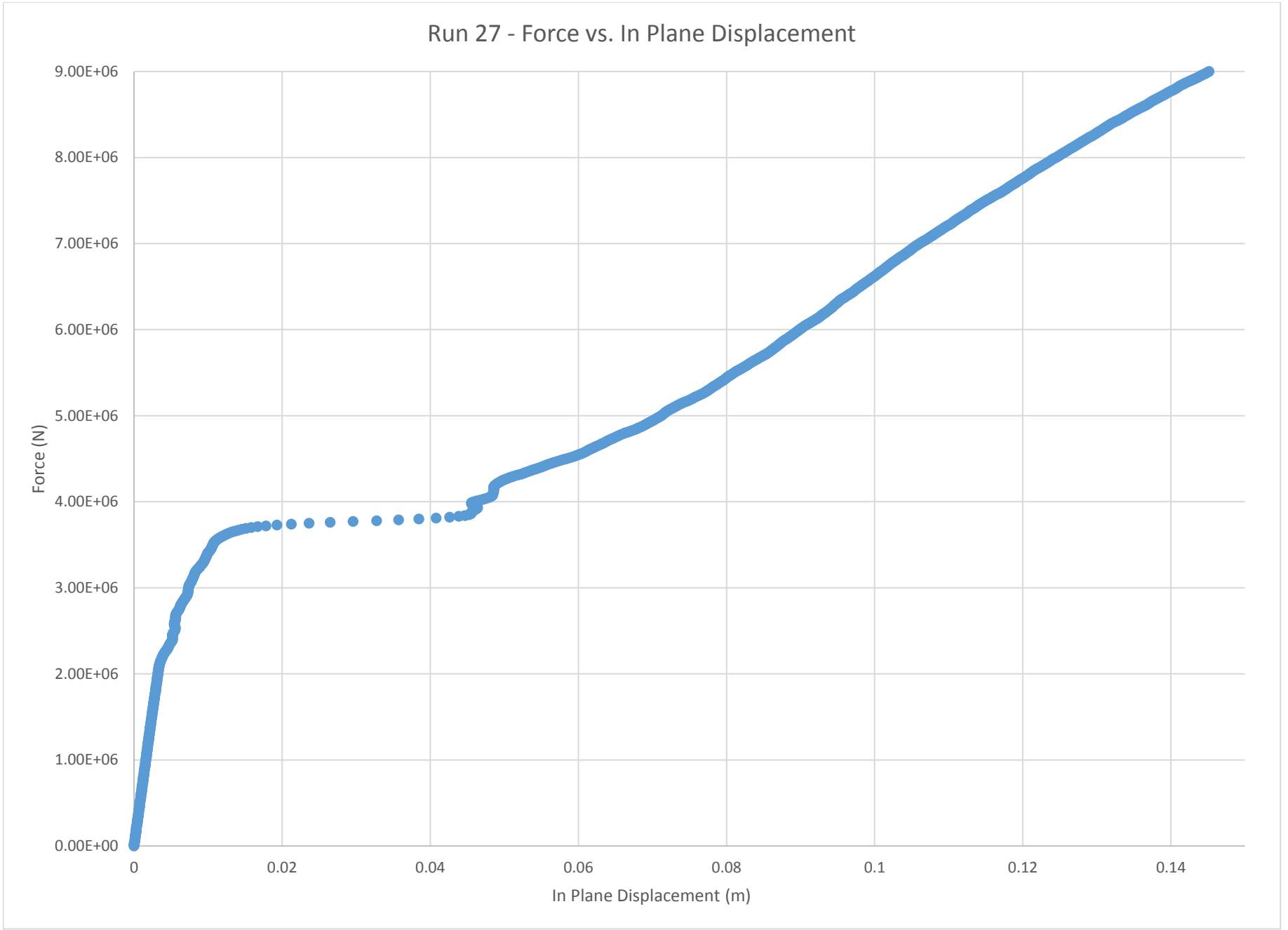
Run 27 - Force vs. In Plane Displacement
Force (N)
9.00E+06
8.00E+06
7.00E+06
6.00E+06
5.00E+06
4.00E+06
3.00E+06
2.00E+06
1.00E+06
0.00E+00
0
0.02
0.04
0.06
0.08
0.1
0.12
0.14
In Plane Displacement (m)

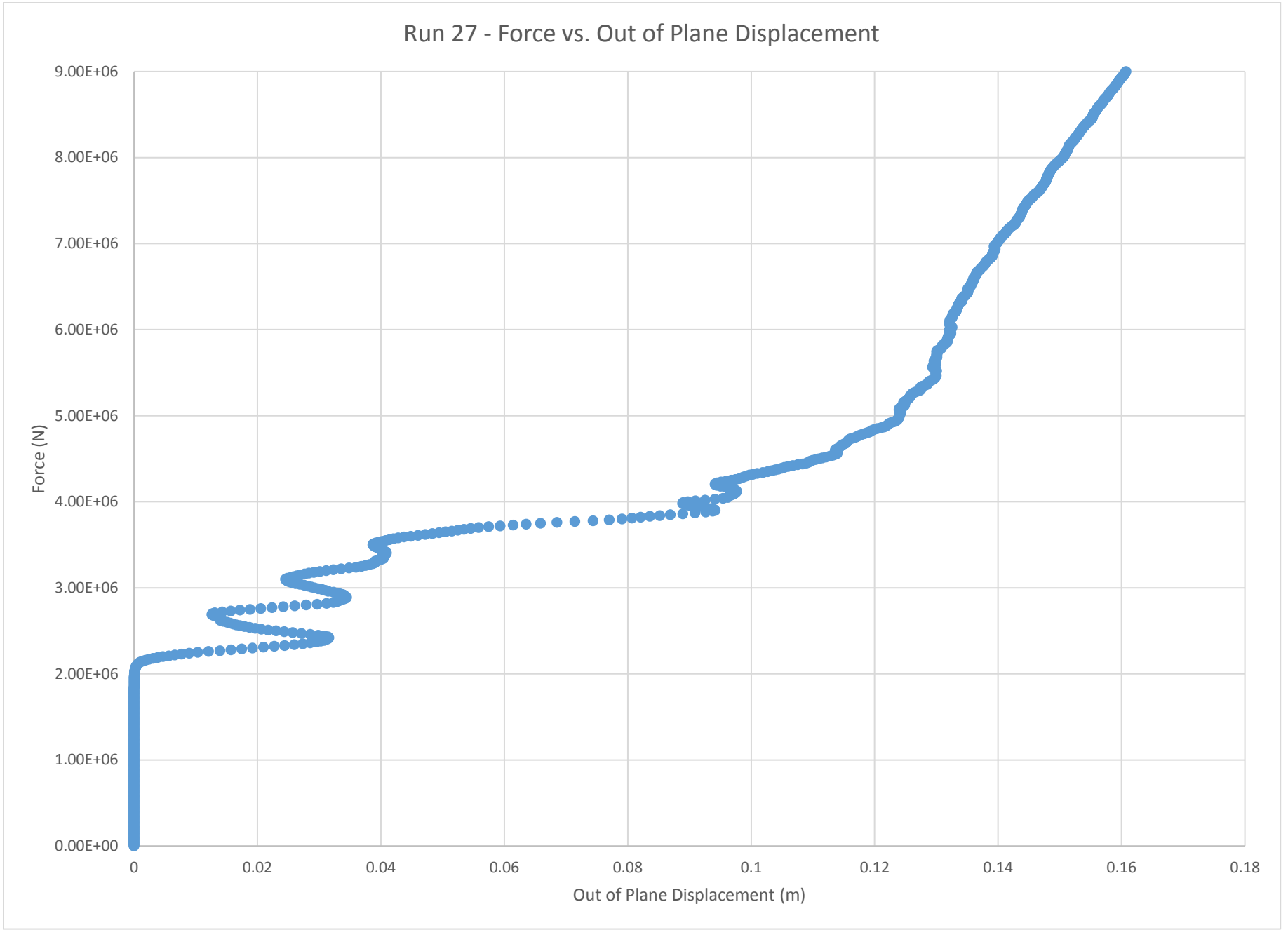
Run 27 - Force vs. Out of Plane Displacement
Force (N)
9.00E+06
8.00E+06
7.00E+06
6.00E+06
5.00E+06
4.00E+06
3.00E+06
2.00E+06
1.00E+06
0.00E+00
0
0.02
0.04
0.06
0.08
0.1
0.12
0.14
0.16
0.18
Out of Plane Displacement (m)

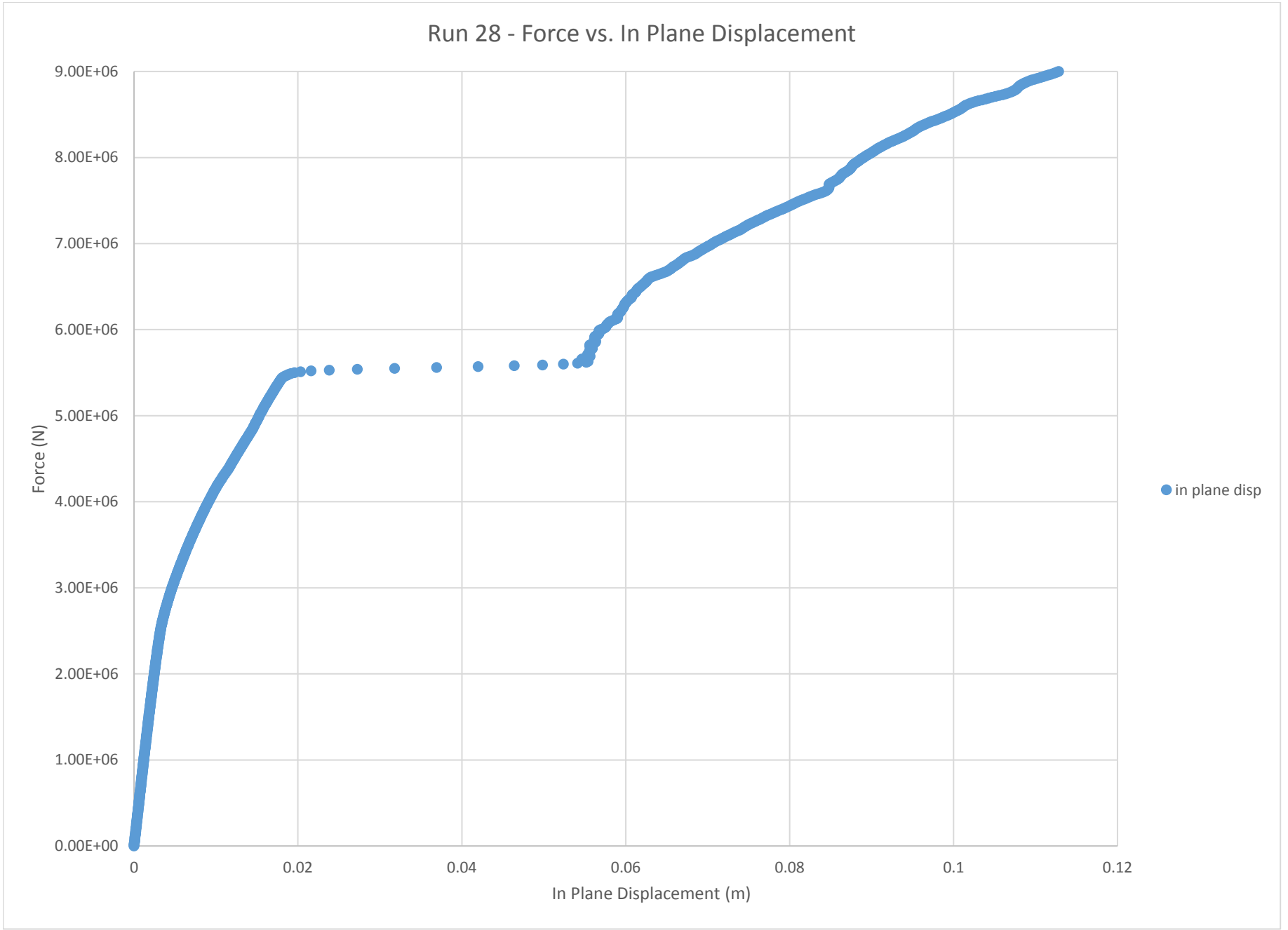
Run 28 - Force vs. In Plane Displacement
9.00E+06
8.00E+06
7.00E+06
6.00E+06
5.00E+06
4.00E+06
3.00E+06
2.00E+06
1.00E+06
0.00E+00
Force (N)
0
0.02
0.04
0.06
0.08
0.1
0.12
In Plane Displacement (m)
in plane disp

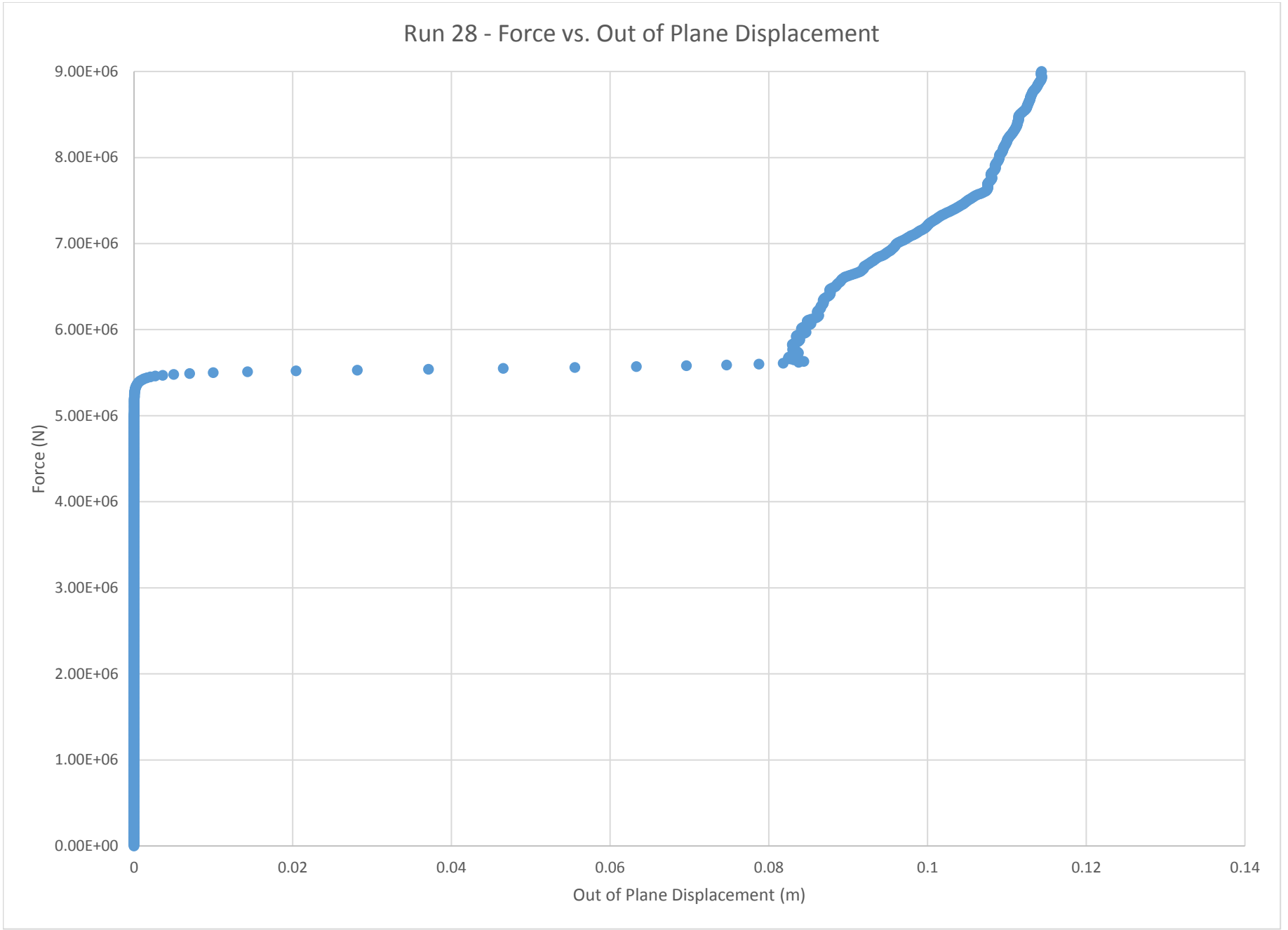
Run 28 - Force vs. Out of Plane Displacement
9.00E+06
8.00E+06
7.00E+06
6.00E+06
5.00E+06
4.00E+06
3.00E+06
2.00E+06
1.00E+06
0.00E+00
Force (N)
0
0.02
0.04
0.06
0.08
0.1
0.12
0.14
Out of Plane Displacement (m)

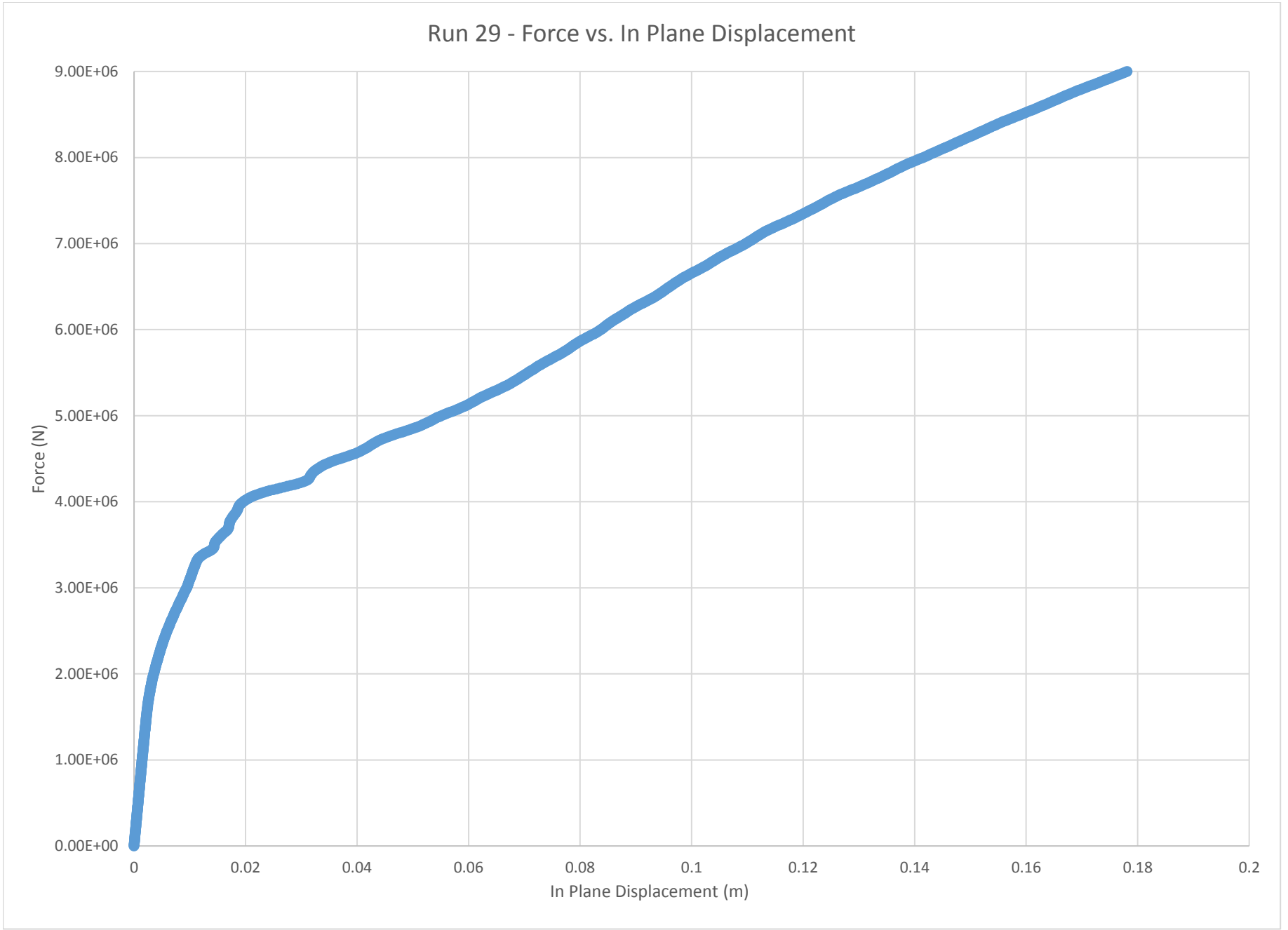
Run 29 - Force vs. In Plane Displacement
Force (N)
9.00E+06
8.00E+06
7.00E+06
6.00E+06
5.00E+06
4.00E+06
3.00E+06
2.00E+06
1.00E+06
0.00E+00
0
0.02
0.04
0.06
0.08
0.1
0.12
0.14
0.16
0.18
0.2
In Plane Displacement (m)

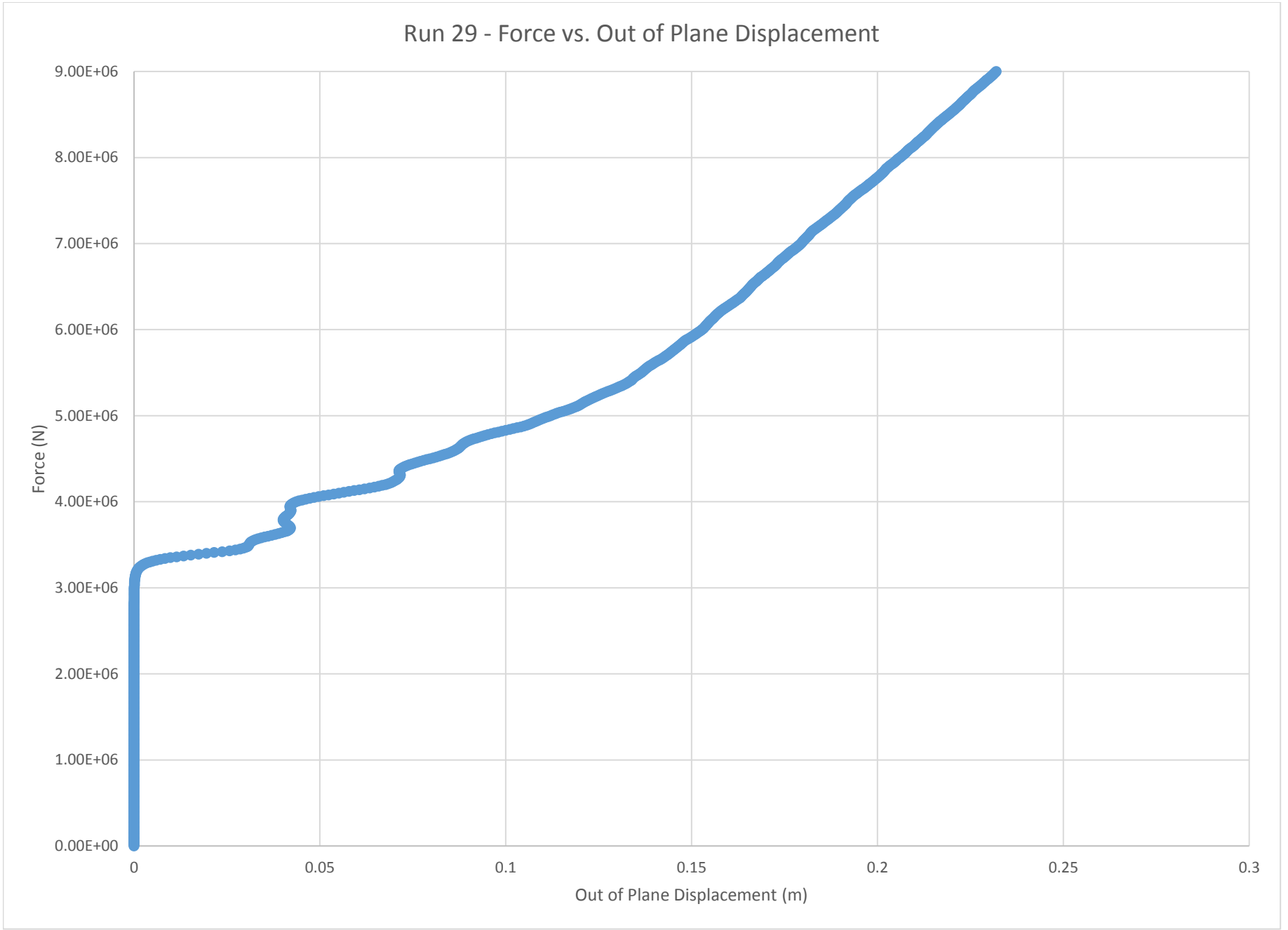
Run 29 - Force vs. Out of Plane Displacement
Force (N)
9.00E+06
8.00E+06
7.00E+06
6.00E+06
5.00E+06
4.00E+06
3.00E+06
2.00E+06
1.00E+06
0.00E+00
0
0.05
0.1
0.15
0.2
0.25
0.3
Out of Plane Displacement (m)

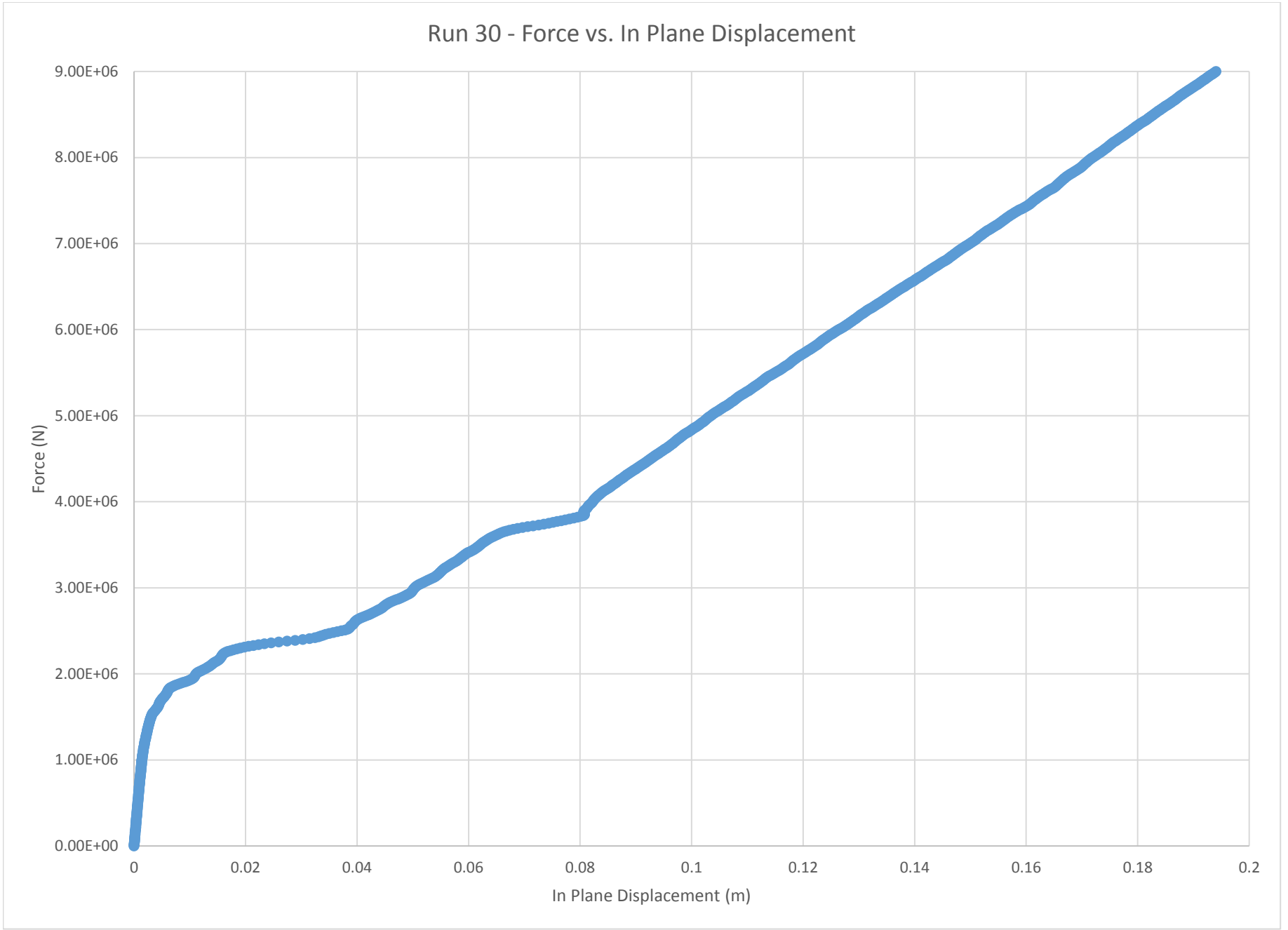
Run 30 - Force vs. In Plane Displacement
9.00E+06
8.00E+06
7.00E+06
6.00E+06
5.00E+06
4.00E+06
3.00E+06
2.00E+06
1.00E+06
0.00E+00
Force (N)
0
0.02
0.04
0.06
0.08
0.1
0.12
0.14
0.16
0.18
0.2
In Plane Displacement (m)

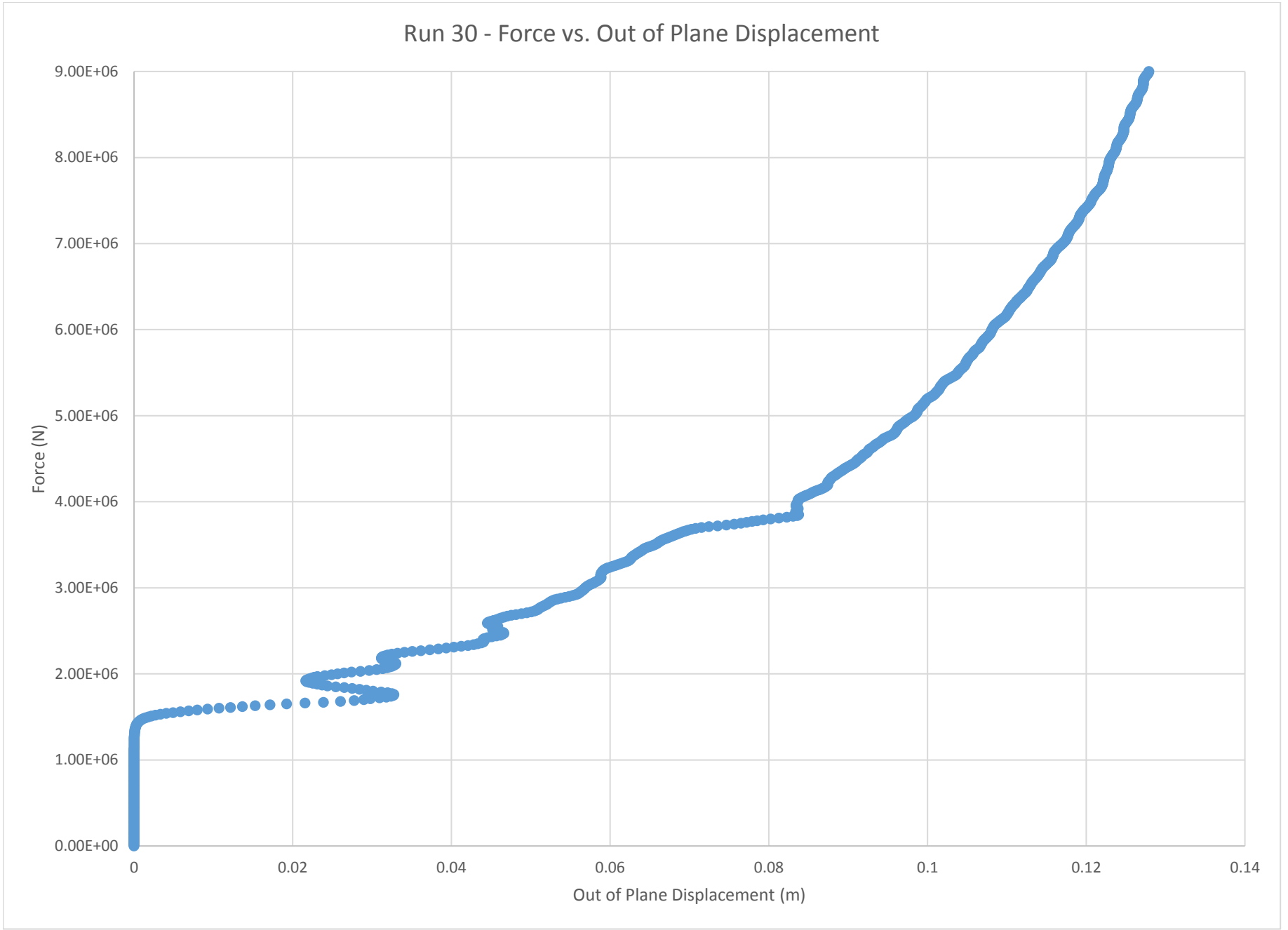
Run 30 - Force vs. Out of Plane Displacement
9.00E+06
8.00E+06
7.00E+06
6.00E+06
5.00E+06
4.00E+06
3.00E+06
2.00E+06
1.00E+06
0.00E+00
Force (N)
0
0.02
0.04
0.06
0.08
0.1
0.12
0.14
Out of Plane Displacement (m)

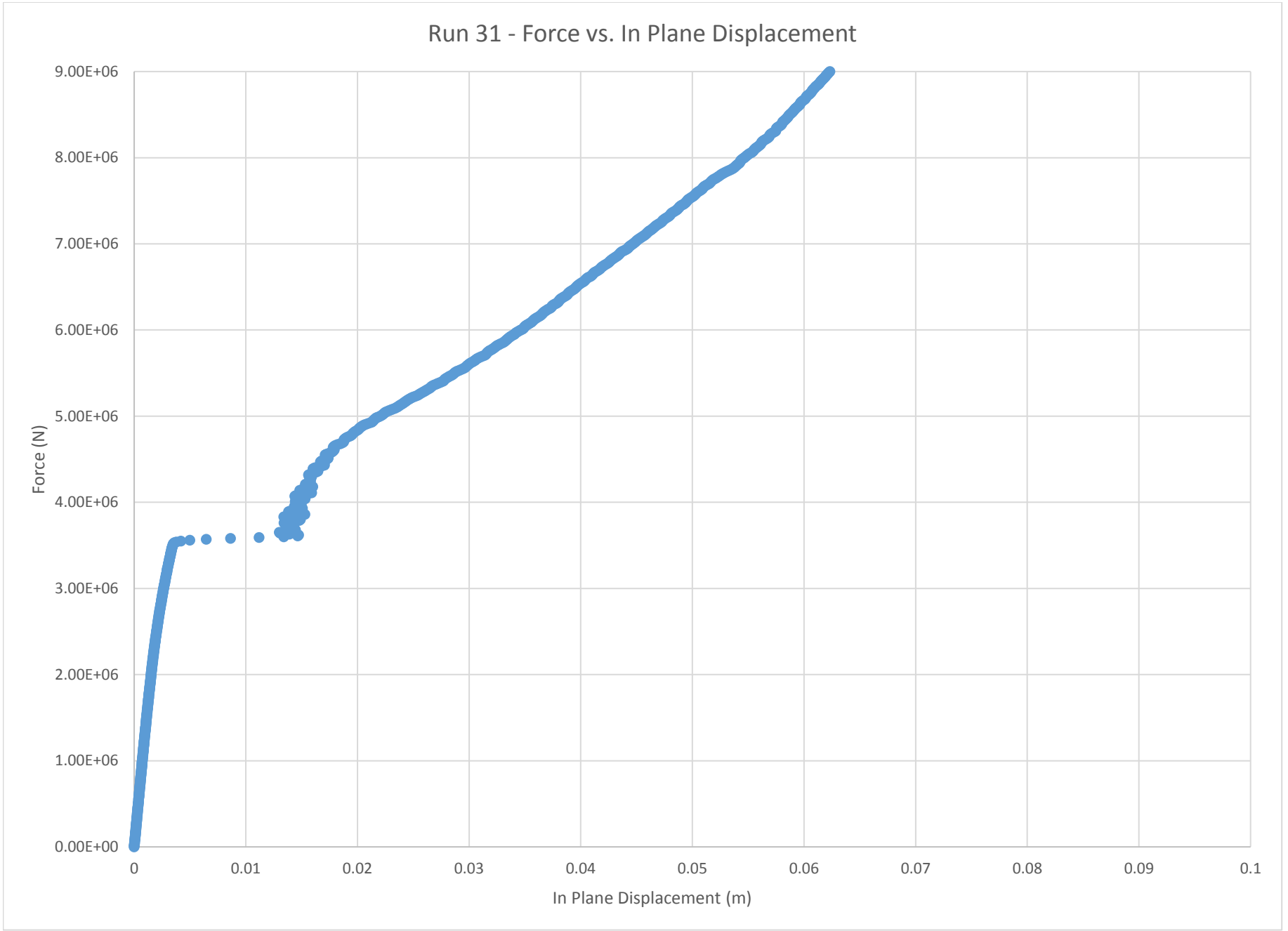
Run 31 - Force vs. In Plane Displacement
9.00E+06
8.00E+06
7.00E+06
6.00E+06
5.00E+06
4.00E+06
3.00E+06
2.00E+06
1.00E+06
0.00E+00
Force (N)
0
0.01
0.02
0.03
0.04
0.05
0.06
0.07
0.08
0.09
0.1
In Plane Displacement (m)

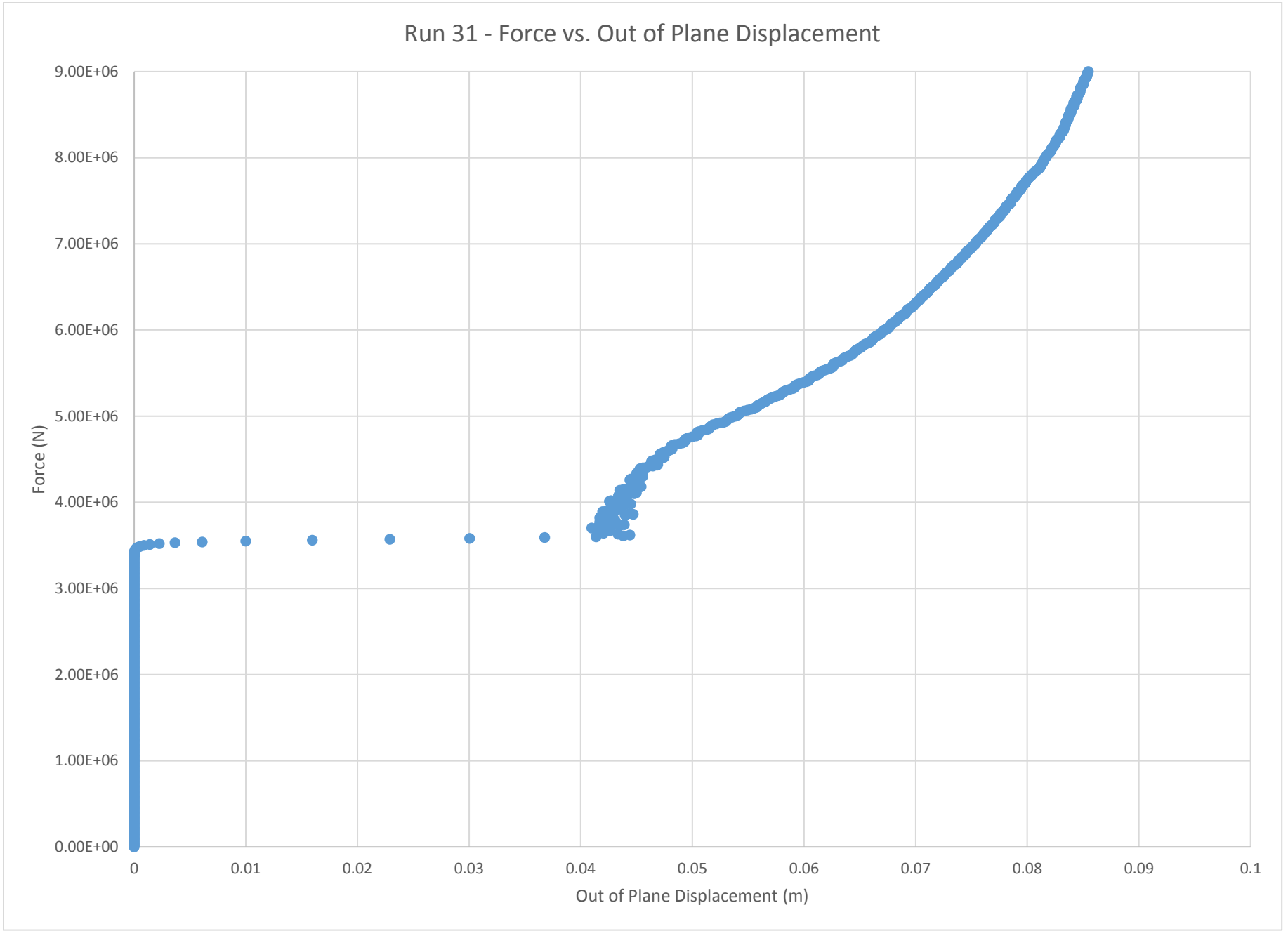
Run 31 - Force vs. Out of Plane Displacement
9.00E+06
8.00E+06
7.00E+06
6.00E+06
5.00E+06
4.00E+06
3.00E+06
2.00E+06
1.00E+06
0.00E+00
Force (N)
0
0.01
0.02
0.03
0.04
0.05
0.06
0.07
0.08
0.09
0.1
Out of Plane Displacement (m)

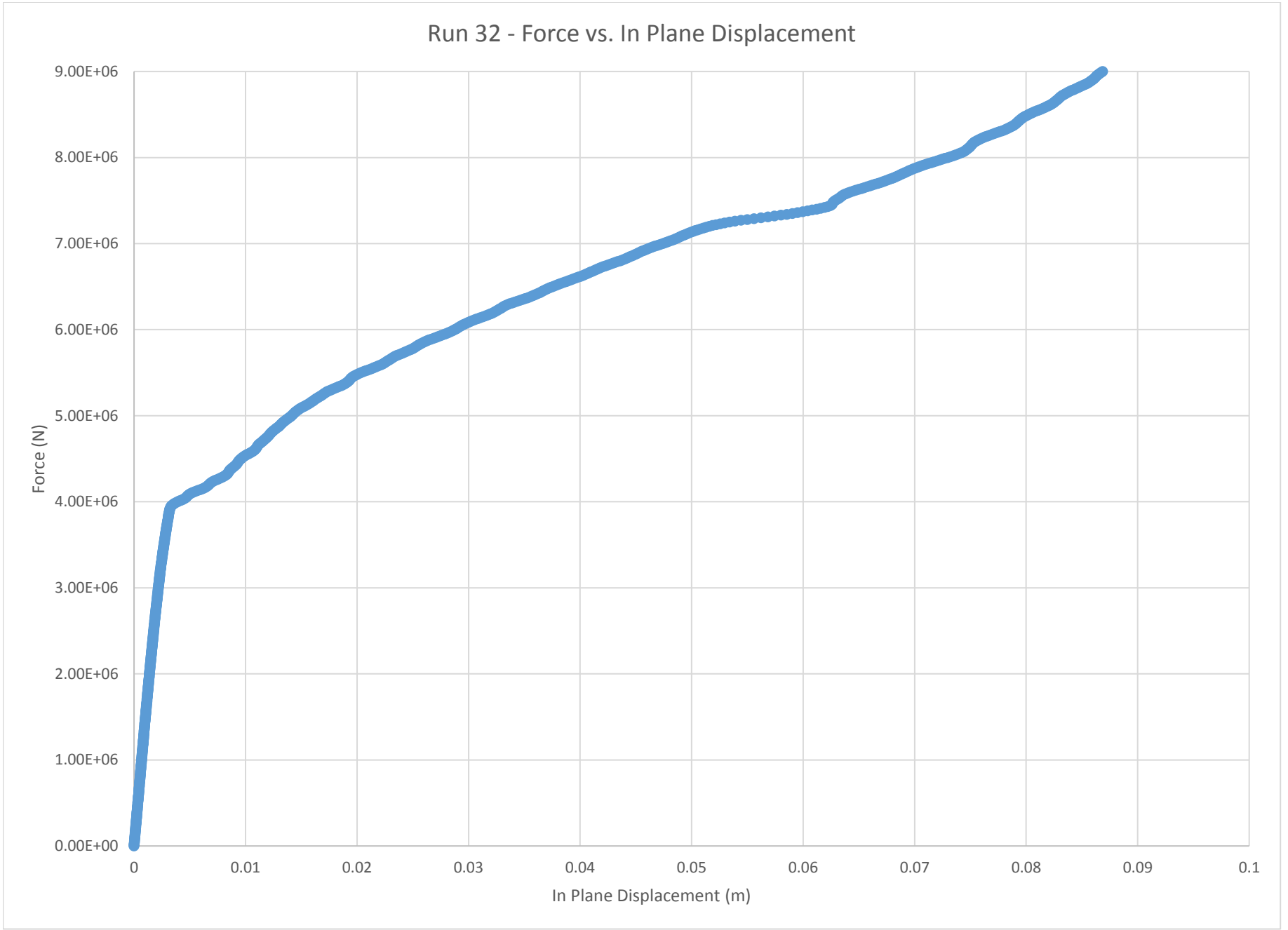
Run 32 - Force vs. In Plane Displacement
9.00E+06
8.00E+06
7.00E+06
6.00E+06
5.00E+06
4.00E+06
3.00E+06
2.00E+06
1.00E+06
0.00E+00
Force (N)
0
0.01
0.02
0.03
0.04
0.05
0.06
0.07
0.08
0.09
0.1
In Plane Displacement (m)

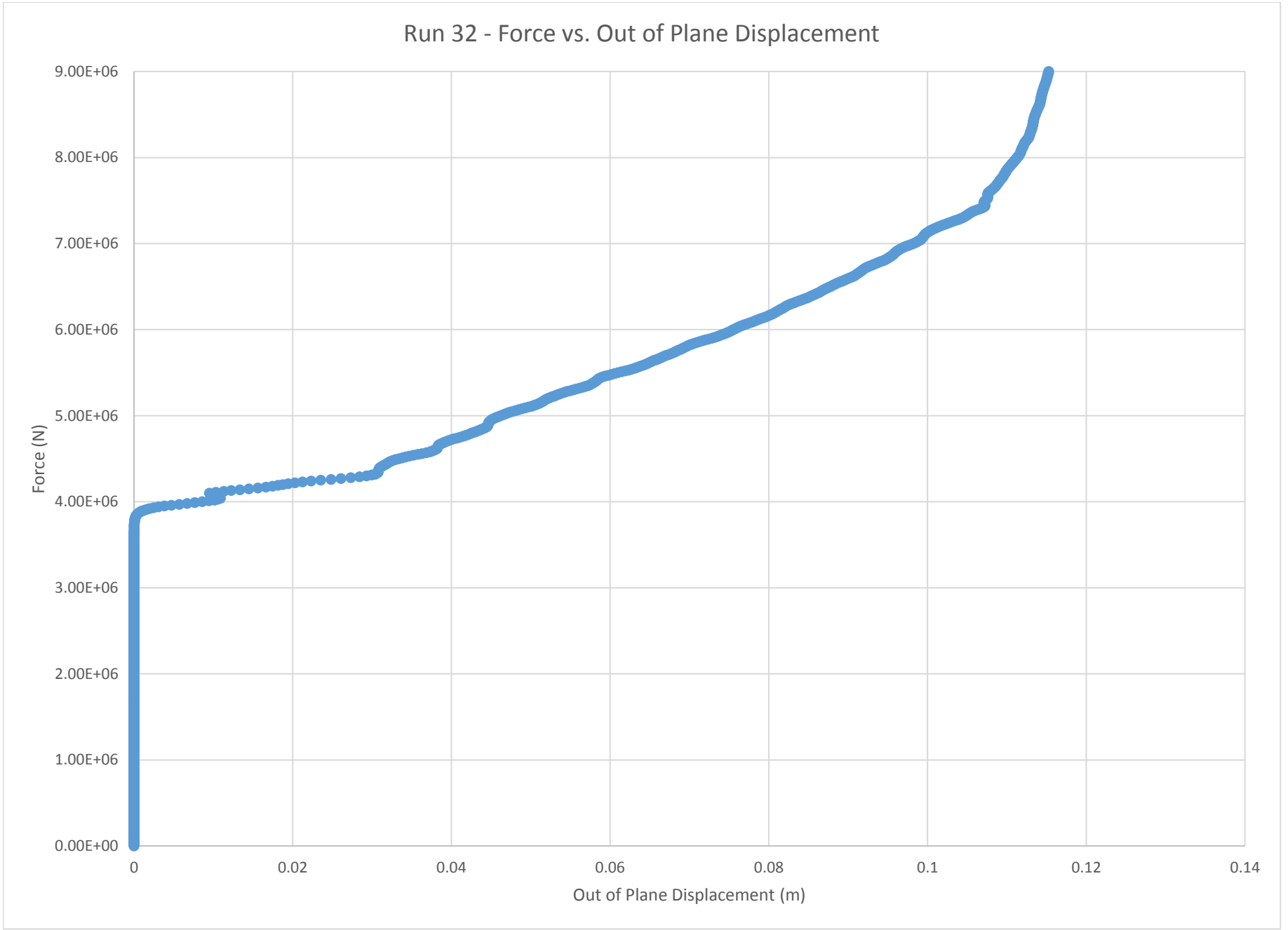
Run 32 - Force vs. Out of Plane Displacement
Force (N)
9.00E+06
8.00E+06
7.00E+06
6.00E+06
5.00E+06
4.00E+06
3.00E+06
2.00E+06
1.00E+06
0.00E+00
0
0.02
0.04
0.06
0.08
0.1
0.12
0.14
Out of Plane Displacement (m)

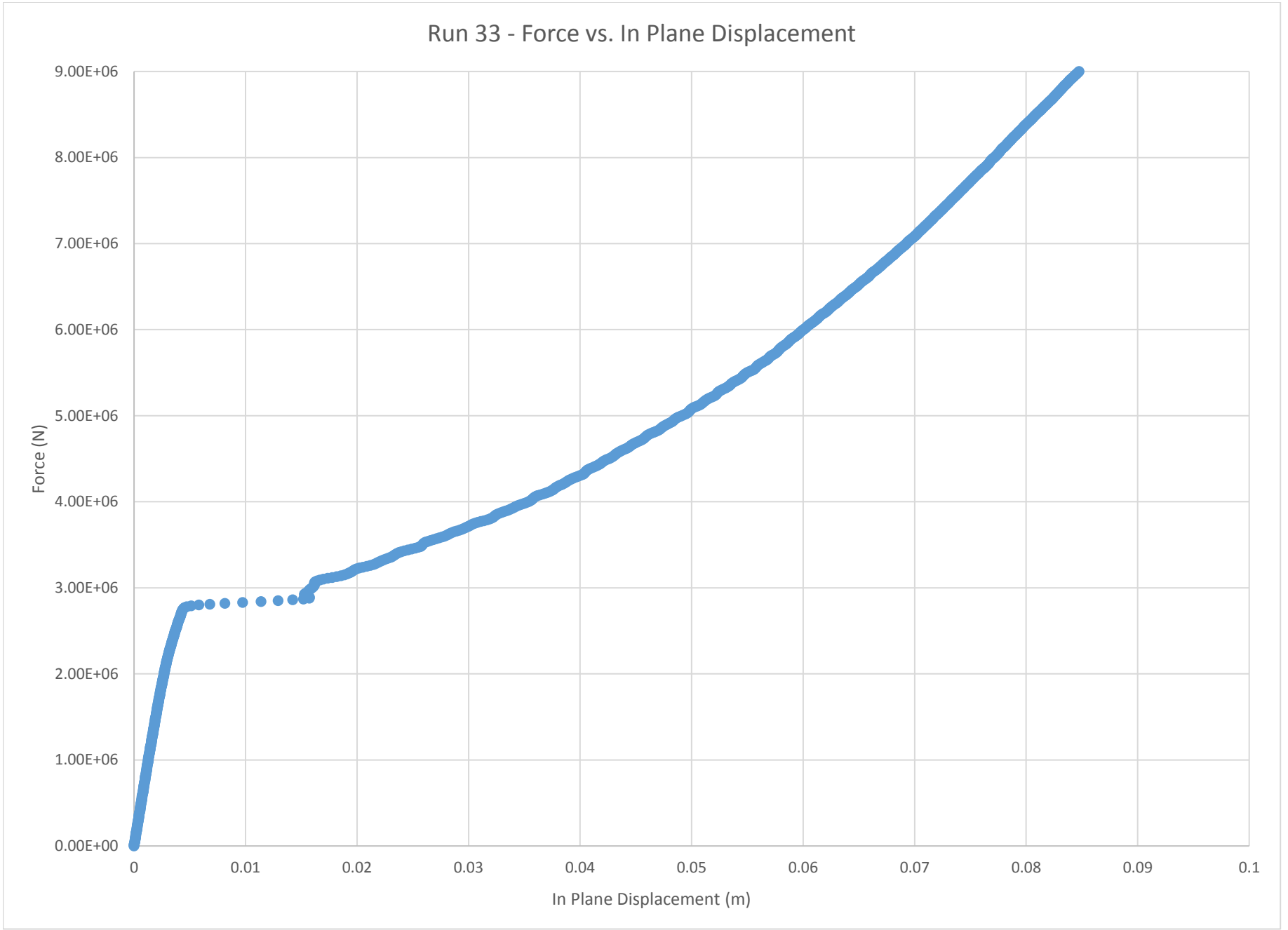
Run 33 - Force vs. In Plane Displacement
9.00E+06
8.00E+06
7.00E+06
6.00E+06
5.00E+06
4.00E+06
3.00E+06
2.00E+06
1.00E+06
0.00E+00
Force (N)
0
0.01
0.02
0.03
0.04
0.05
0.06
0.07
0.08
0.09
0.1
In Plane Displacement (m)

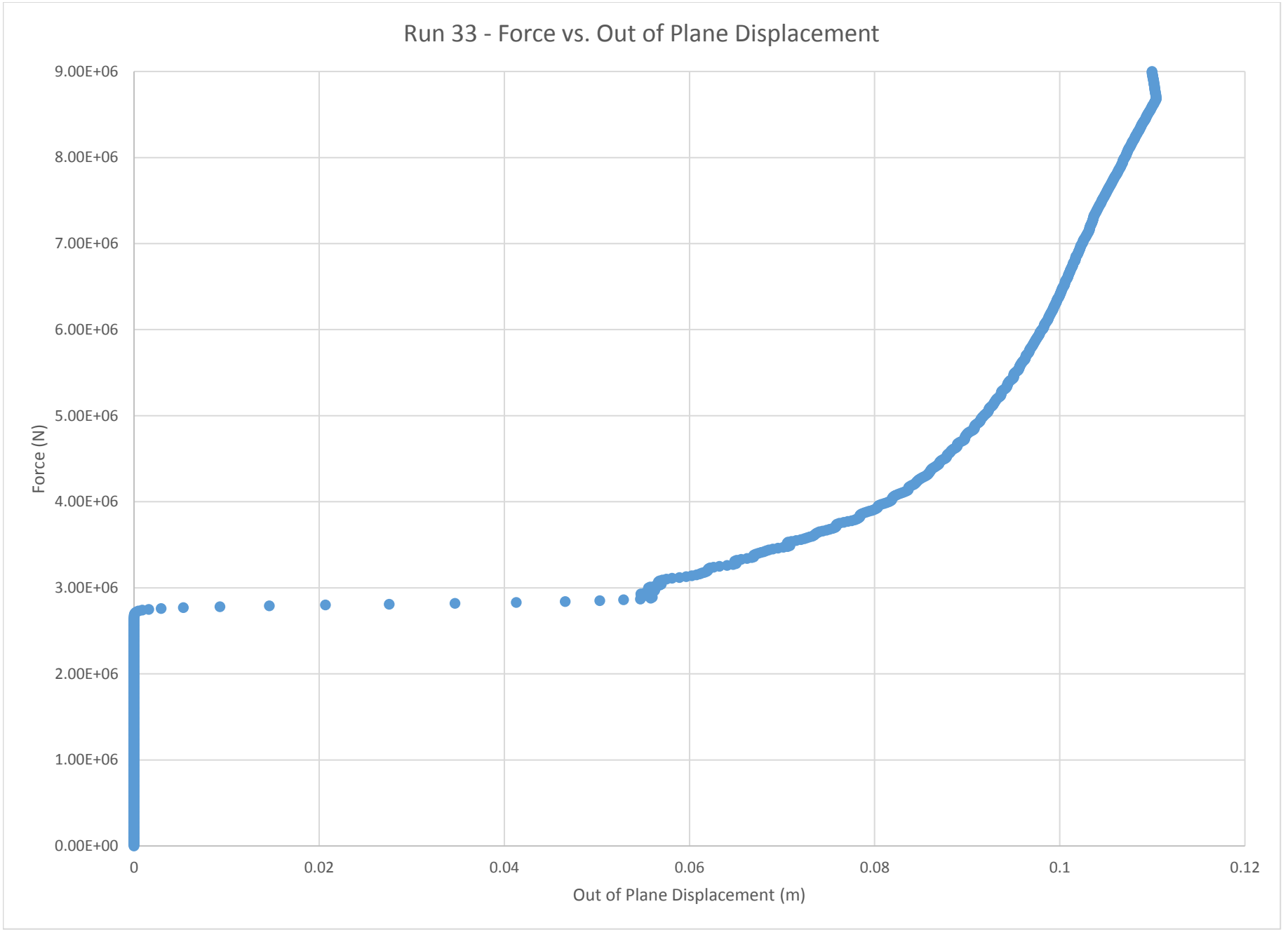
Run 33 - Force vs. Out of Plane Displacement
9.00E+06
8.00E+06
7.00E+06
6.00E+06
5.00E+06
4.00E+06
3.00E+06
2.00E+06
1.00E+06
0.00E+00
Force (N)
0
0.02
0.04
0.06
0.08
0.1
0.12
Out of Plane Displacement (m)

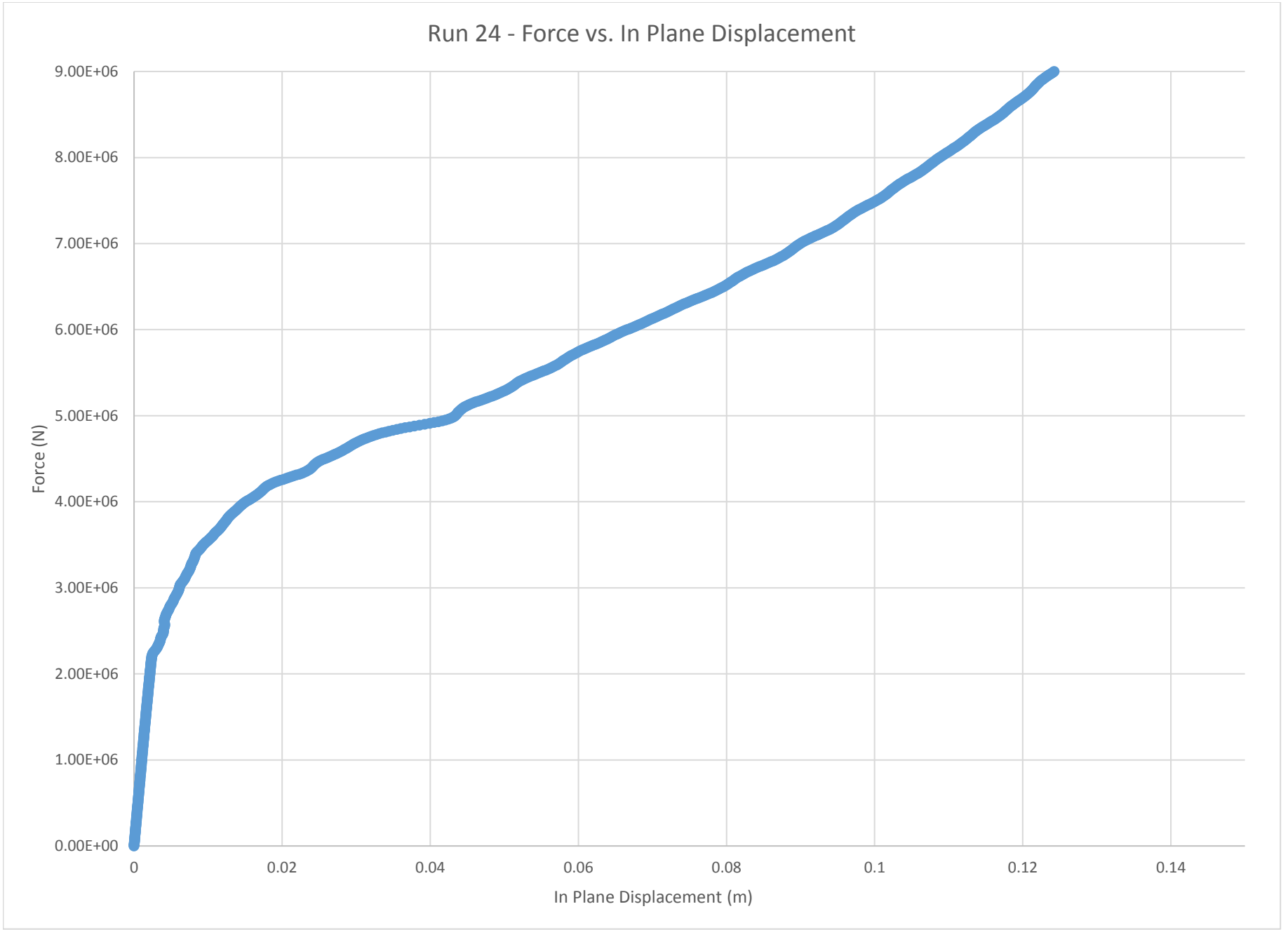
Run 24 - Force vs. In Plane Displacement
9.00E+06
8.00E+06
7.00E+06
6.00E+06
5.00E+06
4.00E+06
3.00E+06
2.00E+06
1.00E+06
0.00E+00
Force (N)
0
0.02
0.04
0.06
0.08
0.1
0.12
0.14
In Plane Displacement (m)

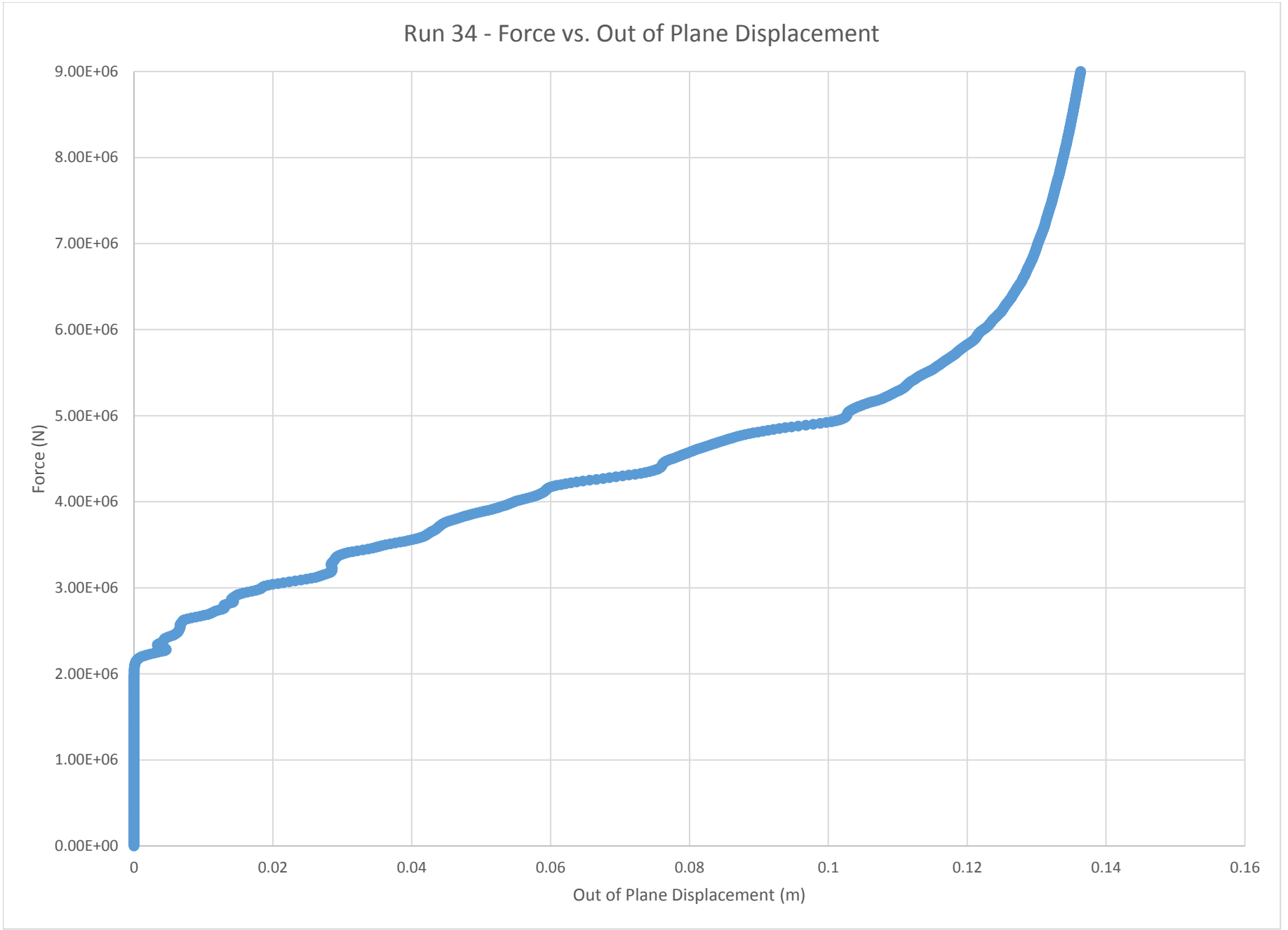
Run 34 - Force vs. Out of Plane Displacement
Force (N)
9.00E+06
8.00E+06
7.00E+06
6.00E+06
5.00E+06
4.00E+06
3.00E+06
2.00E+06
1.00E+06
0.00E+00
0
0.02
0.04
0.06
0.08
0.1
0.12
0.14
0.16
Out of Plane Displacement (m)

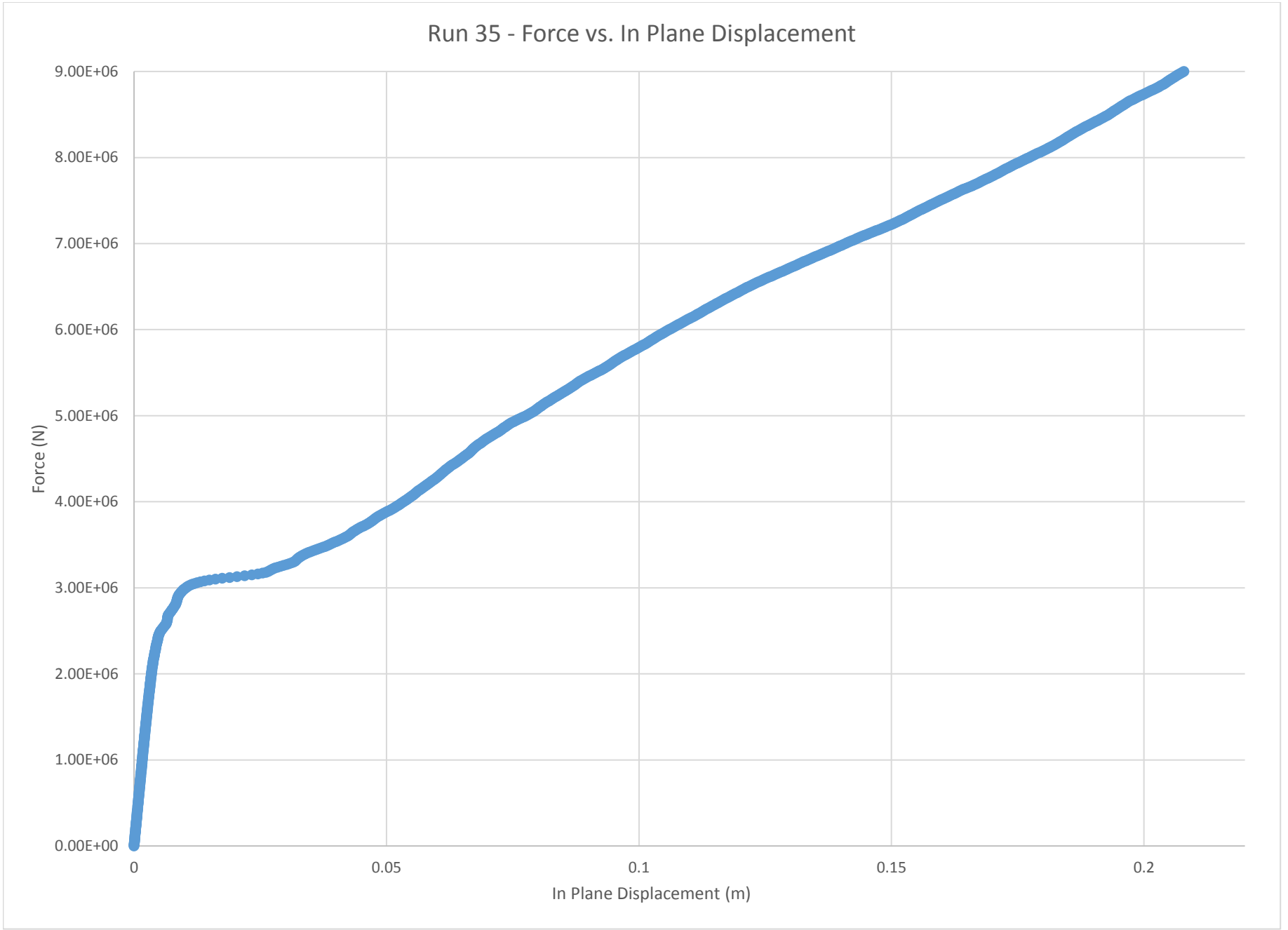
Run 35 - Force vs. In Plane Displacement
9.00E+06
8.00E+06
7.00E+06
6.00E+06
5.00E+06
4.00E+06
3.00E+06
2.00E+06
1.00E+06
0.00E+00
Force (N)
0
0.05
0.1
0.15
0.2
In Plane Displacement (m)

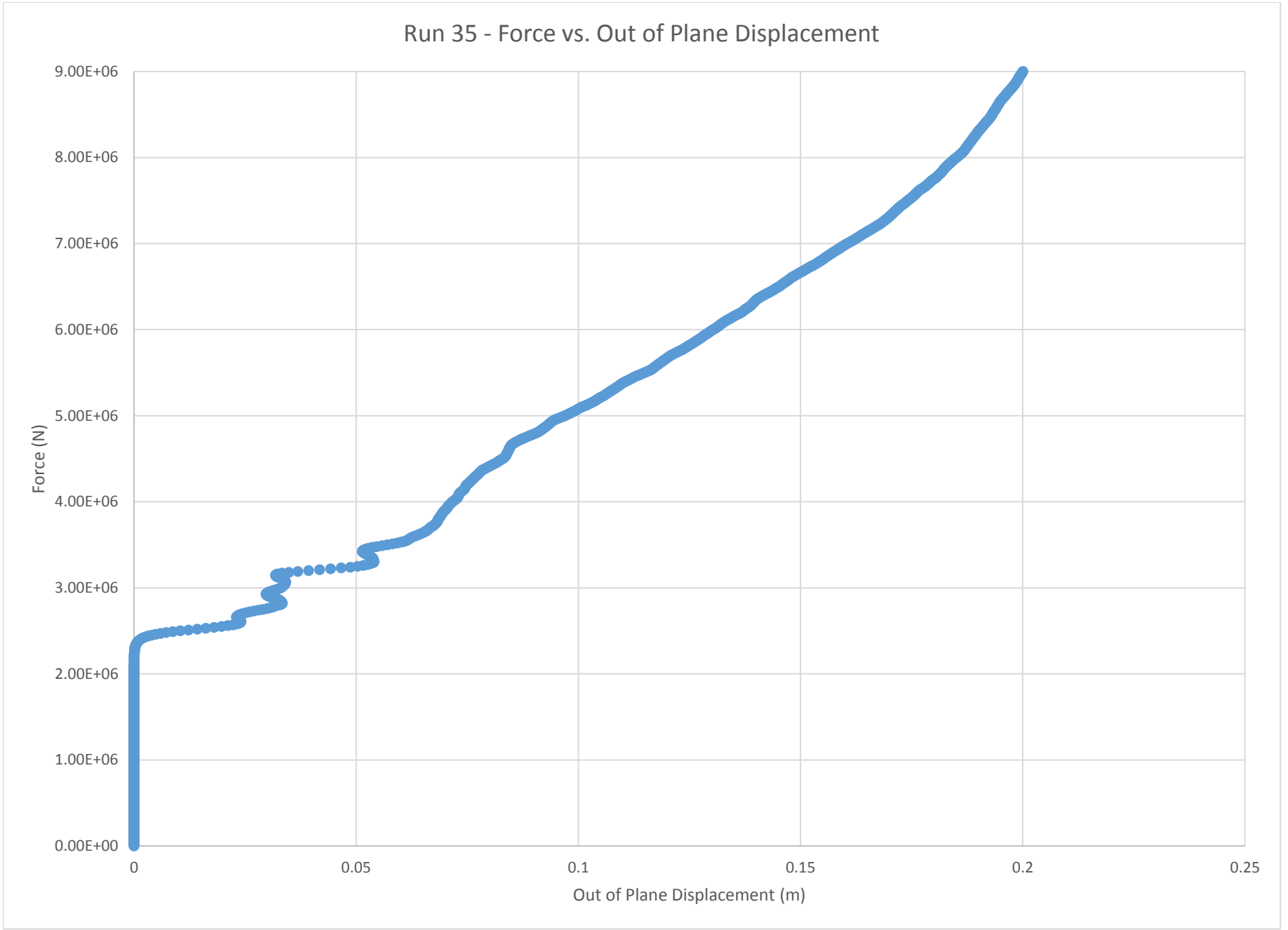
Run 35 - Force vs. Out of Plane Displacement
9.00E+06
8.00E+06
7.00E+06
6.00E+06
5.00E+06
4.00E+06
3.00E+06
2.00E+06
1.00E+06
0.00E+00
Force (N)
0
0.05
0.1
0.15
0.2
0.25
Out of Plane Displacement (m)

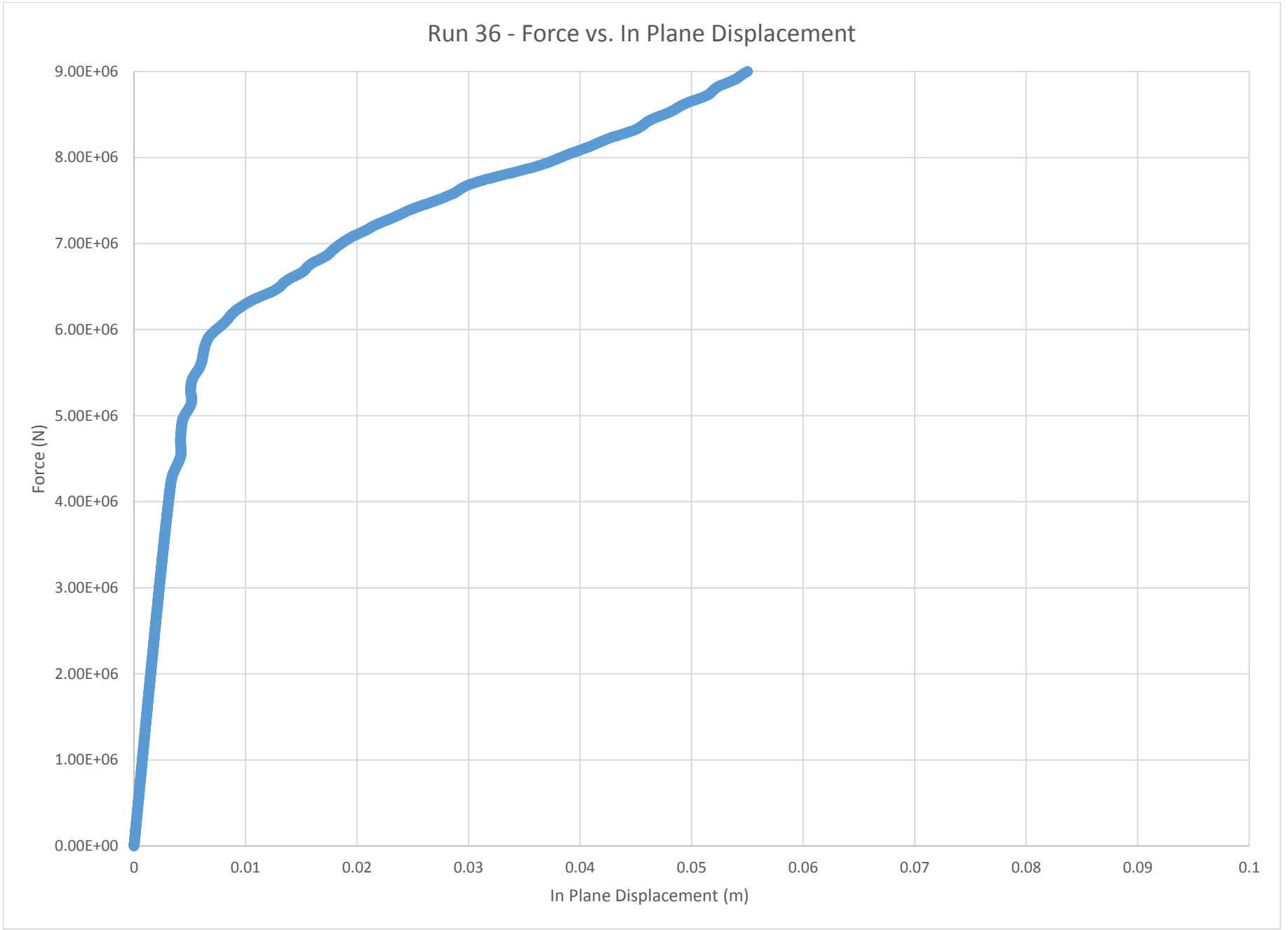
Run 36 - Force vs. In Plane Displacement
9.00E+06
8.00E+06
7.00E+06
6.00E+06
5.00E+06
4.00E+06
3.00E+06
2.00E+06
1.00E+06
0.00E+00
Force (N)
0
0.01
0.02
0.03
0.04
0.05
0.06
0.07
0.08
0.09
0.1
In Plane Displacement (m)

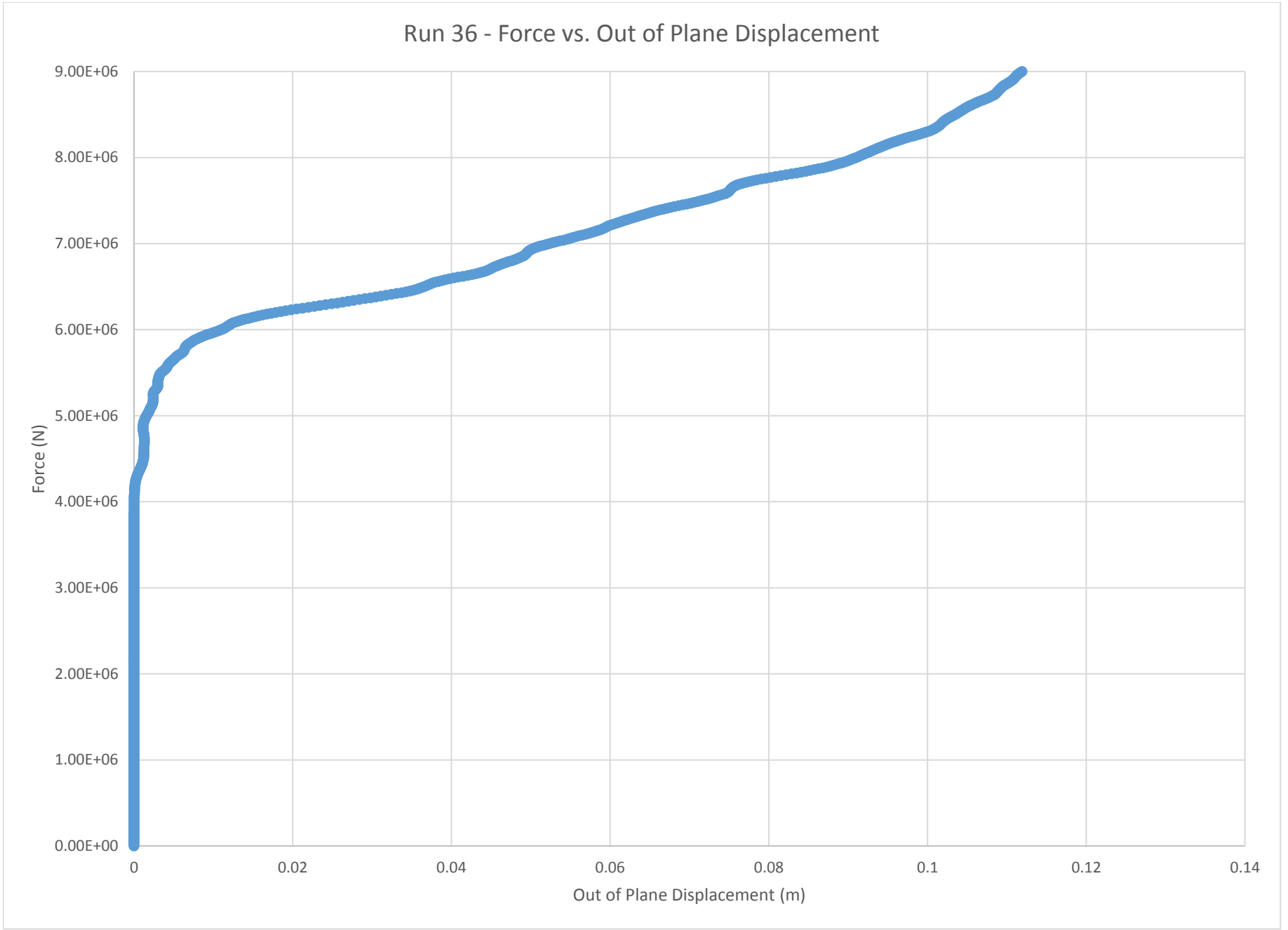
Run 36 - Force vs. Out of Plane Displacement
9.00E+06
8.00E+06
7.00E+06
6.00E+06
5.00E+06
4.00E+06
3.00E+06
2.00E+06
1.00E+06
0.00E+00
Force (N)
0
0.02
0.04
0.06
0.08
0.1
0.12
0.14
Out of Plane Displacement (m)

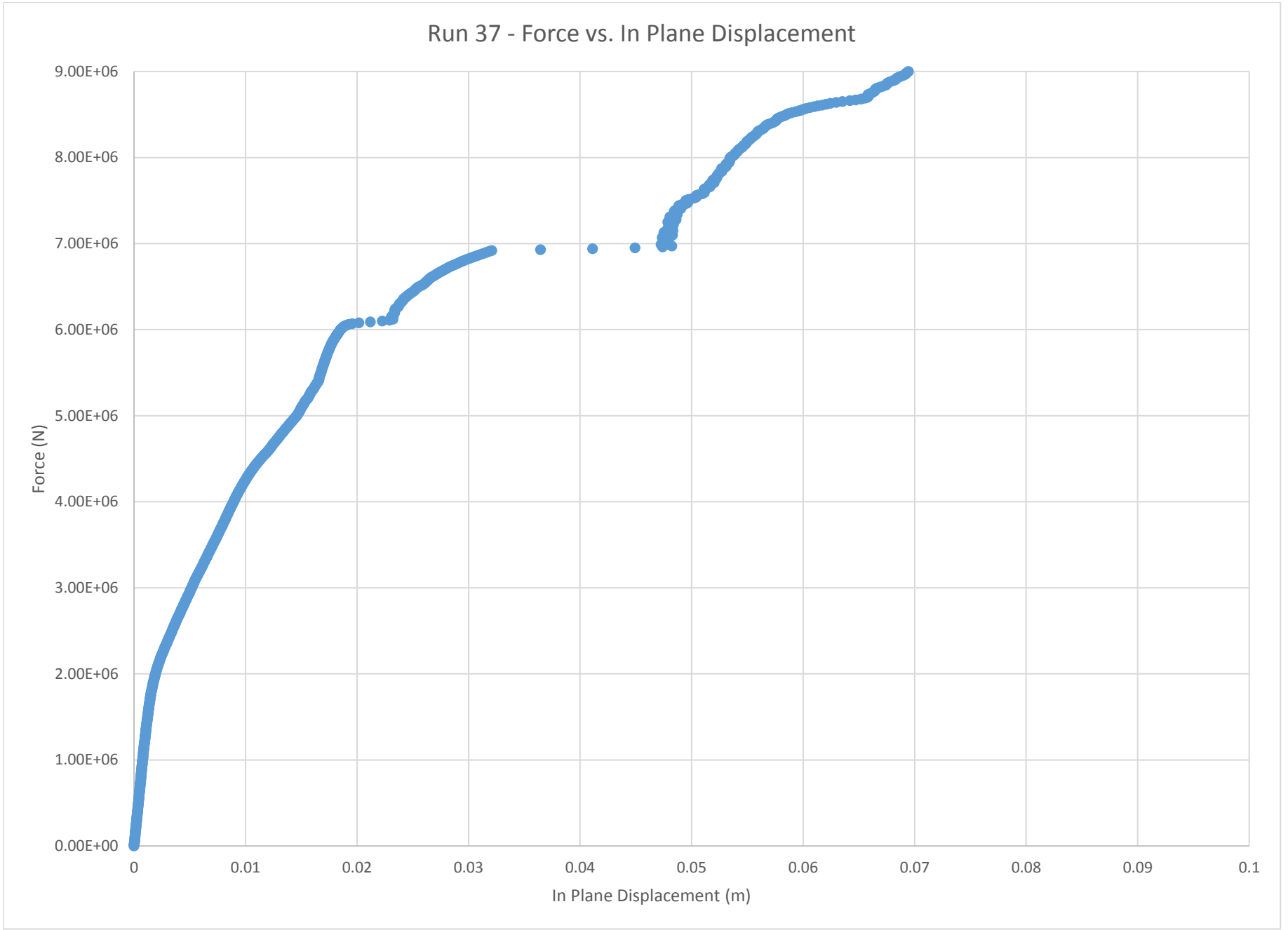
Run 37 - Force vs. In Plane Displacement
9.00E+06
8.00E+06
7.00E+06
6.00E+06
5.00E+06
4.00E+06
3.00E+06
2.00E+06
1.00E+06
0.00E+00
Force (N)
0
0.01
0.02
0.03
0.04
0.05
0.06
0.07
0.08
0.09
0.1
In Plane Displacement (m)

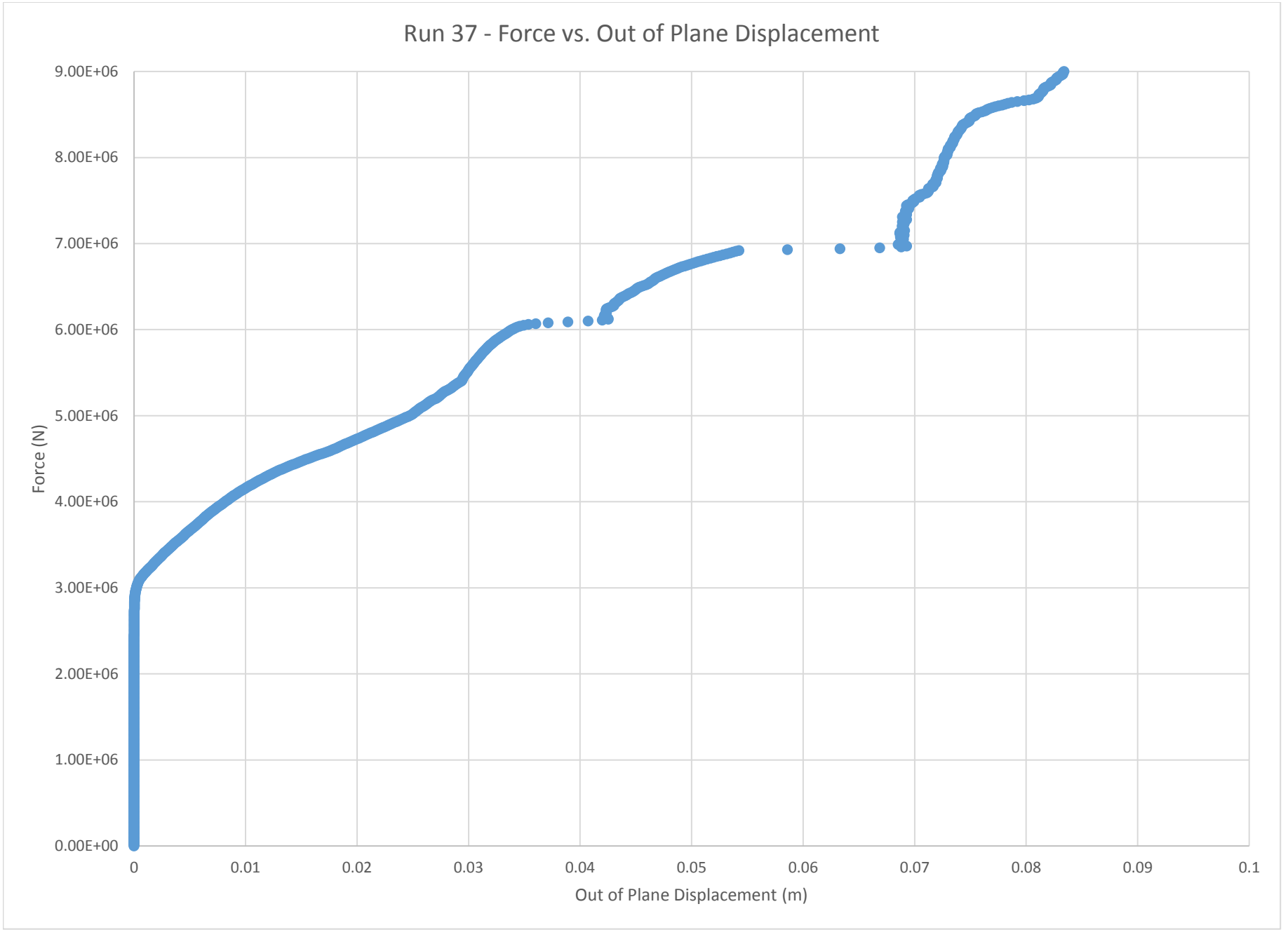
Run 37 - Force vs. Out of Plane Displacement
Force (N)
9.00E+06
8.00E+06
7.00E+06
6.00E+06
5.00E+06
4.00E+06
3.00E+06
2.00E+06
1.00E+06
0.00E+00
0
0.01
0.02
0.03
0.04
0.05
0.06
0.07
0.08
0.09
0.1
Out of Plane Displacement (m)

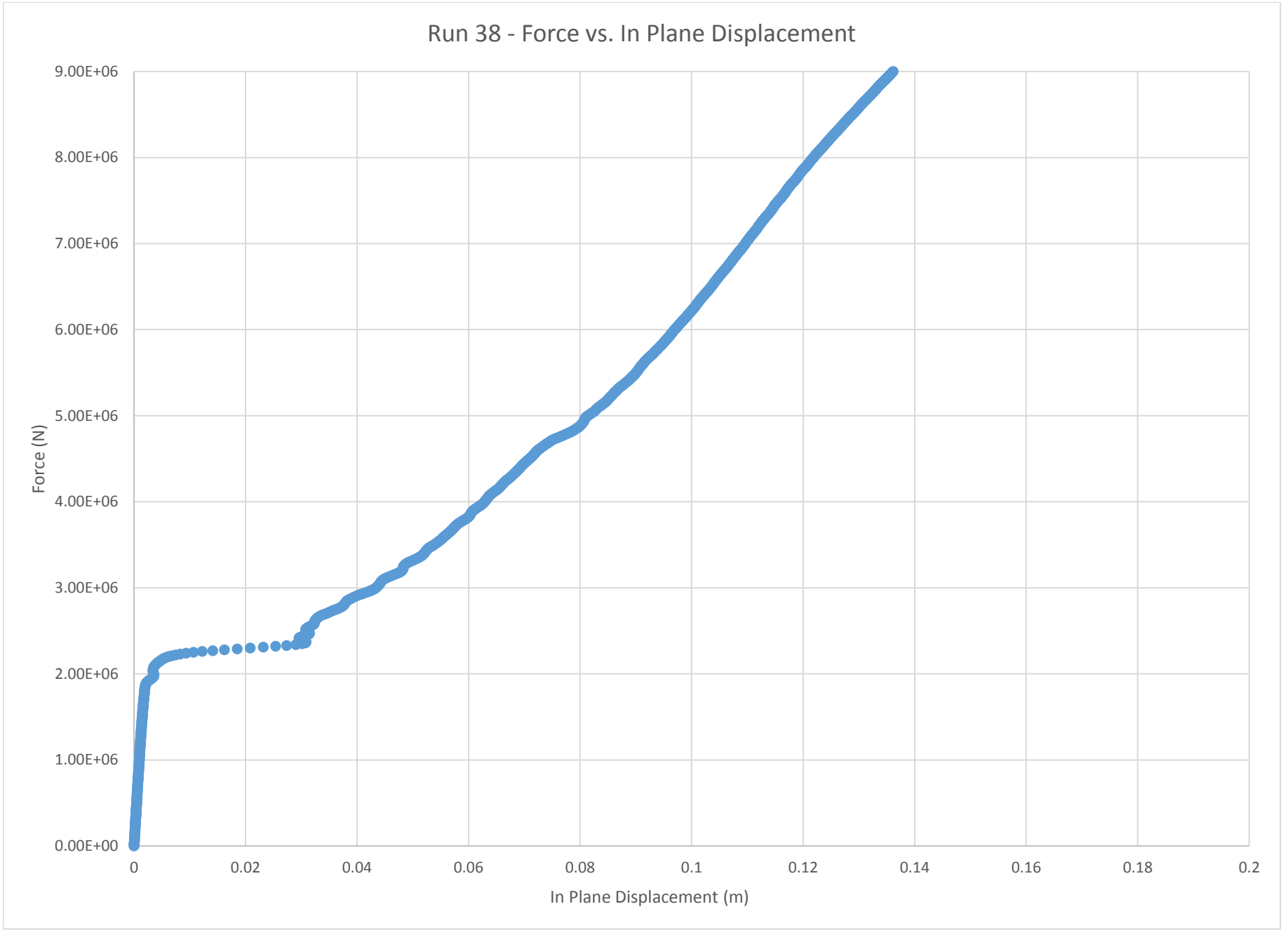
Run 38 - Force vs. In Plane Displacement
Force (N)
9.00E+06
8.00E+06
7.00E+06
6.00E+06
5.00E+06
4.00E+06
3.00E+06
2.00E+06
1.00E+06
0.00E+00
0
0.02
0.04
0.06
0.08
0.1
0.12
0.14
0.16
0.18
0.2
In Plane Displacement (m)

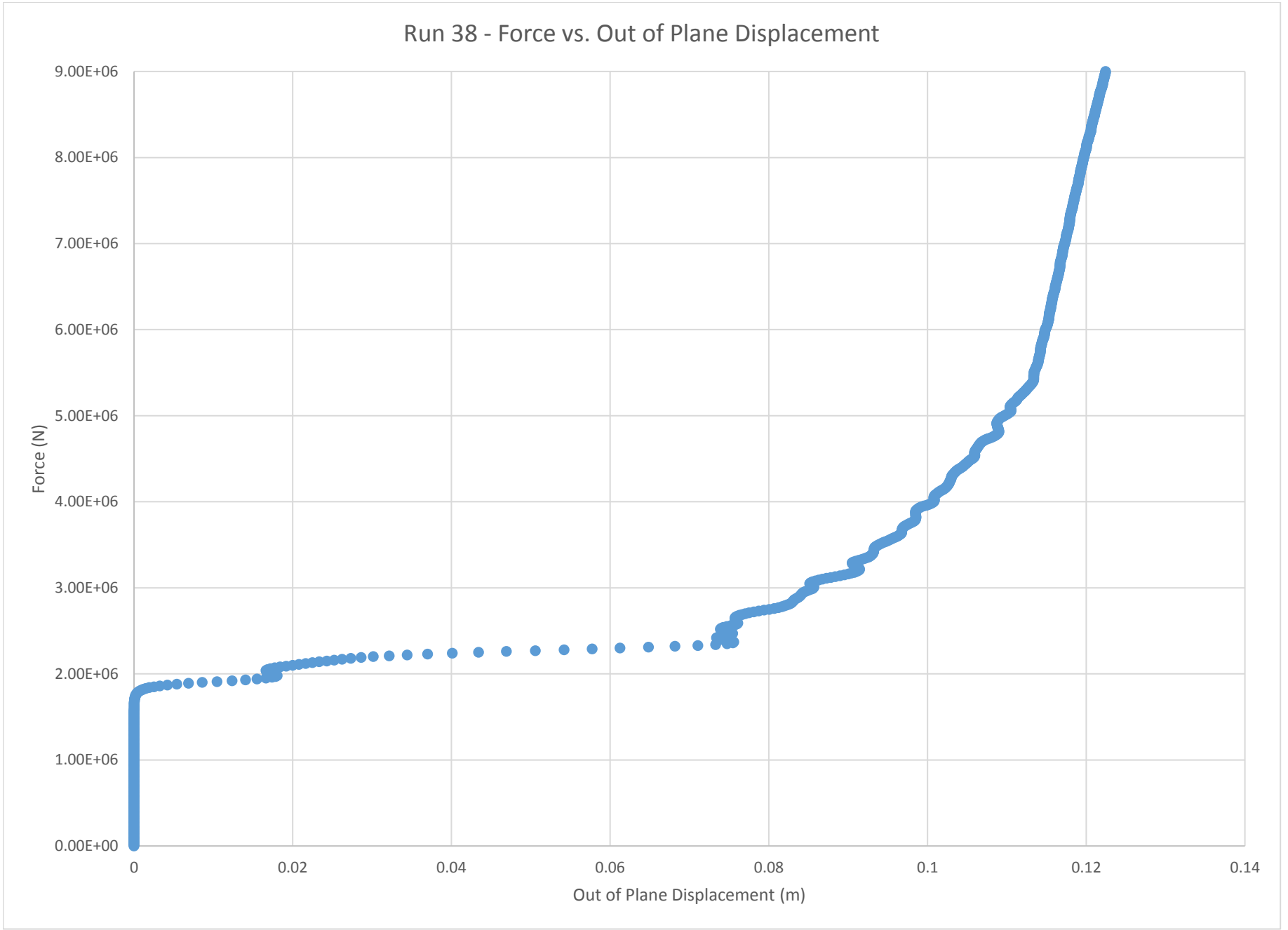
Run 38 - Force vs. Out of Plane Displacement
Force (N)
9.00E+06
8.00E+06
7.00E+06
6.00E+06
5.00E+06
4.00E+06
3.00E+06
2.00E+06
1.00E+06
0.00E+00
0
0.02
0.04
0.06
0.08
0.1
0.12
0.14
Out of Plane Displacement (m)


Run 39 - Force vs. In Plane Displacement
9.00E+06
8.00E+06
7.00E+06
6.00E+06
5.00E+06
4.00E+06
3.00E+06
2.00E+06
1.00E+06
0.00E+00
Force (N)
0
0.01
0.02
0.03
0.04
0.05
0.06
0.07
0.08
0.09
0.1
In Plane Displacement (m)

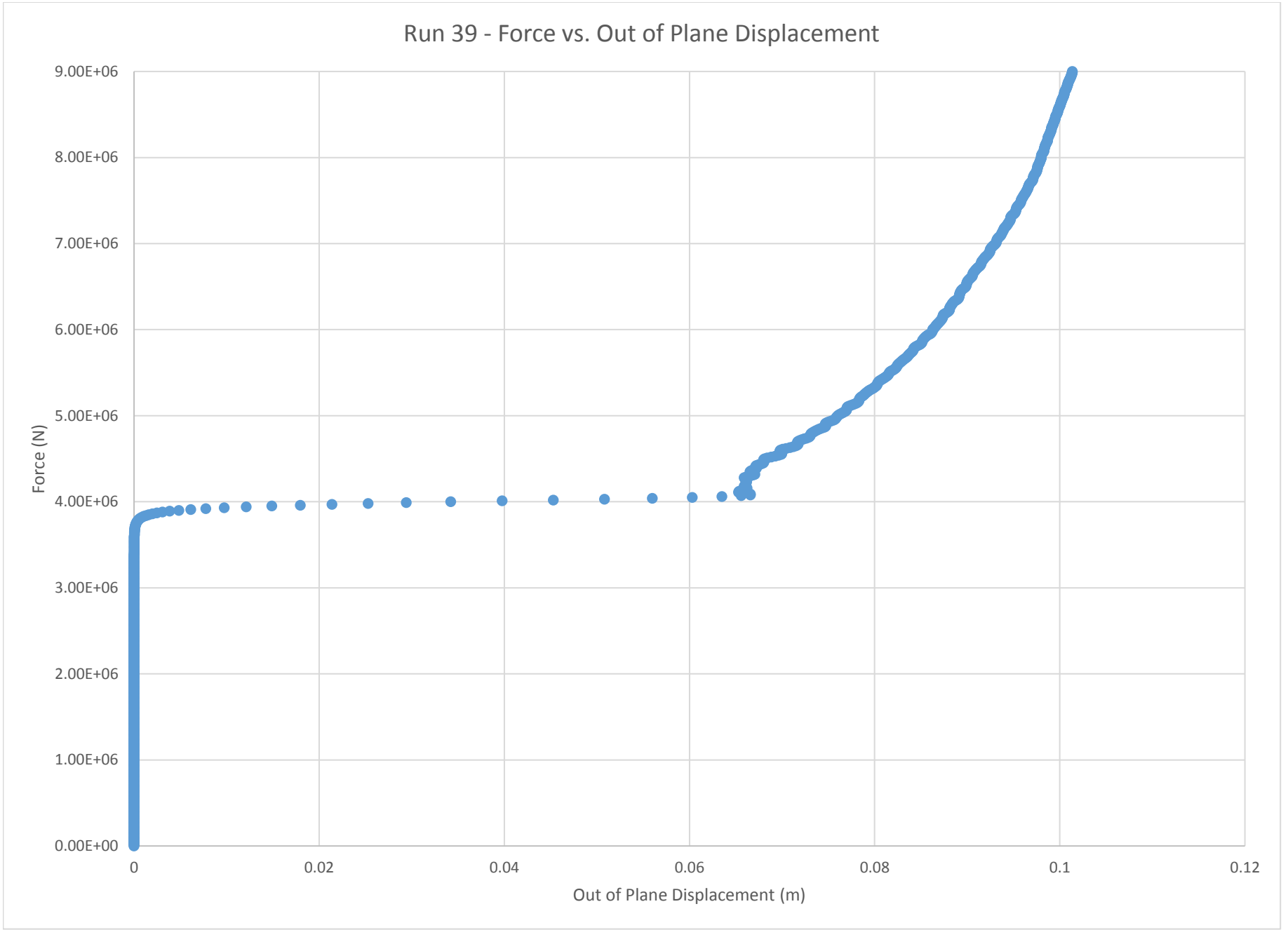
Run 39 - Force vs. Out of Plane Displacement
9.00E+06
8.00E+06
7.00E+06
6.00E+06
5.00E+06
4.00E+06
3.00E+06
2.00E+06
1.00E+06
0.00E+00
Force (N)
0
0.02
0.04
0.06
0.08
0.1
0.12
Out of Plane Displacement (m)

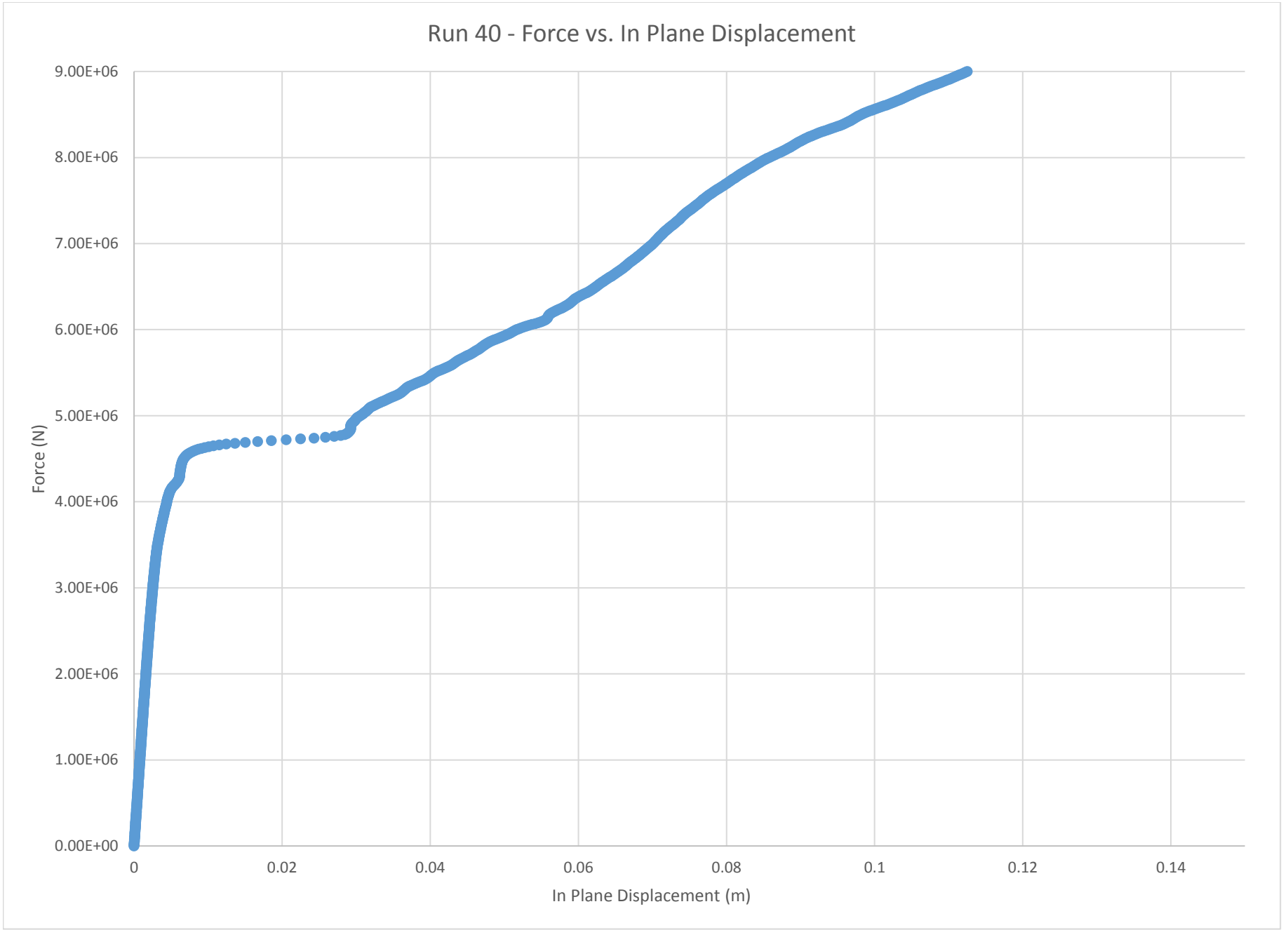
Run 40 - Force vs. In Plane Displacement
9.00E+06
8.00E+06
7.00E+06
6.00E+06
5.00E+06
4.00E+06
3.00E+06
2.00E+06
1.00E+06
0.00E+00
Force (N)
0
0.02
0.04
0.06
0.08
0.1
0.12
0.14
In Plane Displacement (m)

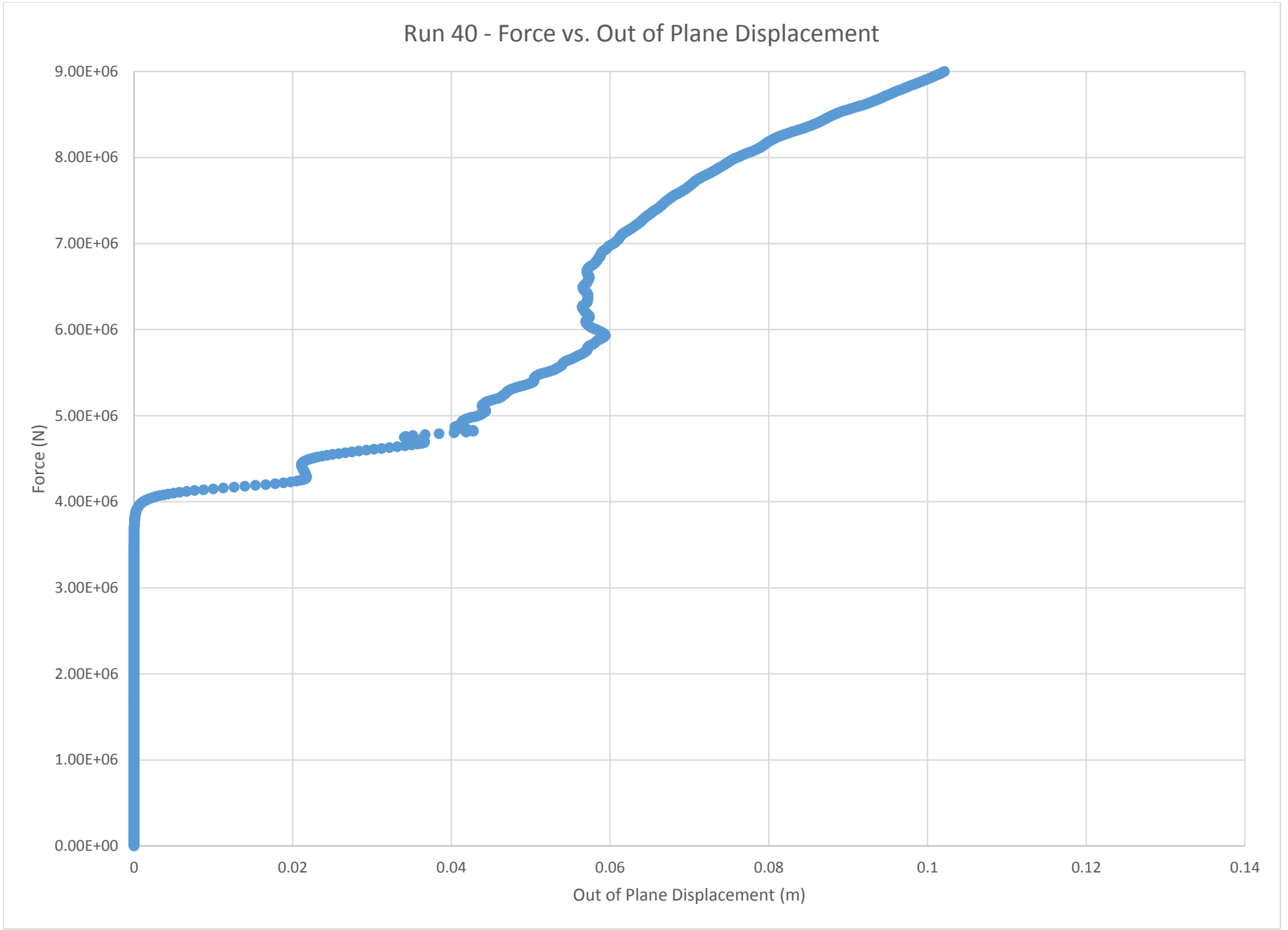
Run 40 - Force vs. Out of Plane Displacement
Force (N)
9.00E+06
8.00E+06
7.00E+06
6.00E+06
5.00E+06
4.00E+06
3.00E+06
2.00E+06
1.00E+06
0.00E+00
0
0.02
0.04
0.06
0.08
0.1
0.12
0.14
Out of Plane Displacement (m)

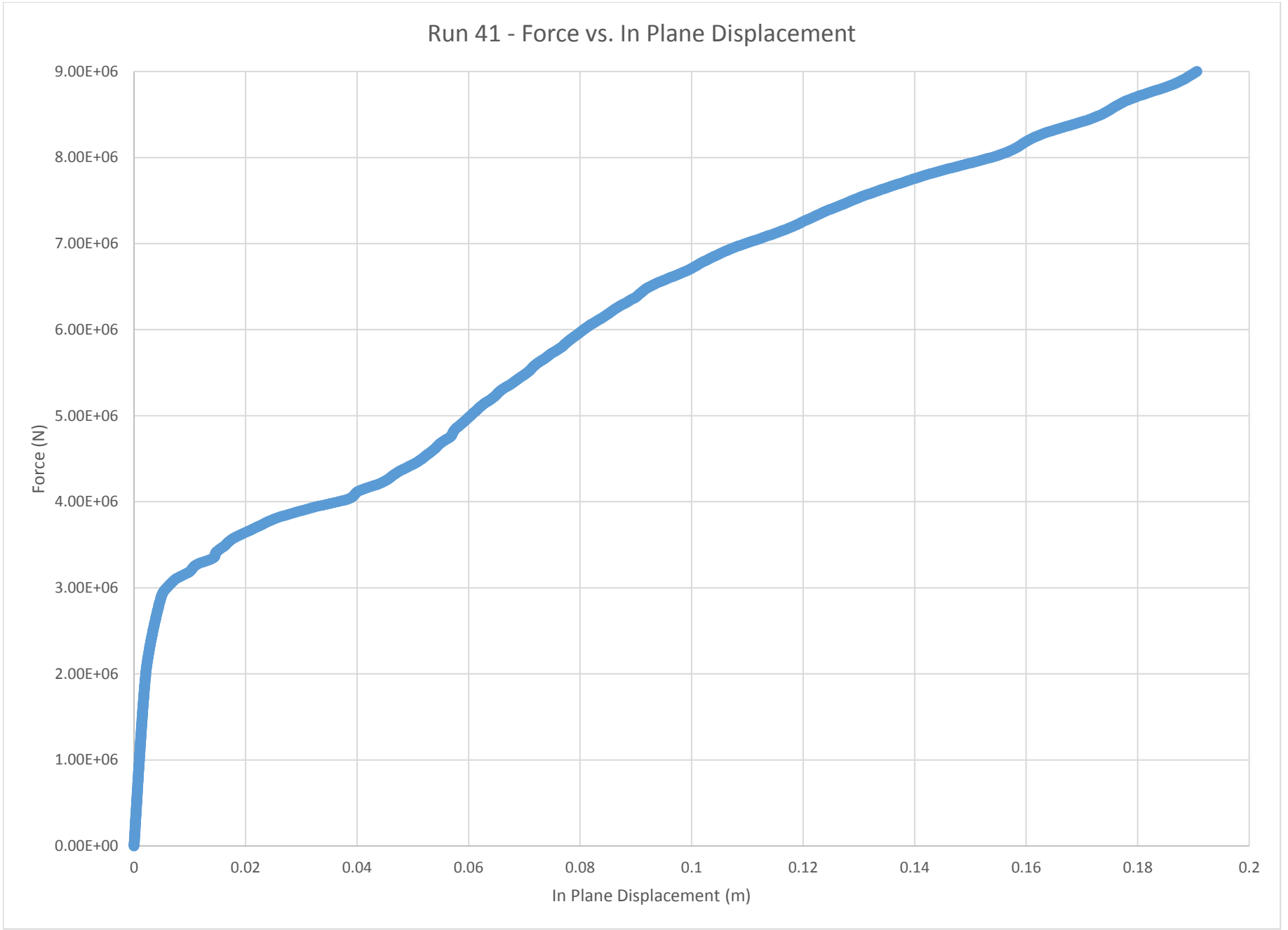
Run 41 - Force vs. In Plane Displacement
9.00E+06
8.00E+06
7.00E+06
6.00E+06
5.00E+06
4.00E+06
3.00E+06
2.00E+06
1.00E+06
0.00E+00
Force (N)
0
0.02
0.04
0.06
0.08
0.1
0.12
0.14
0.16
0.18
0.2
In Plane Displacement (m)

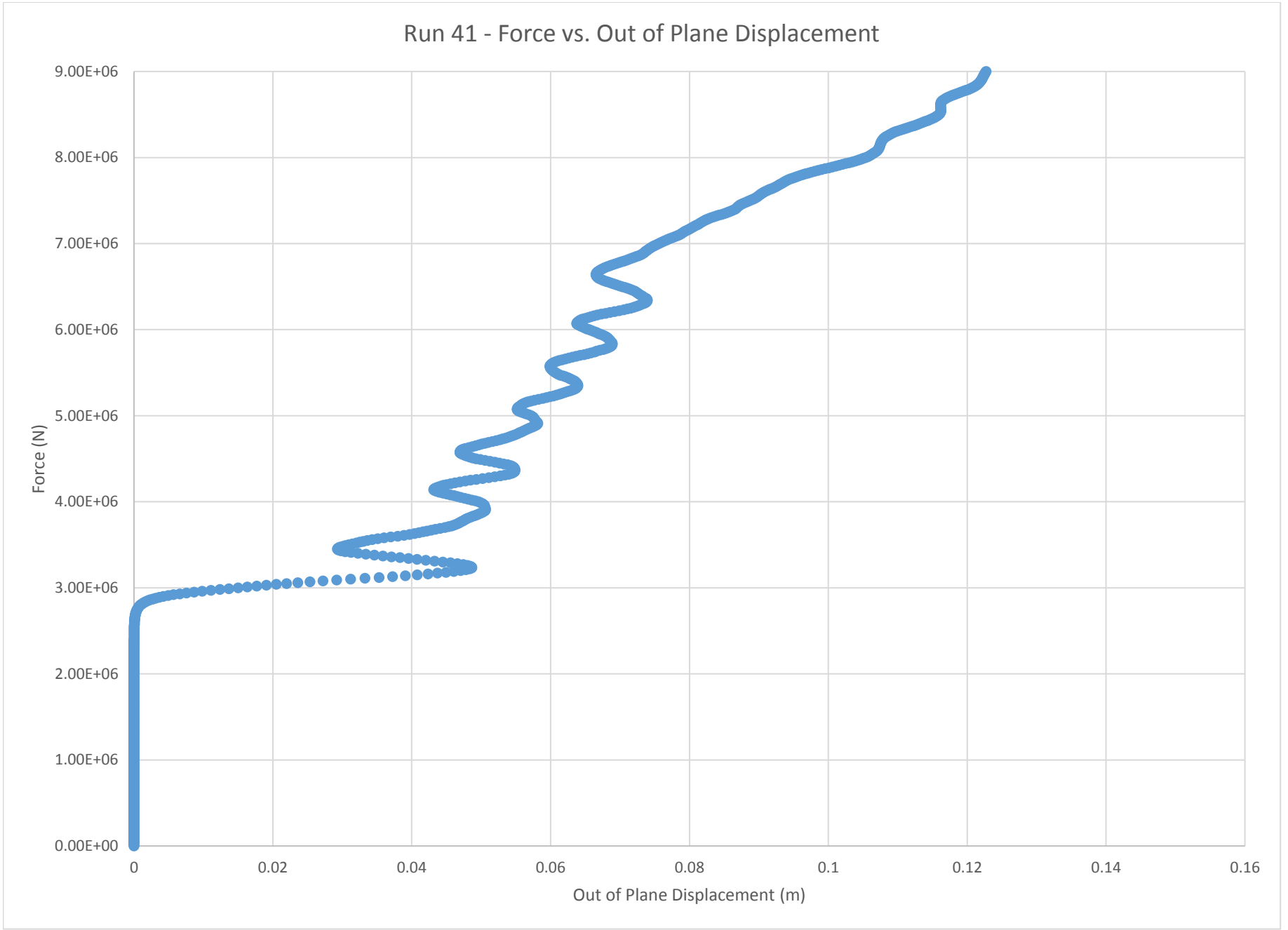
Run 41 - Force vs. Out of Plane Displacement
Force (N)
9.00E+06
8.00E+06
7.00E+06
6.00E+06
5.00E+06
4.00E+06
3.00E+06
2.00E+06
1.00E+06
0.00E+00
0
0.02
0.04
0.06
0.08
0.1
0.12
0.14
0.16
Out of Plane Displacement (m)

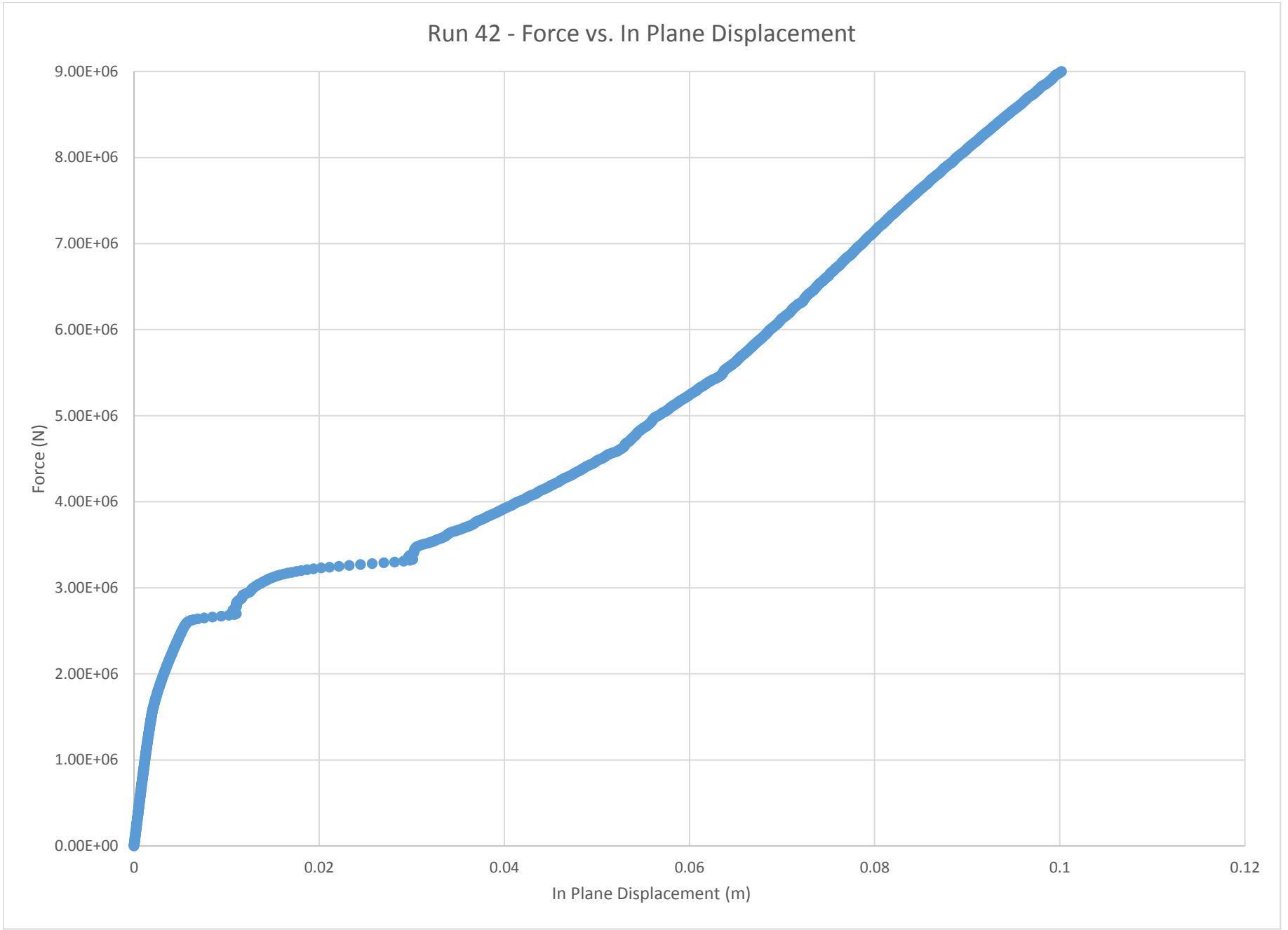
Run 42 - Force vs. In Plane Displacement
9.00E+06
8.00E+06
7.00E+06
6.00E+06
5.00E+06
4.00E+06
3.00E+06
2.00E+06
1.00E+06
0.00E+00
Force (N)
0
0.02
0.04
0.06
0.08
0.1
0.12
In Plane Displacement (m)


Run 42 - Force vs. Out of Plane Displacement
9.00E+06
8.00E+06
7.00E+06
6.00E+06
5.00E+06
4.00E+06
3.00E+06
2.00E+06
1.00E+06
0.00E+00
Force (N)
0
0.02
0.04
0.06
0.08
0.1
0.12
0.14
Out of Plane Displacement (m)

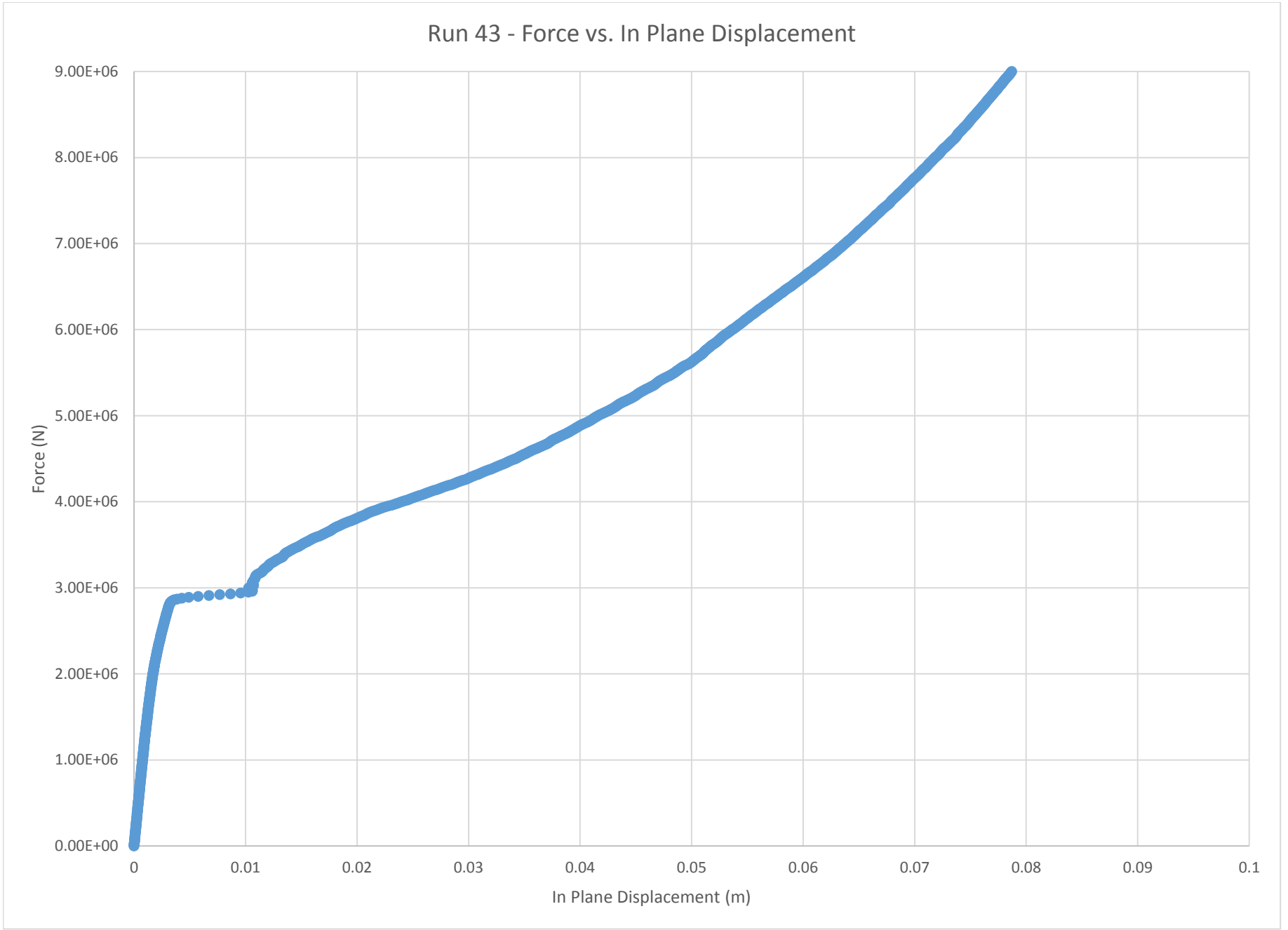
Run 43 - Force vs. In Plane Displacement
9.00E+06
8.00E+06
7.00E+06
6.00E+06
5.00E+06
4.00E+06
3.00E+06
2.00E+06
1.00E+06
0.00E+00
Force (N)
0
0.01
0.02
0.03
0.04
0.05
0.06
0.07
0.08
0.09
0.1
In Plane Displacement (m)

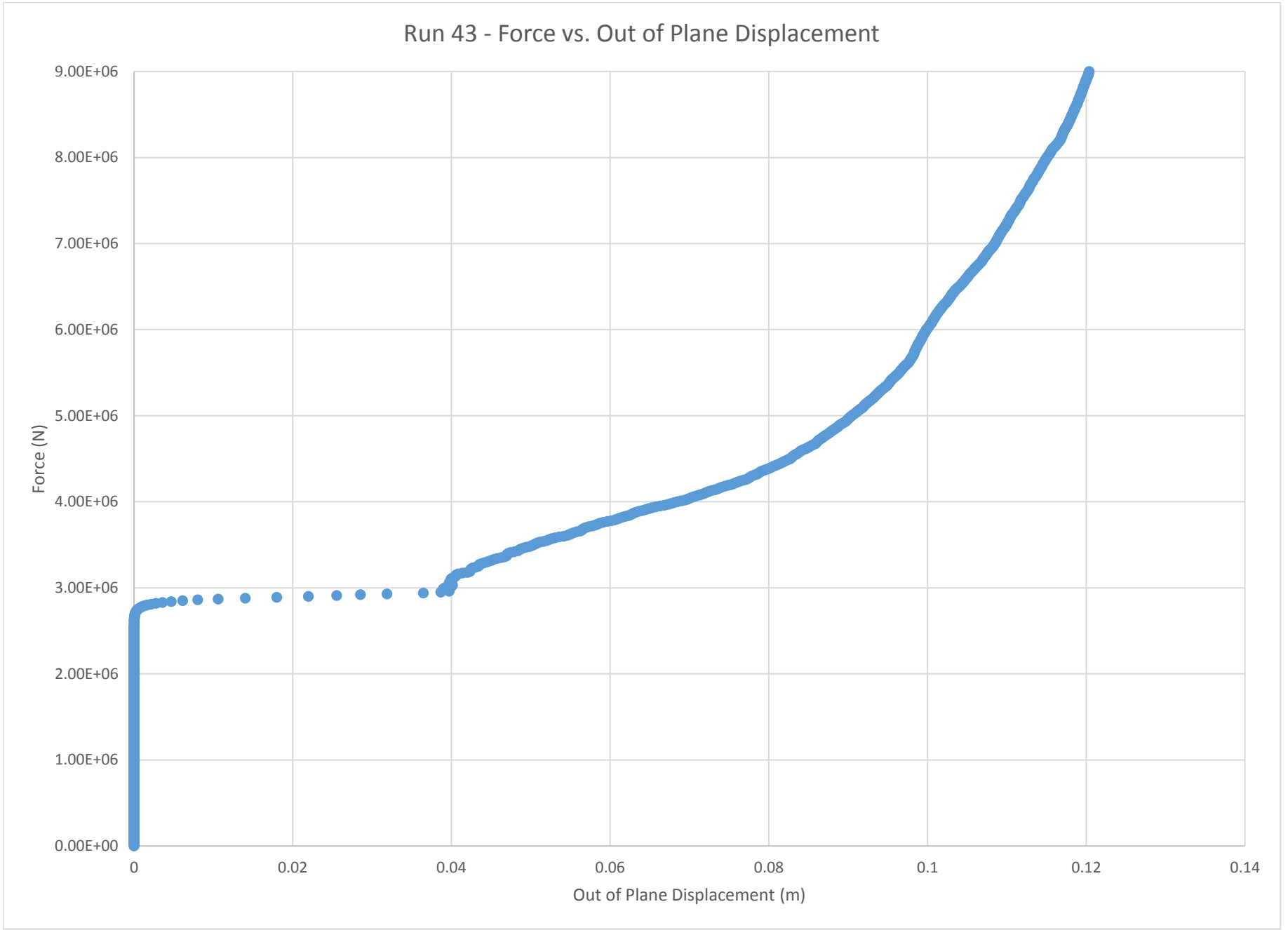
Run 43 - Force vs. Out of Plane Displacement
9.00E+06
8.00E+06
7.00E+06
6.00E+06
5.00E+06
4.00E+06
3.00E+06
2.00E+06
1.00E+06
0.00E+00
Force (N)
0
0.02
0.04
0.06
0.08
0.1
0.12
0.14
Out of Plane Displacement (m)

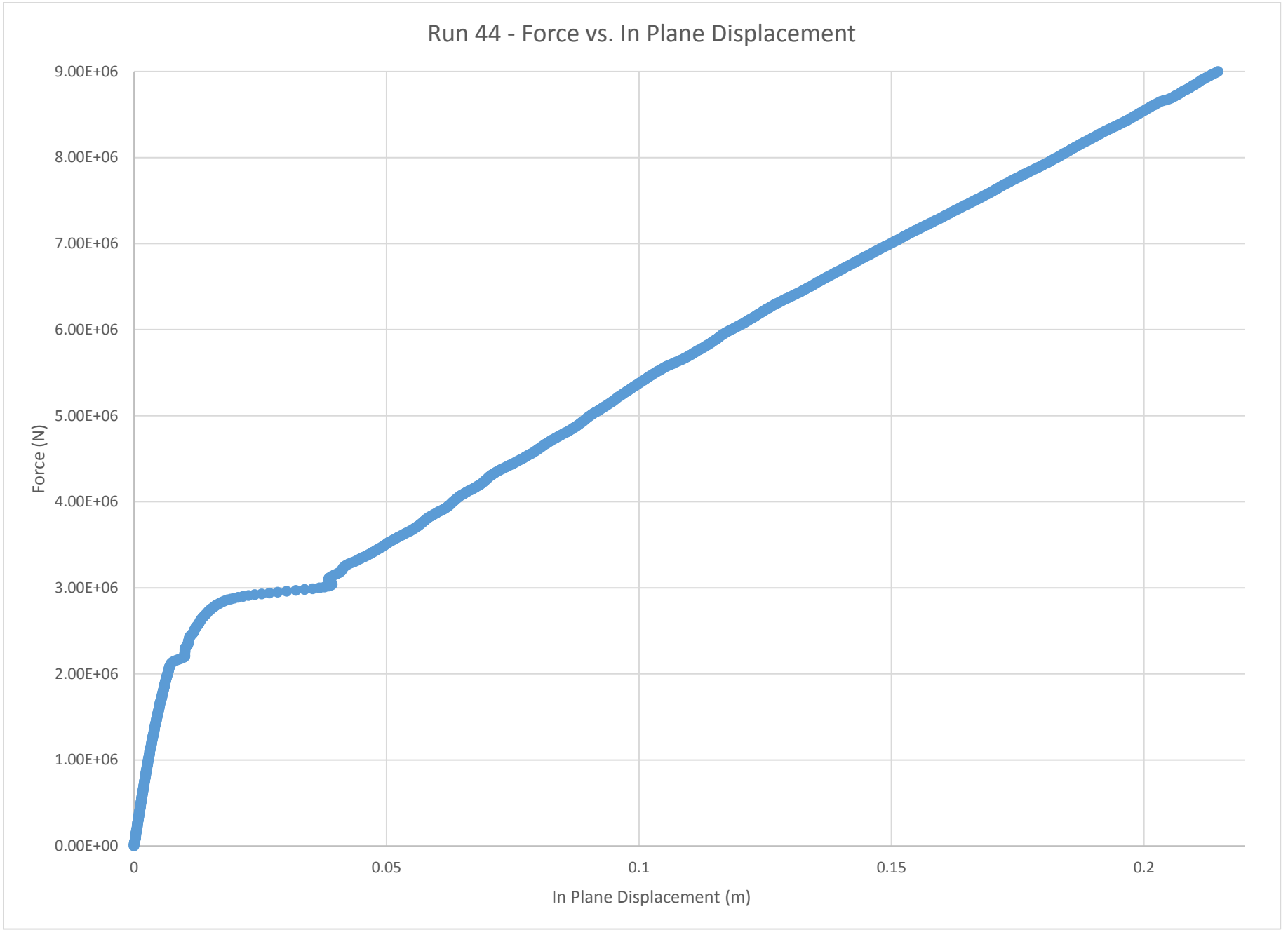
Run 44 - Force vs. In Plane Displacement
9.00E+06
8.00E+06
7.00E+06
6.00E+06
5.00E+06
4.00E+06
3.00E+06
2.00E+06
1.00E+06
0.00E+00
Force (N)
0
0.05
0.1
0.15
0.2
In Plane Displacement (m)

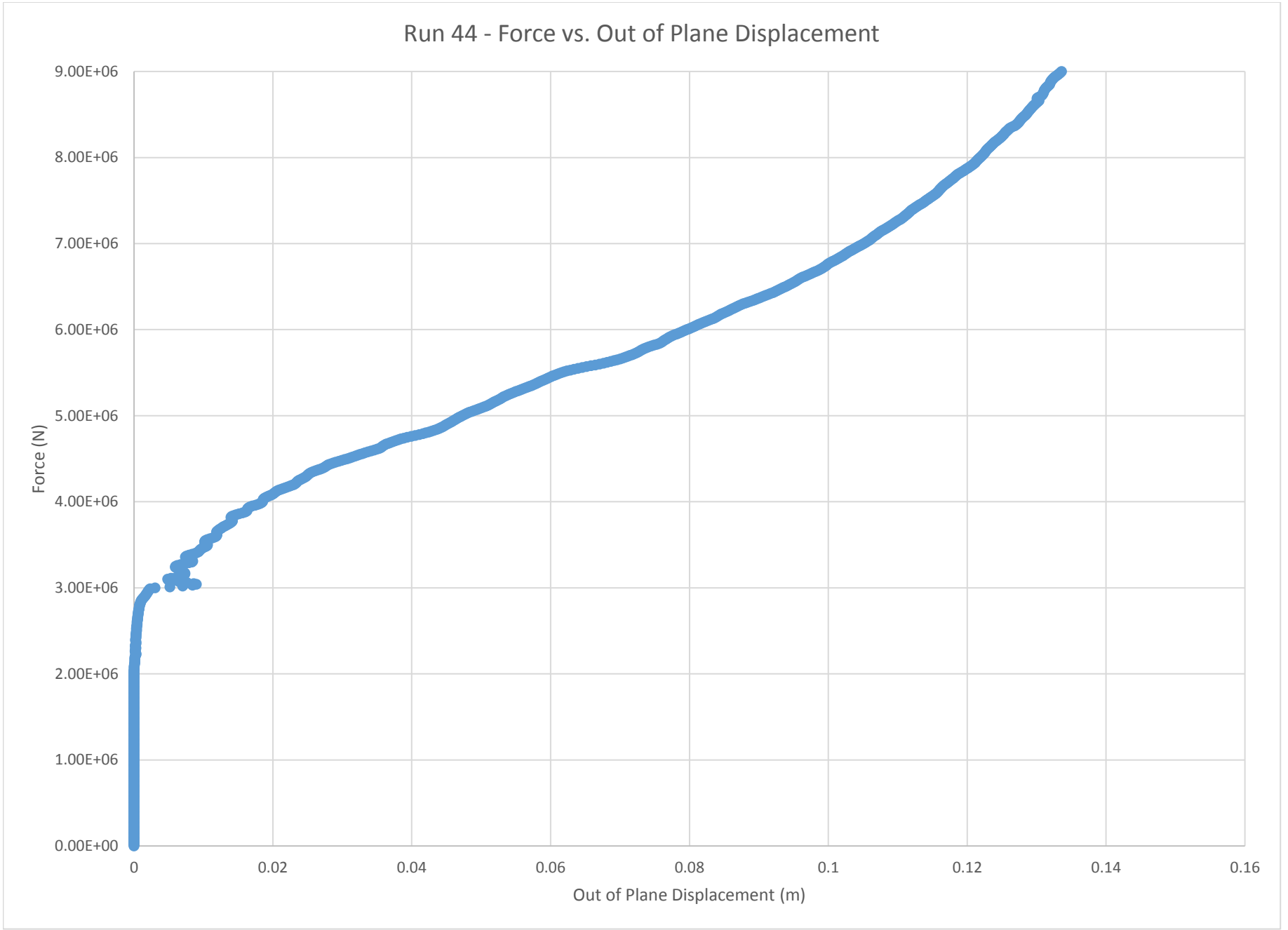
Run 44 - Force vs. Out of Plane Displacement
Force (N)
9.00E+06
8.00E+06
7.00E+06
6.00E+06
5.00E+06
4.00E+06
3.00E+06
2.00E+06
1.00E+06
0.00E+00
0
0.02
0.04
0.06
0.08
0.1
0.12
0.14
0.16
Out of Plane Displacement (m)

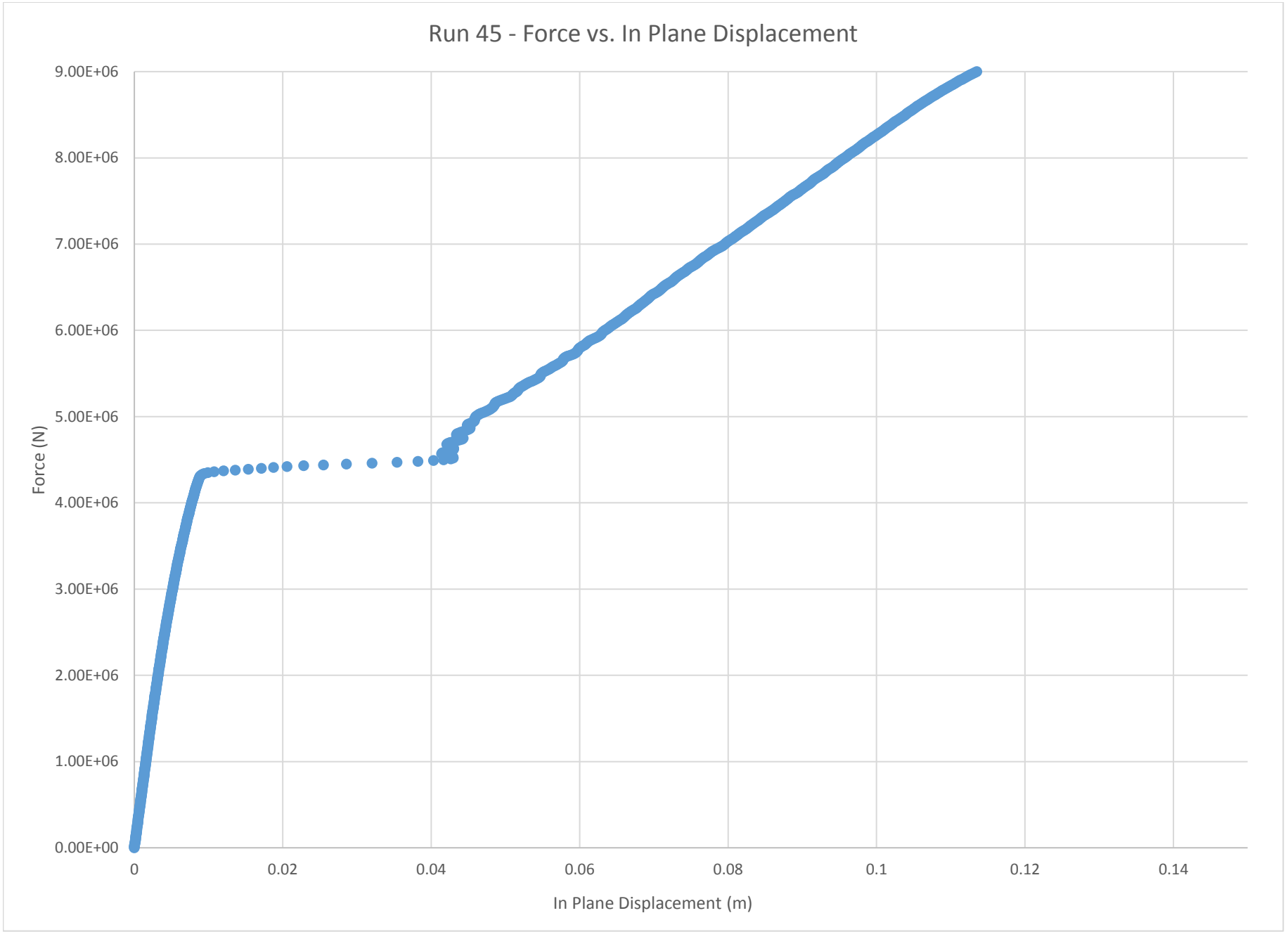
Run 45 - Force vs. In Plane Displacement
9.00E+06
8.00E+06
7.00E+06
6.00E+06
5.00E+06
4.00E+06
3.00E+06
2.00E+06
1.00E+06
0.00E+00
Force (N)
0
0.02
0.04
0.06
0.08
0.1
0.12
0.14
In Plane Displacement (m)

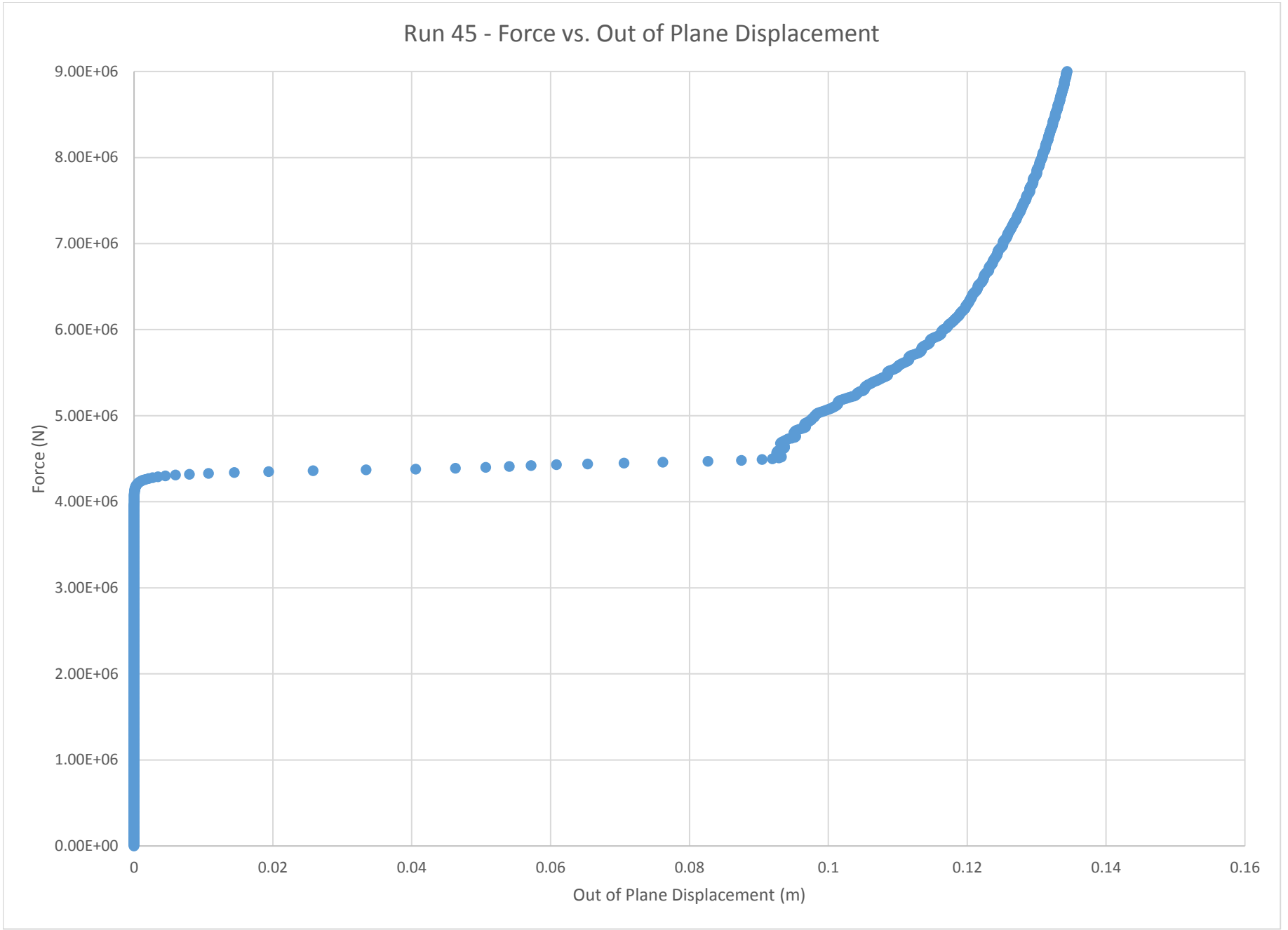
Run 45 - Force vs. Out of Plane Displacement
Force (N)
9.00E+06
8.00E+06
7.00E+06
6.00E+06
5.00E+06
4.00E+06
3.00E+06
2.00E+06
1.00E+06
0.00E+00
0
0.02
0.04
0.06
0.08
0.1
0.12
0.14
0.16
Out of Plane Displacement (m)

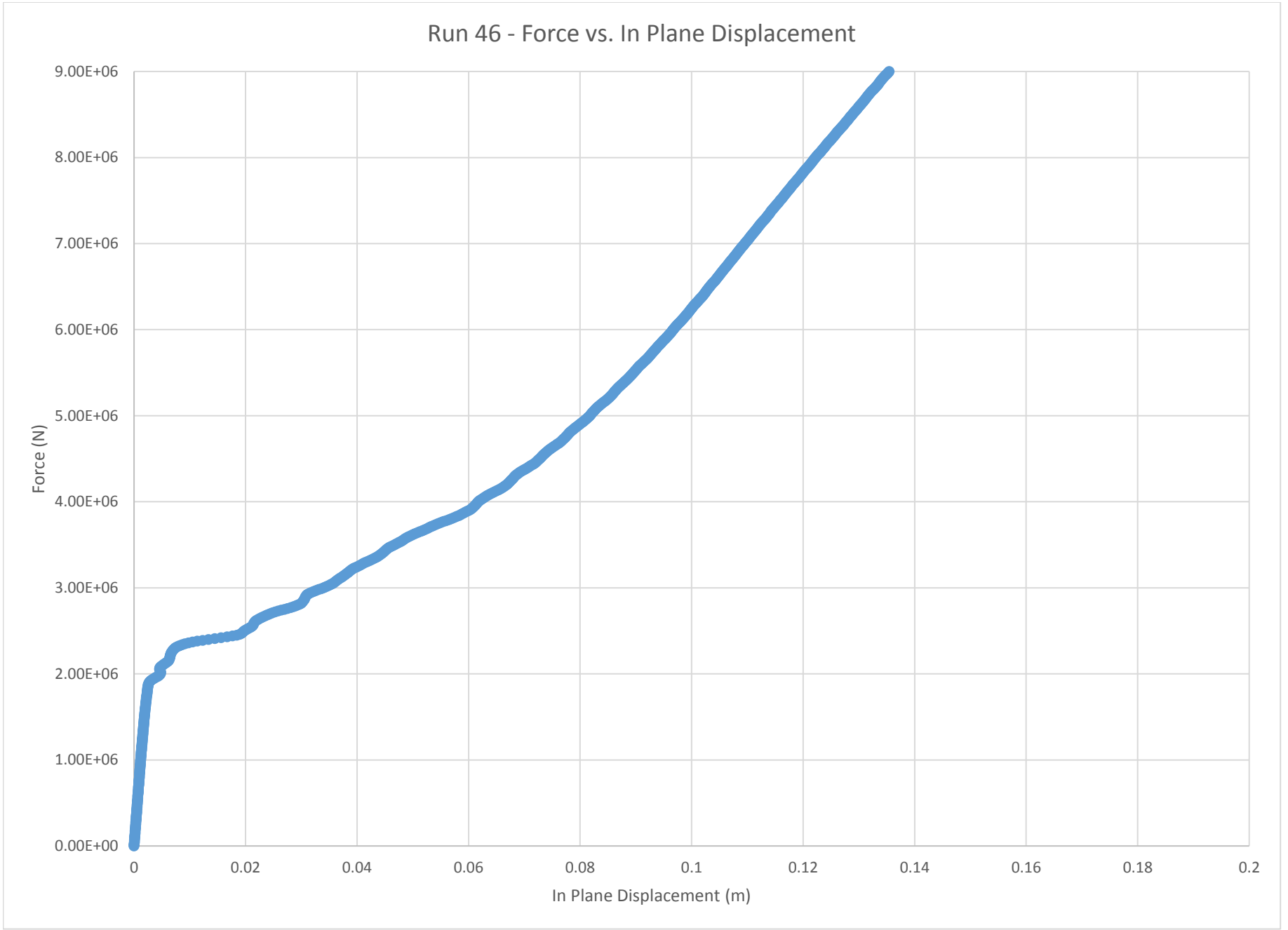
Run 46 - Force vs. In Plane Displacement
Force (N)
9.00E+06
8.00E+06
7.00E+06
6.00E+06
5.00E+06
4.00E+06
3.00E+06
2.00E+06
1.00E+06
0.00E+00
0
0.02
0.04
0.06
0.08
0.1
0.12
0.14
0.16
0.18
0.2
In Plane Displacement (m)

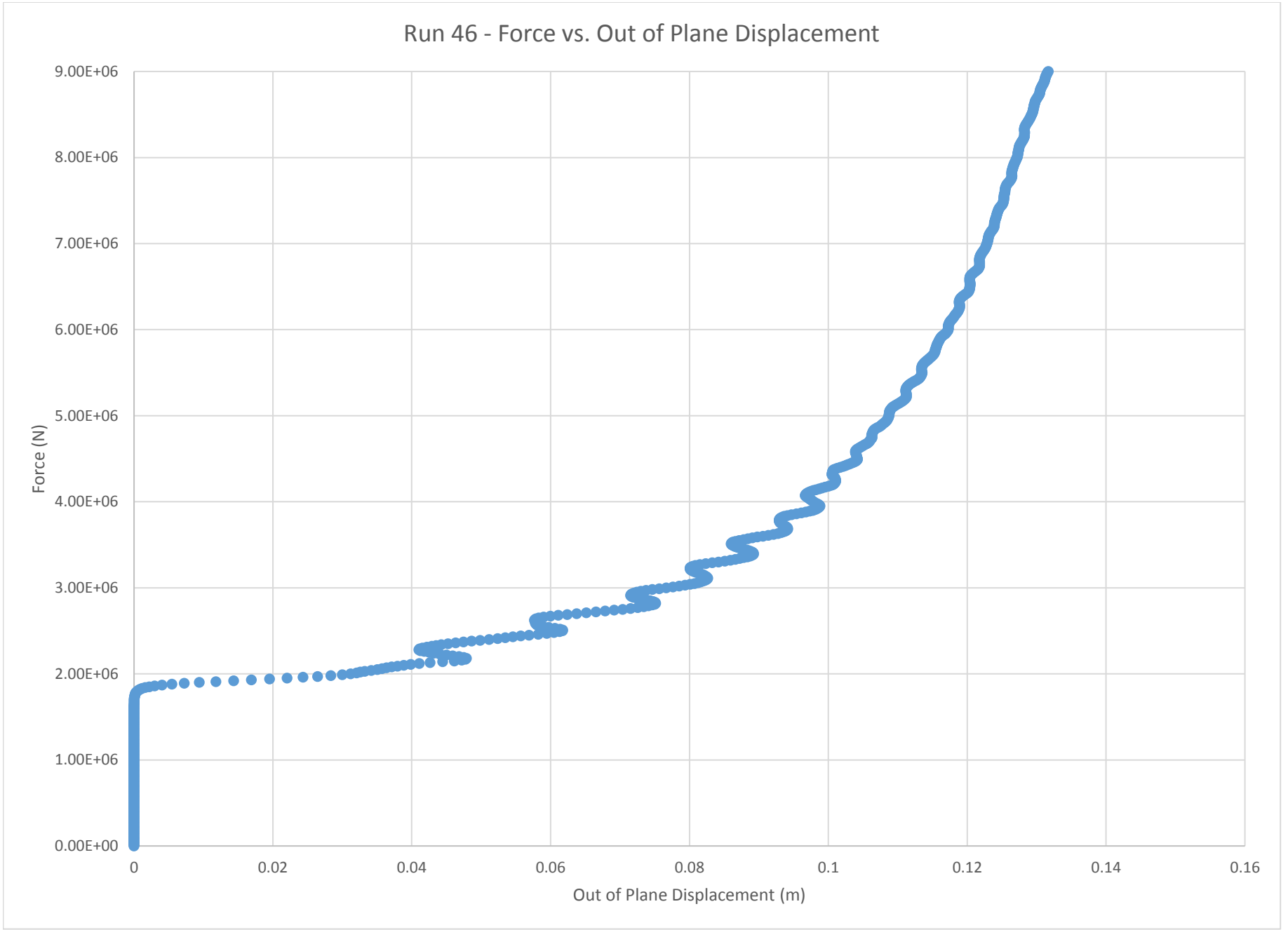
Run 46 - Force vs. Out of Plane Displacement
Force (N)
9.00E+06
8.00E+06
7.00E+06
6.00E+06
5.00E+06
4.00E+06
3.00E+06
2.00E+06
1.00E+06
0.00E+00
0
0.02
0.04
0.06
0.08
0.1
0.12
0.14
0.16
Out of Plane Displacement (m)

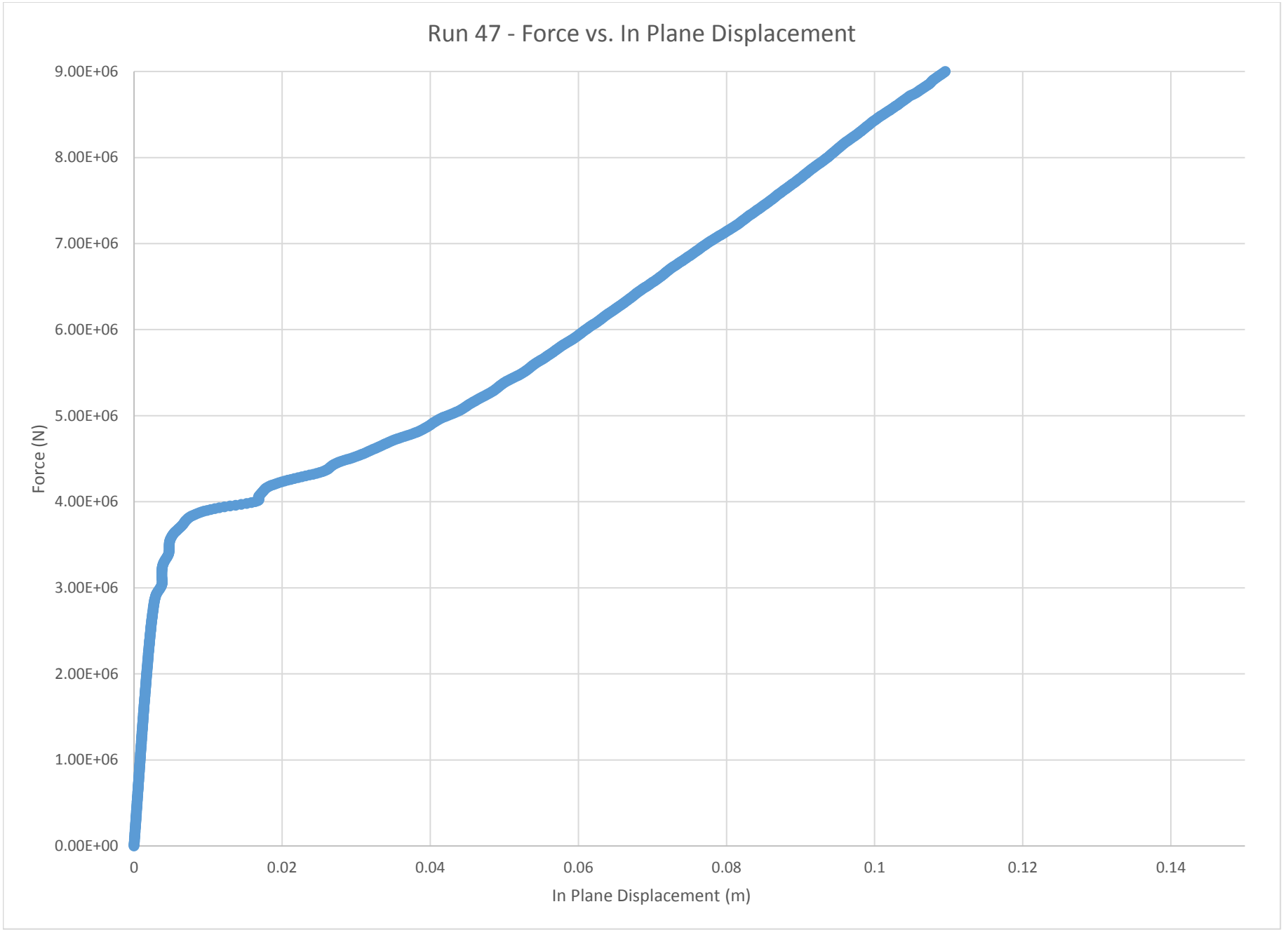
Run 47 - Force vs. In Plane Displacement
9.00E+06
8.00E+06
7.00E+06
6.00E+06
5.00E+06
4.00E+06
3.00E+06
2.00E+06
1.00E+06
0.00E+00
Force (N)
0
0.02
0.04
0.06
0.08
0.1
0.12
0.14
In Plane Displacement (m)

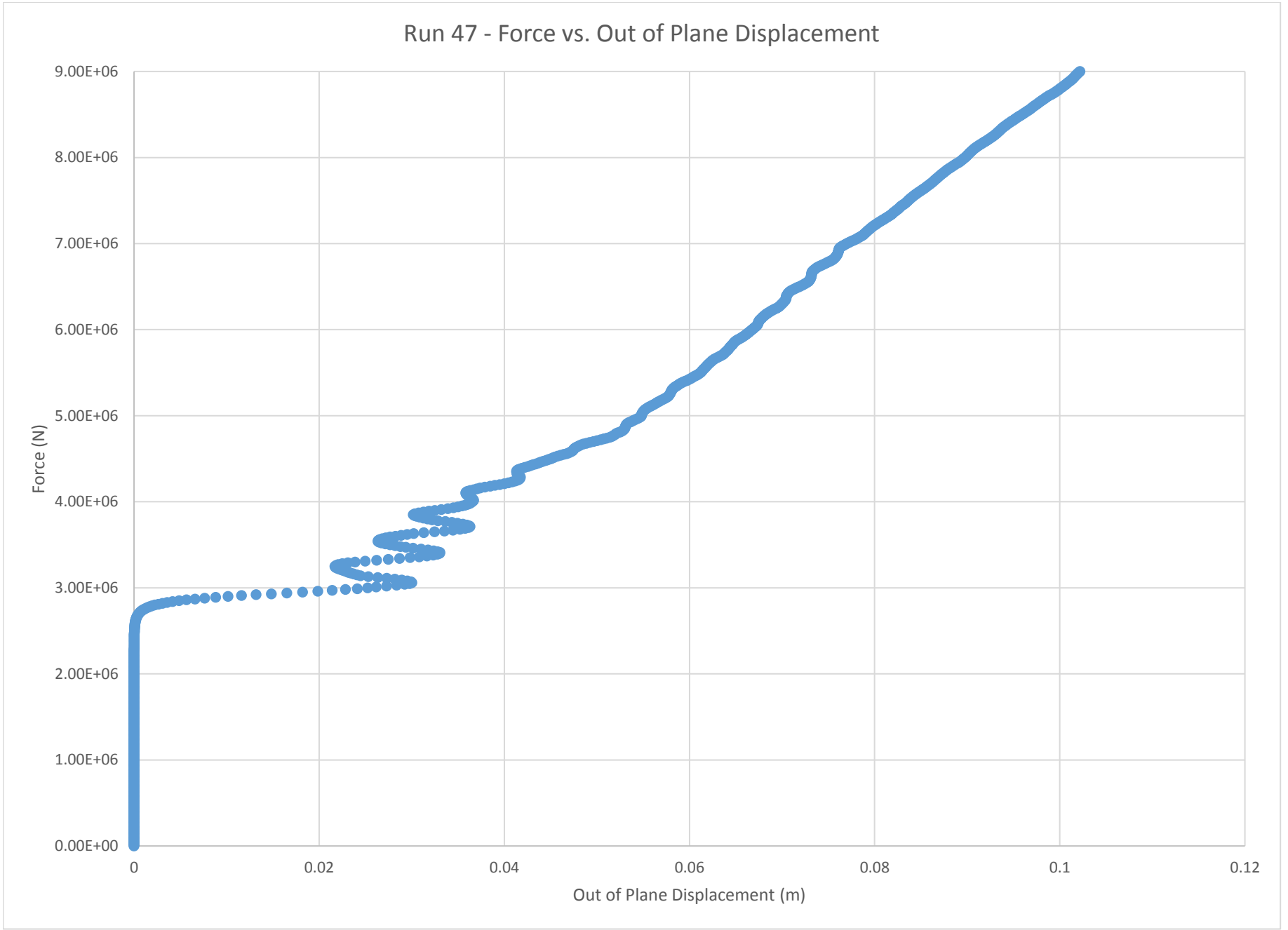
Run 47 - Force vs. Out of Plane Displacement
9.00E+06
8.00E+06
7.00E+06
6.00E+06
5.00E+06
4.00E+06
3.00E+06
2.00E+06
1.00E+06
0.00E+00
Force (N)
0
0.02
0.04
0.06
0.08
0.1
0.12
Out of Plane Displacement (m)

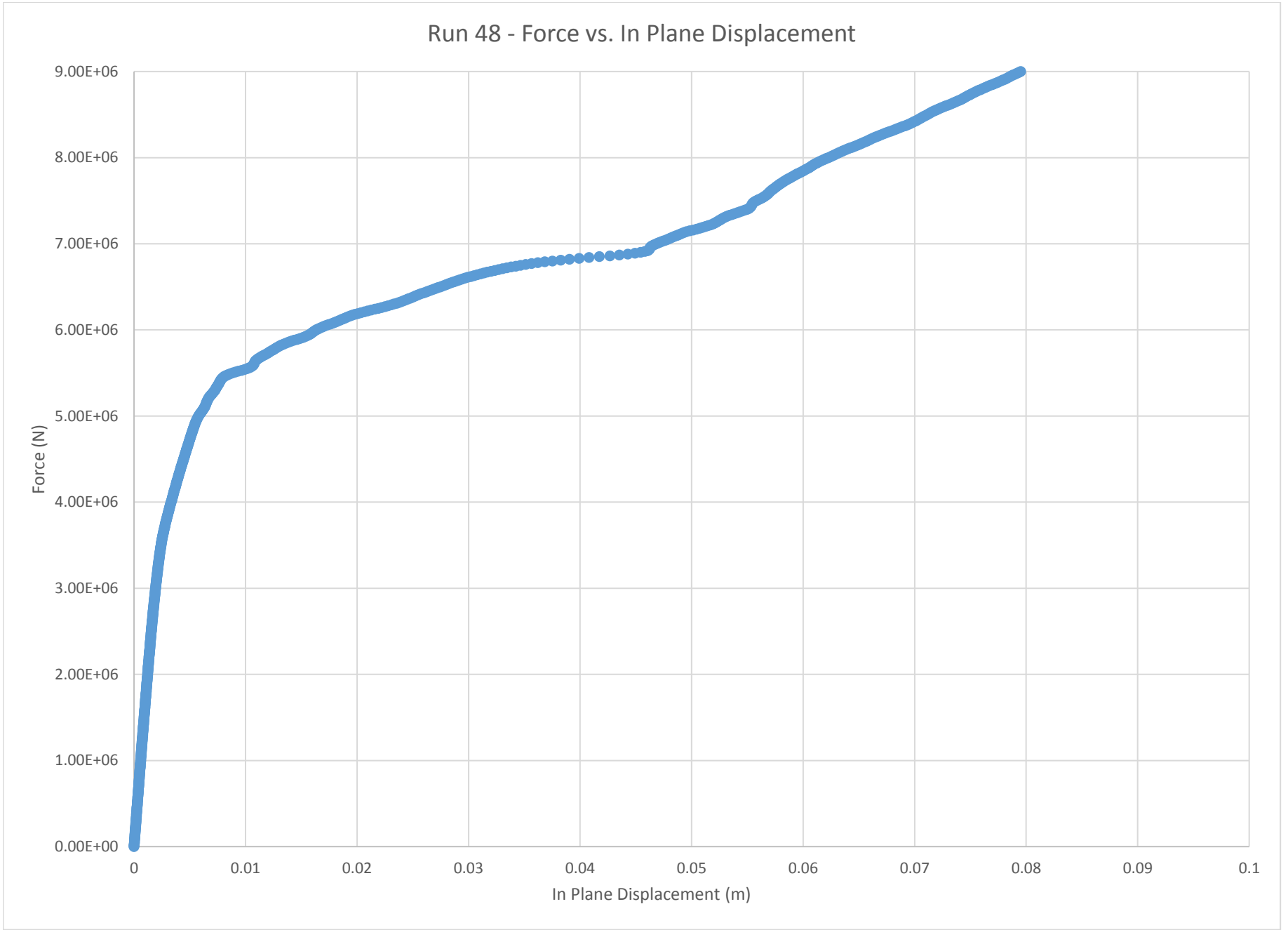
Run 48 - Force vs. In Plane Displacement
Force (N)
9.00E+06
8.00E+06
7.00E+06
6.00E+06
5.00E+06
4.00E+06
3.00E+06
2.00E+06
1.00E+06
0.00E+00
0
0.01
0.02
0.03
0.04
0.05
0.06
0.07
0.08
0.09
0.1
In Plane Displacement (m)

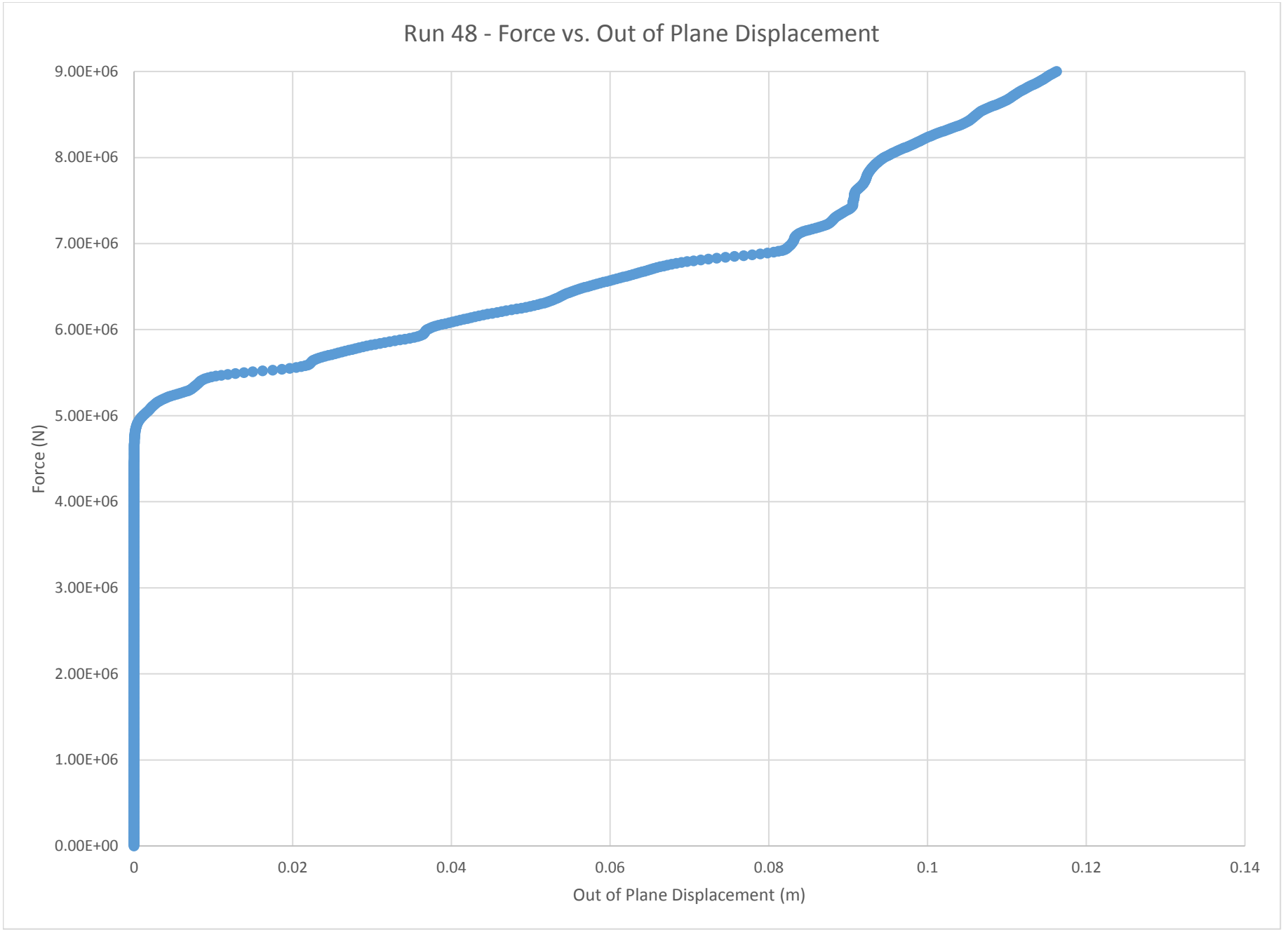
Run 48 - Force vs. Out of Plane Displacement
9.00E+06
8.00E+06
7.00E+06
6.00E+06
5.00E+06
4.00E+06
3.00E+06
2.00E+06
1.00E+06
0.00E+00
Force (N)
0
0.02
0.04
0.06
0.08
0.1
0.12
0.14
Out of Plane Displacement (m)

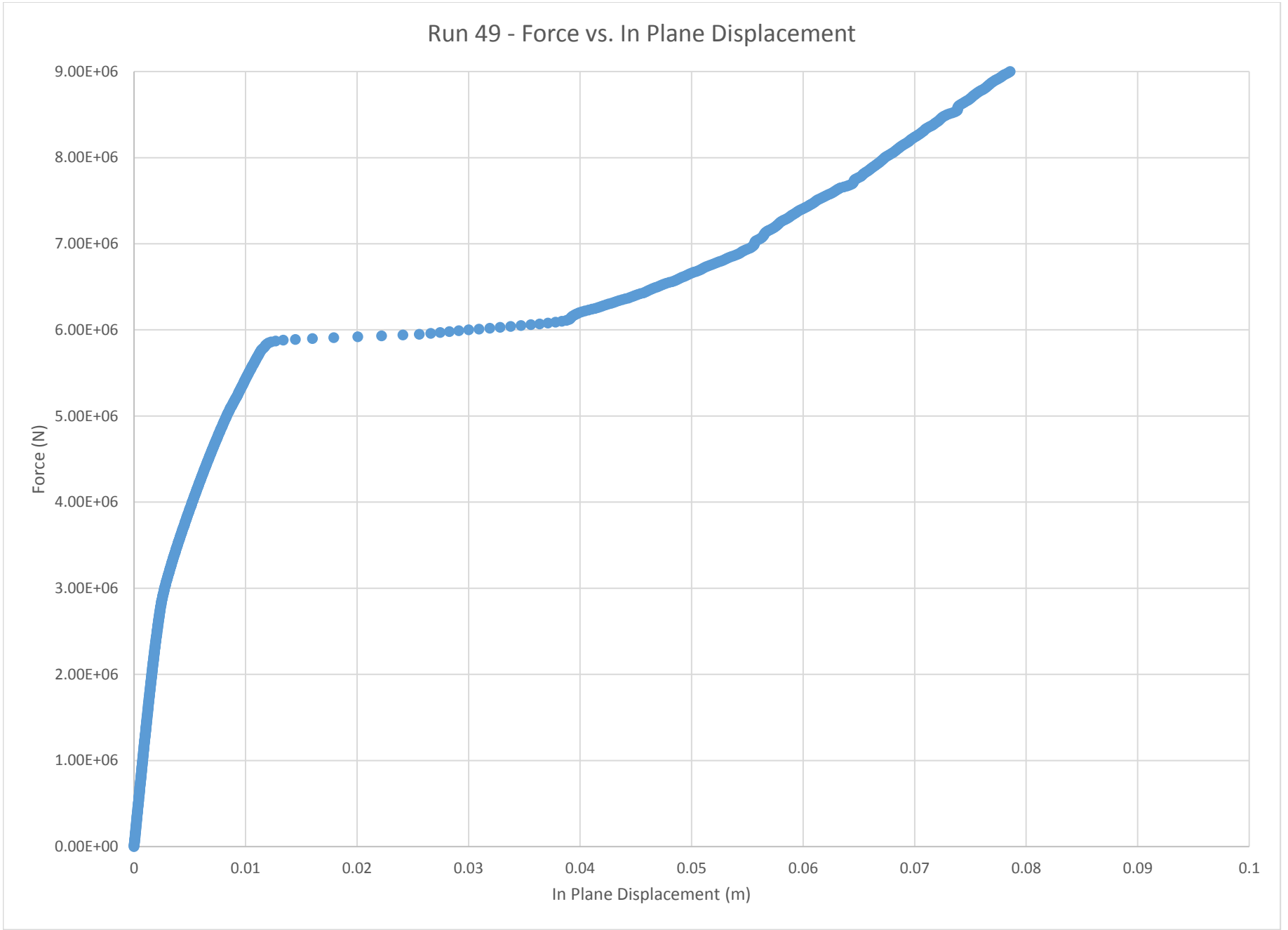
Run 49 - Force vs. In Plane Displacement
9.00E+06
8.00E+06
7.00E+06
6.00E+06
5.00E+06
4.00E+06
3.00E+06
2.00E+06
1.00E+06
0.00E+00
Force (N)
0
0.01
0.02
0.03
0.04
0.05
0.06
0.07
0.08
0.09
0.1
In Plane Displacement (m)

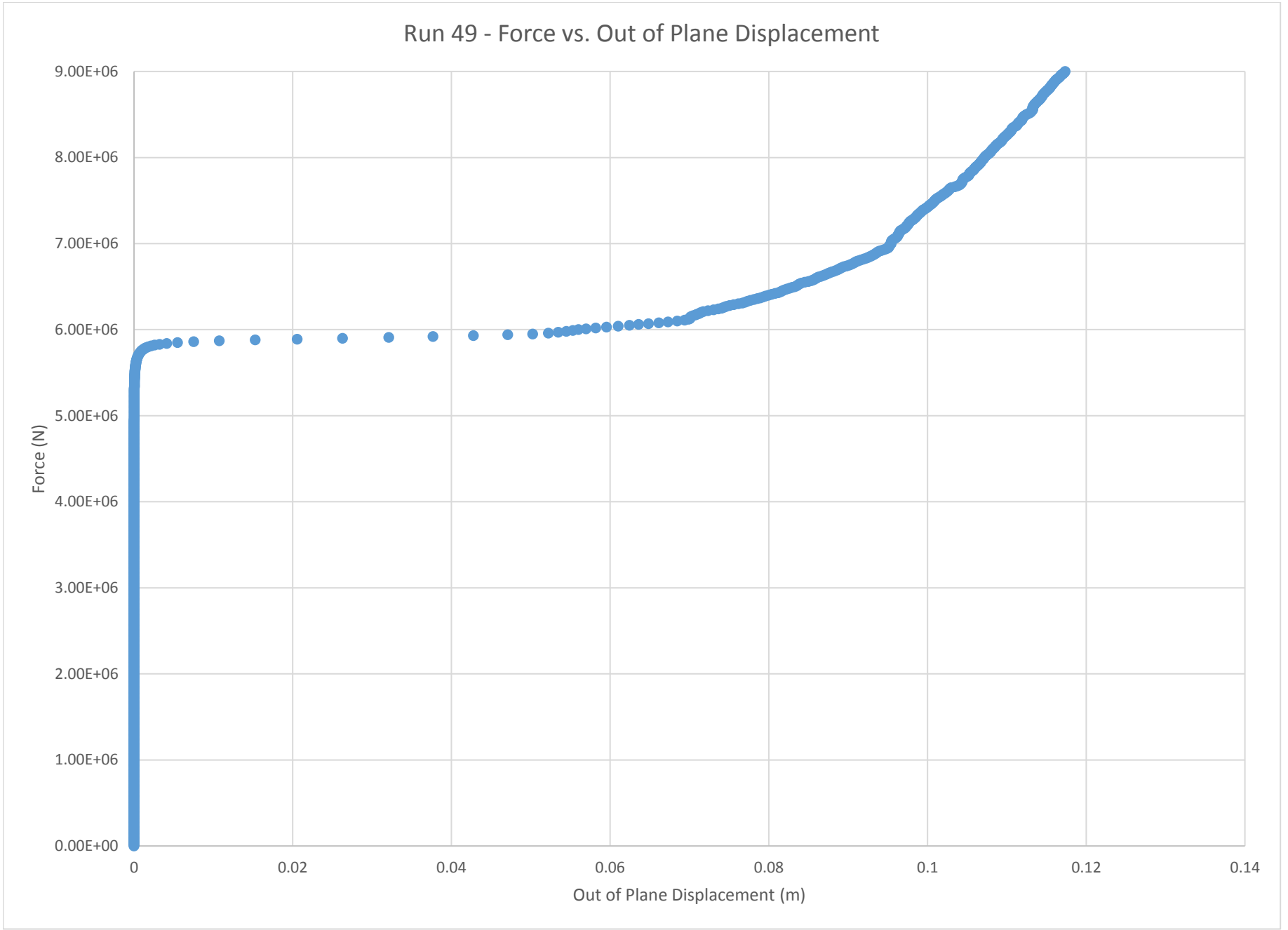
Run 49 - Force vs. Out of Plane Displacement
9.00E+06
8.00E+06
7.00E+06
6.00E+06
5.00E+06
4.00E+06
3.00E+06
2.00E+06
1.00E+06
0.00E+00
Force (N)
0
0.02
0.04
0.06
0.08
0.1
0.12
0.14
Out of Plane Displacement (m)

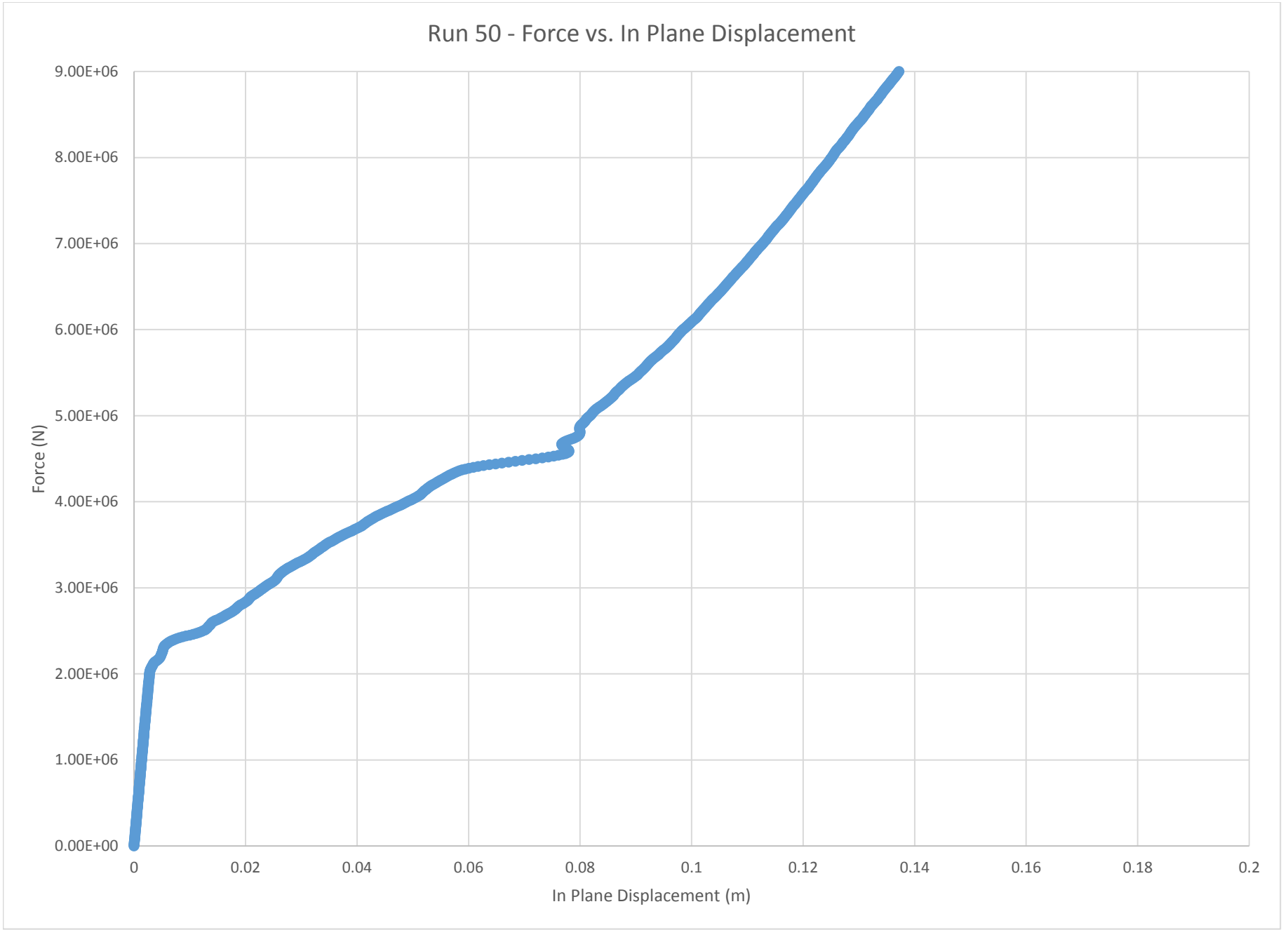
Run 50 - Force vs. In Plane Displacement
Force (N)
9.00E+06
8.00E+06
7.00E+06
6.00E+06
5.00E+06
4.00E+06
3.00E+06
2.00E+06
1.00E+06
0.00E+00
0
0.02
0.04
0.06
0.08
0.1
0.12
0.14
0.16
0.18
0.2
In Plane Displacement (m)

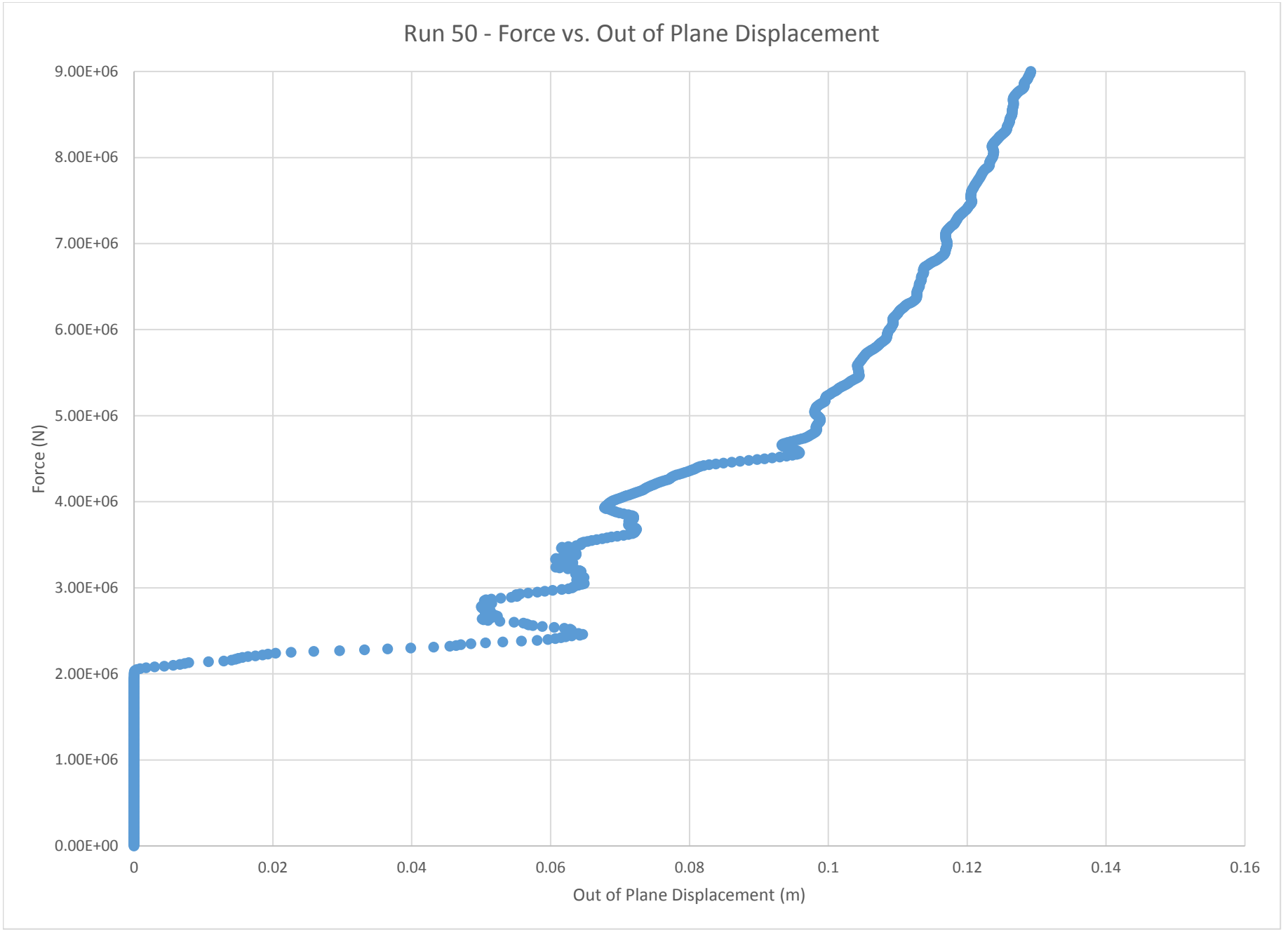
Run 50 - Force vs. Out of Plane Displacement
Force (N)
9.00E+06
8.00E+06
7.00E+06
6.00E+06
5.00E+06
4.00E+06
3.00E+06
2.00E+06
1.00E+06
0.00E+00
0
0.02
0.04
0.06
0.08
0.1
0.12
0.14
0.16
Out of Plane Displacement (m)

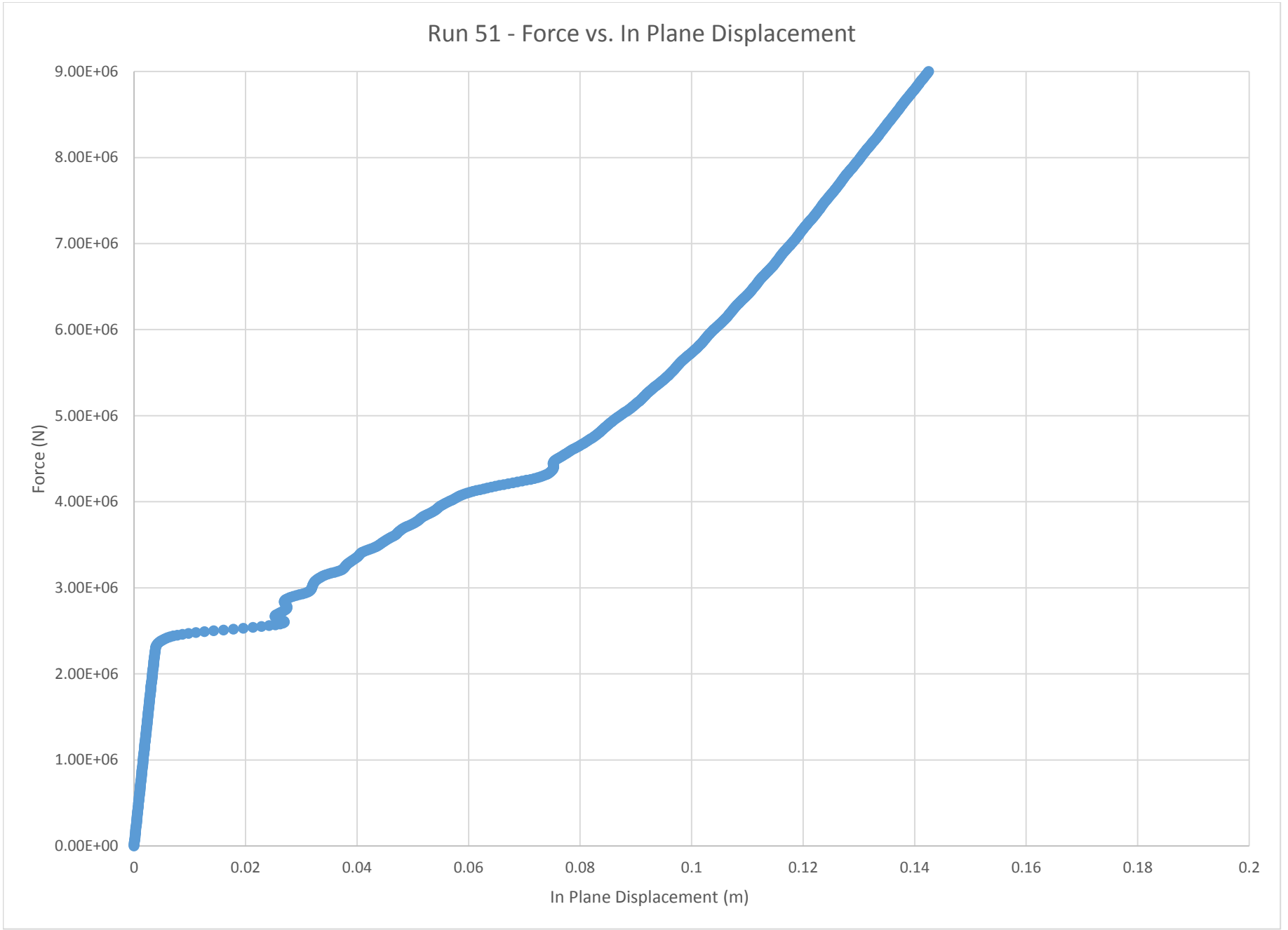
Run 51 - Force vs. In Plane Displacement
Force (N)
9.00E+06
8.00E+06
7.00E+06
6.00E+06
5.00E+06
4.00E+06
3.00E+06
2.00E+06
1.00E+06
0.00E+00
0
0.02
0.04
0.06
0.08
0.1
0.12
0.14
0.16
0.18
0.2
In Plane Displacement (m)

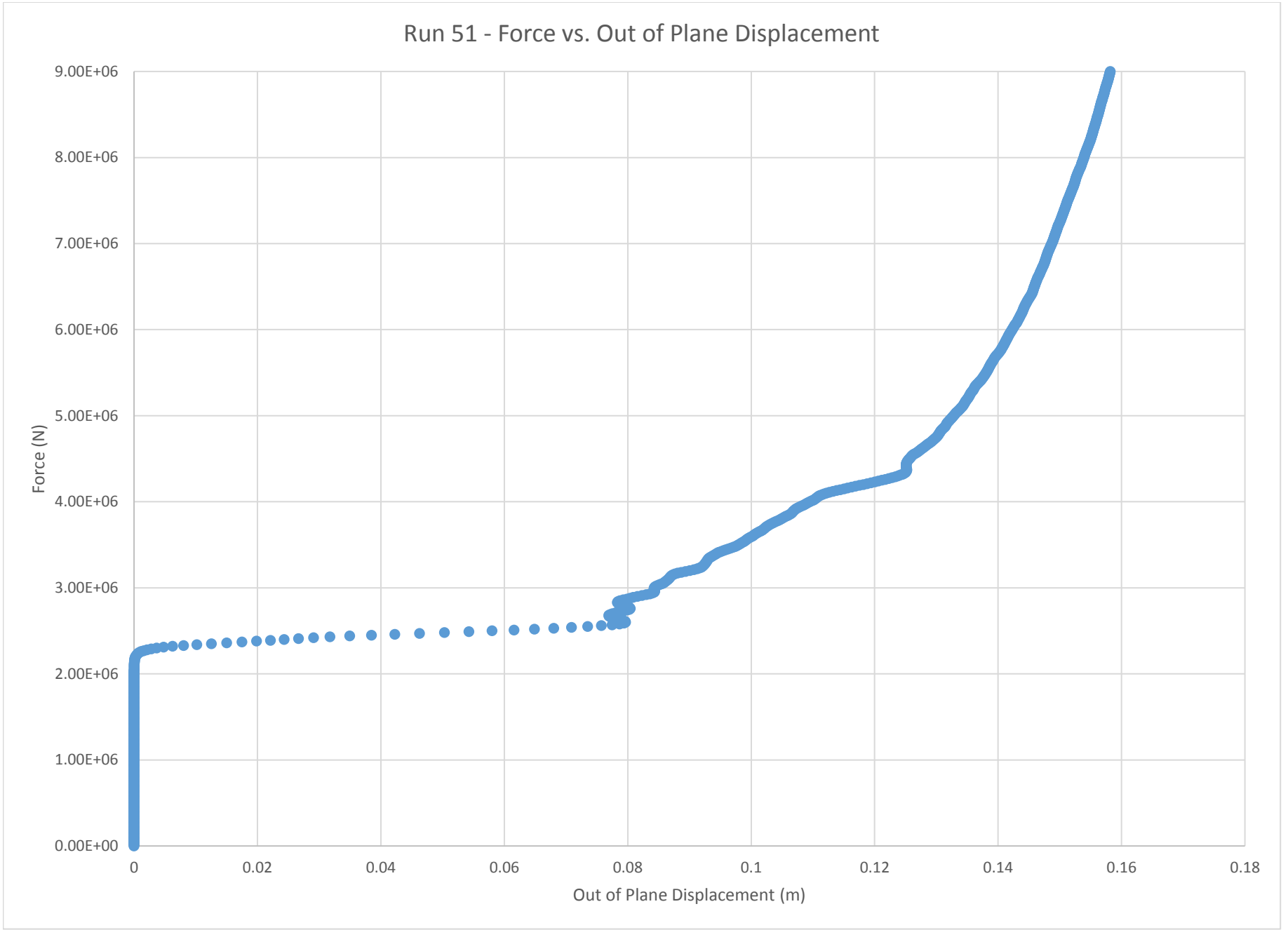
Run 51 - Force vs. Out of Plane Displacement
9.00E+06
8.00E+06
7.00E+06
6.00E+06
5.00E+06
4.00E+06
3.00E+06
2.00E+06
1.00E+06
0.00E+00
Force (N)
0
0.02
0.04
0.06
0.08
0.1
0.12
0.14
0.16
0.18
Out of Plane Displacement (m)